



PB99-164113

# CONNECTICUT TRANSPORTATION INSTITUTE

## Protection of Reinforcement with Corrosion Inhibitors, Phase I

Final Report  
November, 1998

JHR 98-266

Project 96-2, Phase I

Principal Investigator(s)  
Mark Allyn, Graduate Student  
Gregory C. Frantz, Professor  
Jack E. Stephens, Professor Emeritus



**SCHOOL OF ENGINEERING  
UNIVERSITY OF CONNECTICUT  
STORRS, CONNECTICUT**

REPRODUCED BY:  
U.S. Department of Commerce  
National Technical Information Service  
Springfield, Virginia 22161

**NTIS**



**Protection of Reinforcement with  
Corrosion Inhibitors, Phase I**

Final Report  
November, 1998

JHR 98-266                      Project 96-2, Phase I


Principal Investigator(s)  
Mark Allyn, Graduate Student  
Gregory C. Frantz, Professor  
Jack E. Stephens, Professor Emeritus

This research was sponsored by the Joint Highway Research Advisory Council (JHRAC) of the University of Connecticut and the Connecticut Department of Transportation and was carried out in the Connecticut Transportation Institute of the University of Connecticut.

The contents of this report reflect the views of the author(s) who are responsible for the facts and accuracy of the data presented herein. The contents do not necessarily reflect the official views or policies of the University of Connecticut or the Connecticut Department of Transportation. This report does not constitute a standard, specification, or regulation.

PROTECTED UNDER INTERNATIONAL COPYRIGHT  
ALL RIGHTS RESERVED.  
NATIONAL TECHNICAL INFORMATION SERVICE  
U.S. DEPARTMENT OF COMMERCE

Technical Report Documentation Page

1. Report No. <b>JHR 98-266</b>	2. Government Accession No.  PB99-164113	3. Recipient's Catalog No.	
4. Title and Subtitle <b>Protection of Reinforcement with Corrosion Inhibitors, Phase I</b>		5. Report Date <b>November, 1998</b>	
7. Author(s) <b>M. Allyn; G.C. Frantz; and J.E. Stephens</b>		6. Performing Organization Code	
9. Performing Organization Name and Address  <b>University of Connecticut Department of Civil and Environmental Engineering 191 Auditorium Road, Box U-37 Storrs, CT 06269</b>		8. Performing Organization Report No. <b>JHR 98-266</b>	
12. Sponsoring Agency Name and Address  <b>Connecticut Department of Transportation 280 West Street Rocky Hill, CT 06067-0207</b>		10 Work Unit No. (TRAIS)	
15 Supplementary Notes		11. Contract or Grant No.	
16. Abstract  Costs due to corrosion of reinforcement in concrete caused by deicing salts has been estimated at up to \$1 billion per year in the US alone. For most situations, corrosion inhibiting admixtures offer significant advantages over other protection methods to delay initiation of corrosion for the service life of the structure.  Two new prototype corrosion inhibiting chemicals were evaluated and compared with two commercial corrosion inhibiting admixtures as well as with a typical air-entrained control concrete. Corrosion testing consisted of weekly wetting (with salt solution) and drying cycles applied to slab type specimens and to both 2-inch and 3-inch diameter lollipop specimens. Some lollipop specimens were also "pre-cracked" prior to corrosion testing. Linear polarization techniques measured corrosion rates. Reinforcing bars were removed and visually examined at completion of testing. Other concrete material test results included compression strength, freeze-thaw resistance, and absorption.  Compared with the control concrete and with the two commercial inhibitors, the new corrosion inhibiting chemicals produced significant improvement. After about 12 months of corrosion monitoring, "uncracked" specimens with the two prototype chemicals showed no sign of corrosion. "Pre-cracked" specimens, which contained the new chemicals, had very greatly reduced amounts of reinforcement corrosion.		13. Type of Report and Period Covered <b>Final Report</b>	
17. Key Words <b>Bridges (concrete), Corrosion; Corrosion Inhibitors; Durability; Pavements (concrete); and Research</b>		14. Sponsoring Agency Code	
19. Security Classif. (of this report)	20. Security Classif. (of this page)	21. No. of Pages	22. Price

## GENERAL DISCLAIMER

This document may be affected by one or more of the following statements:

- This document has been reproduced from the best copy furnished by the sponsoring agency. It is being released in the interest of making available as much information as possible.
- This document may contain data which exceeds the sheet parameters. It was furnished in this condition by the sponsoring agency and is the best copy available.
- This document may contain tone-on-tone or color graphs, charts and/or pictures which have been reproduced in black and white.
- The document is paginated as submitted by the original source.
- Portions of this document are not fully legible due to the historical nature of some of the material. However, it is the best reproduction available from the original submission.



# SI\* (MODERN METRIC) CONVERSION FACTORS

## APPROXIMATE CONVERSIONS TO SI UNITS

## APPROXIMATE CONVERSIONS TO SI UNITS

Symbol	When You Know	Multiply By	To Find	Symbol
--------	---------------	-------------	---------	--------

Symbol	When You Know	Multiply By	To Find	Symbol
--------	---------------	-------------	---------	--------

### LENGTH

in	inches	25.4	millimetres	mm
ft	feet	0.305	metres	m
yd	yards	0.914	metres	m
mi	miles	1.61	kilometres	km
<u>AREA</u>				
in <sup>2</sup>	square inches	645.2	millimetres squared	mm <sup>2</sup>
ft <sup>2</sup>	square feet	0.093	metres squared	m <sup>2</sup>
yd <sup>2</sup>	square yards	0.836	metres squared	m <sup>2</sup>
ac	acres	0.405	hectares	ha
mi <sup>2</sup>	square miles	2.59	kilometres squared	km <sup>2</sup>

### LENGTH

mm	millimetres	0.039	inches	in
m	metres	3.28	feet	ft
m	metres	1.09	yards	yd
km	kilometres	0.621	miles	mi
<u>AREA</u>				
mm <sup>2</sup>	millimetres squared	0.0016	square inches	in <sup>2</sup>
m <sup>2</sup>	metres squared	10.764	square feet	ft <sup>2</sup>
ha	hectares	2.47	acres	ac
km <sup>2</sup>	kilometres squared	0.386	square miles	mi <sup>2</sup>

### VOLUME

fl oz	fluid ounces	29.57	millilitres	mL
gal	gallons	3.785	Litres	L
ft <sup>3</sup>	cubic feet	0.028	metres cubed	m <sup>3</sup>
yd <sup>3</sup>	cubic yards	0.765	metres cubed	m <sup>3</sup>

### VOLUME

mL	millilitres	0.034	fluid ounces	fl oz
L	litres	0.264	gallons	gal
m <sup>3</sup>	metres cubed	35.315	cubic feet	ft <sup>3</sup>
m <sup>3</sup>	metres cubed	1.308	cubic yards	yd <sup>3</sup>

NOTE: Volumes greater than 1000 L shall be shown in m<sup>3</sup>

### MASS

oz	ounces	28.35	grams	g
lb	pounds	0.454	kilograms	kg
T	short tons (2000 lb)	0.907	megagrams	Mg

### MASS

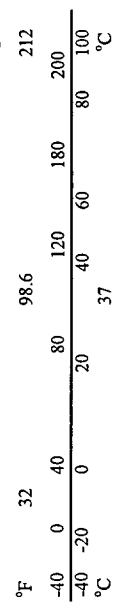
g	grams	0.035	ounces	oz
kg	kilograms	2.205	pounds	lb
Mg	megagrams	1.102	short tons (2000 lb)	T

### TEMPERATURE (exact)

°F	Fahrenheit temperature	5(F-32)/9	Celcius temperature	°C
----	------------------------	-----------	---------------------	----

### TEMPERATURE (exact)

°C	Celcius temperature	1.8C+32	Fahrenheit temperature	°F
----	---------------------	---------	------------------------	----



\* SI is the symbol for the International System of Measurement

## PREFACE

This is the final report on the JHRAC Project 96-2 Phase 1 entitled "Protection of Reinforcement with Corrosion Inhibitors." This work was sponsored by the Joint Highway Research Advisor Council of the University of Connecticut and the Connecticut Department of Transportation. This work was originally presented in the first author's thesis to the Graduate Faculty of the University of Connecticut in partial fulfillment of the requirements for the degree of Master of Science. The support of the Connecticut Department of Transportation is gratefully acknowledged.



# TABLE OF CONTENTS

Title Page .....	i
Technical Report Documentation .....	ii
Metric Conversion Sheet .....	iii
Preface .....	iv
Table of Contents .....	v
List of Tables .....	viii
List of Figures .....	ix
Chapter 1 INTRODUCTION .....	1
1.1 Problem Statement .....	1
1.2 Intent of Research .....	3
1.3 Organization of Report .....	4
Chapter 2 PRINCIPLES OF CORROSION .....	5
2.1 Basic Mechanisms of Corrosion .....	5
2.2 Different Forms of Corrosion .....	9
2.3 Passivity of Steel .....	11
2.4 Factors That Affect Corrosion of Steel in Concrete .....	13
2.4.1 Carbonation .....	14
2.4.2 Chlorides ... ..	15
2.4.3 Absorption/Permeability .....	16
2.4.4 Depth of Cover .....	17
2.5 Typical Corrosion Cells Formed .....	18
2.6 Corrosion Inhibitors .....	19
Chapter 3 CORROSION MONITORING TECHNIQUES .....	21
3.1 General .....	21
3.2 Half Cell Measurements .....	21
3.3 Macro-Cell Measurements .....	22
3.4 Linear Polarization .....	24
3.4.1 Polarization Technique .....	24
3.4.2 IR Drop Correction Techniques .....	26
3.5 AC Impedance .....	27
Chapter 4 LITERATURE REVIEW .....	32
4.1 General .....	32
4.2 Studies of Varying Concrete and Reinforcement Properties .....	32
4.3 Evaluation of Corrosion Inhibitors .....	34
4.4 Monitoring of Existing Structures .....	36

Chapter 5	CORROSION EXPERIMENTAL PROGRAM .....	38
5.1	General .....	38
5.2	Materials .....	39
5.2.1	Mix Design .....	39
5.2.2	Mixing Procedure.....	43
5.2.3	Cement .....	45
5.2.4	Reinforcement Bars .....	45
5.2.5	Deicing Salt .....	47
5.3	Corrosion Specimen Design and Test Environment .....	47
5.3.1	Lollipop Specimens .....	47
5.3.2	"Cracked" Lollipop Specimens .....	48
5.3.3	Slab Specimens .....	50
5.4	Specimen Fabrication and Curing .....	52
5.4.1	General .....	52
5.4.2	Lollipop Specimens: Standard and "Cracked" .....	52
5.4.3	Slab Specimens .....	54
5.4.4	Strength Cylinders .....	56
5.4.5	Curing Procedure .....	56
5.5	Wetting and Drying Procedure .....	57
Chapter 6	CORROSION TESTING METHODS .....	60
6.1	General .....	60
6.2	Polarization Resistance Measurements .....	60
6.3	IR Drop .....	66
Chapter 7	PRESENTATION AND DISCUSSION OF RESULTS .....	70
7.1	Compression Strength, Freeze-Thaw and Absorption .....	70
7.2	Solution Resistance .....	73
7.2.1	General .....	73
7.2.2	Control Specimens .....	73
7.2.3	Inhibitor A and Inhibitor B Specimens .....	77
7.2.4	DAS and DSS Specimens .....	78
7.3	Corrosion Rates .....	79
7.3.1	General .....	79
7.3.2	Control Specimens .....	85
7.3.3	Inhibitor A and Inhibitor B Specimens .....	85
7.3.4	DAS and DSS Specimens .....	86
7.4	Visual Examination of Specimens .....	87
7.4.1	General .....	87
7.4.2	Corrosion Monitored Specimens .....	96
7.4.3	"Cracked" Lollipop Specimens .....	97
7.5	Corrosion Summary .....	98
7.6	Overall Performance Summary: DAS and DSS Chemicals .....	99

Chapter 8	CONCLUSIONS AND RECOMMENDATIONS .....	101
8.1	Conclusions .....	101
8.2	Recommendations for Future Research .....	102
REFERENCES	.....	104
APPENDIX A	FREEZE-THAW TESTING .....	109
A1.0	Specimen Preparation and Test Protocol .....	109
A2.0	Discussion of Results .....	113
A2.1	General .....	113
A2.2	Control Specimens .....	114
A2.3	Inhibitor A & Inhibitor B Specimens .....	121
A2.4	DAS Specimens .....	122
A2.5	DSS Specimens .....	124
A2.6	Summary of Results .....	126
A3.0	Conclusions .....	128
APPENDIX B	ABSORPTION TESTING .....	132
B1.0	Specimen Preparation and Test Protocol .....	132
B2.0	Discussion of Results .....	135
B3.0	Conclusions .....	141
APPENDIX C	COMPRESSION STRENGTH .....	143
C1.0	Specimen Preparation and Test Protocol .....	143
C2.0	Discussion of Results .....	144
C3.0	Conclusions .....	150
APPENDIX D	SOLUTION RESISTANCE AND CORROSION RATE DATA .....	151

## LIST OF TABLES

3.0	Interpretations of Half Cell Reading (Copper-Copper Sulfate Reference Electrode) .....	22
5.0	Aggregate Properties .....	40
5.1	Corrosion Mix Proportions .....	43
5.2	Chemical Analysis of Type I/II Cement .....	46
5.3	Mechanical and Chemical Analysis of No.4 Grade 60 Reinforcement .....	46
6.0	Typical Standard Deviation and Coefficient of Variation for Actively Corroding Specimens (Based on Three Runs/Test) .....	66
6.1	2-Inch Cylinders: Comparison of Positive Feedback (PF) and AC Impedance (I) Methods for Measuring the Solution Resistance .....	68
6.2	3-Inch Cylinders: Comparison of Positive Feedback (PF) and AC Impedance (I) Methods for Measuring the Solution Resistance .....	69
7.0	Corrosion Mixes: 28 and 56 Day Compression Strengths .....	71
7.1	Corrosion Mixes: Average Time to Corrosion .....	84
7.2	Corrosion Rates for All Specimens at Approximately 47 Weeks ...	84
7.3	Visual Inspection Results for the Standard Lollipops .....	95
7.4	Visual Inspection Results for the Slab Specimens .....	95
7.5	Visual Inspection Results for the "Cracked" Lollipops .....	96
A-1	Freeze-Thaw Mix Proportions .....	110
A-2	Relative Dynamic Modulus of Elasticity, Weight Loss, and Appearance Ratings Values .....	115
A-3	Air Bubble Characteristics of the Control, 2%DAS and 2%DSS Mixes .....	126
A-4	Summary of Relative Dynamic Modulus of Elasticity, Weight Loss, and Appearance Ratings Values for the Best Performing Mixes .....	127
B-1	Absorption Mix Proportions .....	133
B-2	Final Absorption: All Specimens .....	135
C-1	Additional Mix Proportions .....	144
C-2	28 Day Strengths for Corrosion and Freeze-Thaw Mixes .....	145

## LIST OF FIGURES

2.0	Metallurgy in Reverse .....	5
2.1	Basic Corrosion Cell Components .....	7
2.2	Pitting Corrosion Process .....	10
2.3	Typical Behavior of an Active-Passive Metal .....	12
2.4	Approximate Pourbiac Diagram for Iron and Water at 25°C .....	14
2.5	Effects of Water-Cement Ratio and Depth of Cover .....	18
3.0	Typical Macro-Cell Corrosion Verses Time .....	23
3.1	Linear Polarization Curve: Over-Potential Shift Equals $\pm 10\text{mV}$ (Note: Plot Shown is in the Form $i_{\text{APP}}$ Vs E) .....	25
3.2	Electrical Circuit Model for a Simple Corrosion System .....	29
3.3	Bode Plot for Electrical Circuit Shown in Figure 3.2 .....	29
3.4	Nyquist Plot for Electrical Circuit Shown in Figure 3.2 .....	30
5.0	2-Inch Diameter Lollipop .....	49
5.1	3-Inch Diameter Lollipop .....	49
5.2	"Cracked" 3-Inch Diameter Lollipop .....	49
5.3	Slab Specimen .....	51
5.4	Lollipop Casting Fixture .....	53
6.0	Lollipop Test Cell Setup .....	62
6.1	Slab Specimen Test Cell Setup .....	62
6.2	Typical Linear Polarization Curve for an Actively Corroding Lollipop Specimen, Not Corrected for IR Drop (Plotted I Vs E) .....	65
6.3	Linear Portion of Figure 6.2, Corrected for IR Drop (Plotted E Vs. I) .....	65
7.0	Compression Strengths: Lollipop Specimens .....	72
7.1	Compression Strengths: Slab Specimens.....	72
7.2	Solution Resistance, 2-Inch Cylinders: Control, Inhibitor A and B Mixes .....	74
7.3	Solution Resistance, 2-Inch Cylinders: Control, DAS and DSS Mixes	74
7.4	Solution Resistance, 3-Inch Cylinders: Control, Inhibitor A and B Mixes .....	75
7.5	Solution Resistance, 3-Inch Cylinders: Control, DAS and DSS Mixes	75
7.6	Solution Resistance, Slabs: Control, Inhibitor A and B Mixes .....	76
7.7	Solution Resistance, Slabs: Control, DAS and DSS Mixes .....	76
7.8	Corrosion Rate, 2-Inch Cylinders: Control, Inhibitors A and B Mixes	80
7.9	Corrosion Rate, 2-Inch Cylinders: DAS and All DSS Mixes .....	81
7.10	Corrosion Rate, 2-Inch Cylinders: DAS and DSS Mixes (Omitting	81

Specimen 1%DSS-1) .....	81
7.11 Corrosion Rate, 3-Inch Cylinders: Control, Inhibitors A and B Mixes	82
7.12 Corrosion Rate, 3-Inch Cylinders: DAS and DSS Mixes .....	82
7.13 Corrosion Rate, Slabs: Control, Inhibitors A and B Mixes .....	83
7.14 Corrosion Rate, Slabs: DAS, DSS, Inhibitor A and B Mixes .....	83
7.15 Visually Examined 2-Inch Diameter Lollipop Specimens .....	89
7.16 Visually Examined 3-Inch Diameter Lollipop Specimens .....	90
7.17a Visually Examined Slab Specimens .....	91
7.17b Visually Examined Slab Specimens, Continued .....	92
7.18a Visually Examined 3-Inch Diameter "Cracked" Lollipop Specimens	93
7.18b Visually Examined 3-Inch Diameter "Cracked" Lollipop Specimens, Continued .....	94
A-1 28 Day Strengths for Freeze-Thaw Mixes .....	116
A-2 Relative Dynamic Modulus of Elasticity, all Specimens at 300 Cycles .....	117
A-3 Relative Dynamic Modulus of Elasticity, all Specimens .....	118
A-4 Weight Loss, all Specimens .....	119
A-5 Appearance Ratings, all Specimens .....	120
A-6 Relative Dynamic Modulus of Elasticity, Control Mixes .....	121
A-7 Relative Dynamic Modulus of Elasticity, Inhibitors A & B Mixes .	122
A-8 Relative Dynamic Modulus of Elasticity, DAS Mixes .....	123
A-9 Relative Dynamic Modulus of Elasticity, DAS-R Mixes .....	123
A-10 Relative Dynamic Modulus of Elasticity, DSS Mixes .....	125
A-11 Relative Dynamic Modulus of Elasticity, DSS-R Mixes .....	125
A-12 Relative Dynamic Modulus of Elasticity, Comparison of Best Performing Mixes .....	128
A-13 Relative Dynamic Modulus of Elasticity at 300 Cycles, DSS, DSS-R, DAS and DAS-R Mixes .....	130
A-14 Weight Loss at 300 Cycles, DSS, DSS-R, DAS and DAS-R Mixes ..	130
A-15 Appearance Rating, DSS, DSS-R, DAS and DAS-R Mixes .....	131
B-1 Final Absorption: all Specimens, Dried at 100 <sup>o</sup> C .....	136
B-2 Final Absorption: all Specimens, Dried at 40 <sup>o</sup> C .....	137
B-3 Absorption Verses Time: Control, Inhibitors A & B, DAS and DSS Specimens, Dried at 100 <sup>o</sup> C .....	138
B-4 Absorption Verses Time: Control, Inhibitors A & B, DAS and DSS Specimens, Dried at 40 <sup>o</sup> C .....	138
B-5 Final Absorption: DAS and DAS-R Specimens, Dried at 100 <sup>o</sup> C .....	140
B-6 Final Absorption: DSS and DSS-R Specimens, Dried at 100 <sup>o</sup> C ...	140
B-7 Final Absorption: DAS and DSS Specimens, Dried at 100 <sup>o</sup> C .....	142

C-1	28 Day Compression Strengths for Corrosion Mixes .....	146
C-2	28 Day Compression Strengths for Freeze-Thaw Mixes .....	147
C-3	Relative 28 Day Compression Strengths: All DAS Mixes (Control Mixes = 100%) .....	148
C-4	Relative 28 Day Compression Strengths: All DSS Mixes (Control Mixes = 100%) .....	148
D-1	Solution Resistance, 2-Inch Diameter Lollipops: Control .....	152
D-2	Solution Resistance, 2-Inch Diameter Lollipops: Inhibitor A .....	152
D-3	Solution Resistance, 2-Inch Diameter Lollipops: Inhibitor B .....	153
D-4	Solution Resistance, 2-Inch Diameter Lollipops: 2%DAS .....	153
D-5	Solution Resistance, 2-Inch Diameter Lollipops: 1%DAS .....	154
D-6	Solution Resistance, 2-Inch Diameter Lollipops: 1/2%DAS .....	154
D-7	Solution Resistance, 2-Inch Diameter Lollipops: 2%DSS .....	155
D-8	Solution Resistance, 2-Inch Diameter Lollipops: 1%DSS .....	155
D-9	Solution Resistance, 3-Inch Diameter Lollipops: Control .....	156
D-10	Solution Resistance, 3-Inch Diameter Lollipops: Inhibitor A .....	156
D-11	Solution Resistance, 3-Inch Diameter Lollipops: Inhibitor B .....	157
D-12	Solution Resistance, 3-Inch Diameter Lollipops: 2%DAS .....	157
D-13	Solution Resistance, 3-Inch Diameter Lollipops: 1%DAS .....	158
D-14	Solution Resistance, 3-Inch Diameter Lollipops: 1/2%DAS .....	158
D-15	Solution Resistance, 3-Inch Diameter Lollipops: 2%DSS .....	159
D-16	Solution Resistance, 3-Inch Diameter Lollipops: 1%DSS .....	159
D-17	Solution Resistance, Slabs, Control-1 Mixes Conn .....	160
D-18	Solution Resistance, Slabs, Control-2 Unconn .....	160
D-19	Solution Resistance, Slabs, Control-2 Mixes Conn .....	161
D-20	Solution Resistance, Slabs, Inhibitor A .....	161
D-21	Solution Resistance, Slabs, Inhibitor B .....	162
D-22	Solution Resistance, Slabs, 2% DAS .....	162
D-23	Solution Resistance, Slabs, 1% DAS .....	163
D-24	Solution Resistance, Slabs, 1/2% DAS .....	163
D-25	Solution Resistance, Slabs, 2% DSS .....	164
D-26	Solution Resistance, Slabs, 1% DSS .....	164
D-27	Corrosion Rate, 2-Inch Diameter Lollipops: Control .....	165
D-28	Corrosion Rate, 2-Inch Diameter Lollipops: Inhibitor A .....	165
D-29	Corrosion Rate, 2-Inch Diameter Lollipops: Inhibitor B .....	166
D-30	Corrosion Rate, 2-Inch Diameter Lollipops: 2%DAS .....	166
D-31	Corrosion Rate, 2-Inch Diameter Lollipops: 1%DAS .....	167
D-32	Corrosion Rate, 2-Inch Diameter Lollipops: 1/2%DAS.....	167
D-33	Corrosion Rate, 2-Inch Diameter Lollipops: 2%DSS .....	168
D-34	Corrosion Rate, 2-Inch Diameter Lollipops: 1%DSS .....	168
D-35	Corrosion Rate, 3-Inch Diameter Lollipops: Control .....	169
D-36	Corrosion Rate, 3-Inch Diameter Lollipops: Inhibitor A .....	169

D-37	Corrosion Rate, 3-Inch Diameter Lollipops: Inhibitor B .....	170
D-38	Corrosion Rate, 3-Inch Diameter Lollipops: 2%DAS .....	170
D-39	Corrosion Rate, 3-Inch Diameter Lollipops: 1%DAS .....	171
D-40	Corrosion Rate, 3-Inch Diameter Lollipops: 1/2%DAS.....	171
D-41	Corrosion Rate, 3-Inch Diameter Lollipops: 2%DSS.....	172
D-42	Corrosion Rate, 3-Inch Diameter Lollipops: 1%DSS .....	172
D-43	Corrosion Rate, Slabs, Control-1 Mixes Conn .....	173
D-44	Corrosion Rate, Slabs, Control-2 Unconn .....	173
D-45	Corrosion Rate, Slabs, Control-2 Mixes Conn .....	174
D-46	Corrosion Rate, Slabs, Inhibitor A .....	174
D-47	Corrosion Rate, Slabs, Inhibitor B .....	175
D-48	Corrosion Rate, Slabs, 2% DAS .....	175
D-49	Corrosion Rate, Slabs, 1% DAS .....	176
D-50	Corrosion Rate, Slabs, 1/2% DAS .....	176
D-51	Corrosion Rate, Slabs, 2% DSS .....	177
D-52	Corrosion Rate, Slabs, 1% DSS .....	177



# CHAPTER 1.0

## INTRODUCTION

### 1.1 PROBLEM STATEMENT

In 1955, the Bureau of Public Roads (now called the Federal Highway Administration) mandated a wet road policy: in the winter, vehicle tires should be in direct contact with pavement on federal funded highways [1]. It is doubtful the public would accept anything else than this bare road policy.

Corrosion of concrete reinforcement is a world wide problem that costs billions of dollars a year. Costs due to corrosion of reinforced concrete caused by the use of deicing salts has been estimated at \$325 million to \$1 billion per year in the U.S. alone [2].

Bridges and parking structures located in harsh winter regions, where large quantities of deicing salts are used, or located in or near marine environments are susceptible to corrosion damage due to the presence of chloride ions. Numerous methods/techniques have been tried to eliminate or at least delay corrosion. To date, an ideal solution to this costly problem has not been found.

When steel is embedded in concrete, the cement paste that surrounds the bar is alkaline in nature, typically with a pH between 12 and 14, which facilitates the formation of a thin passive film that protects the steel from corroding. However, this naturally occurring passive layer can be destroyed by the presence of chloride ions, such as from the use of deicing salts that migrate through the hardened concrete.

Various methods have been tried to prevent or delay corrosion of steel reinforcement embedded in concrete, for example: increased concrete cover over the rebars, reduced water/cement ratios, denser concretes, latex or polymer modified concrete overlays, waterproofing membrane with asphalt overlays, epoxy coated rebars, cathodic protection, and corrosion inhibiting admixtures.

Reduced water/cement ratios, increased cover, denser concretes, and membranes attempt to prevent or limit the ingress of chlorides into the concrete. The epoxy coating on epoxy coated rebars provide a protective barrier around the steel reinforcement that is presumed to isolate the bar from destructive chloride ions. Cathodic protection uses an external power source in conjunction with a external sacrificial anode, which forces the reinforcing steel to become the cathode of the system (see Chapter 2.0), thereby protecting it from corrosion even in the presence of chlorides. Corrosion inhibiting admixtures either prevent or delay the onset of corrosion (see Chapter 2.0).

The use of epoxy coated rebars was initially believed to be the "ideal" solution to prevent corrosion of rebars, but its long-term effectiveness is being questioned [3].

Cathodic protection systems protect steel reinforcement in concrete contaminated with high levels of chloride but is rather expensive and a source of electricity must be available.

The use of corrosion inhibiting admixtures have several advantages over other methods:

1. The admixture is uniformly distributed throughout the concrete, hence, equally protecting all the steel in the structure.

2. The use of inhibiting admixtures is not skill dependent, only the correct amount needs to be added to the concrete mix for it to work.
3. Construction quality control (e.g., damaging of epoxy coatings, difficulty of working with low water/cement ratio or low slump concretes) generally is not a concern with inhibiting admixtures.
4. Inhibiting admixtures do not require maintenance, whereas other systems do (e.g., membranes, cathodic protection).

Many chemicals/compounds have been investigated in the past for use as concrete corrosion inhibitors [4, 5]. Some showed promise as an inhibitor, but had detrimental effects on certain concrete properties or were expensive.

The "ideal" concrete corrosion protection system would prevent the initiation of corrosion for the service life of the structure. Corrosion inhibiting admixtures look to be, currently, the best chance for this solution based on their non-skill dependent usage and low maintenance characteristics. To date, only a few concrete corrosion inhibitors exist that do not have adverse effects on concrete properties and generally only delay (not prevent) corrosion initiation in laboratory testing [6].

## **1.2 INTENT OF RESEARCH**

The objective of this research program was to evaluate two prototype concrete corrosion inhibitors and compare their performance with a standard air entrained control

concrete as well as with two existing commercial concrete corrosion inhibitors. Also, different corrosion specimen types were evaluated.

Linear polarization measurements and visual inspections were utilized to evaluate the corrosion performance of the various mixes. Furthermore, specific hardened concrete properties (durability, strength and absorption) of each mix were evaluated.

### **1.3 ORGANIZATION OF REPORT**

Chapter 2.0 presents a limited explanation of the basic principles of corrosion and specifically steel corrosion. Electrochemical techniques commonly used to monitor the corrosion of steel reinforcement in concrete are described in Chapter 3.0. A literature review of some past research on corrosion of steel reinforcement embedded in concrete is presented in Chapter 4.0. Chapter 5.0 discusses the variables for the corrosion experimental program including mix design, specimen fabrication and testing environment. Test assumptions, geometry of test cells, testing procedures and data reduction are discussed in Chapter 6.0. Results for the corrosion testing program are presented in Chapter 7.0 and project conclusions & recommendations for future studies are presented in Chapter 8.0. Appendices A, B, and C discuss test parameters, test results and conclusions for the freeze-thaw, absorption and compression strength testing programs, respectively. Appendix D presents the solution resistances and corrosion rates (verses time) for each specimen for each variable tested.

Mr. Mark Allyn, former Graduate Research Assistant, prepared this report as part of the requirements for the Master of Science degree (48).

# CHAPTER 2.0

## PRINCIPLES OF CORROSION

### 2.1 BASIC MECHANISMS OF CORROSION

Corrosion is defined as the destruction or deterioration of a material caused by a chemical or electrochemical reaction with its environment. Sometimes this definition is applied only to metals but it also pertains to non-metals, such as plastics, ceramics and rubber. This discussion will be limited to metallic corrosion of iron only.

Metallic corrosion is a process by which a metal returns to its natural form. It has been compared to extractive metallurgy in reverse (Fig. 2.0) [7]. Large amounts of energy must be added to iron ore during the refining process. In the case of corroding steel, there is a tendency for the iron to revert back to its natural and more thermodynamically stable state, iron oxide.

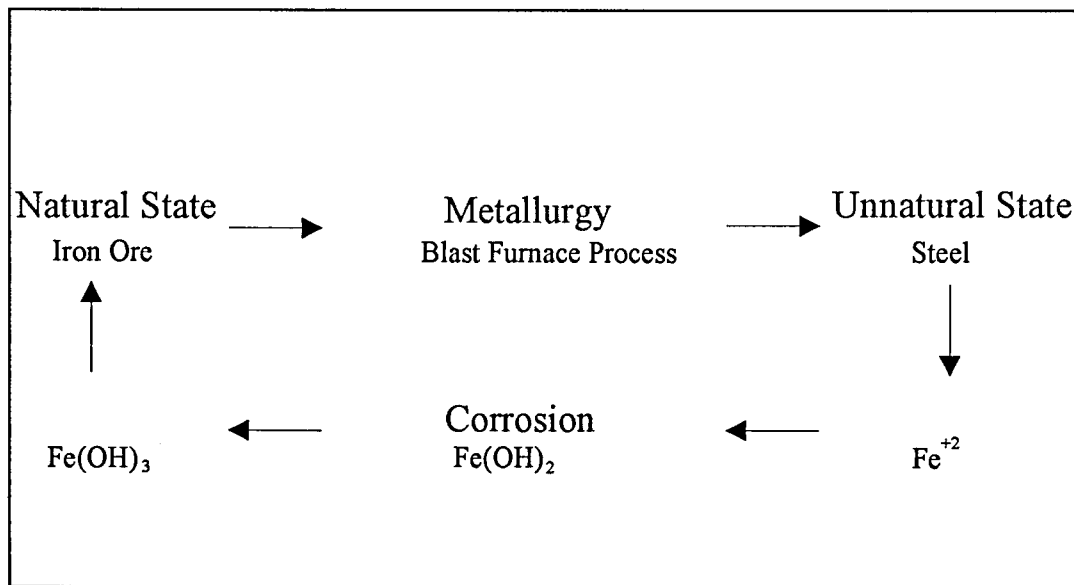


Figure 2.0 Metallurgy in Reverse.

Corrosion can be classified into two categories, dry corrosion and wet corrosion [7]. Dry corrosion is most often associated with high temperatures and occurs without the presence of an aqueous solution. Vapors or gases are usually the corrosive agent, as in the corrosion of steel by furnace gases. Wet corrosion occurs when an electrolyte or aqueous solution is present, for example, the corrosion of steel in salt water. Wet corrosion accounts for the majority of metal deterioration and pertains to the corrosion of steel reinforcement in concrete. This discussion will focus on wet corrosion only. For a more detailed discussion, refer to References 6, 7, 8, and 9.

Corrosion is an electrochemical process that can be defined as any reaction that can be divided into a partial oxidation and a partial reduction reaction. More than one oxidation or reduction reaction can occur [7]. An electrical circuit must be present for metallic corrosion to occur, and the circuit is usually made up of three components: anode, cathode and electrolyte. When potential gradients form in the electrolyte between anodic and cathodic areas on the metal surface, corrosion occurs since the system strives to reach equilibrium. Electrons flow through the metal from anodic sites to cathodic sites located on the metal surface (Fig 2.1). The flow of current (i.e., charge transfer) is completed through the electrolyte due to its ionic conductivity, thereby completing the electrical circuit.

The anode electrode is where metal dissolution (oxidation process) occurs and electrons are lost. The anodic reaction in every metallic corrosion reaction is the oxidation of the metal into its ion:

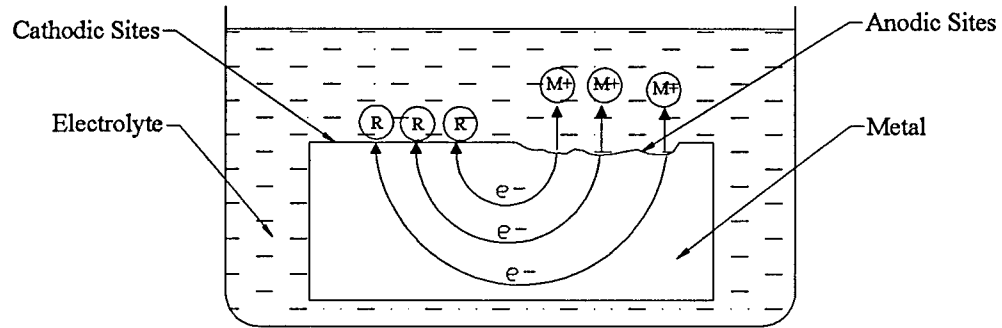
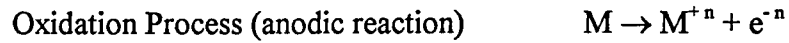


Figure 2.1 Basic Corrosion Cell Components.

A reduction process (gaining of electrons) occurs at metal areas, called cathodes, that receive electrons. The most common cathodic reactions (reduction processes) that occur in metallic corrosion are (represented as R in Figure 2.1):

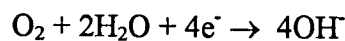
Hydrogen Evolution	$2H^{+} + 2e^{-} \rightarrow H_2$
Oxygen Reduction (acidic solution)	$O_2 + 4H^{+} + 4e^{-} \rightarrow 2H_2O$
Oxygen Reduction (neutral and basic solutions)	$O_2 + 2H_2O + 4e^{-} \rightarrow 4OH^{-}$
Metal Ion Reduction	$M^{3+} + e^{-} \rightarrow M^{+2}$
Metal Deposition	$M^{+} + e^{-} \rightarrow M$

The first three are quite common. Metal ion reduction and metal deposition are less common and are usually found in chemical process streams.

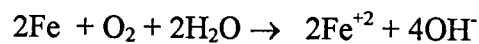
One of the most important basic principles of corrosion is that "during metallic corrosion, the rate of oxidation must equal the rate of reduction (in terms of electrical production and consumption)" [7]. The electrochemical process of corrosion can be demonstrated by using the example of steel in salt water. The corrosion process of steel in salt water can be separated into anodic and cathodic reactions with the salt water acting as the electrolytic solution. The anodic reaction that occurs is:



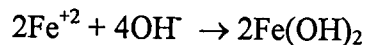
The electrolyte is exposed to the atmosphere and therefore contains dissolved oxygen. Since salt water is generally considered a neutral solution, the cathodic reaction process is oxygen reduction:



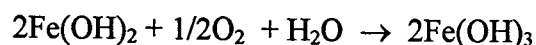
The sodium ions ( $\text{Na}^{+}$ ) and chloride ions ( $\text{Cl}^{-}$ ) do not participate in the electrochemical reactions. Therefore, the overall corrosion process of steel in salt water can be shown as:



The ferrous ions ( $\text{Fe}^{+2}$ ) and the hydroxyl ions ( $\text{OH}^{-}$ ) combined to form ferrous hydroxide:



Ferrous hydroxide, usually dark green in color, then precipitates out of solution. This compound is unstable in oxygenated environments and oxidizes into ferric hydroxide, which is the familiar red rust commonly associated with the corrosion of steel:



Moisture (electrolyte) and oxygen must be present for corrosion to occur. If either is not present, no corrosion will occur.



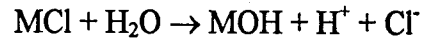
## 2.2 DIFFERENT FORMS OF CORROSION

Corrosion takes many forms such as: uniform/general corrosion, pitting corrosion, galvanic corrosion, crevice corrosion, stress corrosion, intergranular corrosion, selective leaching, and erosion corrosion. Only the first four are significant in the corrosion of reinforcing steel in concrete, and these will be discussed in further detail. For a thorough discussion on forms of corrosion see References 7 and 10.

Uniform corrosion occurs over relatively large exposed areas with anodic and cathodic regions spread throughout. Since the corrosion product occupies a much larger volume than the original bar, high tensile stresses develop in the concrete. This causes degradation of the concrete by cracking and spalling. Loss of mechanical bond between the reinforcing bar and concrete can also occur.

Pitting corrosion is a form of localized corrosion and is usually considered one of the most destructive types of corrosion. Pitting corrosion is a self sustaining process and metal dissolution occurs at a relatively small area. Therefore, failure can occur quite suddenly and without visual warning since considerable amounts of corrosion can occur before cracks and spalls are visible in the concrete. For example, consider the case where metal M is submerged in an aerated sodium chloride solution (Fig. 2.2). As the metal dissolution occurs at a localized area, a pit is formed. The metal dissolution process creates an abundance of positively charged ions ( $M^+$ ) in the pit, which subsequently attract more negatively charged ions ( $Cl^-$ ), which results in an increase of metal salts ( $MCl$ ) in the pit. The solution in the pit becomes oxygen depleted and oxygen reduction ceases in the pit. Metal dissolution continues in the pit and is fueled by oxygen reduction

occurring on surface areas outside the pit (Fig. 2.2), which become cathodically protected from corrosion while the pit is active. The metal salts hydrolyze in the pit, a process called hydrolysis:



The solution in the pit becomes acidic (i.e., the pH is reduced) due to the increase of hydrogen ions ( $\text{H}^+$ ). As a result of the chloride migration and hydrolysis reaction, the dissolution process increases rapidly and becomes autocatalytic.

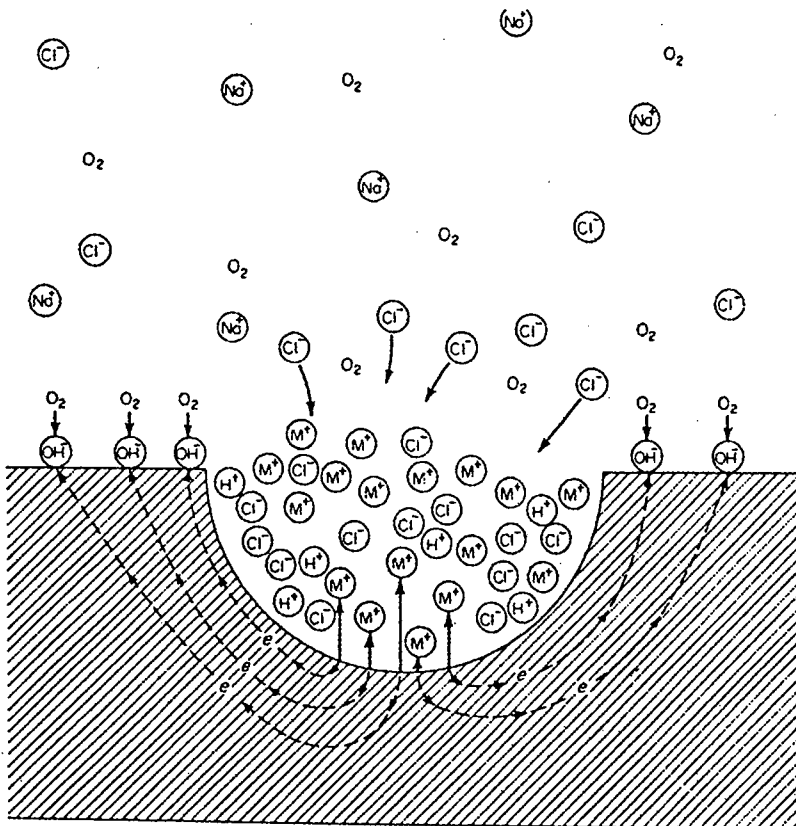


Figure 2.2 Pitting Corrosion Process [7].

Galvanic corrosion occurs when two dissimilar metals are electrically connected in a conductive or corrosive solution. The extent of corrosion is dependent on the areas or relative areas of connected metals, solution conductivity, and the potential difference between the metals. The potential difference is the driving force, and the larger it is, the more severe the corrosion will be. The potential difference of various metals and alloys are usually obtained from electromotive force (EMF) and Galvanic series charts, which aid in predicting the possibility of galvanic corrosion between two dissimilar metals. Galvanic corrosion can also occur when two similar metals are electrically connected and a potential difference exists between the two metals. The potential difference can be caused by differential concentrations of oxygen, chlorides, or moisture or a combination.

Crevice corrosion is very similar to pitting corrosion, except it occurs within crevices or other shielded areas that are usually only a few thousandths of an inch, or less, in width [7]. Cracks in reinforced concrete that propagate down to the reinforcing steel and coating defects on reinforcing bars are areas that could be susceptible to crevice corrosion. The process of crevice corrosion is very similar to that of pitting corrosion.

General corrosion, pitting corrosion and crevice corrosion are more prevalent in the corrosion of reinforcing bars in concrete. However, galvanic corrosion can occur if dissimilar metals are connected together, such as attaching ducts or hangers. Care should be used when selecting material types so that galvanic couples can not form.

### **2.3 PASSIVITY OF STEEL**

Iron is considered an active-passive metal. The typical behavior of an active-passive metal is shown in Figure 2.3. Active-passive metals have three distinct regions:

active region - the metal is actively corroding,

passive region - the metal is somewhat inert and the corrosion rate is very low, and  
 transpassive region - the metal loses its passive film and starts actively corroding.

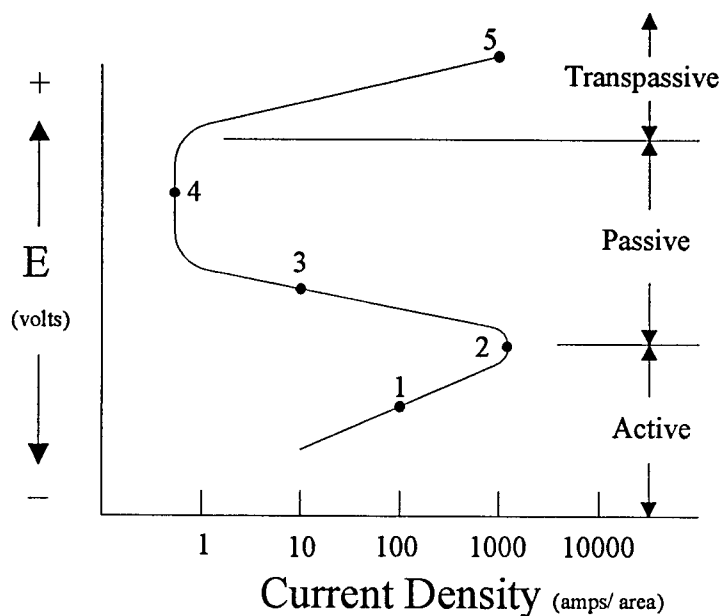


**Figure 2.3 Typical Behavior of an Active-Passive Metal.**

Passivity, defined simply, refers to a loss of chemical reactivity under certain conditions [7]. This definition can be explained by looking at Figure 2.3. When the oxidation and reduction reactions are occurring at point No.1, the current density of the system, which is proportional to the corrosion rate, is 100 amps/cm<sup>2</sup>. If an oxidation agent (anodic inhibitor) is added to the system or the potential of the system is increased, the oxidation rate increases. Remembering that the oxidation rate must equal the reduction rate, as the system moves from point No.1 to point No.4 the current density first increases

to over 1000 amps/cm<sup>2</sup> (point No. 2) and then decreases to less than 1 amp/cm<sup>2</sup> (point No. 4). This increase in oxidation results in the formation of a passive film that acts as a barrier preventing further oxidation of the underlying metal. Also, the potential is increasing and becoming more noble (i.e., the system is being pushed anodically). Therefore, at point No.4 the steel is said to be passivated, and the corrosion rate is significantly reduced. Note that the current density and therefore corrosion rate will increase greatly if the system passes from the passive to the transpassive region (from point No.4 to point No.5).

The passive surface film formed on the steel is very thin and fragile. There is still much debate about the exact structure of the passive film, i.e., amorphous or crystalline. Kruger [11] published a review on the nature of the passive film on iron and ferrous alloys and suggested that more protective films are amorphous. More recent work by Toney et al.[12] showed, by use of X-ray scattering, that the structure of the passive film on iron is a spinel based on Fe<sub>3</sub>O<sub>4</sub>, but with cation vacancies on octahedral and tetrahedral sites. The structure is Fe<sub>3</sub>O<sub>4</sub>, but the chemistry is analogous to Fe<sub>2</sub>O<sub>3</sub>.

## **2.4 FACTORS THAT AFFECT CORROSION OF STEEL IN CONCRETE**

When steel is embedded in concrete, the cement paste that surrounds the bar is alkaline in nature, typically with a pH between 12 and 14. Many researchers believe the alkaline environment in concrete facilitates the formation of a thin passive film that protects the steel from corroding [4, 6, 8, 9, 13, 14]. The Pourbaix diagram for iron (Fig. 2.4), based on thermodynamics, shows that iron remains passive and thermodynamically

stable when the pH is between 8 and 13. This diagram does not include the effects caused by the presence of chloride ions or the presence of a concrete environment (e.g., cement, aggregates, etc.). Also, thermodynamics cannot predict whether or not a film will be protective of its substrate [15]. Some people believe the formation of mineral scales, not a passive film, provides the main protection for the reinforcement [15]. Damage to the protective layer can occur either mechanically or chemically. Examples of the latter are carbonation and chloride ingress.

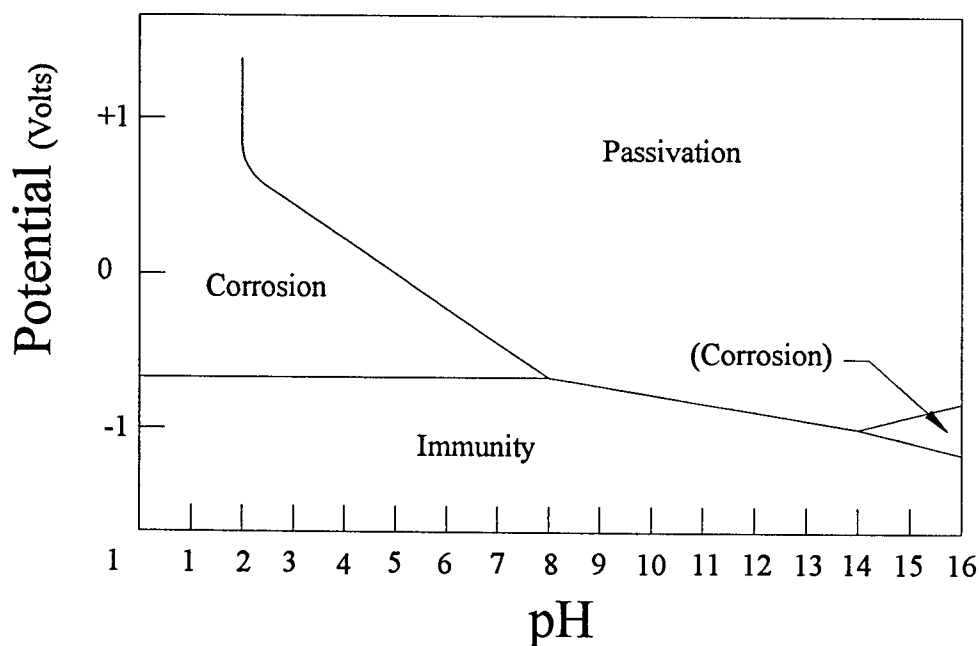
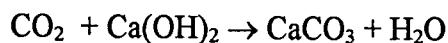


Figure 2.4 Approximate Pourbaix Diagram for Iron and Water at 25°C.

### 2.4.1 Carbonation

Carbonation occurs from the reaction between atmospheric carbon dioxide ( $\text{CO}_2$ ) and the hydroxides ( $\text{Ca}(\text{OH})_2$ ) in the cement paste to form carbonates ( $\text{CaCO}_3$ ) and water:



The formation of the carbonates can reduce the pH of the concrete to a range below 8.0, thereby depassivating the steel and leaving it susceptible to corrosion (Fig. 2.4). The magnitude of carbonation damage is essentially proportional to the impermeability characteristics of the concrete and the depth of concrete cover over the reinforcing bars. Carbonation is generally not a significant concern today when using good quality and sound concrete mixes in conjunction with adequate reinforcement cover.

#### 2.4.2 Chlorides

Ingress of chlorides is more destructive, by far, to reinforced concrete than carbonation in the United States. Reinforced concrete can be subjected to chloride damage from exposure to marine environments, deicing salts, admixtures containing chlorides, and chloride contaminated cements, aggregates and batch water. Most people believe that chlorides that migrate into hardened concrete, such as from marine environments and deicing salts, are more destructive [14]. Migrating chlorides can also cause potential differences to develop in the pore solution (i.e., electrolyte) between anodic and cathodic sites. The system wants to remain in equilibrium, thereby causing corrosion to occur. This is more prevalent in galvanic cells. Bridge decks, which can act as galvanic cells, have upper and lower mats of reinforcement that are electrically connected. Migrating chloride ions contaminate the upper layer of concrete, whereas the lower layer remains relatively uncontaminated. A large potential difference develops between the mats and corrosion can be quite severe [13].

Most researchers believe that the depassivation of reinforcing steel is caused by the presence of chlorides [6, 8, 9, 16, 17]. The exact cause of steel depassivation due to the presence of chloride ions is not yet completely known or agreed upon. The penetrating chlorides do not significantly reduce the pH of the concrete, therefore chlorides cause corrosion even in high pH environments where the steel should be passivated. The chloride ion concentration required to initiate corrosion in normal concrete is about 1.0 to 1.6 lbs acid soluble chloride ions per cubic yard of concrete [18]. Borgard et. al. [15.], suggested that corrosion of steel embedded in concrete is not related to the break down of passive films on carbon steel, since relatively large quantities of chloride are required to initiate corrosion in concrete and the fact that chlorine can reduce corrosion in some cases.

#### **2.4.3 Absorption/Permeability**

The absorption/permeability of concrete determines the rate that moisture, oxygen and chlorides diffuse through uncracked concrete to the steel. The moisture together with salt (sodium chloride) acts as an electrolyte to facilitate the flow of ionic current, the oxygen fuels the cathodic reaction, and chlorides initiate the corrosion process. Therefore, the lower the concrete absorption/permeability, the longer it will take for corrosion to initiate. Many factors affect the absorption/permeability of concrete such as water-cement ratio, degree of consolidation, and adequacy of curing. Many studies have shown that the ingress of chlorides is reduced by lowering the water-cement ratio [18, 19]. But, reducing the water-cement ratio alone will not assure chloride reduction. Proper consolidation and curing of the concrete must also be provided. Pozzolans are commonly utilized to



decrease the permeability of concrete, thereby increasing the time to the initiation of corrosion.

Concrete resistivity and resistance are functions of the absorption/permeability characteristics of concrete. Resistance is related to resistivity by the following:

$$R = \rho(L/A), \text{ where}$$

R = Resistance (ohms)

$\rho$  = Resistivity (ohms-cm)

L = Length (cm)

A = Cross sectional area (cm<sup>2</sup>)

Resistivity has a value at every point in a body, while resistance applies to a single value for the entire body. Concrete with low absorption/permeability, and therefore a low moisture and chloride content, usually has a very high electrical resistivity. Many people equate low absorption/permeability and high resistivity to good quality mixes that protect concrete reinforcement from corrosion. The presence of moisture and chlorides can reduce concrete resistivity significantly.

#### 2.4.4 Depth Of Cover

Increasing the depth of concrete cover significantly increases the time to corrosion due to the increased depth of chloride diffusion required to initiate corrosion. Figure 2.5 shows the typical effects of water-cement ratio and depth of cover on chloride penetration. Chlorides primarily migrate into the concrete by diffusion. Fick's Second Law of Diffusion can determine the chloride concentration at any depth and time. The diffusion constant and

surface chloride concentration must be accurately known to obtain meaningful results from this method.

## 2.5 TYPICAL CORROSION CELLS FORMED

Generally, two types of corrosion cells, macro-cell and micro-cells, can develop during the corrosion of steel reinforcement bars embedded in concrete. A macro-cell forms when the anode and cathode regions are relatively large and located relatively far apart on the same bar or are located on different bars or different levels of bars, which are electrically connected. When the anode and cathode areas are relatively close together on the same reinforcing bar, a micro-cell is said to form. A large potential difference can

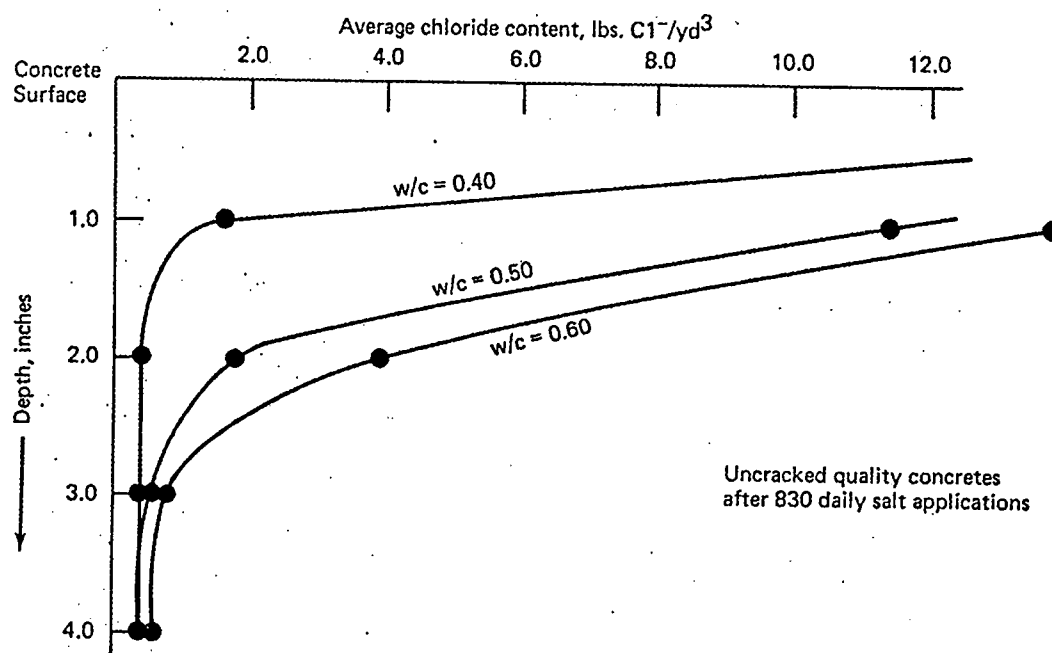


Figure 2.5 Effects of Water-Cement Ratio and Depth of Cover [19].

develop in the electrolyte between the anode and cathode for both types of cells, such as caused from chloride ingress, and under the right conditions (i.e., presence of oxygen, electrolyte and chlorides) a corrosion cell could initiate. Both general/uniform and localized corrosion can occur in a macro-cell.

## 2.6 CORROSION INHIBITORS

Corrosion inhibitors are chemical compounds that reduce the corrosion rate of metals in aggressive environments. Hundreds of corrosion inhibitors have been developed over the years for specific applications such as cooling systems, water systems, oil refining and other chemical process industries.

The use of corrosion inhibitors to reduce the corrosion of reinforcing steel is relatively new. A number of corrosion inhibitors have been tested with concrete (see Chapter 4.0). Many chemicals are capable of inhibiting corrosion on bare steel but have undesirable effects on the plastic or hardened properties of the concrete, such as setting time, strength and durability. Few chemicals meet the requirements necessary to be used as commercial corrosion inhibitors in concrete. This is evident since only a few commercial concrete corrosion inhibitors are used regularly. The ones that do satisfy these requirements fall into two categories, inorganic and organic inhibitors. Common substances in inorganic inhibitors, not necessarily used in concrete, are chromates and nitrites, whereas organic inhibitors contain carbon based compounds such as amines.

Corrosion inhibitors are generally classified as either anodic, cathodic or mixed. Anodic inhibitors increase the oxidation rate of the metal, which promotes the formation

of a protective oxide film. This is accomplished by shifting the metal from the active region to the passive region (refer to Fig. 2.3). Cathodic inhibitors reduce the rate of metal dissolution by inhibiting the reduction reaction by forming an insoluble or insulating film over the cathodic sites. Insoluble films block the supply of oxygen, whereas insulating films increase the resistance to charge transfer at the metal/solution interface. The cathodic reaction is prevented or reduced if either type of film is present. Mixed inhibitors function as a combination of both.

Unlike anodic inhibitors, cathodic inhibitors do not accelerate the metal dissolution rate. Anodic inhibitors increase the metal dissolution rate in order to shift the metal into the passive range. The danger with anodic inhibitors is that if the inhibitor concentration is not sufficient, the metal may be left in the active region, thereby actually accelerating the corrosion process rather than inhibiting it.

Corrosion protection of steel reinforcement embedded in concrete can be provided by concrete corrosion inhibitors or by preventing or reducing the rate of chloride ingress to the steel reinforcement. An ideal system would offer both types of corrosion protection.

## CHAPTER 3.0

### CORROSION MONITORING TECHNIQUES

#### 3.1 GENERAL

There are many different ways to monitor the corrosion of reinforcing steel in concrete in the laboratory. Some popular techniques are the half cell, macro-cell, linear polarization and AC impedance methods. The first method can only predict the probability of corrosion activity, whereas the latter two methods can measure the corrosion rate occurring in a system. The macro-cell method can not measure the true corrosion rate.

#### 3.2 HALF CELL MEASUREMENTS

The half cell method measures the open circuit potential between the steel reinforcing bar, called the working electrode, and a reference electrode. This technique is able to detect the *probability* of corrosion activity. ASTM C-876-91 [20] is a standardized test procedure and provides guidelines (Table 3.0) for the interpretation of the potential measurements for a copper-copper sulfate reference electrode. Other commonly used reference electrodes are silver-silver chloride and saturated calomel electrodes. These electrodes are stable and accurate but somewhat fragile. Therefore, they are mostly utilized for laboratory experiments. The copper-copper sulfate is very durable and relatively inexpensive. It is normally used for field testing of existing structures. One disadvantage of the copper-copper sulfate electrode is that it is unstable with respect to

temperature; but, if the user is aware of the temperature variation, it can be accounted for.

The advantages of this technique are relatively fast testing time, non-intrusive method, test simplicity and low cost. The major limitation is that it can only predict if corrosion might be occurring. It cannot determine a corrosion rate. Also, the interpretation ranges are quite large and leave much uncertainty.

**Table 3.0 Interpretations of Half Cell Reading (Copper-Copper Sulfate Reference Electrode).**

Half Cell Readings (Volts)	Corrosion Activity
> -0.20	90% chance of no corrosion
-0.20 to -0.35	uncertain range
< -0.35	90% chance of corrosion

### 3.3 MACRO-CELL MEASUREMENTS

Macro-cell techniques are mainly used in the laboratory for monitoring concrete environments that are susceptible to general/uniform corrosion. Macro-cell is usually considered a time to corrosion method that evaluates corrosion inhibitors, concrete mixes specially designed to increase time to corrosion, or a combination of both. Generally, this method utilizes slab type specimens with two layers of reinforcement. The bottom layer usually contains twice the amount of reinforcement in the top layer. The bottom layer acts as the cell cathode and the top layer acts as the cell anode. The reinforcing layers are electrically connected externally by a 100 ohm external resistor. Some researchers believe it is more appropriate to use a 10 ohm resistor depending on the type of measuring

equipment used [18, 21]. The slabs are subjected to continuous wet/dry cycles; first ponded with a salt solution (two weeks) and then dried at 100°F (two weeks). The voltage drop across the resistor is monitored at specific intervals and macro-cell currents are calculated from Ohm's Law. This current is plotted versus time and is a representation of the corrosion of the system (Figure 3.0). This method is very basic, easily executed and inexpensive but does not allow a reasonable corrosion rate to be obtained. ASTM G-109-92 has standardized the macro-cell method [22]. This method is adequate for time to corrosion studies, but the overall test duration required to obtain adequate results is quite long in most cases. Also, the macro-cell currents measured are not the true corrosion current of the system since localized corrosion currents are not accounted for.

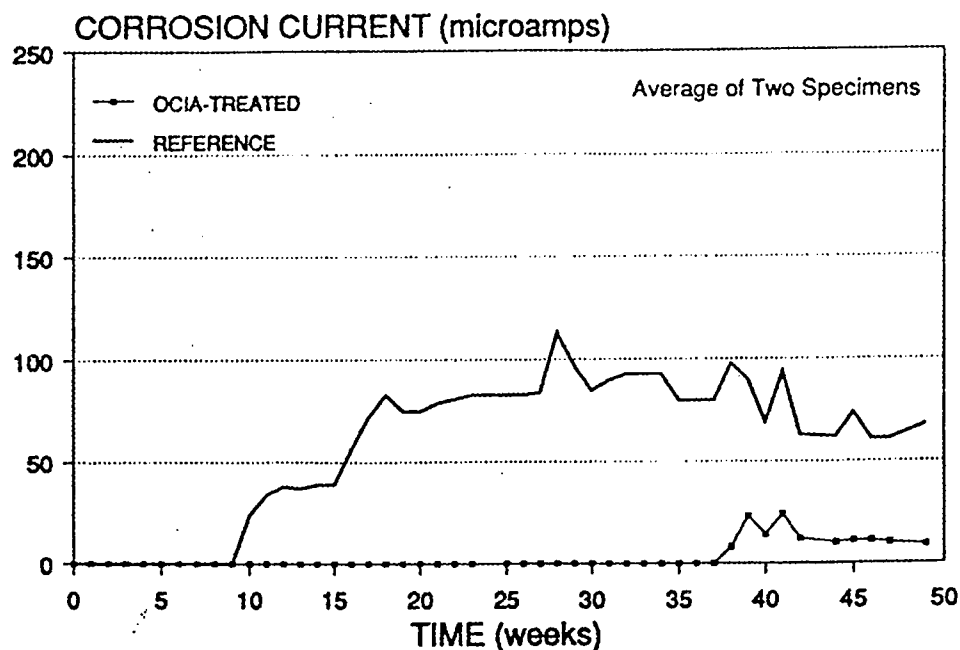


Figure 3.0 Typical Macro-Cell Corrosion Verses Time [23].

### 3.4 LINEAR POLARIZATION

#### 3.4.1 Polarization Technique

Linear polarization can determine the corrosion rate of a system. In this method, a current is applied to the system to shift the "at rest" open circuit potential in increments, called over-potentials, with a maximum total shift of  $\pm 20\text{mV}$ . The over-potential and applied current are recorded and plotted. The end result is a polarization curve ( Figure 3.1). Since the open circuit potential is only shifted  $\pm 20\text{mV}$ (max.), the polarization curve obeys a quasi-linear relationship [24]. The slope in the form of  $\Delta E / \Delta i_{\text{app}}$ , where the current is zero, is equal to the polarization resistance ( $R_p$ ). Hence, the method is called "Linear" polarization. A corrosion rate can then be related by the Stern-Geary equation:

$$R_p = \frac{\Delta E}{\Delta i_{\text{app}}} \quad B = \frac{\beta_a \beta_c}{2.3 (\beta_a + \beta_c)} \quad I_{\text{corr}} = \frac{B}{R_p}$$

where  $\beta_a$  and  $\beta_c$  are the anodic and cathodic Tafel slopes, respectively, B is the Tafel constant, and  $I_{\text{corr}}$  is the corrosion current. The corrosion current density,  $i_{\text{corr}}$ , is obtained by dividing  $I_{\text{corr}}$  (Amps) by the surface area ( $\text{cm}^2$ ) of steel polarized. A corrosion rate (mpy) can be calculated by multiplying  $i_{\text{corr}}$  by a constant, C, ( 457164 for steel).

The Tafel slopes are obtained from the linear segments of the anodic and cathodic polarization curves. These Tafel polarization curves require large over-potentials (up to 250mV or more) to be applied to the system. These large over-potentials can damage the



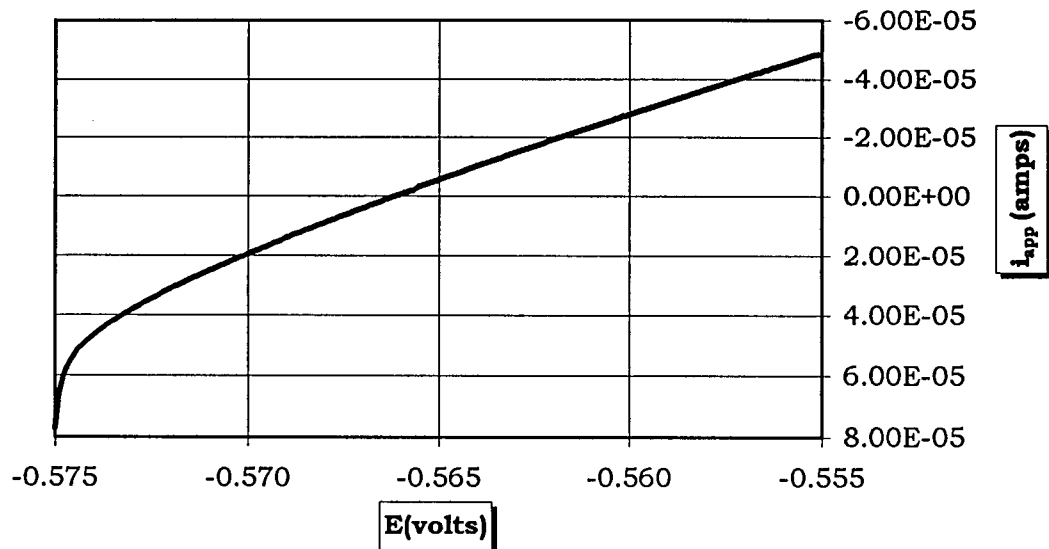


**Figure 3.1 Linear Polarization Curve :Over-Potential Shift equals  $\pm 10\text{mV}$  (Note: Plot Shown is in the Form  $i_{APP}$  Vs E).**

system and render it unusable. Also, depending on the system environment it is sometimes difficult to obtain these values. To avoid these problems, many researchers assume values for the Tafel slopes based on related published work. Anodic and cathodic Tafel slopes for reinforcement corrosion in concrete environments are usually assumed to be  $0.120\text{V}$ , which translates to a Tafel constant,  $B$ , of  $26\text{mV}$ . Some researchers use a  $B$  value of  $26\text{mV}$  for actively corroding systems and  $52\text{mV}$  for passive systems [6].

It is important to adjust the linear polarization curve for the ohmic resistance of the solution for the system. The solution resistance,  $R_s$ , for the steel reinforcement in the concrete environment is the resistance of the concrete that is subjected to polarization currents. The  $R_s$  for concrete is usually a large value and when combined with the

polarization currents (used to produce the over-potential) produces an IR drop. The IR drop becomes significant and should be accounted for when the  $R_s$  and/or currents become large. If the ohmic resistance is not corrected for, an overestimation of the polarization resistance will occur and the corrosion rate will be underestimated.

### 3.4.2 IR Drop Correction Techniques

There are various methods to correct for the IR drop such as positive feedback, current interrupt and impedance measurements.

Positive feedback is a method that multiplies the applied current by a fraction of the uncompensated resistance,  $R_U$ . That product is then added to the electrode potential via a current-voltage converter and then inputted back into the potentiostat [25]. The fraction multiplication of  $R_U$  continues until the compensated resistance,  $R_C$ , is equal to  $R_U$ . A disadvantage of this technique is that it can cause the potentiostat to become unstable at 100% compensation. Therefore, the total compensation is usually limited to 75% to 90% [26]. Also, this technique assumes that  $R_U$  is constant. If  $R_U$  does vary, the applied correction to the polarization resistance data would be incorrect. An advantage of this technique is that the correction is continuous and can be used during fast scan rates (100mv/s or greater). The IR drop can be mathematically corrected by using positive feedback if the  $R_s$ , which is primarily  $R_U$  when neglecting the electrolytic and connection lead resistances, can be assumed constant during each polarization. If this is assumed, the  $R_s$  is only measured once per test day. The polarization potentials are corrected by subtracting the product of the current and  $R_s$  (i.e., IR drop) at each step.

Current interrupt is a technique that abruptly interrupts the cell current. During this time of zero current, the IR drop instantly disappears but the cell potential discharges at the rate determined by the double layer capacitance [27]. If the decay time is long enough for the potentiostat to make a voltage measurement, a true cell potential can be obtained. An advantage of this technique is that  $R_U$  can be highly compensated. A disadvantage is that this method is not suitable for rapid scan rates because the correction occurs at finite intervals. The scan rate should be limited to 100mV/s and lower [26]. Also, this method can cause the potentiostat to become unstable in certain instances, and, if the correction is not updated often, the IR correction could become invalid.

AC impedance can also determine the  $R_S$  of a cell. A small sinusoidal voltage is applied at a relatively high frequency (10 kHz or greater, depending on cell environment). The double layer capacitance shorts out at high frequencies and the remaining impedance is equal to the  $R_S$  of the cell. The frequency magnitude must be chosen to ensure that the actual  $R_S$  is determined. If a large enough frequency is not used, the  $R_S$  will not be fully measured. The advantage of this method is that the  $R_S$  can be accurately determined even if the DC current is zero[27]. This is not a continuous method. Therefore, for this method to be used in conjunction with linear polarization, the  $R_S$  must be assumed constant and the IR drop mathematically corrected for.

### 3.5 AC IMPEDANCE

AC impedance, also called Electrochemical Impedance Spectroscopy, can also determine the corrosion rate of a system. This method shifts the open circuit potential of

the system by applying a small sinusoidal over-potential,  $\Delta E_\omega$ , while monitoring the current,  $\Delta I_\omega$ , required to produce the shift, over a wide range of frequencies,  $\omega$ . The electrochemical impedance,  $Z$ , is the AC equivalent of the resistance of a DC circuit and is defined as the ratio of  $\Delta E_\omega / \Delta I_\omega$ . Linear polarization is measured in direct current and AC impedance is measured in alternating current. The magnitude of the over-potential is usually less than  $\pm 20$  mV, therefore this method is nondestructive to the system.

During a typical AC impedance test, the frequency is scanned from a high value (20kHz or greater) to a low value (1 mHz or lower). The impedance and phase angle,  $\phi$ , are measured and recorded at each frequency step. The data is then plotted with either a Bode plot or Nyquist plot. The Bode plot actually consists of two graphs which are  $\log |Z|$  versus  $\log \omega$ , and phase angle,  $\phi$ , versus  $\log \omega$ . The Nyquist plot is a graph where the real component of the impedance,  $Z'$ , is plotted on the horizontal axis and the imaginary part of the impedance,  $Z''$ , is plotted on the vertical axis.

Models consisting of electronic circuits are commonly used to represent corroding systems. Figure 3.2 shows a model of a simple corrosion system. In this figure  $R_s$  is the solution resistance,  $R_p$  is the polarization resistance, and  $C_{dl}$  is called the double layer capacitance, which is equal to the capacitance of the corroding interface.

A theoretical Bode plot for the above model is shown in Figure 3.3. Here the solution resistance,  $R_s$ , is taken as the magnitude of the impedance,  $Z$ , at the higher frequencies. This is valid because the double layer capacitance shorts out the polarization resistance at high frequencies. The double layer acts as an open circuit at low frequencies.

Therefore, the magnitude of the impedance at low frequencies equals the total resistance,  $R_T$ . Hence, the polarization resistance,  $R_p$ , is the difference between  $R_T$  and  $R_s$ .

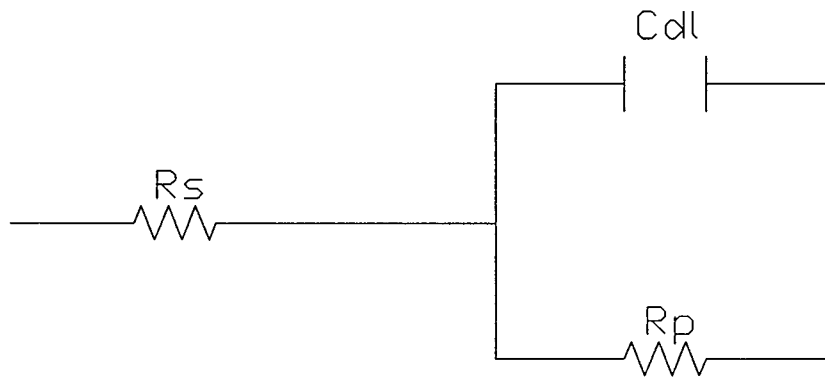


Figure 3.2 Electrical Circuit Model for a Simple Corrosion System.

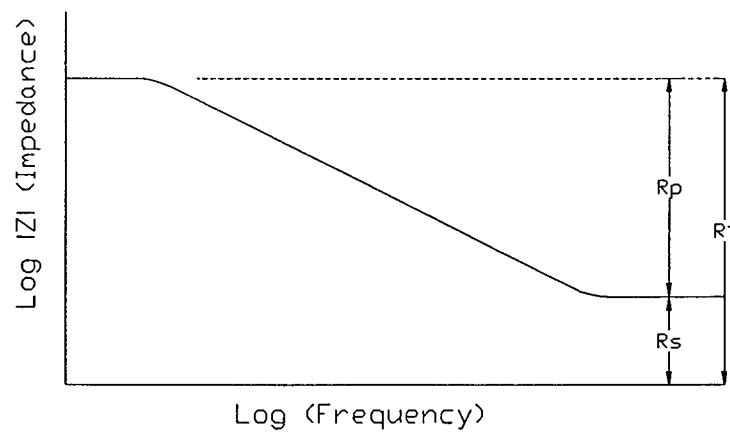


Figure 3.3 Bode Plot for Electrical Circuit Shown in Figure 3.2.

Figure 3.4 shows a theoretical Nyquist plot of the simple corrosion model. The plot consists of a semicircle that crosses the  $Z'$  axis in two locations. The intersection closest to the  $Z''$  axis represents the solution resistance and the diameter of the circle is equal to the polarization resistance.



Figure 3.4 Nyquist Plot for Electrical Circuit Shown in Figure 3.2.

Real corrosion systems are usually more complex than the model shown in Figure 3.2. and therefore the model must be modified. For instance, if the corrosion process is diffusion controlled, an additional electrical element, called the Warburg impedance, must be added in series with the polarization resistance.

Advantages of using AC impedance are the ability to measure very low corrosion rates, IR compensation is not required, and mechanistic information about the corrosion

process can usually be obtained. Some disadvantages are the high equipment costs and the relatively long test duration required to obtain low frequency data. If the system is not scanned to low enough frequencies, the results could be highly inaccurate especially if the Bode plots are used. Also, curve fitting or other methods might be required to interpolate and extrapolate limited data when Nyquist plots are used.

## **CHAPTER 4.0**

### **LITERATURE REVIEW**

#### **4.1 GENERAL**

Much research has been conducted over the last 20 years in an attempt to understand and eliminate the corrosion of steel reinforcement embedded in concrete. As discussed in Chapter 2.0, there are many factors that affect corrosion of reinforcing steel. Although a great deal of research has been performed, the corrosion problem has still not been eliminated.

#### **4.2 STUDIES OF VARYING CONCRETE AND REINFORCEMENT PROPERTIES**

Clear et. al. [19] used half cell potentials, visual surveys, and chloride analyses to monitor 124 - 5ft. by 4 ft. by 6 in. reinforced concrete slabs. The slabs were fabricated using various mix designs, construction methods, and special treatments. The slab reinforcement consisted of No. 4 steel reinforcing bars in a grid pattern. The slabs were subjected to daily ponding with a 3% sodium chloride solution for about six years. Results indicated that w/c ratio, depth of cover, and degree of consolidation have a significant effect on time to corrosion.

Lorentz et. al., from the University of Minnesota, [9] evaluated the impact of w/c ratio, silica fume content, entrained air content, type of reinforcing steel and coating, and cracked verses uncracked concrete on corrosion of steel reinforcement embedded in



concrete. A total of 96 concrete prisms (12.5 inches by 12.5 inches by 7 inches) and cracked slabs (12 inches by 48 inches by 7 inches) were cast. Some had chloride mixed into the top layer of the concrete (seeded) to create an aggressive corrosive environment. The specimens were subjected to cyclic wet (15% NaCl) and dry (air) periods for 35 to 40 months. Both the prisms and slabs had two layers of reinforcing, consisting of two rebars in the upper mat (1 inch cover) and four rebars in the bottom layer. The two layers were electrically connected to form a galvanic corrosion cell. The researchers used macro-cell current measurements, instant off potential measurements, concrete resistance measurements, and half cell potentials measurements to monitor the specimens over time. Their results indicated that 85% of the specimens did form the traditional macro-cell, where the upper mat functions as the anode and the bottom mat acts as the cathode. The reverse occurred in 15% of the specimens, and corrosion products were found on the bottom mat when visually examined. They attributed this to the formation of a differential concentration cell of either oxygen, chlorides, moisture or possibly a combination of all three. The addition of condensed silica fume reduced the corrosion macro-cell current and significantly increased the concrete resistance. Epoxy coated rebars with intentionally damaged coating still out performed plain rebars and had only light corrosion at the damaged areas. No signs of coating delamination or corrosion migration under the coating (crevice corrosion) was observed. The University of Minnesota research also found that there was no apparent relationship between air entrainment and corrosion resistant properties of concrete. Other researchers [18, 14] have performed similar experiments that assess the impact of varying concrete properties and/or bar types on rebar corrosion.

The performance of epoxy rebars was evaluated by Clear et. al. [3] after concerns arose after the premature and extensive corrosion of epoxy coated rebars in bridge structures in Florida. The researchers used AC impedance to assess coating quality (e.g., holidays) as well as the coating performance in preventing/reducing corrosion. Slab specimens similar to ASTM G-109 specimens were monitored by measuring the macro-cell current over time. AC impedance measurements were also periodically taken. The results indicated there were numerous problems with epoxy coated rebar technology as practiced at that time. The researchers made suggestions they felt would enhance the performance of epoxy coated rebars. The potentially poor performance of damaged epoxy coated rebars has been questioned by some researchers [21, 9]. Some studies even evaluated the corrosion resistance of "exotic" rebars [28].

#### **4.3 EVALUATION OF CORROSION INHIBITORS**

Many corrosion inhibitors have been investigated in the past [4, 5, 6]. Some showed promise and others caused problems with certain concrete properties. Inhibitors were generally evaluated using either simulated pore solution testing [29, 30] or using actual concrete or mortar specimens [6, 17, 23, 30, 31, 32, 33, 34] or using a combination of both.

Simulated pore solution testing is a screening process that evaluates the performance of chemicals for inhibiting steel rebar corrosion in a high alkaline environment, usually simulated by saturated calcium hydroxide. Linear polarization or AC impedance techniques are commonly used for these tests.

Slab and lollipop specimens are commonly used to investigate potential corrosion inhibitors in concrete and are monitored by either macro-cell, linear polarization, or AC impedance techniques. Berke et. al. [31] compared macro-cell and linear polarization monitoring techniques on evaluating the inhibiting effects of a calcium nitrite on galvanized steel and aluminum in concrete. He used corrosion specimens similar to ASTM G-109 slabs, exposed continuously to wet/dry cycling consisting of two weeks of ponding with 3% NaCl and two weeks of air drying at room temperature. Results showed that linear polarization was preferred since this method detected both localized corrosion and macro-cell corrosion. He concluded that both methods were adequate, but if a true corrosion rate is desired, one should use linear polarization.

Trepanier [6], from Queen's University, evaluated four commercial concrete corrosion inhibitors utilizing 2-inch diameter lollipop specimens made of mortar and ASTM G-109 slab specimens made of concrete. The lollipops were constantly submerged, to about mid height, in 3.5% NaCl solution. The slabs followed ASTM G-109 procedures. Half cell potentials, linear polarization, and AC impedance techniques were used to monitor the lollipop specimens, and macro-cell currents were measured for the slabs. Results showed that all four inhibitors delayed the initiation of corrosion by varying degrees, but none completely prevented corrosion from occurring. The inhibitors performance increased as the w/c ratio decreased. Also, AC impedance measurements correlated well with linear polarization data. After 343 days of cyclic ponding, only the control ASTM G-109 slabs were actively corroding (corrosion initiated at 271 days). This demonstrated the significant time duration required to obtain results from the ASTM G-

109 test. It is felt that evaluation of corrosion inhibitors, both short term testing and long term testing, should be conducted using concrete specimens, representative of real world conditions, even though such tests require more time and effort [35].

#### **4.4 MONITORING OF EXISTING STRUCTURES**

In the past, the detection of corrosion in existing bridges has usually been limited to visual inspection and to half cell potential mapping. SHRP-S-323 Volume I [36] provided a critical evaluation of exiting methods for assessing the condition of actual concrete bridge components. The advantages and disadvantages of using half cell potential mapping to assess corrosion activity were discussed. The report indicated that the only field-ready method available at that time (1993) was the half cell technique, which can only give the probability that corrosion is or is not occurring. A corrosion rate can not be obtained from this method.

SHRP-S-323 Volume II [37] described the evaluation, in the laboratory and in the field, of three commercially developed corrosion detection devices that measure corrosion rates. Two of the devices were based on the linear polarization technique and the third used the AC impedance technique that superimposed two current pulses, a high frequency and a low frequency. Some of the devices used guard electrodes for current confinement. This created a more defined polarization area, and therefore a more accurate instantaneous corrosion rate was obtained. Results indicated that the three devices gave comparable results in the laboratory for small mortar specimens and large slabs with actively corroding steel. However, these instruments were unable to confine signal distribution for large slabs

with passive steel. Based on this research , SHRP published "Standard Test Method for Determining Instantaneous Corrosion Rate of Uncoated Steel in Reinforced Concrete" [38]. Some of these devices have been used by other researchers to monitor concrete specimens in the laboratory [17].

## CHAPTER 5.0

### CORROSION EXPERIMENTAL PROGRAM

#### 5.1 GENERAL

The experimental program was divided into four sections consisting of corrosion testing, absorption testing, freeze-thaw testing and strength testing. The corrosion testing program used both 2-inch and 3-inch diameter lollipop specimens and slab specimens. These tests evaluated and compared several commercial and new concrete corrosion inhibitors and also evaluated different specimen geometries. The absorption testing helped to evaluate the permeability characteristics of the concrete modified with inhibitors, which helped to classify the inhibitors. The freeze-thaw testing and compression strength testing determined the durability and strength characteristics of the concrete mixes. Information on the freeze-thaw, absorption, and strength testing programs are located in Appendices A, B & C.

The prototype inhibitors evaluated were called DAS and DSS. The DAS was evaluated at concentrations of 2%, 1%, and 1/2%; the DSS at 2% and 1% concentrations. Concentrations were based on batch weight of cement.

Two commercially available corrosion inhibitors, referred to as Inhibitor A and Inhibitor B, which are commonly used in reinforced concrete, were also evaluated. Inhibitor A was a calcium nitrite based chemical and was recommended to be used in concentrations of 2.0, 4.0 and 6.0 gallons per cubic yard depending on the degree of protection required. A 4.0 gallons per cubic yard dose was chosen for this study.

Inhibitor B was an organic based chemical consisting of esters and amines and is described to act as a dual protection inhibitor by also reducing the ingress of moisture and chlorides. One dosage of inhibitor B, 1.0 gallon per cubic yard, was recommended by the manufacturer for all corrosive environments.

Comparisons were made between the individual inhibitors as well as with a good quality air-entrained control concrete.

## 5.2 MATERIALS

### 5.2.1 Mix Design

The basic control concrete mix was based on Connecticut Department of Transportation (ConnDot) Form 814 [39], the guidelines in the Portland Cement Association's (PCA) "Design and Control of Concrete Mixtures"[40] and the ConnDot Bridge Design Manual [41]. This mix was developed on a previous research project [42]. It conformed to ConnDot's Class F concrete for bridges with requirements of:

Minimum 28 day compressive strength ( $f'_c$ ) = 4000 psi

Maximum water/cement ratio (w/c) = 0.44

Minimum cement content = 658 pounds per cubic yard

Due to the relatively small sizes of specimen types utilized on this project, the coarse aggregate was limited to a 3/8 inch crushed basaltic trap rock instead of the 3/4 inch and 1/2 inch aggregate blend normally used for Class F concrete. The 3/8 inch trap rock, obtained from a local quarry and delivered in 55 gallon drums, satisfied ConnDot gradation specifications. As delivered the stone was moderately dirty (i.e. high quantity of

fines), which would have effected reproducibility of the mixes. To achieve better control, all stone was washed over a large No.30 pan sieve and then dried in an oven at 200°F for one day.

The fine aggregate was a bank sand obtained from a local gravel plant and was delivered in one bulk load. It conformed to the ConnDot requirements for graduation. The sand was also oven dried.

The coarse and fine aggregates were obtained from the same sources as a recently completed University of Connecticut research project. Therefore, the absorption and specific gravity values for the coarse and fine aggregates were assumed unchanged and were used for this project (Table 5.0) [42].

**Table 5.0 Aggregate Properties [42].**

Properties	Coarse Aggregate	Fine Aggregate
Bulk Specific Gravity (dry)	2.88	2.73
Bulk Specific Gravity (saturated-surface-dry)	2.92	2.75
Absorption	1.29%	0.85%
Fineness Modulus	N/A	2.73

The maximum water/cement ratio specified by ConnDot was assumed to be based on saturated-surface-dry aggregates. Since the coarse and fine aggregates were oven dried, additional batch water was added to the mix to account for aggregate absorption. Batch water was also adjusted for water content of the corrosion inhibitors except for Inhibitor B, where no adjustment was necessary based on the manufacture's literature.



As stated previously, the main objective of this project was to evaluate two chemicals for their corrosion inhibiting effects on steel reinforcement in concrete and to compare them with two existing commercial inhibitors. For this reason, it was decided that the cement content would be kept constant for all mixes. To eliminate any affects that might occur with other admixtures, such as superplasticizers, retarders or pozzolans, only air-entraining admixtures, as specified by the inhibitor manufacturers, were added to the mixes if required.

The maximum allowable water/cement, w/c, ratio was set at 0.44 with a slump of 4 inches. If the chemical properties of a certain inhibitor allowed a reduction in the w/c ratio while achieving the desired consistency, then that was accepted as an advantage of that particular inhibitor. In other words the w/c ratio was not held constant. To achieve constant w/c ratios, the amount of cement in each mix would have to be varied. Cement content can have an effect on the performance of some inhibitors, so it was held constant instead of the w/c ratio. W/c ratios for the mixes generally varied between 0.41 and 0.38. There were a few exceptions where the w/c ratio was 0.45, but these mixes were used because of the small divergence from the maximum.

The air content for concrete with a maximum aggregate size of 3/8 inch and exposed to "severe" conditions is recommended to be 7.5% with a range of -1% to +2% [40]. This range was generally adhered to for air-entrained mixes. Air entraining admixtures used for this project complied with ASTM C260-94 requirements [43]. Mixes with Inhibitor A or B used the particular brand and type of air entraining agent as specified by the inhibitor supplier.

The target slump of each mix was set to be about 4 inches. However, slumps varied to allow proper consolidation based on individual mix characteristics. Certain inhibitors made the mix more cohesive and therefore required a higher slump to achieve proper consolidation. The slumps varied from 2.75 to 4.75 inches.

Numerous trial mixes were performed with batch sizes of 1.0 and 1.25 cu. ft. Due to the large scope of this project as well as the miscellaneous delays and problems encountered, the lollipop and slab corrosion specimens were cast in different batches on different days. Mix proportions for the corrosion specimens are shown in Table 5.1.

Two balances were utilized in the weighing of all batch water and the DAS and DSS inhibitors. Both balances were calibrated at the start of the project. Unfortunately, one of the balances became uncalibrated, and this was not discovered until after most of the specimens had been cast. It is impossible to speculate exactly when the malfunction occurred or for how long the balance was used after the problem occurred. That balance underestimated the weight by about 7.5%. This would possibly increase the w/c ratios of some mixes and would increase the amount of the DAS and DSS actually used, which were added by weight. The mix water, though, was generally weighed out on the functioning balance. The quantity of Inhibitor A, Inhibitor B, or air entraining agents were not effected because these items were added to the mix based on volume, not weight. Cement and aggregates were weighed on a separate, larger balance.

### 5.2.2 Mixing Procedure

The mixing procedure was kept as consistent as possible for all mixes. The sequence of adding the inhibitor and air entraining agent (if required) into the mix was based on the manufacturer's recommendations. A drum mixer with a maximum batch capacity of 2.0 cu. ft., was utilized. For practical reasons the maximum batch size was limited to 1.5 cu. ft. Corrosion specimens were made with 1.25 cu. ft. batches except for the controls, which used two 1.0 cu. ft. batches.

**Table 5.1 Corrosion Mix Proportions.**

Mix Type <sup>1</sup>	W/C Ratio	Air-Entrain Admixture	Inhibitor Concentration <sup>2</sup>	Air Content	Slump (in)
<b>Slab Specimens</b>					
Control -1	0.38	Yes	None	7.5%	3.00
Control - 2	0.38	Yes	None	8.0%	3.75
Inhibitor A	0.40	Yes	4.0 gal/c.y.	7.0 %	4.50
Inhibitor B	0.45	Yes	1.0 gal/c.y.	8.5 %	2.75
2% DAS	0.41	No	2%	6.0 %	4.00
1% DAS	0.39	No	1%	7.0 %	3.00
1/2% DAS	0.39	No	1/2%	7.0 %	3.00
2% DSS	0.40	No	2%	8.0%	4.50
1% DSS	0.40	No	1%	8.0%	3.00
<b>Lollipop Specimens</b>					
Control - 2	0.38	Yes	None	8.0%	3.75
Inhibitor A	0.38	Yes	4.0 gal/c.y.	8.0 %	4.00
Inhibitor B	0.39	Yes	1.0 gal/c.y.	9.0 %	4.75
2% DAS	0.41	No	2%	6.5 %	4.25
1% DAS	0.40	No	1%	8.0 %	3.75
1/2% DAS	0.40	No	1/2%	8.5 %	4.25
2% DSS	0.41	No	2%	7.0%	4.25
1% DSS	0.40	No	1%	8.0%	4.75

<sup>1</sup> All mixes contained Type I/II cement @ 27.85 lb., coarse agg. (oven-dried) @ 48.59 lb., and fine agg. (oven-dried) @ 54.26 lb. - Based on 1.0 cu. ft. mix.

<sup>2</sup> Concentrations for Inhibitors A and B were as suggested by the supplier. Concentrations for the DAS and DSS were based on weight of cement.

The general mixing procedure was as follows:

1. Wet the inside of the drum. Drain all excess water from drum.
2. Place all coarse and fine aggregate in mixer and mix for 1.5 minutes.
3. With mixer running, add approximately 85% of batch water to mixer and mix for 2.0 minutes.
4. Add air entraining admixture, or DAS, or DSS (as required) and mix for 2.0 minutes.
5. Add all cement (in 1.0 minute) and mix for 1.0 minute.
6. Add Inhibitor A or B (as required) and mix for 1.0 minute.
7. Stop mixer and scrape drum ( in approximately 1.0 minute). Restart mixer.
8. Add rest of batch water as needed. Mix for 2.0 minutes
9. Stop mixer and rest for 2.0 minutes.
10. Restart mixer and mix for 2.0 minutes.
11. Pour mixture into pre-wetted floor pan.
12. Perform a slump test and an air content test.
13. Cast specimens.

The concrete slump was determined in accordance with ASTM C143-90a [44].

The air content was measured by the pressure method, ASTM C231-91b [45], except the concrete was placed in the measuring bowl in two layers instead of three and an aggregate correction factor was not applied.

The air-entrained control concrete followed the general mixing procedure. Due to the large number of control corrosion specimens, 2.0 cu. ft. of concrete was required. This was accomplished by using two 1.0-cu.-ft. batches that were deposited into a large steel pan and thoroughly hand blended to form a uniform mix. To retard the set and allow for sufficient time to cast specimens, refrigerated water (approximately 46°F) was utilized for both batches.

### **5.2.3 Cement**

Type I/II cement, all from the same manufacturer, was utilized for this project. The chemical analysis of the cement (from supplier) is shown in Table 5.2.

### **5.2.4 Reinforcement Bars**

Reinforcement for all specimens was No. 4 Grade 60 rebar. All bars were from the same production lot to ensure similar material properties. The mechanical and chemical analysis for the reinforcement (from supplier) are in Table 5.3.

Twenty foot bars were cut into 14.75-inch lengths, brushed with a wire wheel mounted on a bench grinder, and stored in an oven at 100°F. The day before casting specimens, the bars to be used in that casting were pickled in a 2.5N sulfuric acid solution for ten minutes, rinsed with tap water, and dried. The bars were then taped at specific locations, depending on specimen type, with electroplaters tape (Fig. 5.0, 5.1 and 5.3) as recommended by ASTM G109-92. The bars were then placed back into the oven. Vinyl

examination gloves were worn during the handling of the pickled bars to prevent contamination.

**Table 5.2 Chemical Analysis of Type I/II Cement.**

SiO <sub>2</sub>	21.0%
Al <sub>2</sub> O <sub>3</sub>	4.7%
Fe <sub>2</sub> O <sub>3</sub>	3.3%
CaO	63.0%
MgO	3.2%
SO <sub>3</sub>	3.1%
Na <sub>2</sub> O Equiv.	0.58%
Ignition Loss	0.90%
Insoluble Residue	0.30%

**Potential Compounds**

C <sub>3</sub> S	52%
C <sub>3</sub> A	7%

**Table 5.3 Mechanical and Chemical Analysis of No. 4 Grade 60 Reinforcement.**

**Mechanical Properties**

Yield Strength (psi)	63000
Tensile Strength (psi)	98500
% Elongation	10.0

**Chemical Analysis**

C	0.45%
Mn	0.84%
P	0.072%
S	0.033%

### **5.2.5 Deicing Salt**

Deicing salt, which was almost entirely sodium chloride with a very small amount of calcium chloride, was provided for this project by ConnDot. It was crushed to aid dissolving, mixed with hot water for a 15% concentration, and stirred periodically for one hour. The solution stood for one day to allow any impurities to settle out and was then filtered through a No. 200 sieve before being placed in multiple five gallon plastic storage containers. Salt solution concentration was 15%.

## **5.3 CORROSION SPECIMEN DESIGN AND TEST ENVIRONMENT**

### **5.3.1 Lollipop Specimens**

The specific geometry and size of the lollipop specimens (Fig. 5.0 and 5.1) were chosen for several reasons. First, the cylindrical shape allows for a more uniform polarization of the specimen. Second, these specimens are easily handled, occupy less space and can be dried efficiently in an oven.

Cylindrical lollipop specimens are usually used in tests to simulate marine environments. Lollipops typically are continuously soaked to mid-level height in a salt solution. This wet/dry interface simulates the spray zone that is created by wave and tidal actions that occur at bridge piers. The chloride ions from the salt water are wicked into the concrete from capillary action. The spray zone creates a prime environment for corrosion due to the abundance of chlorides, oxygen, and moisture. Corrosion below the water line can occur but is usually minor in comparison since it is diffusion controlled due to the limited quantity of dissolved oxygen in the salt water.

This research program focused more on corrosion in bridge decks rather than in bridge piers. Therefore, the typical ponding procedure for the lollipop specimens was modified. To simulate the effect of deicer salts on bridge decks, all specimens were placed in wet/dry cycles to simulate more precisely the actual environment of bridge decks. The specific ponding and drying procedure for the lollipop specimens is detailed in Section 5.5.

Both 2-inch diameter and 3-inch diameter lollipop specimens were used to allow comparisons between the two sizes. In past studies, 2-inch diameter lollipops have usually been limited to only mortars [6]. To rule out specimen quality concerns, preliminary castings of the 2-inch diameter lollipops (using 3/8 inch aggregate) were made and examined. The results indicated homogeneous concrete surrounding the reinforcing bar.

The length of both the 2-inch diameter and 3-inch diameter lollipop specimens was 6 inches and the clear cover was 3/4 inch and 1-1/4 inch, respectively. Both specimens had the same exposed bar area (Fig. 5.0 and 5.1). Three 2-inch diameter and three 3-inch diameter lollipop specimens were cast for each non-control mix and six specimens of each diameter were cast for the control mix. This allowed three control specimens of each diameter to be cut opened and physically examined periodically throughout the duration of the project.

### **5.3.2 "Cracked" Lollipop Specimens**

To simulate an existing cracked concrete environment, some additional 3-inch diameter lollipop specimens were saw cut longitudinally on one side (Fig. 5.2). The additional lollipop specimens were generally cast from the first set of corrosion mixes that



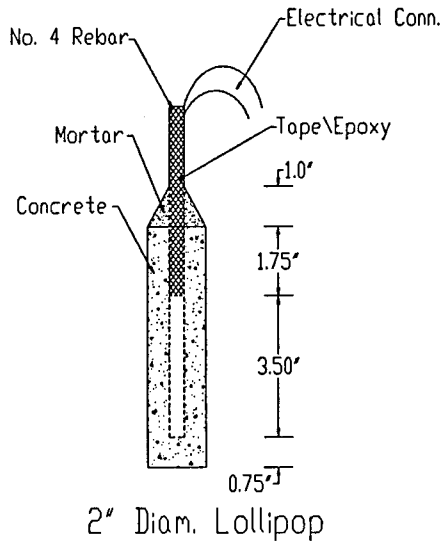


Figure 5.0 2-Inch Diameter Lollipop.

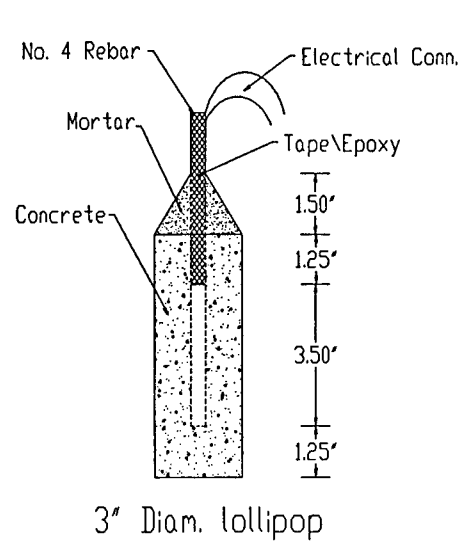


Figure 5.1 3-Inch Diameter Lollipop.

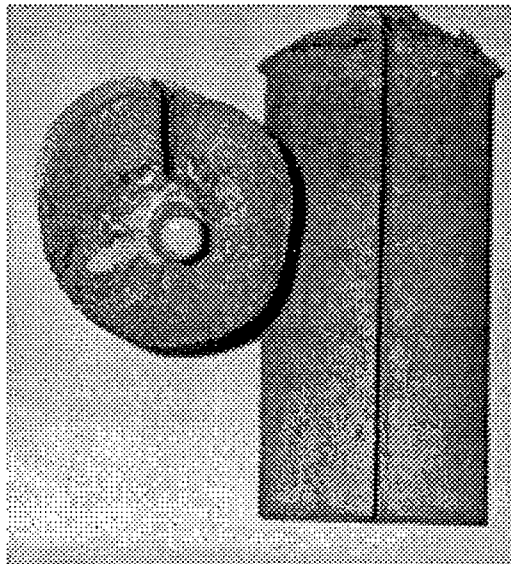


Figure 5.2 "Cracked" 3-Inch Diameter Lollipop.

were not used for the corrosion rate monitoring program due to minor surface irregularities. Since the "crack" created a direct path for the salt water to migrate to the reinforcing bar, the minor surface irregularities were insignificant. These specimens were visually inspected only and no electrochemical measurements were taken (i.e., linear polarization).

### 5.3.3 Slab Specimens

This slab specimen simulates an actual bridge deck very well. As discussed in Section 3.3, this type of specimen is not only subjected to localized corrosion but also macro-cell corrosion, which can occur in bridge decks. The disadvantages of this specimen are:

1. Slabs are large and awkward to handle,
2. Localized polarization effects occur due to specimen geometry, and
3. Slabs require a large storage area and are difficult to enclose for drying.

The slab design was based on ASTM G-109-92 [22]. The overall dimensions were 11-inches long by 4.5-inches wide by 6-inches high. Each slab contained one No. 4 Grade 60 rebar in the top layer and two No. 4 Grade 60 rebars in the bottom layer (Fig. 5.3). A 0.75-inch cover was used for the top reinforcing bar and a 1.0-inch cover for the lower bars. Since macro-cell measurements were not taken, a resistor was not placed in the electrical connection of the upper and lower layers of reinforcement as specified by ASTM G-109-92. Instead, a "banana plug" was inserted into the electrical connection. This

allowed the upper mat to be isolated during a corrosion test and allowed both mats to be continuously connected at all other times.

The number of slab specimens cast for each mix was the same as for the lollipops, three each for non-control mixes and six for the control mix.

The testing environment for the slab specimens also used wet/dry cycles, but the slabs were air dried at room temperature instead of oven dried. Also, one-inch-square wood strips were placed under the slabs to provide adequate oxygen flow. The specific ponding and drying procedure for the slab specimens is detailed in Section 5.5.

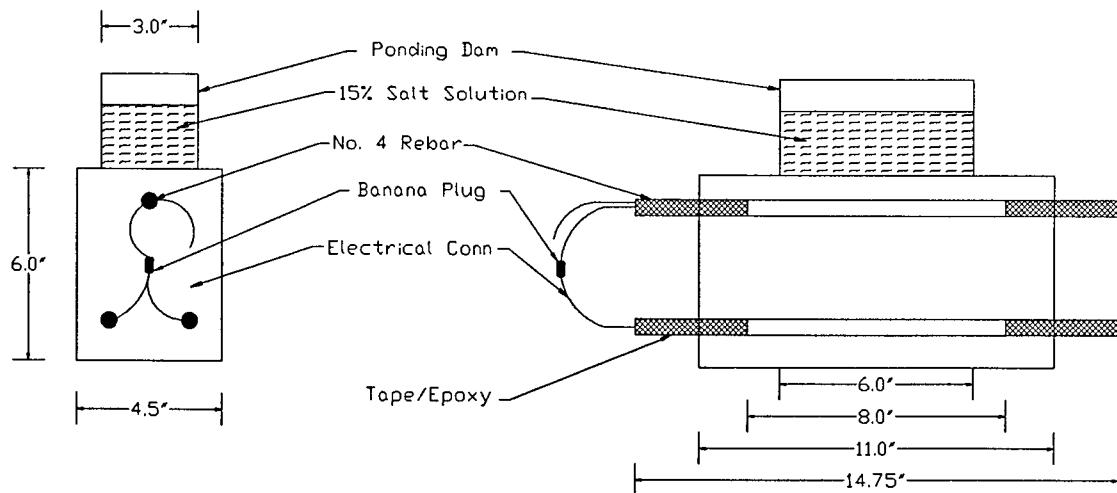


Figure 5.3 Slab Specimen.

## 5.4 SPECIMEN FABRICATION AND CURING

### 5.4.1 General

All specimens were consolidated with the aid of a 20 inch by 20 inch vibration table with the table's output range set at the maximum. Rodding and tapping of the molds were also utilized with the lollipop specimens.

### 5.4.2 Lollipop Specimens: Standard and "Cracked"

The lollipop specimens were cast in standard 3 inch x 6 inch and modified 2 inch x 6 inch plastic cylinder molds, coated with a thin film of mineral oil, before rebar placement, to act as a form release agent. All excess oil was allowed to drain out. The modified 2 inch x 6 inch plastic cylinder molds were constructed by cutting off the top two inches of a standard 2 inch x 4 inch mold and attaching that piece to the top of a standard 2 inch x 4 inch plastic cylinder mold using duct tape. The plastic cylinder molds fit tightly through holes cut into the upper and lower plywood decks of the 24 inch x 24 inch special casting fixture (Fig. 5.4). A maximum of six specimens of each size could be made on each casting fixture.

The crucial step for casting the lollipop specimens was to center the rebar. This was accomplished easily with the special casting fixtures. Three casting fixtures permitted casting up to three mixes per day. The rebar was centered in the cylinder mold via a two-piece nylon template. Two nylon templates were fabricated, one for the 2-inch diameter lollipops and another for the 3-inch diameter lollipops. The nylon templates were a 4-inch-long cylinder, 2 inches or 3 inches in diameter, with a longitudinal through-hole for the

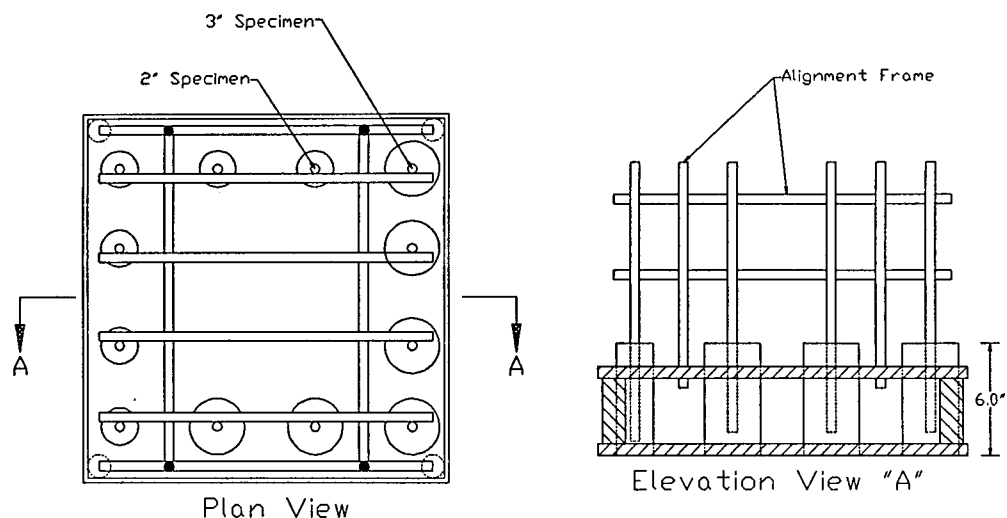


**Figure 5.4 Lollipop Casting Fixture.**

rebar, and sawed longitudinally into two pieces. A thin milled "collar" held the template at the top of the molds. After centering the rebar at the proper height, the upper portion of the rebar was clamped to the steel alignment frame of the casting fixture with dial gage clamps to prevent movement during casting. The four horizontal arms (on each level) of the alignment frame were movable and positioned snugly against the vertical rebars in the specimens. The horizontal arms were then clamped to the alignment frame and specimen rebar at each of the two frame levels. The two-piece nylon template was then easily slid out of the cylinder without disturbing the bar. Careful fabrication of the casting fixtures and nylon templates made rebar placement very easy and very accurate.

The casting fixtures were clamped one at a time to the vibration table. The lollipop specimens were cast in three layers. Each layer was rodded approximately ten times using 3/16-inch or 3/8-inch diameter rods and vibrated for 25 seconds. The molds were also tapped on the sides with a 3/8-inch diameter rod during the vibration of each layer. This

procedure eliminated any surface honeycombing problems encountered with some preliminary batches that only used vibration. A mortar cone was applied to the top of the lollipop specimens approximately one to two hours after casting. The mortar cones ensured that any water accidentally spilled on the specimen would run off (See Figures 5.0 and 5.1). The mortar consisted of water, cement and sand in the ratio of 1:2.5:6.9, respectively.

After moist curing and after about a week of air curing, rebars were cut to a final length at 3 inches above the top of the concrete. Two electrical wires were brazed with silver solder on the top of each rebar of the standard lollipops, one at the end (the sense connection) and one approximately 1/2 inch from the end (the working electrode connection). The rebar was wrapped with a wet rag to help prevent excessive heat from passing into the concrete from the brazing operation. Electrical banana connection plugs were then soldered to the exposed wire ends. The protruding rebars, including all electrical connections, were then covered with epoxy sealer.

Note that no wires were attached to the "cracked" specimens, but the protruding rebars were covered with epoxy sealer. After about 6.5 months of total curing, some 3-inch diameter lollipops were saw cut longitudinally on one side using a masonry saw to create the "cracked" specimen (Fig. 5.2). The saw cut was about 1/8 inch width and extended down to about 1/8 inch from the rebar.

### **5.4.3 Slab Specimens**

Plywood forms were fabricated to cast the slabs. Mineral oil was applied to the

forms the day before a casting to act as a form release and then the forms were covered with plastic. On the day of a casting, the top and bottom rebars were installed and positioned so that the longitudinal ribs were vertical. A small bead of acrylic latex caulk was placed around the rebars at their intersection with the forms. The extruding rebars were then securely taped together on the outsides of the forms to prevent movement during casting .

Two forms were clamped on the vibration table at one time. The slabs were cast in two layers and each layer was vibrated for fifteen seconds. The tops of the slabs were finished with a hand trowel three times at twenty minute intervals to eliminate any plastic shrinkage cracking of the concrete over the top rebar.

Four electrical wires, two on the top rebar (one sense wire and one working electrode wire) and one on each of the bottom rebars, were attached with silver solder during the time of air curing. The rebars were wrapped with wet rags to help absorb heat generated from the brazing operation. Electrical banana connection plugs were then attached to the wire ends.

After the slabs had cured, 6 inch x 3 inch x 3-inch deep Plexiglas dams were attached to the slab tops with silicone caulking. Also at this time, the sides and top areas outside the dam were coated with a concrete epoxy sealer to prevent loss of moisture. The bottom was not sealed. The taped rebar ends projecting from the slabs, including electrical connections, were also covered with the epoxy sealer.

#### 5.4.4 Strength Cylinders

Six 3-inch x 6-inch cylinders were cast with each batch to obtain strength data. A plywood fixture, similar to the lollipop casting apparatus and approximately 24 inches x 24 inches, was constructed to securely hold sixteen 3 inch x 6 inch plastic cylinder molds on the vibration table. Mineral oil was applied to the molds the day of casting. The molds were turned upside down until casting time to allow excess oil to drain out. The cylinders were cast in two layers and each layer was vibrated for fifteen seconds. The tops of the cylinders were finished with a hand trowel.

#### 5.4.5 Curing Procedure

After casting, the specimens were covered with 4 mil plastic sheeting. The next morning, all specimens were demolded and placed in a moist curing room at 70°F for varying times depending on specimen type. The curing room was equipped with shelves as well as open water tanks and had multiple misting jets that maintained the relative humidity at 95% ( $\pm$  5%). After wet curing, all specimens were stored in a dry store room, kept at room temperature and relative humidity, until needed for testing.

The lollipop specimens were wet cured for 14 days on shelves in the moist cure room. On the fifteenth day, the specimens were placed in the dry store room for about fourteen more days. After a total of 28 days minimum, the specimens were introduced to the wet/dry cycling test schedule. Some specimens began testing slightly longer than 28 days based on when they could be introduced into a cycle.



The "cracked" 3-inch diameter lollipop specimens were cured essentially the same as the standard lollipop specimens, except the "cracked" specimens were stored in air in the store room for about six months before being saw cut and then placed into the wet/dry cyclic environment.

The slab specimens were wet cured for 14 days, the same as the lollipop specimens. The slab specimens were air cured for a longer period of time, approximately 32 days instead of 14 days due to problems with the corrosion monitoring equipment as well as due to problems in casting some of the lollipop specimens. The slab specimens were then placed into the wet/dry cycles.

The cylinders used for strength monitoring of the corrosion specimens were wet cured for fourteen days on shelves in the moist cure room. The specimens were then placed in the dry store room until required for testing. The strength cylinders were tested at 28 days and 56 days of age.

## **5.5 WETTING AND DRYING PROCEDURE**

The wet cycle consisted of either soaking or ponding the specimens with a 15% salt solution for four consecutive days. Past research has typically used either a 3.0% [6, 14, 19, 31] or a 15% [9, 18, 32, 34] salt solution. The 15% salt solution creates a harsher environment, thereby expediting the overall test time. Also, salt concentrations on actual bridge decks from the use of deicing salts have been shown to vary between 7% and 15%.

The drying cycle lasted for three days and consisted of either air drying (for slabs) at room temperature or oven drying (for lollipops) at 100°F ( $\pm 3^\circ\text{F}$ ). The drying oven was a 50-inch high x 24-inch wide x 24-inch deep oven that was vented to exhaust moisture.

This particular wet/dry cycle simulates a "southern exposure" environment and creates an aggressive corrosion environment with an abundance of chlorides and oxygen, which should accelerate the overall test time.

The ponding and drying procedure for the lollipop specimens, for both standard and "cracked" specimens, was as follows:

1. Place the lollipop specimens in their individual ponding containers, 4-inch diameter by 6-inch tall containers for the 2-inch diameter specimens and 6-inch diameter by 6-inch containers for the 3-inch diameter specimens. Containers were made from standard plastic cylinder molds.
2. Fill the ponding containers with fresh 15% salt solution to a level of 1.0 inch below the top of the container.
3. Four days later, remove the specimens from their ponding containers and rinse the specimens with warm water to remove any exterior salt buildup.
4. Place the specimens on the racks in the drying oven.
5. Empty the ponding containers and rinse with warm water.
6. After three days of drying, remove the specimens from the oven and proceed to step one. Repeat steps one through six.

The ponding and drying procedure for the slab specimens was as follows:

1. Fill each ponding dam to a depth of 2.0 inches with fresh 15% salt solution.
2. Place a plastic cover over each dam during the ponding cycle to prevent evaporation of the salt solution.
3. Four days later, vacuum out the salt solution. (Once a month rinse out the ponding dams and exposed concrete to remove any salt buildup).
4. Let the slabs air dry for three days at room temperature.
5. Proceed to step one. Repeat steps one through five.

## CHAPTER 6.0

### CORROSION TESTING METHODS

#### 6.1 GENERAL

The corrosion testing program to evaluate the two prototype inhibitors, as well as two commercial inhibitors, used two different geometrically shaped specimen types. One type consisted of 2-inch or 3-inch diameter cylindrical lollipop specimens. The other type was a rectangular slab specimen.

Linear polarization was selected to measure the polarization resistance of the specimens based on its accuracy, moderate cost, and ability to measure both macro-cell and localized corrosion. Linear polarization does require a slightly higher knowledge of elementary electrochemical theories than half cell potential or macro-cell methods do. Analysis of the data is relatively easy with readily available commercial software used in conjunction with a data reduction program developed "in house". This method is also more accurate than half cell potential and macro-cell techniques. AC Impedance is used by some researchers [6, 46], but the instrumentation required is quite extensive and costly. Also, test time can be extremely lengthy and analysis of the data can be fairly complex. Polarization measurements were take at the end of a wet cycle.

#### 6.2 Polarization Resistance Measurements

Polarization measurements were made using an EG&G PARC Potentiostat/Galvanostat Model 273A. Corrosion monitoring equipment tested by SHRP [37] was

considered but not chosen, since the SHRP equipment does not have the flexibility to change certain test parameters, operate accurately in high concrete solution resistance environments, or perform other types of electrochemical experiments, whereas a potentiostat does. Also, it was questionable whether the SHRP equipment would be compatible with the lollipop specimen geometry. A three electrode probe cell setup was used and consisted of:

1. One saturated calomel reference electrode, RE,.
2. One working electrode, WE, (No. 4 reinforcing bar).
3. 1/2-inch diameter graphite counter electrode, CE, ( two used for the lollipop specimens and one used for the slab specimens).

Figures 6.0 and 6.1 show the actual geometry of the test cells. The test cell for the lollipop specimens consisted of a plastic container and a plexiglass "lid" to hold the reference and counter electrodes in place. The two counter electrode setup (Fig. 6.0) provided a more uniform polarization for the round lollipop specimens. The test cell for the slab specimens was the ponding dam attached to the top of each slab. The working electrode of all specimens, both lollipops and slabs, had a separate sense wire attached, as specified in Section 5.4., to help stabilize the linear polarization measurements in the case of high currents, which would create a significant voltage drop in the working electrode lead. Both types of test cells were filled with the same 15% salt solution used for the wetting/ponding cycle.

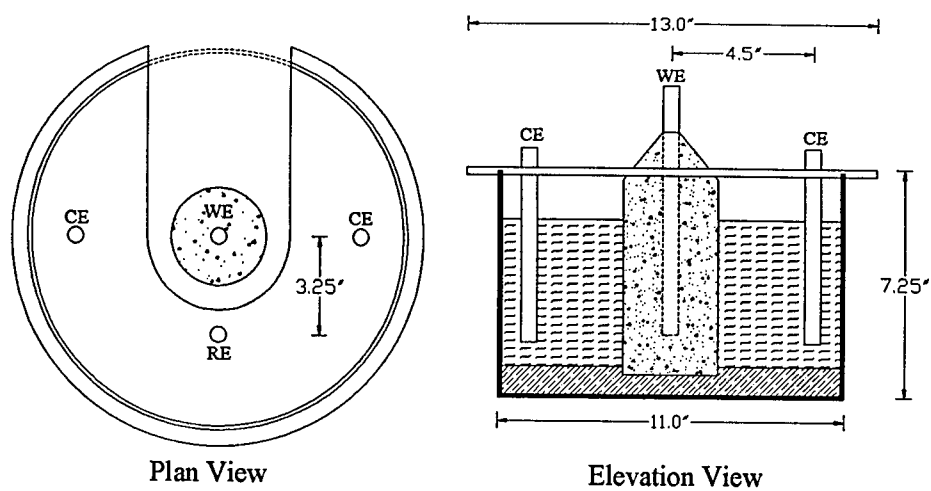


Figure 6.0 Lollipop Test Cell Setup.

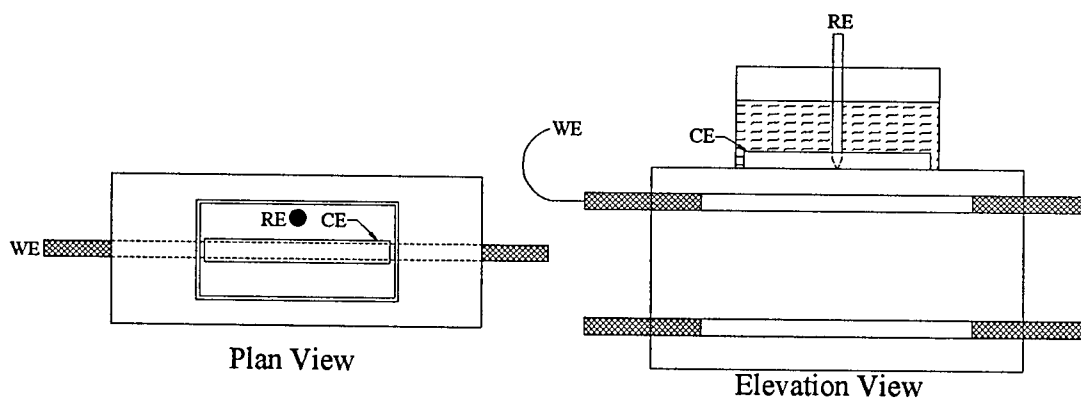


Figure 6.1 Slab Specimen Test Cell Setup.

Tests were initially controlled by EG&G PARC M352 SoftCorr<sup>TM</sup> III software on a Gateway P133 Pentium Processor Computer through a National Instruments® GPIB-PCII A interface. However, problems developed during the use of this software. The

M352 software would intermittently "reverse polarize" a specimen by first pushing the cell's open circuit potential approximately 200mV (anodically) and then polarizing from that new open circuit potential. The potential verses current curve would occur in the opposite direction, hence, called "reverse polarization". Consequently, the software was changed to CorrWare, by Scribner Associates, Inc, for the duration of the project. This software change eliminated the reverse polarization problem.

The Tafel constant, B, of 0.026V was used to calculate the corrosion current. The same value was used for both passive and active systems. Specific Tafel slopes were not obtained because the same working electrode material, iron, was used for all the specimens.

When calculating the corrosion rate, it was assumed that the corrosion was occurring over the entire exposed area of the bar. This is not usually the case, however this assumption is typically made by researchers. In most instances, the corrosion is localized. Thus, an average corrosion rate is calculated. Therefore, calculated corrosion rates are nominal at best.

The cell was polarized  $\pm 10$ mV about the open circuit potential at a scan rate of 0.1mV/sec. The IR drop was not accounted for during the linear polarization test but was corrected for as described in Section 6.3 by use of a data reduction program, specially written "in-house" for this project.

The same data reduction program that corrected for the IR drop, also calculated the actual  $R_p$  value. The  $R_p$  for each test was calculated from the slope of the corrected current verses potential curve between these two points:

1. The potential where the current equals zero,  $E_{I=0}$ , the true open circuit potential.
2. The potential +5mV above  $E_{I=0}$ .

Accuracy is maintained by limiting the  $R_p$  calculation to 5mV above the true open circuit potential. Figure 6.2 shows a typical polarization curve (voltage verses current) for an actively corroding lollipop specimen that has not been corrected for the IR drop. Figure 6.3 shows the linear region that has been corrected for the IR drop. The slope(  $\Delta E/\Delta I$ ) of the "best fit" linear line (Figure 6.3) equals the  $R_p$  of the specimen, which is shown as the "x" coefficient in the line equation shown. The negative sign is disregarded.

The lollipop specimens were tested every two weeks and the slabs were tested once a month. Three linear polarization measurements were initially taken for each specimen on each test day and then an average  $R_p$  was calculated. This proved to be very time consuming because of the large number of specimens being monitored. As the project progressed and more experience was attained, it became apparent that the  $R_p$  values varied more when corrosion was not present and varied only very slightly when corrosion initiated or was active (Table 6.0). The condition of active corrosion was more important. Therefore, the number of linear polarization measurements per specimen was reduced to one, which allowed more specimens to be monitored without a substantial loss in accuracy. Each polarization run was scrutinized upon completion and a second run was performed if deemed necessary.



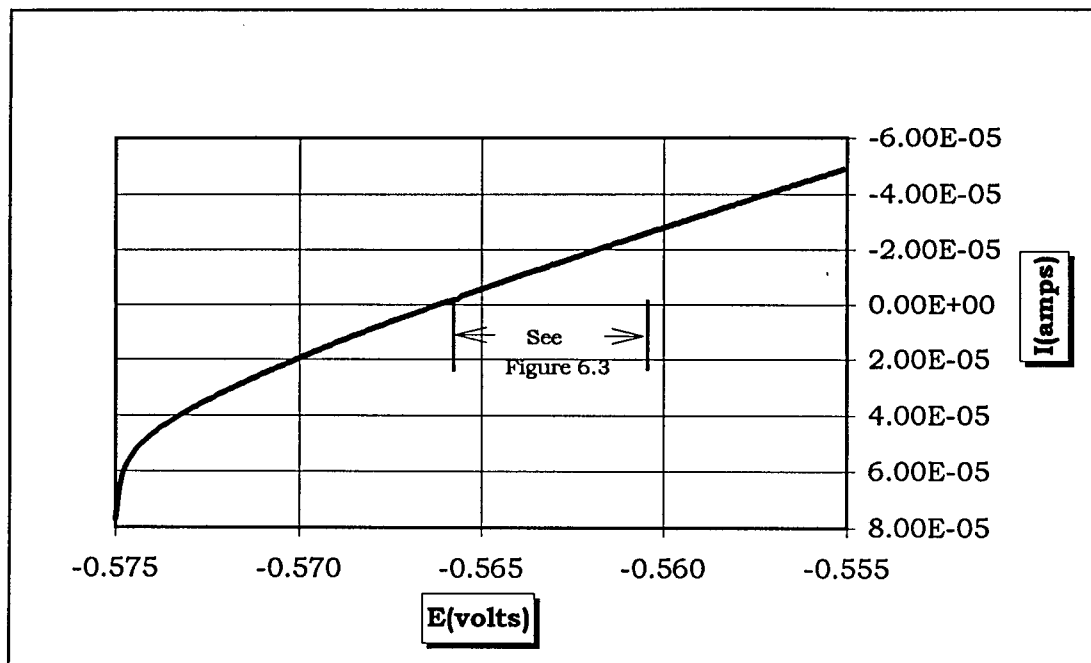


Figure 6.2 Typical Linear Polarization Curve for an Actively Corroding Lollipop Specimen, Not Corrected for IR Drop (Plotted I Vs E).

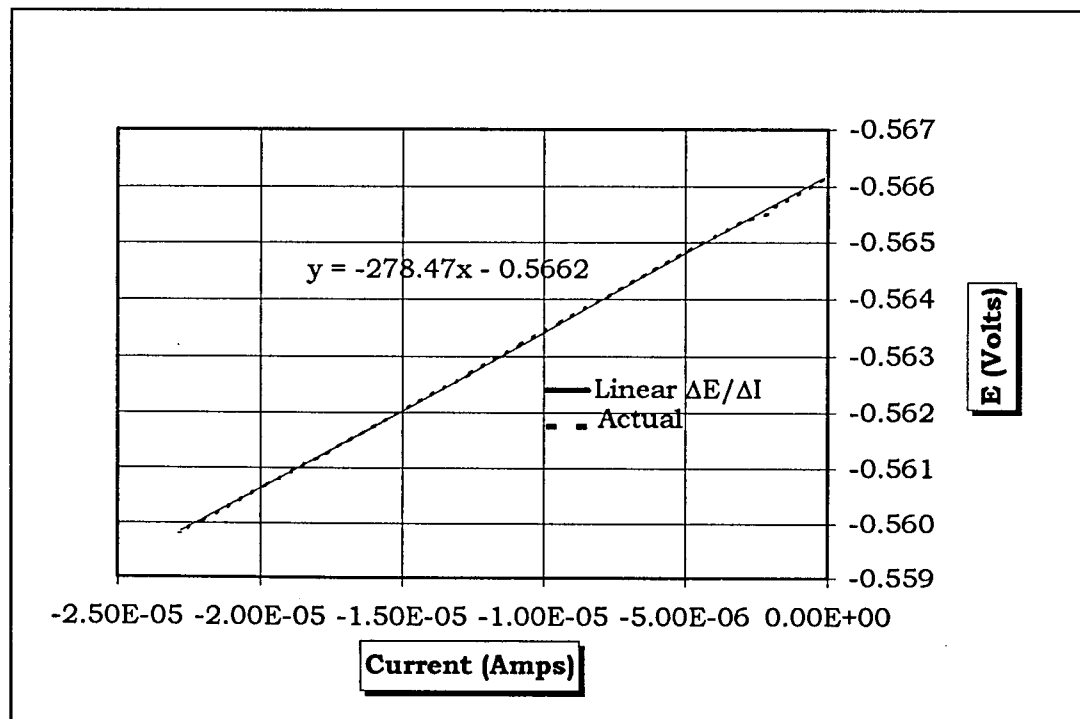


Figure 6.3 Linear Portion Of Figure 6.2 That Has Been Corrected For The IR Drop (Plotted E Vs I).

**Table 6.0 Typical Standard Deviation and Coefficient of Variation for Actively Corroding Specimens (Based on Three Runs/Test).**

Test No.	R <sub>p</sub> (Ave.) (ohms-cm <sup>2</sup> )	S <sup>1</sup>	V <sup>2</sup> (%)
1	185605	176.66	3.44
2	197097	109.19	2.00
3	203494	197.78	3.51
4 <sup>3</sup>	24348	1.48	0.22
5	16789	4.36	0.94
6	13566	0.54	0.14

<sup>1</sup> S is the sample standard deviation.

<sup>2</sup> V is the coefficient of variation.

<sup>3</sup> Corrosion initiated.

### 6.3 IR DROP

The solution resistance was measured by the positive feedback method with EG&G PARC M270 software utilizing the same three electrode probe cell described previously. The compensation was set at 85% and the pulse height at 10mV. Current ranges were set at 100uA for the low solution resistance specimens and 10uA for the higher solution resistance specimens. The resistance of the concrete was assumed to be constant for each test period. This assumption is valid since the resistance of the concrete should vary only slightly, if any, during a test period. The IR drop was then accounted for mathematically as described in 3.4.2.

The solution resistance was assumed to be the resistance of the concrete only. The resistance of the electrolyte solution and of the testing leads can increase the IR drop in certain cases. However, the 15% salt solution was very conductive and only moderate length leads were used. Their contribution to the total solution resistance of the system

would be relatively small as compared to the concrete resistance and was subsequently ignored.

The values obtained by positive feedback were checked periodically with AC impedance and the results corresponded quite well. Some results are in Tables 6.1 and 6.2. The AC Impedance measurements were performed by a Solartron system that consisted of a Model SI 1287 Electrochemical Interface and a Model SI 1250 Frequency Response Analyzer using Zplot software by Scribner Associates, Inc. To obtain the  $R_s$  measurements, the frequency response analyzer was set to the maximum frequency (20kHz for the Model SI 1250). The impedance equipment was on loan to the project, from the University of Connecticut's Chemical Engineering Department, for only very brief intervals.

Table 6.1 2-Inch Cylinders: Comparisons of Positive Feedback (PF) and AC Impedance (I) Methods for Measuring the Solution Resistance.

Spec. No.	Test Date: 8/11/97			Test Date: 10/6/97			Test Date: 12/15/97		
	PF <sup>1</sup> (ohms)	I <sup>2</sup> (ohms)	% Diff.	PF (ohms)	I (ohms)	% Diff.	PF (ohms)	I (ohms)	% Diff.
Control - C2-#1	40	50.86	21.35	---	---	---	70	55.64	-25.81
Control - C2-#3	40	58.18	31.25	---	---	---	60	51.29	-16.98
Control - C2-#4	40	43.77	8.61	---	---	---	60	50.32	-19.24
Control - C2-#6	---	---	---	---	---	---	60	49.34	-21.61
2%DAS - #1	2070	1942.6	-6.56	5700	3997	-42.61	12500	9248.3	-35.16
2%DAS - #2	2840	2648.1	-7.25	5370	5350	-0.37	17000	12390	-37.21
2%DAS - #3	3070	2875.3	-6.77	5650	5657.3	0.13	18000	13232	-36.03
1%DAS - #1	---	---	---	2930	2900.9	-1.00	7500	6026.3	-24.45
1%DAS - #2	---	---	---	3370	3378.1	0.24	9000	7423.4	-21.24
1%DAS - #3	---	---	---	3670	3669.8	-0.01	9800	8114.3	-20.77
1/2%DAS - #1	---	---	---	1940	1770.3	-9.59	2800	2657.9	-5.35
1/2%DAS - #2	---	---	---	2240	1890.5	-18.49	3500	2766.4	-26.52
1/2%DAS - #3	---	---	---	2470	2112.8	-16.91	4100	3394.6	-20.78
2%DSS - #1	1930	1960.3	1.55	4210	3780.8	-11.35	10800	7954	-35.78
2%DSS - #2	2020	2077.5	2.77	4720	4192.3	-12.59	12300	9385.7	-31.05
2%DSS - #3	2560	2522.8	-1.47	5780	6008.8	3.81	25400	16907	-50.23
1%DSS - #1	---	---	---	3650	3129.4	-16.64	7400	5987.8	-23.58
1%DSS - #2	---	---	---	6050	5760.7	-5.02	19200	13372	-43.58
1%DSS - #3	---	---	---	4350	3662.8	-18.76	13200	9666.9	-36.55

<sup>1</sup> PF - Positive Feedback method.

<sup>2</sup> I - AC impedance method.

Table 6.2 3-Inch Cylinders: Comparisons of Positive Feedback (PF) and AC Impedance (I) Methods for Measuring the Solution Resistance.

Spec. No.	Test Date : 8/11/97			Test Date : 10/6/97			Test Date : 12/15/97		
	PF <sup>1</sup> (ohms)	I <sup>2</sup> (ohms)	% Diff.	PF (ohms)	I (ohms)	% Diff.	PF (ohms)	I (ohms)	% Diff.
Control -#1	80	108.46	26.24	---	---	---	---	---	---
Control -#2	90	119.79	24.87	---	---	---	---	---	---
Control -#3	80	91.82	12.87	---	---	---	---	---	---
Control -#4	80	90.54	11.64	---	---	---	---	---	---
Control -#5	70	84.88	17.53	---	---	---	80	89.31	10.42
Control -#6	80	93.43	14.37	---	---	---	---	---	---
2%DAS - #1	2160	2141	-0.89	5550	4994.4	-11.12	18700	13885	-34.68
2%DAS - #2	1370	1412	2.97	2730	2613.3	-4.47	5900	5697.6	-3.55
2%DAS - #3	1660	1692.9	1.94	3560	3208.6	-10.95	9300	7683	-21.05
1%DAS - #1	1580	1585.6	0.35	3280	3031.8	-8.19	8200	6929.9	-18.33
1%DAS - #2	750	808.42	7.23	1140	1182.2	3.57	1800	2004.9	10.22
1%DAS - #3	1560	1552.6	-0.48	3030	2766.1	-9.54	7200	6096.9	-18.09
1/2%DAS - #1	1120	1193.9	6.19	1720	1765.8	2.59	2800	2943.8	4.88
1/2%DAS - #2	940	1037.5	9.40	1400	1446.7	3.23	2100	2319.4	9.46
1/2%DAS - #3	1120	1219.2	8.14	1670	1712.4	2.48	2800	2961.8	5.46
2%DSS - #1	1520	1562.4	2.71	5230	4739.9	-10.34	21600	16199	-33.34
2%DSS - #2	1700	1672.1	-1.67	5750	5320.4	-8.07	24100	17745	-35.81
2%DSS - #3	1640	1668.7	1.72	5610	5026.3	-11.61	24600	17447	-41.00
1%DSS - #1	1600	1691.1	5.39	5130	4695	-9.27	18800	14069	-33.63
1%DSS - #2	1050	1146.7	8.43	2080	2152.6	3.37	4800	4704.5	-2.03
1%DSS - #3	1650	1750.7	5.75	5040	4642.7	-8.56	18600	14661	-26.87

<sup>1</sup> PF - Positive Feedback method.

<sup>2</sup> I - AC impedance method.

## CHAPTER 7.0

### PRESENTATION AND DISCUSSION OF RESULTS

#### 7.1 COMPRESSION STRENGTH, FREEZE-THAW AND ABSORPTION

The 28 day and 56 day compression strength results for the corrosion specimens are shown in Table 7.0, Figures 7.0 and 7.1. For a more detailed discussion, see Appendix C.

As stated in Section 5.2.1, the lollipop and slab specimens were cast in different batches on different days due to various delays and problems. The compression strengths of the slab mixes were up to 16% higher than the lollipop mixes and averaged approximately 7% higher. Inhibitor A mixes had the highest strength of all the mixes (at 120%, relative to control) and the 2%DSS without de-foaming agent had the lowest strength (at 60%, relative to control). Inhibitor B was consistently at about 84% the strength of Control-2.

Increasing the concentration of DAS or DSS produced lower strengths, without much difference between the two chemicals. Except for a few DSS mixes, all the DAS and DSS mixes had 28 day compression strengths greater than 4000 psi, which satisfied the requirements of ConnDot's Class "F" concrete for bridges, the original basis for the "control" mix design.

Appendices A and B present test procedures and test results for freeze-thaw resistance and absorption tests, respectively. The remainder of this chapter will focus on the corrosion test results.

Table 7.0 Corrosion Mixes: 28 and 56 Day Compression Strengths.

Mix Type <sup>1</sup>	w/c	Air Content	28 Day (psi)	56 Day (psi)	Relative 28 Day (psi) <sup>2</sup>
<b>Slab Specimens</b>					
Control -1	0.38	7.5%	----	7049	----
Control - 2	0.38	8.0%	5941	5904	1.00
Inhibitor A	0.40	7.0 %	7381	6984	1.24
Inhibitor B	0.45	8.5 %	4932	5132	0.83
2% DAS	0.41	6.0 %	5217	5394	0.88
1% DAS	0.39	7.0 %	5038	5398	0.85
1/2% DAS	0.39	7.0 %	5367	5420	0.90
2% DSS	0.40	8.0%	3744	4263	0.63
1% DSS	0.40	8.0%	4232	4593	0.71
<b>Lollipop Specimens</b>					
Control - 2	0.38	8.0%	5941	5904	1.00
Inhibitor A	0.38	8.0 %	6884	6339	1.16
Inhibitor B	0.39	9.0 %	4839	4627	0.81
2% DAS	0.41	6.5 %	4489	5018	0.76
1% DAS	0.40	8.0 %	4758	5057	0.80
1/2% DAS	0.40	8.5 %	4996	5040	0.84
2% DSS	0.41	7.0%	3741	4094	0.63
1% DSS	0.40	8.0%	3873	4331	0.65

<sup>1</sup> All mixes contained Type I/II cement @ 27.85 lb., coarse agg. (oven-dried) @ 48.59 lb., and fine agg. (oven-dried) @ 54.26 lb. - Based on 1.0 cu. ft. mix.

<sup>2</sup> Relative strength: Control-2 mix equals 100%.

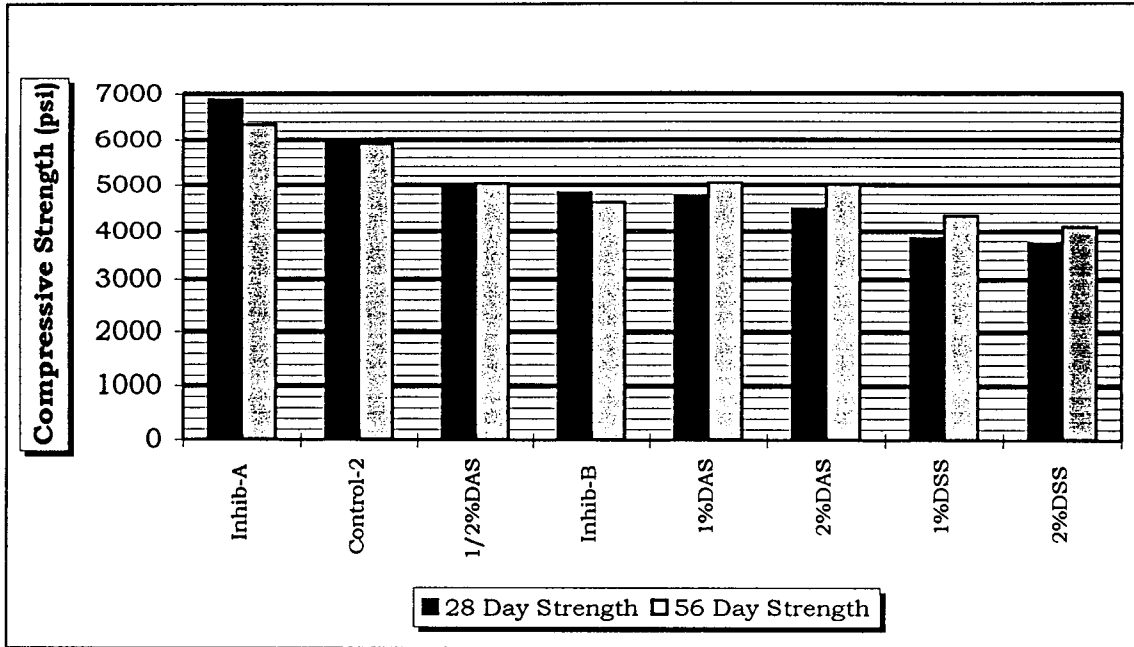


Figure 7.0 Compression Strengths: Lollipop Specimens.

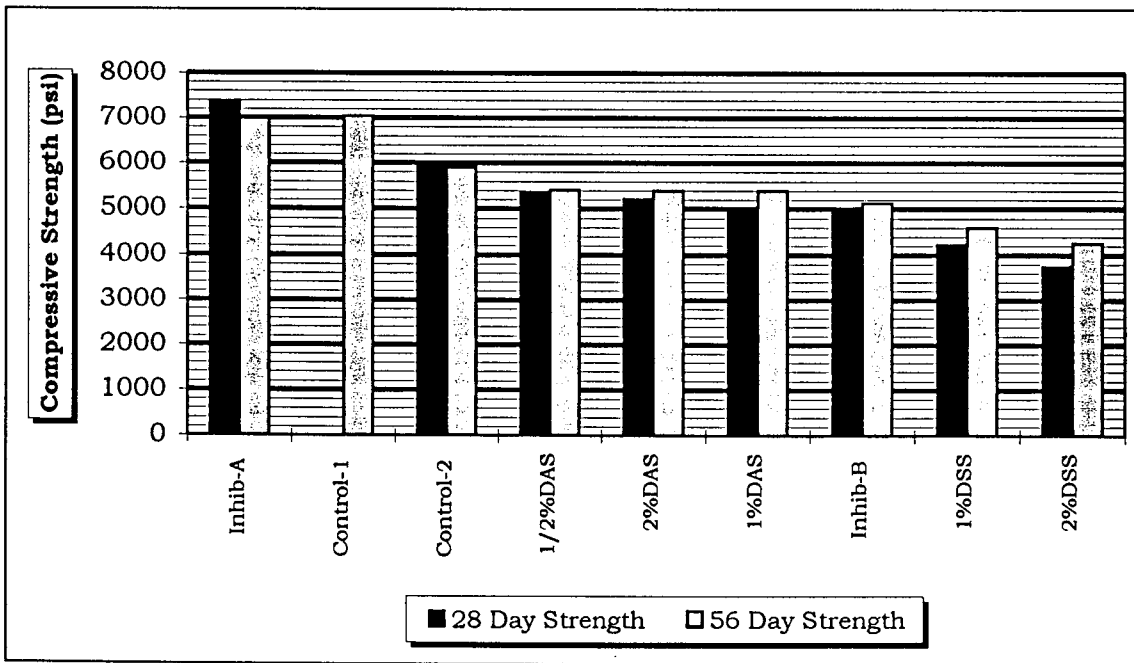


Figure 7.1 Compression Strengths: Slab Specimens.



## 7.2 SOLUTION RESISTANCE

### 7.2.1 General

The solution resistance,  $R_s$ , versus time plots for the lollipop and slab specimens are shown in Figures 7.2 through 7.7. Note the significant difference in vertical scales in these figures for the various specimens. The solution resistances shown were based on an average of three replicate specimens for all the specimen groups, except for the lollipop control specimens and the slab Control-1 specimens, which were based on an average of six and two specimens, respectively.  $R_s$  versus time plots for each individual specimen of each group and type (i.e., not averaged) are shown in Appendix D.

During ponding of the slab specimens, the top and bottom reinforcing mats of the specimens were either electrically connected together or were not electrically connected. These specimens are referred to as either "conn" or "unconn", respectively, in the discussion.

Note that the monitoring of the corrosion specimens is still ongoing. This discussion is based on a monitoring period of about 48 weeks for the lollipops and about 45 weeks for the slabs.

### 7.2.2 Control Specimens

The solution resistance of the 2-inch diameter and 3-inch diameter lollipop specimens and slabs specimens remained relatively constant with values of about 50, 80 and 100 ohms, respectively. The only exception was the slab Control-1 connected

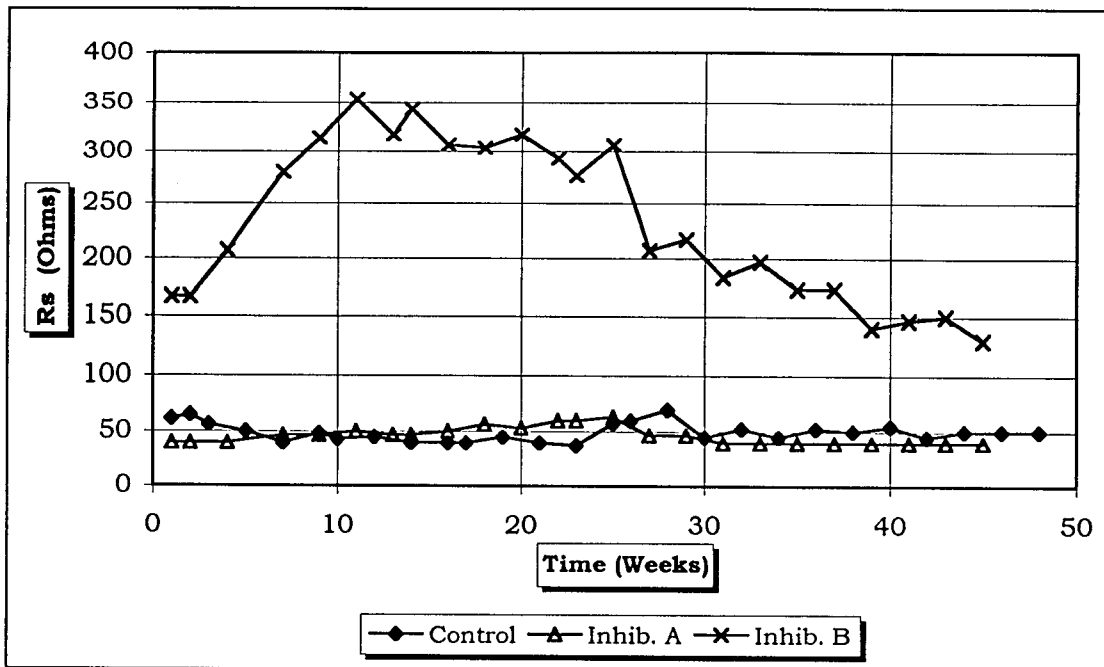


Figure 7.2 Solution Resistance, 2-Inch Cylinders: Control, Inhibitor A and B Mixes.

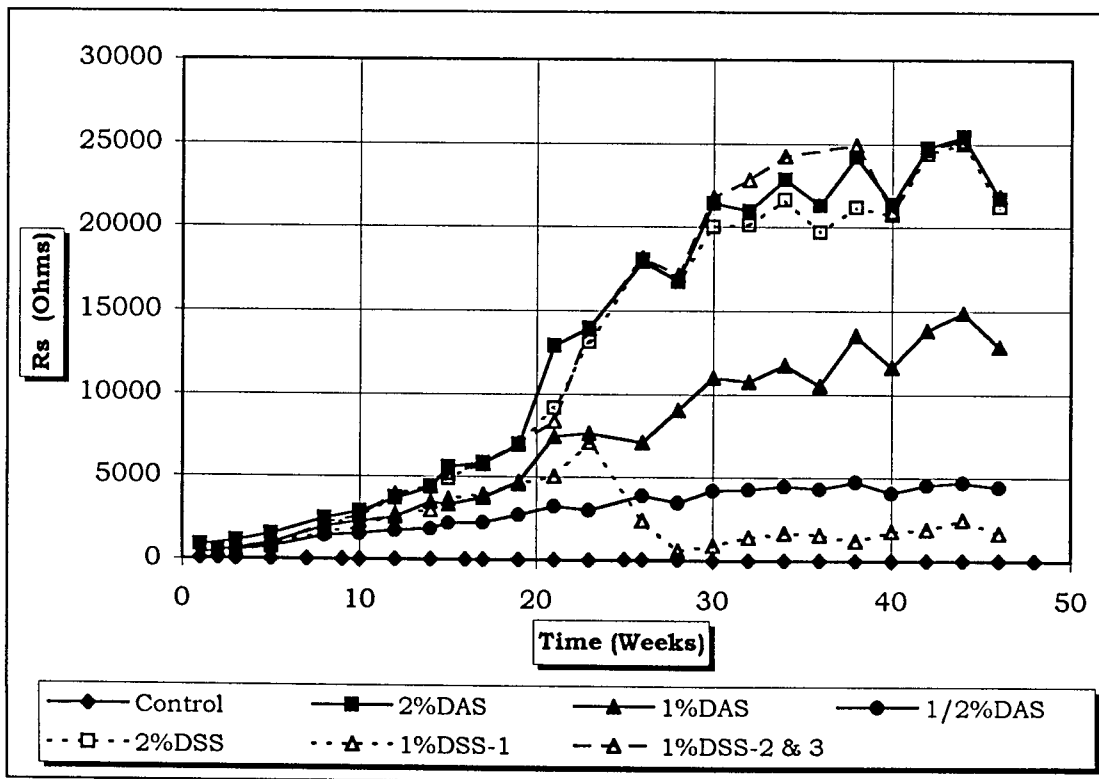


Figure 7.3 Solution Resistance, 2-Inch Cylinders: Control, DAS and DSS Mixes.

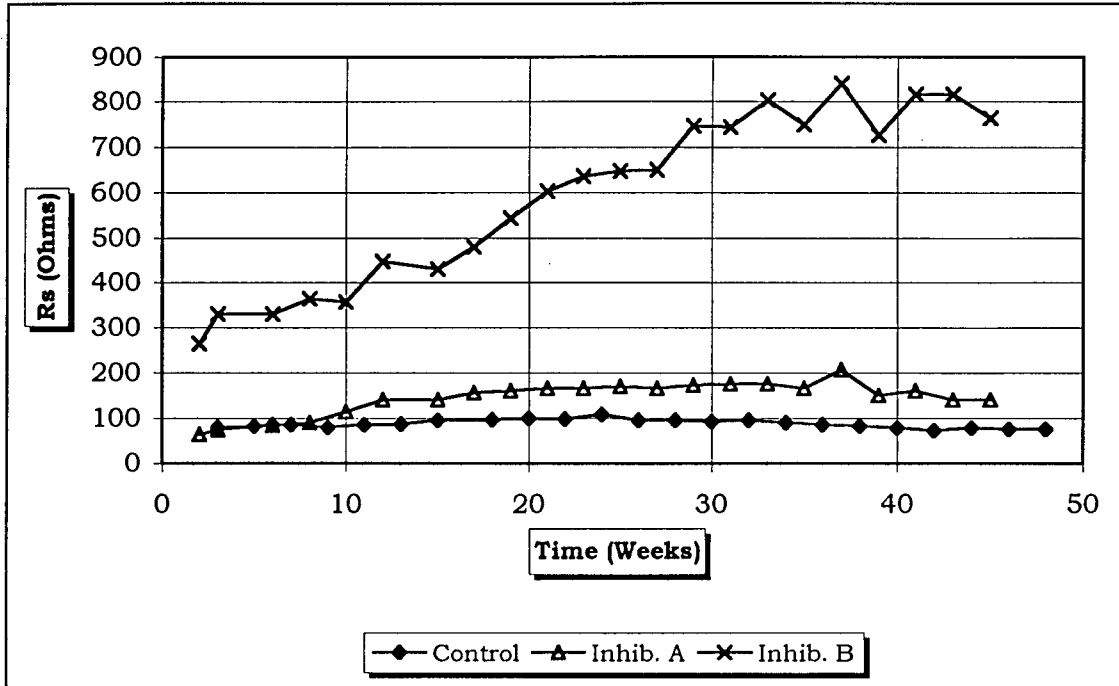


Figure 7.4 Solution Resistance, 3-Inch Cylinders: Control, Inhibitor A and B Mixes.

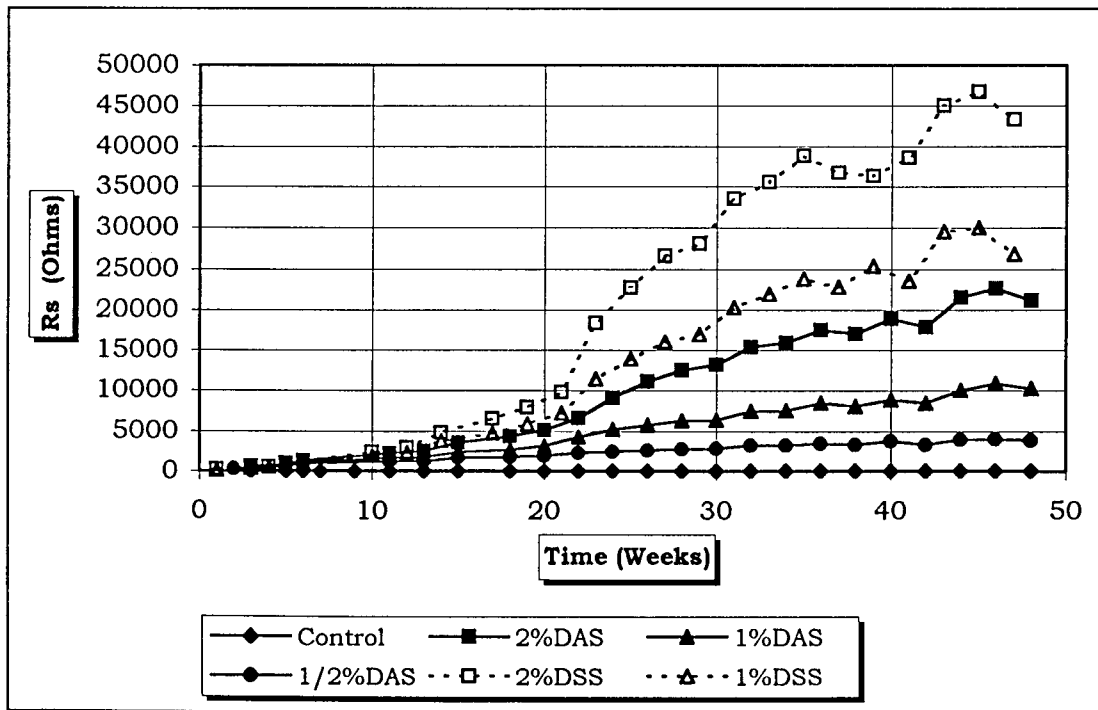


Figure 7.5 Solution Resistance, 3-Inch Cylinders: Control, DAS and DSS Mixes.

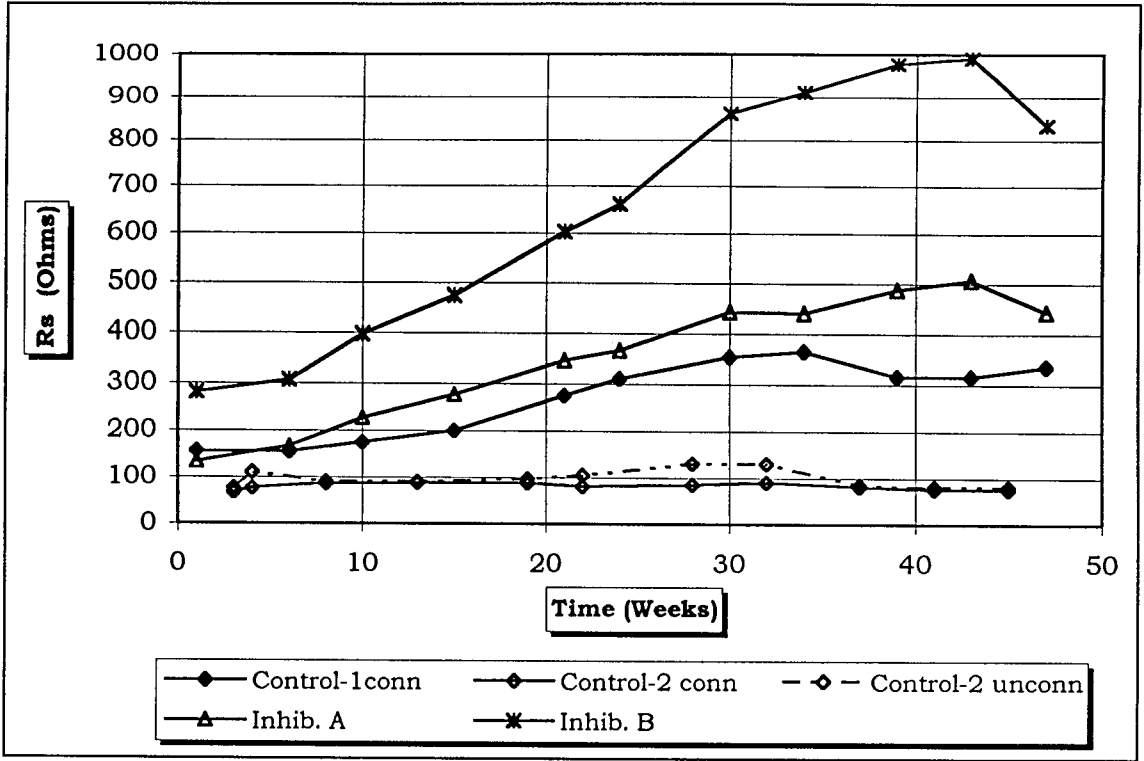


Figure 7.6 Solution Resistance, Slabs: Control, Inhibitor A and B Mixes.

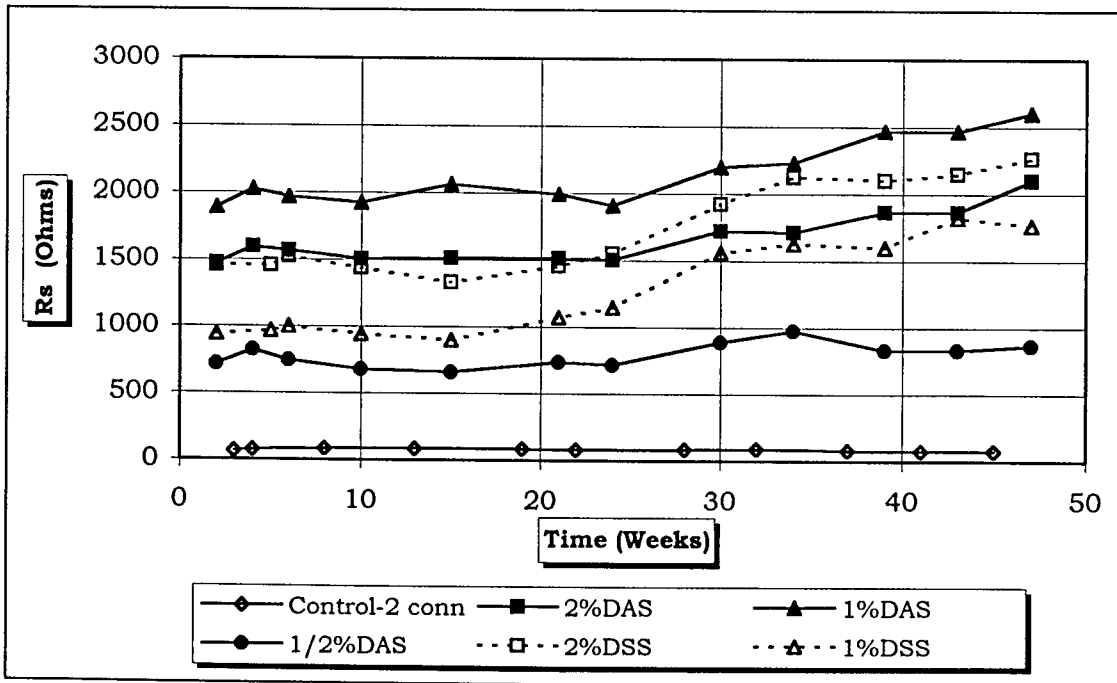


Figure 7.7 Solution Resistance, Slabs: Control, DAS and DSS Mixes.

specimens, where  $R_S$  values increased from 120 to 380 ohms. The 3-inch diameter lollipop specimens and slab Control-2 specimens, both connected and unconnected, had  $R_S$  values approximately double of the 2-inch diameter lollipop specimens. It is not known why the Control-1 specimens had higher  $R_S$  values than the Control-2 specimens. Both mixes had similar w/c ratios, air contents and curing environments. Also, the compression strength of the Control-1 mix was about 20% stronger than the Control-2 mix.

### 7.2.3 Inhibitor A and Inhibitor B Specimens

For Inhibitor A, the lollipop and slab specimens had  $R_S$  results about the same as the geometrically similar control specimens. Only the slab specimens had a significant increase in  $R_S$  with time, from 140 to 500 ohms, similar to Control-1. Recall, the slab specimens were dried at room temperature, whereas the lollipops were oven dried at 100°C. Absorption results (Appendix B) indicated that absorption is reduced for specimens dried at lower temperatures, which might explain why only the slab  $R_S$  increased over time.

The  $R_S$  of all specimens types for Inhibitor B initially increased over time. The slab and 3-inch diameter lollipops had similar  $R_S$  values that were approximately twice those of the 2-inch diameter lollipops. The  $R_S$  values for the 2-inch diameter lollipop specimens and slab specimens started to decline after about 13 weeks and 44 weeks, respectively, indicating an increasing presence of moisture and chlorides in the concrete. The 3-inch diameter lollipop specimens had solution resistances that continually increased during this monitoring period.

#### 7.2.4 DAS and DSS Specimens

The  $R_s$  values generally increased with time for the DAS and DSS specimens. This increase was not as profound for the slab specimens. The DAS and DSS lollipop specimens had  $R_s$  values 50 to 450 times greater than the control lollipop specimens (and also generally than the Inhibitor A specimens) and averaged about 250 times greater. The DAS and DSS lollipop specimens had  $R_s$  values that also were significantly greater than for Inhibitor B, generally by one or two orders of magnitude.

The DAS and DSS slab specimens had  $R_s$  values about 10 to 25 times greater than the control. The difference in  $R_s$  values for the lollipop and slab specimens showed the significant effect of oven drying as compared to the air drying for the DAS and DSS specimens. The two chemicals allowed moisture to evaporate from the concrete during either the oven drying or air drying cycles, but they prevented re-absorption during the wetting cycle.

For the 3-inch diameter DAS and DSS lollipop specimens, the solution resistance increased as the concentration of either DAS or DSS increased. The 2-inch diameter lollipops and slab specimens also generally followed this trend. Note that the 2-inch diameter 1%DSS-1 lollipop specimen was accidentally dropped after completing 23 cycles. In that specimen a crack then immediately developed, which created a direct path for moisture and chlorides to the reinforcing bar. This explained why the  $R_s$  for this specimen decreased so significantly at that time (Fig. 7.3), contrary to the other DAS or DSS specimens.

## 7.3 CORROSION RATES

### 7.3.1 General

Corrosion rates (CR) are calculated by multiplying the current density ( $i_{\text{corr}}$ ) by a constant (see Section 3.4.1), where:

$$I_{\text{corr}} = \frac{B \text{ (Volts)}}{R_p \text{ (ohms)}} \quad i_{\text{corr}} = \frac{I_{\text{corr}}}{\text{Electrode Area (cm}^2\text{)}}$$

$$\text{CR} = i_{\text{corr}} * \text{Constant}$$

Therefore, corrosion rates are inversely proportional to  $R_p$ . In this work, the corrosion rate is expressed as:

$$\text{CR} = \frac{1}{(R_p) * (\text{electrode area})}$$

The electrode area ( $\text{cm}^2$ ) is included to allow comparisons of specimens with different exposed electrode areas (i.e., exposed rebar area) and is implied when written as  $1/R_p$ . Higher values of  $1/R_p$  indicate higher corrosion rates. The units for  $1/R_p$  are  $\mu\text{mhos}/\text{cm}^2$  and is called the area specific conductance, where  $(\text{ohms})^{-1}$  equals  $\mu\text{mhos}$ .

The corrosion rates, expressed as  $1/R_p$ , for the lollipops and slabs specimens are shown in Figures 7.8 through 7.14. The rates were averaged, for each specimen type, as explained in Section 7.2. In some cases (i.e., specimens 1%DSS-[2"] and Inhibitor B-[3"]) if a specimen behaved significantly different than the other replicate specimens, the

individual result (not averaged) is presented. Plots,  $1/R_p$  verses time, for each individual specimen of each group and type (i.e., not averaged) are shown in Appendix D.

The exposed reinforcing bar area (e.g., electrode area) was  $36.10 \text{ cm}^2$  and  $81.07 \text{ cm}^2$  for the lollipop and slab specimens, respectively. Initiation of corrosion was assumed to occur when there was a noticeable relative increase in the corrosion rate. Average time to corrosion for each mix and specimen type is shown in Table 7.1. The final corrosion rates to date of all the specimens are shown in Table 7.2.

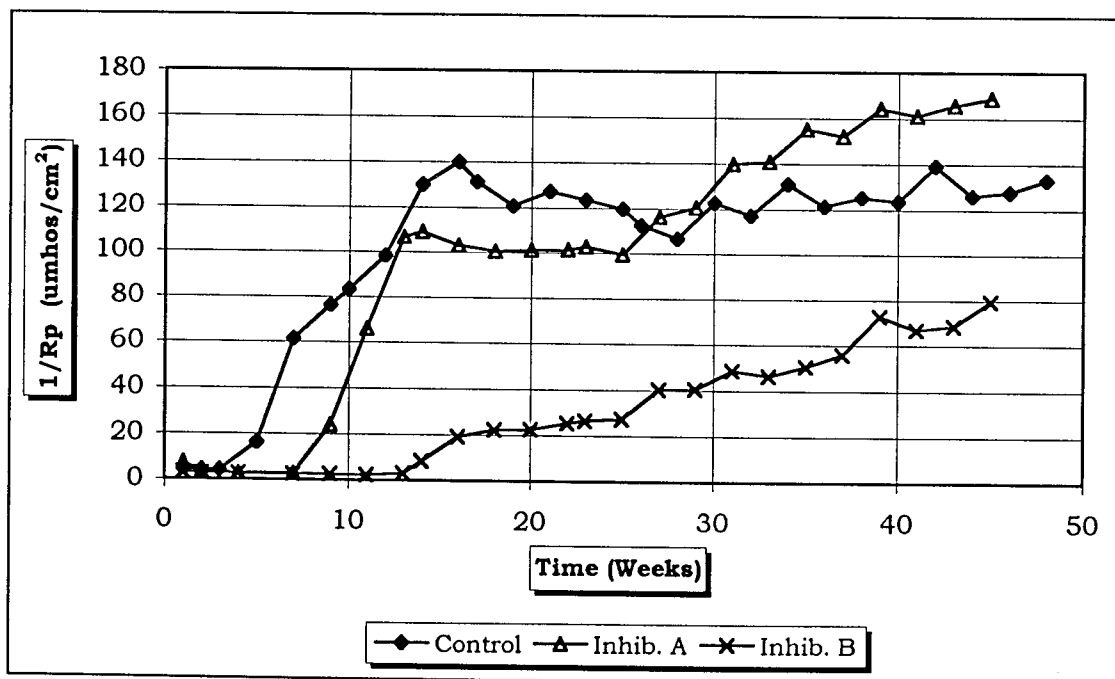


Figure 7.8 Corrosion Rate, 2-Inch Cylinders: Control, Inhibitors A and B Mixes.



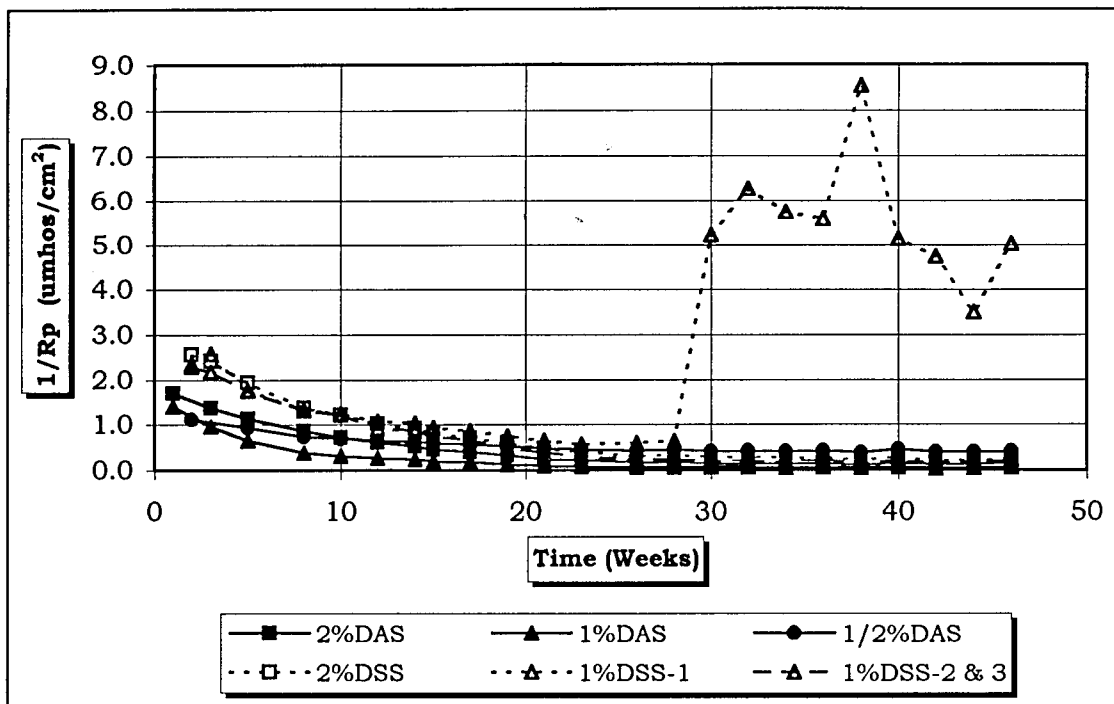


Figure 7.9 Corrosion Rate, 2-Inch Cylinders: DAS and All DSS Mixes.

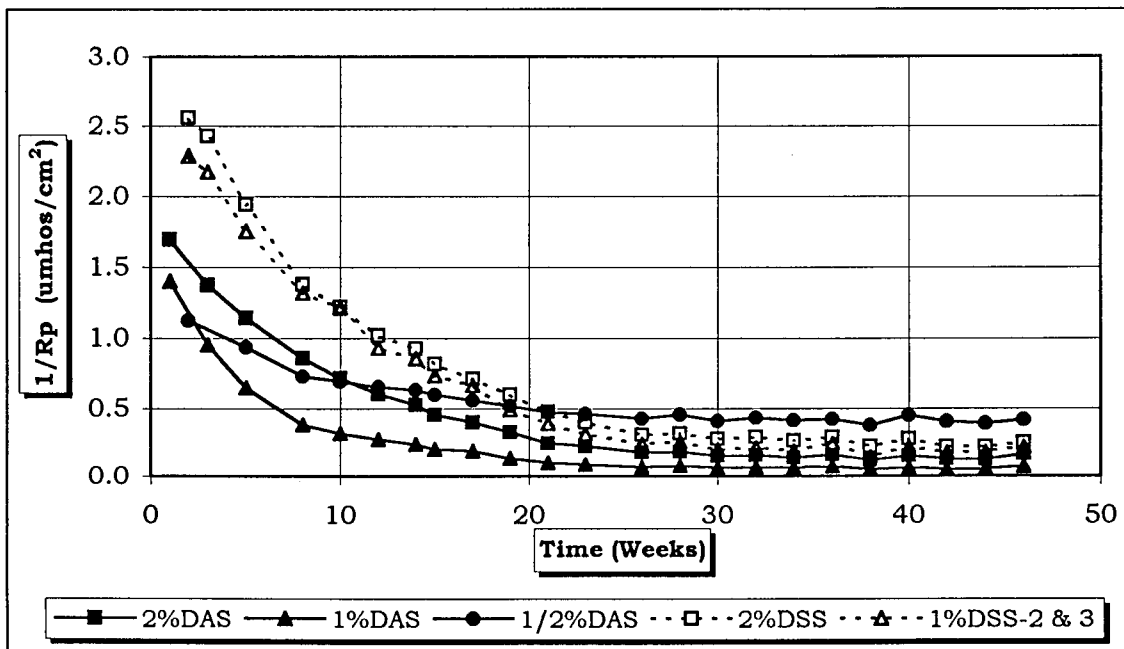


Figure 7.10 Corrosion Rate, 2-Inch Cylinders: DAS and DSS Mixes (Omitting Specimen 1%DSS-1).

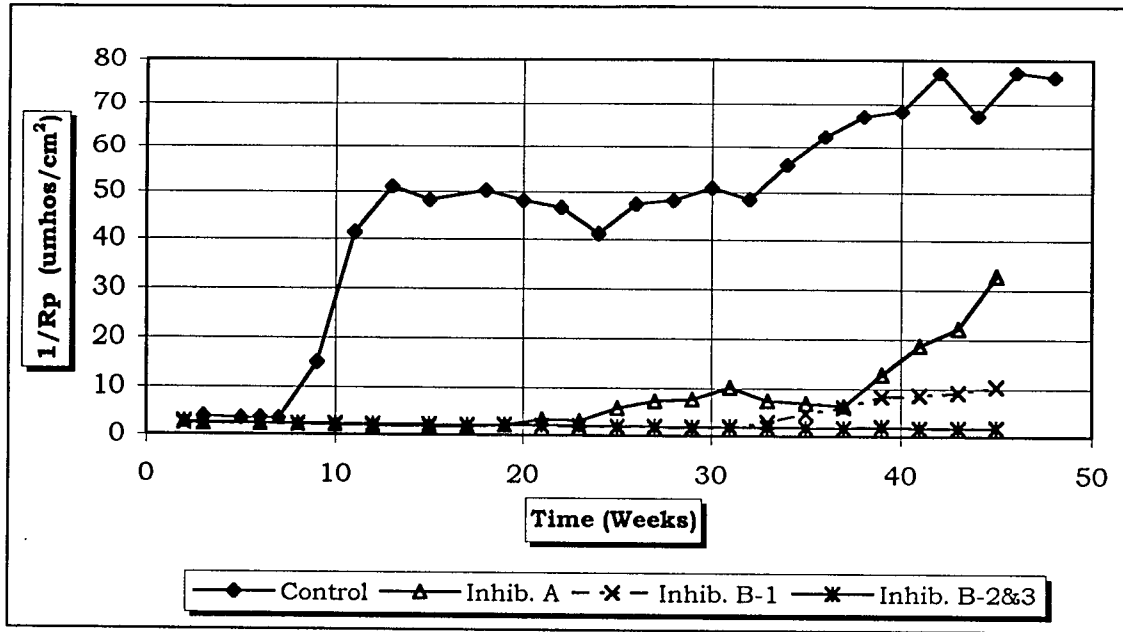


Figure 7.11 Corrosion Rate, 3-Inch Cylinders: Control, Inhibitors A and B Mixes.

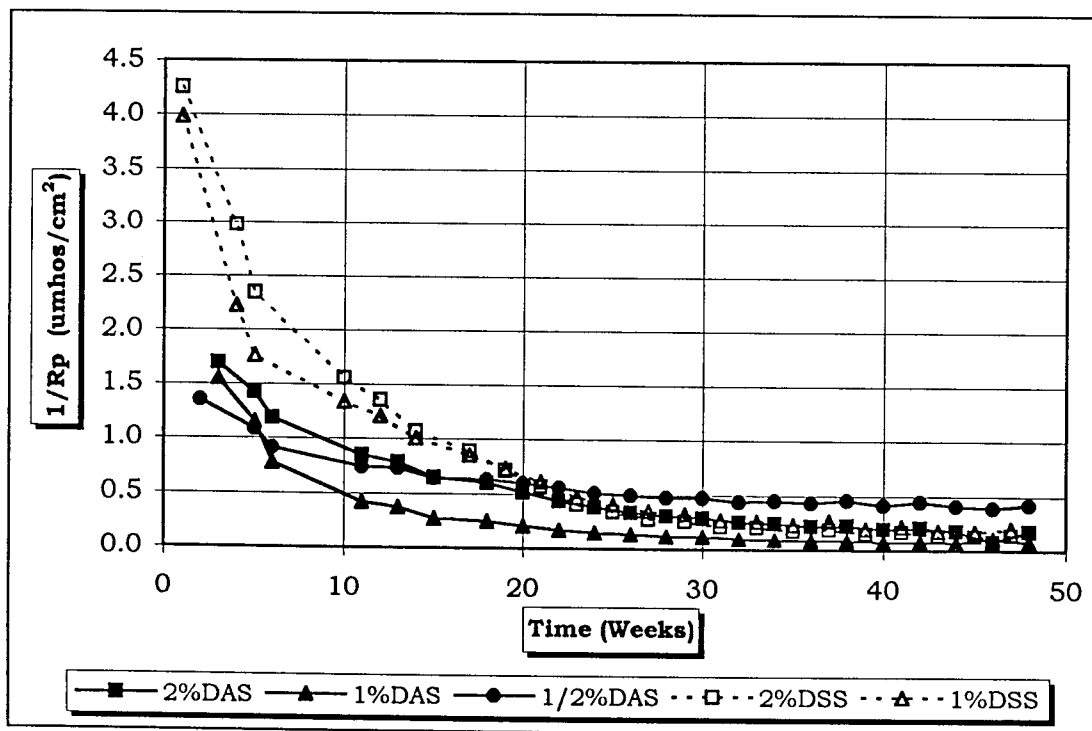


Figure 7.12 Corrosion Rates, 3-Inch Cylinders: DAS and DSS Mixes.

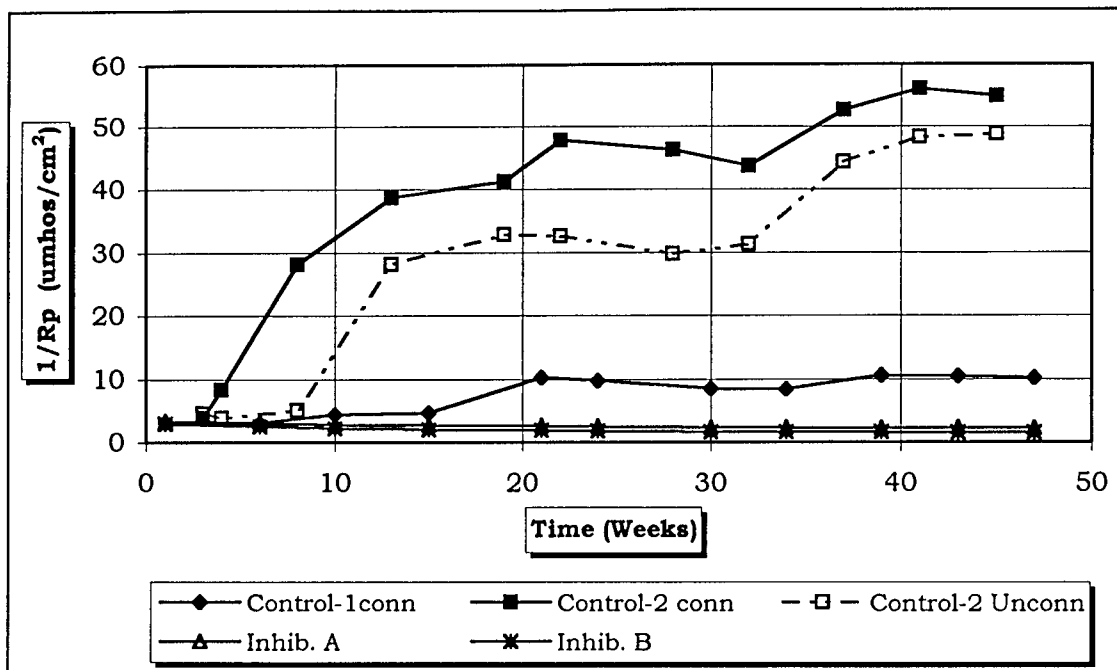


Figure 7.13 Corrosion Rate, Slabs: Control, Inhibitors A and B Mixes.

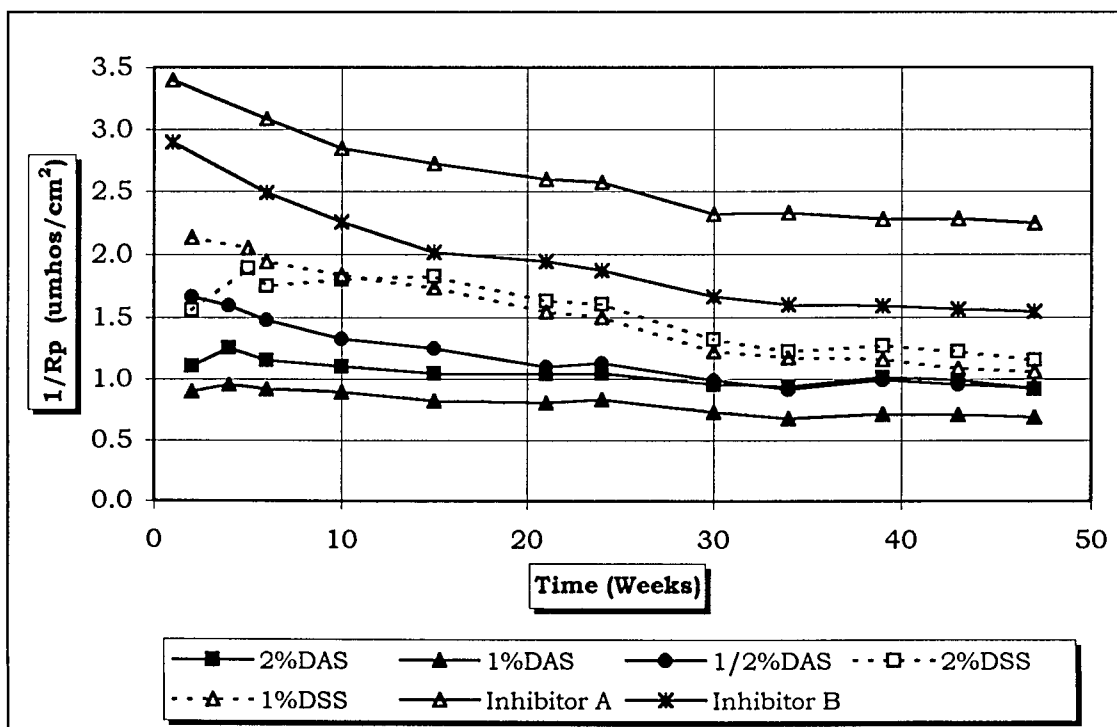


Figure 7.14 Corrosion Rate, Slabs: DAS, DSS, Inhibitor A and B Mixes.

**Table 7.1 Corrosion Mixes: Average Time To Corrosion.**

Mix Type	2-Inch Lollipop (weeks)	3-Inch Lollipop (weeks)	Slab (weeks)
Control -1	----	----	15
Control - 2	5	9	----
Control - 2-conn	----	----	4
Control - 2-unconn	----	----	8
Inhibitor A	9	25	*
Inhibitor B	14	39 <sup>1</sup>	*
2% DAS	*	*	*
1% DAS	*	*	*
1/2% DAS	*	*	*
2% DSS	*	*	*
1% DSS	30 <sup>1</sup>	*	*

\* No corrosion had occurred after about 48 weeks for the lollipops and 45 weeks for the slabs

<sup>1</sup> Corrosion only initiated in one of three specimens.

**Table 7.2 Corrosion Rates for all Specimens at Approximately 47 Weeks.**

Mix Type	2-Inch Lollipop ( $\mu\text{mhos}/\text{cm}^2$ )	3-Inch Lollipop ( $\mu\text{mhos}/\text{cm}^2$ )	Slab ( $\mu\text{mhos}/\text{cm}^2$ )
Control -1	----	----	10
Control - 2	133	76	----
Control - 2-conn	----	----	55
Control - 2-unconn	----	----	48
Inhibitor A	169	33	2.3
Inhibitor B	80	1.8 <sup>1</sup>	1.5
2% DAS	0.16	0.18	0.92
1% DAS	0.07	0.08	0.69
1/2% DAS	0.42	0.42	0.93
2% DSS	0.25	0.14	1.2
1% DSS	0.22 <sup>1</sup>	0.20	1.1

<sup>1</sup> Corrosion rate based on average of specimens No.2 and No.3 only.

### 7.3.2 Control Specimens

Corrosion initiated in the control 2-inch and 3-inch diameter lollipop specimens after 5 and 9 weeks of cycling, respectively. Increasing the concrete cover by 1/2-inch, from 3/4 to 1-1/4 inch, delayed the initiation of corrosion by about a factor of two. There was a significant difference in time to corrosion between the Control-1 and Control-2 slab specimens. The reason for this is not known at this time.

The slab Control-2-unconn specimens had corrosion initiate at 8 weeks, twice the 4 weeks of the Control-2-conn specimens. This result was expected since the connected specimens function both as a micro-cell and as a macro-cell (i.e., localized and galvanic corrosion), whereas the unconnected specimens function only as a micro-cell.

At 48 weeks of monitoring, the corrosion rates were 133  $\mu\text{mhos}/\text{cm}^2$  and 77  $\mu\text{mhos}/\text{cm}^2$  for the 2-inch and 3-inch diameter lollipop, respectively. After 45 weeks of monitoring, the Control-1-conn, Control-2-conn and Control-2-unconn slab specimens had corrosion rates of 10  $\mu\text{mhos}/\text{cm}^2$ , 55  $\mu\text{mhos}/\text{cm}^2$  and 49  $\mu\text{mhos}/\text{cm}^2$ , respectively.

### 7.3.3 Inhibitor A and Inhibitor B Specimens

Inhibitor A had corrosion initiate after 9 weeks for the 2-inch diameter lollipop specimens and after 25 weeks for the 3-inch diameter specimens. Therefore, Inhibitor A delayed the onset of corrosion by a factor of about 2 to 3 when compared to the control lollipop specimens (5 and 9 weeks for the 2-inch and 3-inch lollipops, respectively). At the end of approximately 47 weeks of monitoring, the maximum corrosion rate in the 2-inch and 3-inch lollipop specimens was about 170  $\mu\text{mhos}/\text{cm}^2$  and 35  $\mu\text{mhos}/\text{cm}^2$ , respectively.

After 30 weeks, the corrosion rate for the 2-inch diameter lollipop exceeded the corrosion rate of the control specimens. This could be an indication that there was an insufficient amount of Inhibitor A present after 30 weeks, and thus corrosion was accelerated for reasons described in Section 2.6. After 45 weeks of cycling, the slabs specimens showed no signs of corrosion.

The Inhibitor B 2-inch diameter lollipop specimens started to corrode after 14 weeks and had an averaged maximum corrosion rate of about  $80 \mu\text{mhos}/\text{cm}^2$ . Only one 3-inch diameter lollipop specimen, Inhibitor B-1, had corrosion initiate after 39 weeks of cycling. It had a relatively low corrosion rate of approximately  $10 \mu\text{mhos}/\text{cm}^2$  after 48 weeks. The solution resistances of the 3-inch diameter lollipop specimens for Inhibitor B were about the same when compared to each other. Therefore, the Inhibitor B data shown in Figure 7.4 was based on the average of all specimens. The slab specimens showed no signs of corrosion after 45 weeks of cycling exposure.

#### 7.3.4 DAS and DSS Specimens

Except for the dropped and damaged specimen, none of the DAS or DSS specimens, lollipops or slabs, had corrosion initiate. Calculated corrosion rates decreased with time. After 48 weeks of exposure, all DAS and DSS lollipop and slab specimens had corrosion rates below  $0.5 \mu\text{mhos}/\text{cm}^2$  and  $1.5 \mu\text{mhos}/\text{cm}^2$ , respectively, very low values. It should be noted that even if corrosion is not actually initiated, the calculated corrosion rate will always have a value unless the polarization resistance has a value of infinity, as shown in the equation used to calculate a corrosion rate:

$$\text{Corrosion rate} \propto \frac{1}{R_p}$$

Recall that the 2-inch diameter lollipop specimen ,1%DSS-1, which had corrosion initiate, had been dropped and cracked (Section 7.2.4). If this specimen had not been cracked, it is unlikely that corrosion would have occurred. Even so after 48 weeks, or 23 weeks after the crack developed, the corrosion was still minimal, only 5  $\mu\text{mhos}/\text{cm}^2$  ( 9  $\mu\text{mhos}/\text{cm}^2$  maximum).

These results indicated an excellent performance by these two chemicals, especially in low concrete cover environments, as shown with the 2-inch diameter specimens. The 1%DAS specimens, both lollipops and slabs, consistently had the lowest corrosion rate out of all specimen types and mixes. The general corrosion performance trend, lowest corrosion rate to highest corrosion rate after about 47 weeks, for the lollipops specimens was 1%DAS, 2%DAS, 1%DSS, 2%DSS, 1/2%DAS, Inhibitor B, Inhibitor A, and Control mixes. The slabs had a similar trend, except that the 1/2% DAS mix had the third lowest rate. All other mixes stayed in the same order thereafter.

## 7.4 VISUAL EXAMINATION OF SPECIMENS

### 7.4.1 General

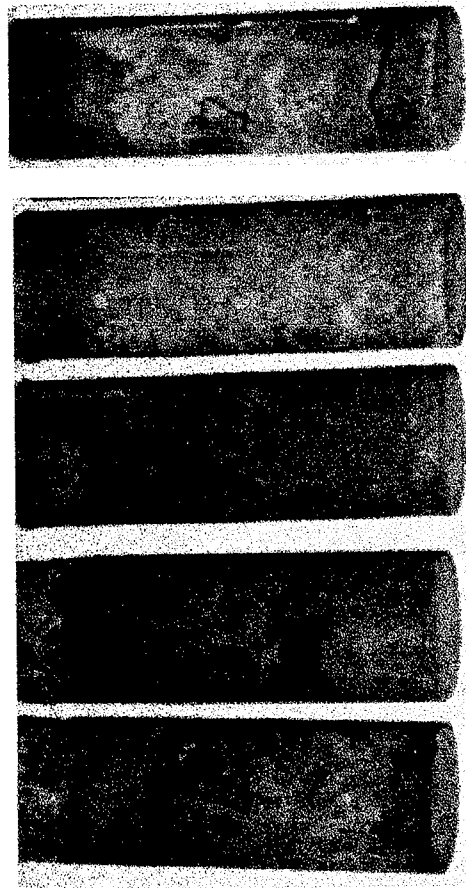
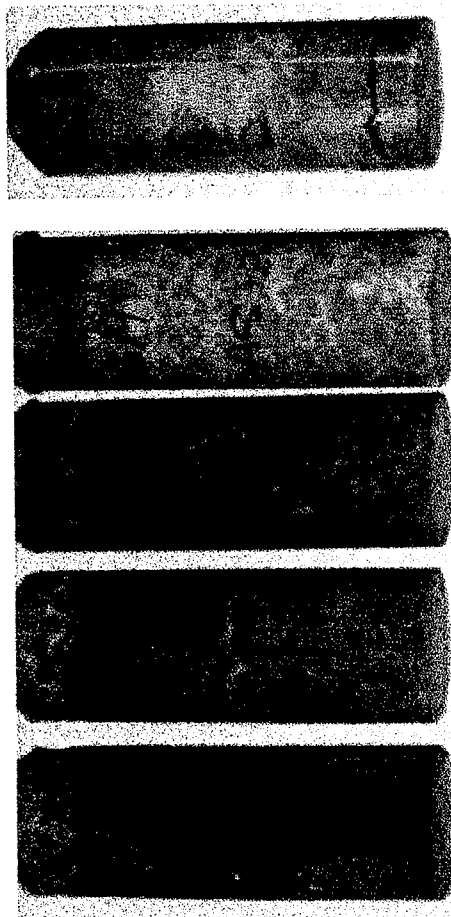
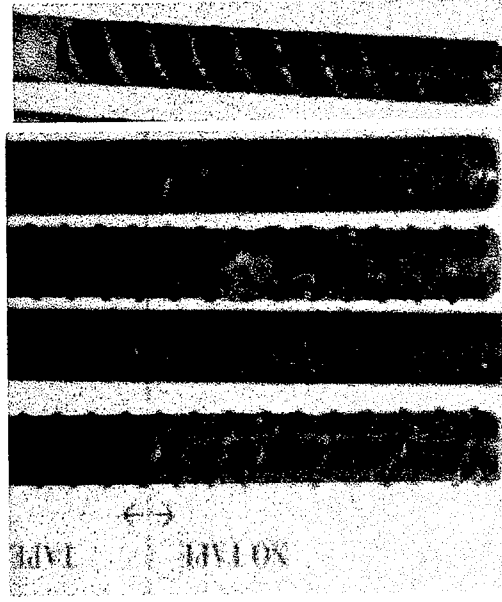
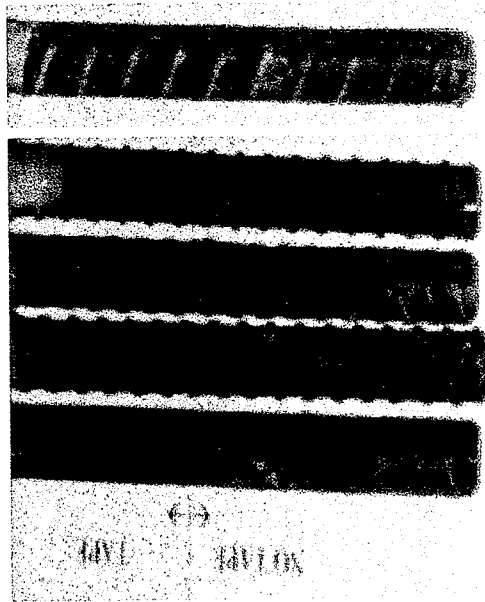
One specimen from each series of lollipop specimens, both standard and "cracked", and slabs specimens was saw cut longitudinally, split open and visually inspected. Since corrosion was not observed in the 2-inch diameter DAS and DSS specimens, no 3-inch

diameter DAS or DSS specimens were cut open and only one 1/2%DAS slab specimen, out of all the DAS and DSS slab specimens, was cut open and visually examined.

Photographs for all specimens that were visually examined are shown in Figures 7.15, 7.16, 7.17 (a & b), and 7.18 (a & b). The letters C, A, and B in these Figures refer to Control, Inhibitor A, and Inhibitor B specimens, respectively. Black magic marker lines on the exterior concrete surface trace cracks that formed over time due to the build up of corrosion byproduct. The top and bottom rows of photos in Figures 7.15 and 7.16 show the front and back views, respectively, of the concrete lollipops and reinforcing bars. Quantitative analyses of the total corroded area on the reinforcing bar of each specimen examined are tabulated in Tables 7.3, 7.4, and 7.5.

Corrosion on the reinforcing bars was generally localized, but was in varying degrees of severity. Immediately after a specimen was cut open, the corrosion products on the reinforcing bar were usually dark green/black in color, which indicated they were in the form of ferrous hydroxide. After a short time of exposure to laboratory air, the corrosion products turned to a red rust color, indicating a transformation into ferric hydroxide due to the abundance of oxygen, as discussed in Chapter 2.0. Some minor corrosion was found under the electroplater's tape of some specimens (crevice corrosion), which indicated that either the amount of tape used was deficient or the tape was not effective at protecting the steel.

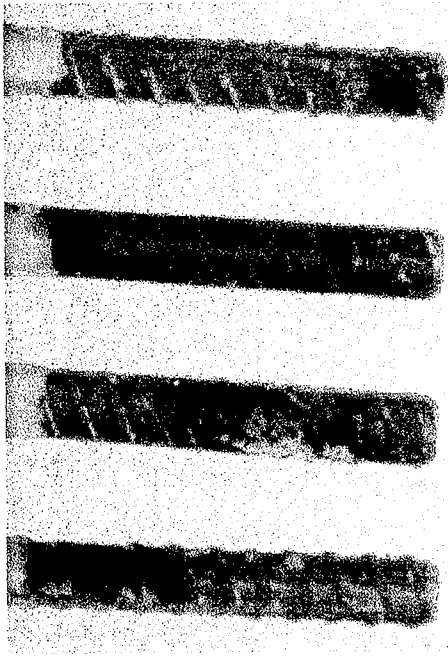




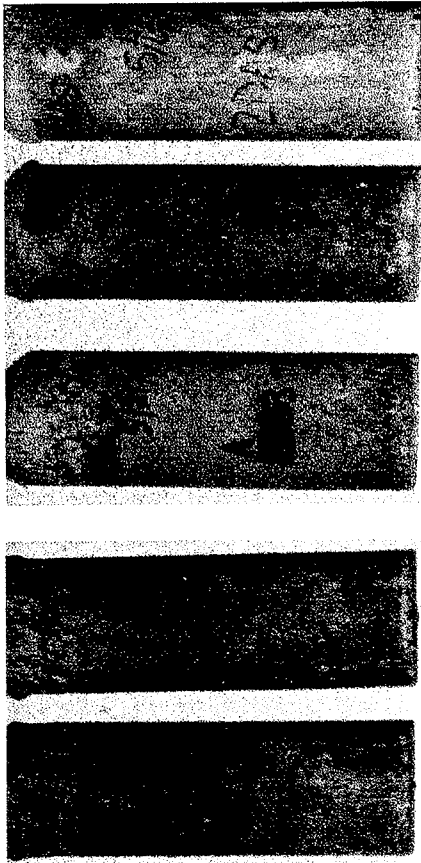
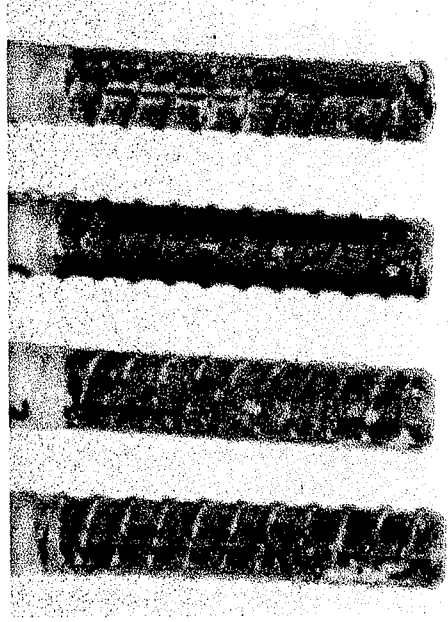
C-4    A    B    2%DAS    1%DSS

Figure 7.15 Visually Examined 2-Inch Diameter Lollipop Specimens.





C-3 C-4 A B



C-3 C-4 A B 2%DAS

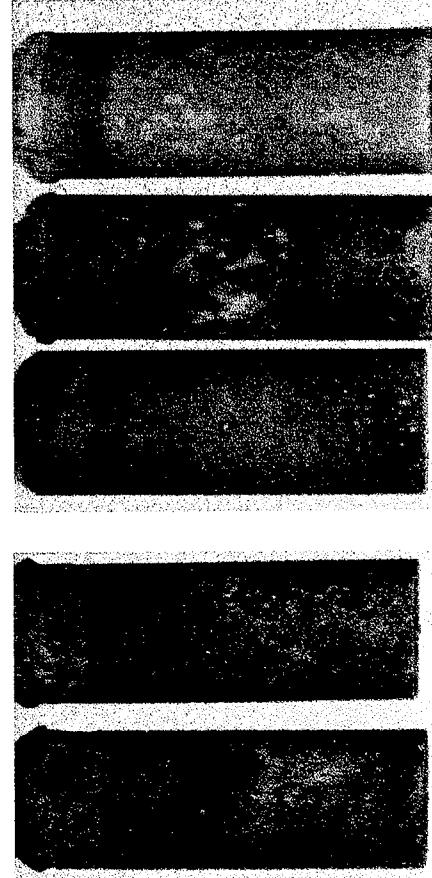
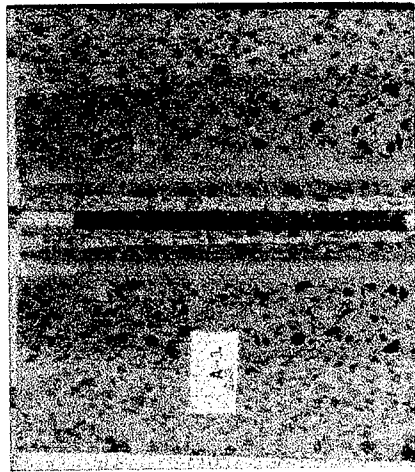
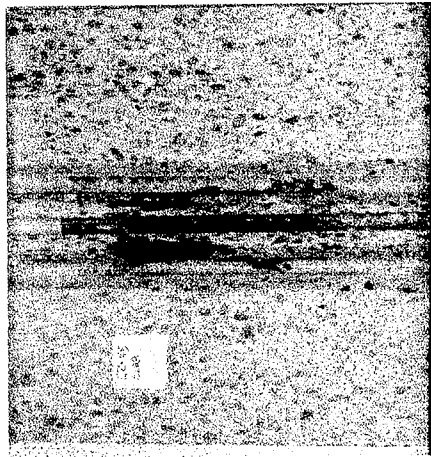


Figure 7.16 Visually Examined 3-Inch Diameter Lollipop Specimens.

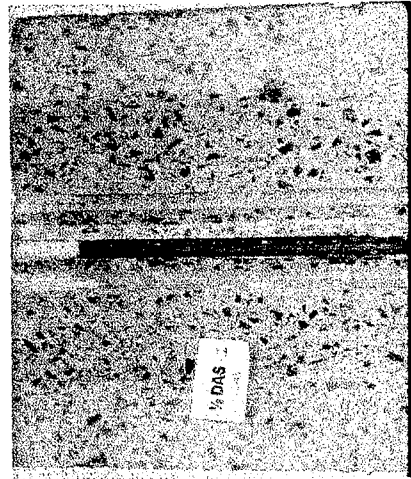




Inhibitor A



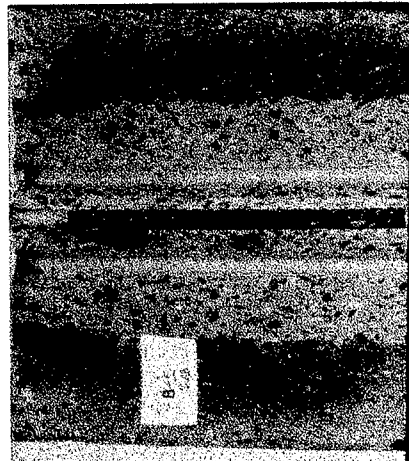
C2-5



1/2%DAS



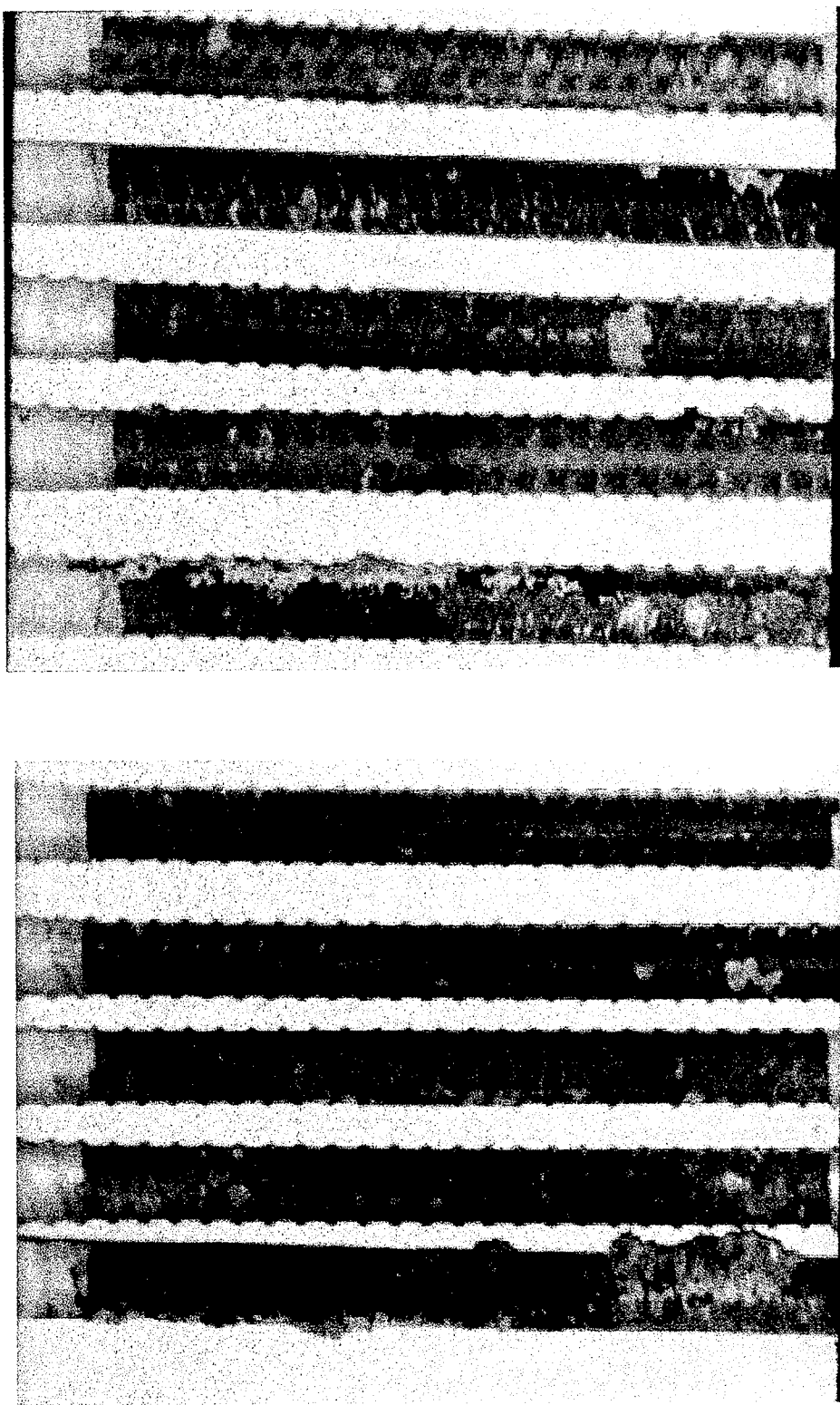
C2-2



Inhibitor B

Figure 7.17a Visually Examined Slab Specimens.





1/2%DAS

Back

C2-2

1/2%DAS

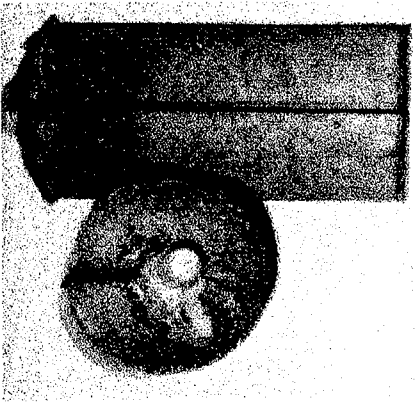
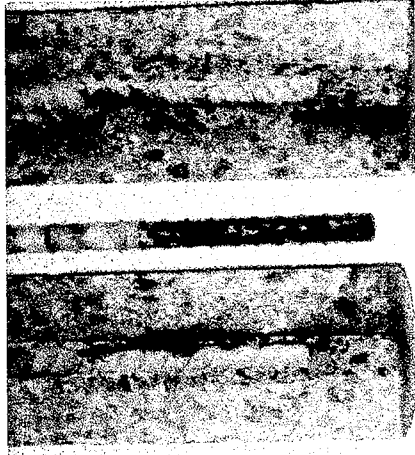
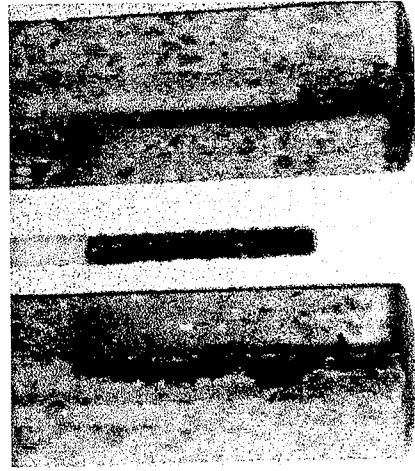
Front

C2-2

Figure 7.17b Visually Examined Slab Specimens, Continued.



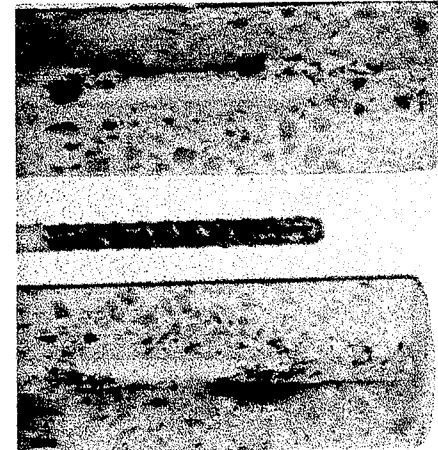
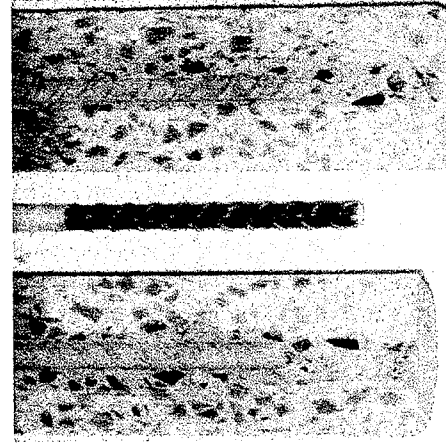
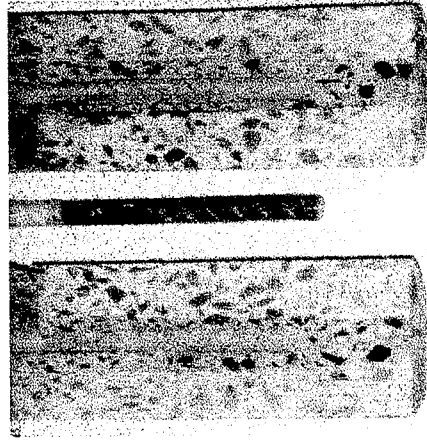




Inhibitor A

Control

Typical Specimen



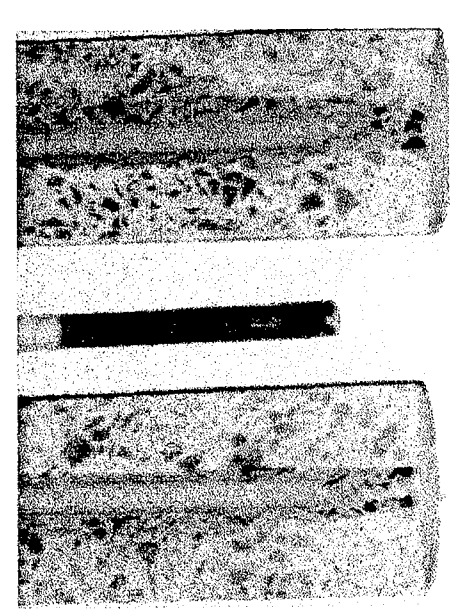
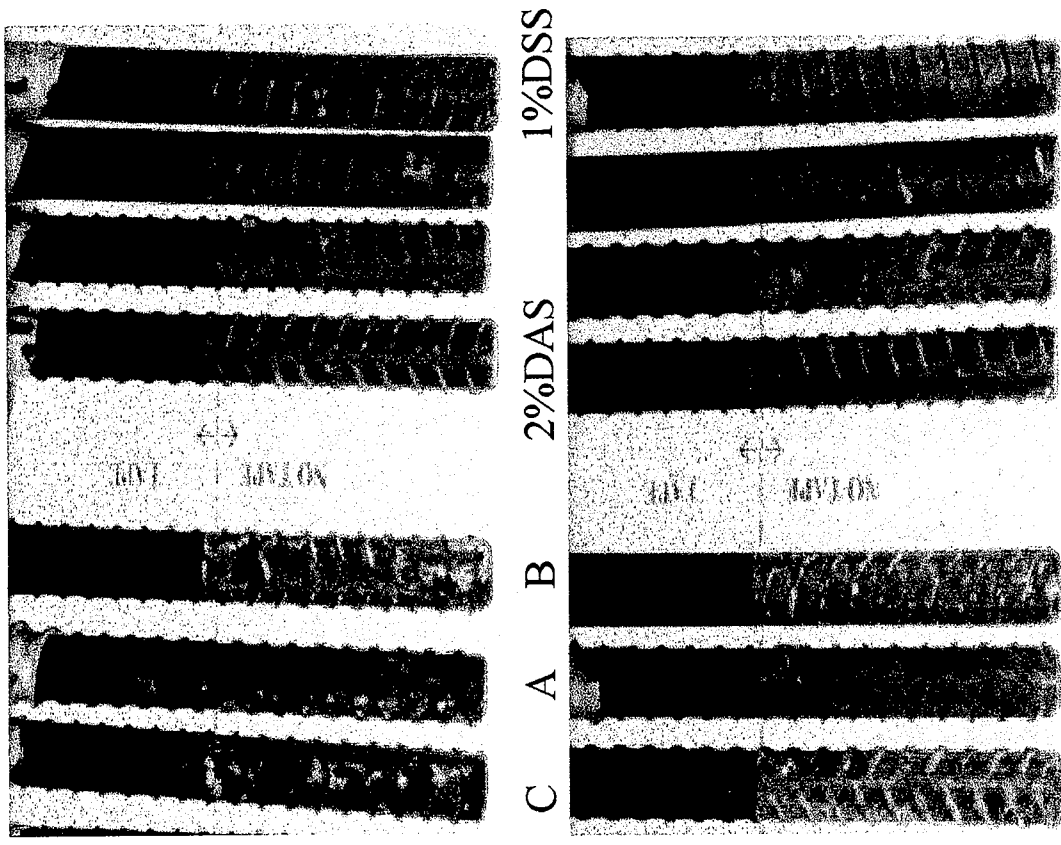
1%DAS

2%DAS

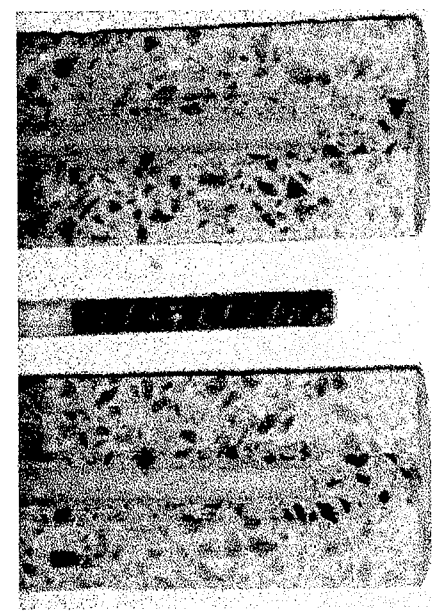
Inhibitor B

Figure 7.18a Visually Examined 3-Inch Diameter "Cracked" Lollipop Specimens.





2%DSS



1%DSS

Figure 7.18b Visually Examined 3-Inch Diameter "Cracked" Lollipop Specimens, Continued.



**Table 7.3 Visual Inspection Results for the Standard Lollipops.**

Specimen <sup>1</sup>	2-inch Diameter Lollipops		3-inch Diameter Lollipops	
	Total Corrosion Area (%)	Heavy Corr. Area (%)	Total Corrosion Area (%)	Heavy Corr. Area (%)
Control-2-#3	---	---	20	20
Control-2-#4	11	11	19	19
Inhibitor A-3-#1	13	13	9	0
Inhibitor B-3-#2	57	57	3	0
2%DAS-2-#3	0	0	---	---
1%DAS-2-#3	0	0	---	---
1/2%DAS-2-#3	0	0	---	---
2%DSS-2-#3	0	0	---	---
1%DSS-2-#1 <sup>2</sup>	1	0	---	---

<sup>1</sup> First number after specimen name indicates batch No. and second number indicates specimen No.

<sup>2</sup> Specimen was dropped and cracked as stated in Section 7.2.4.

**Table 7.4 Visual Inspection Results for the Slab Specimens.**

Specimen <sup>1</sup>	Total Area With Corrosion (%)	Area With Heavy Corrosion (%)
Control-2-#2 conn	44	44
Control -2-#5 unconn	31	31
Inhibitor A-1-#1	0	0
Inhibitor B-1- #1	0	0
1/2%DAS-1-#1	0	0

<sup>1</sup> First number after specimen name indicates batch No. and second number indicates specimen No.

**Table 7.5 Visual Inspection Results for the "Cracked" Lollipops.**

Specimen <sup>1</sup>	Total Area With Corrosion (%)	Area With Heavy Corrosion (%)
Control-1-#3	21	21
Control-1-#9	21	21
Inhibitor A-2-#1	33	33
Inhibitor B-2-#1	12	12
2%DAS-1-#1	~ 0	0
1%DAS-1-#2	2	2
2%DSS-1-#1	1/2	0
1%DSS-1-#2	1/2	0

<sup>1</sup> First number after specimen name indicates batch No. and second number indicates specimen No.

#### 7.4.2 Corrosion Monitored Specimens

Visual examination results of the lollipop and slab specimens correlated well with results from the linear polarization testing. All specimens that had indicated corrosion occurring during the linear polarization testing were, in fact, actively corroding. Also, specimens with linear polarization results that implied no corrosion was occurring had no signs of corrosion when examined.

The DAS and DSS lollipop and slab specimens had an impressive performance (Table 7.3 and 7.5). The superb condition of the concrete exterior of all the 2-inch diameter and 3-inch diameter DAS and DSS specimens was very similar and therefore, only a 2%DAS specimen is shown in Figure 7.15 and Figure 7.16. Also, the 2-inch diameter 1%DAS specimen that was dropped is shown in Figure 7.15. Note that in Figure 7.16, the rebar for the 2%DAS lollipop specimen is not shown since it was not cut open (as stated above).

The 2-inch diameter lollipop specimens had the most dramatic visual results (Fig. 7.15 ). The 2-inch diameter Control, Inhibitor A and Inhibitor B specimens had numerous cracks and/or rust stains on the exterior of the concrete, whereas the DAS and DSS specimens did not.

Only some of the Control specimens, out of all the other 3-inch diameter lollipops (Figure 7.16) and slab specimens (Figure 7.17 a & b), had cracking and/or rust stains visible on the exterior surface of the concrete. Note that the darken areas on the concrete of the Inhibitor B slab specimen (Figure 7.17a) is due to moisture from the saw cutting process.

#### **7.4.3 "Cracked" Lollipop Specimens**

The visual results ( Figure 7.18 a & b, and Table 7.5) show the dramatic reduction in corrosion even in "pre-cracked" specimens containing DAS or DSS. The "cracked" DAS and DSS specimens had only very minor corrosion indicating very good protection of the rebar. The corrosion that did occur in the DAS and DSS concretes was very localized at the saw cut and was usually at a defect (e.g. large air bubble) in the concrete immediately over the reinforcing bar. Furthermore, the corrosion did not spread around the perimeter of the bar due to the low absorption/permeability properties of the DAS and DSS concrete. For specimens without DAS or DSS, the corrosion was much more severe and extended around the bar perimeter.

## 7.5 CORROSION SUMMARY

After approximately one year of salt exposure for the lollipop specimens (2- inch and 3-inch diameter) and slab specimens, DAS and DSS prevented corrosion from initiating. After about six months of salt exposure for the "cracked" lollipop specimens, DAS and DSS either prevented the initiation of corrosion or reduced the amount of corrosion dramatically (Table 7.5). Adding DAS or DSS to concrete significantly increased the concrete's solution resistance, especially when the drying cycles were 100°F. DAS and DSS acted as dual protection inhibitors by reducing the permeability of the concrete as well as inhibiting corrosion even when chlorides were present at the bar.

All the concentrations of DAS and DSS tested performed extremely well. If the best performing mix had to be selected based on corrosion performance and economics, either the 1/2% DAS mix or the 1%DSS mix would be selected. Each was the lowest concentration tested of each chemical, but still prevented corrosion from initiating in all specimen types. A problem was encountered with the DAS chemical whereby a strong ammonium odor developed during the mixing and hydration processes. No unusual odor occurred when the DSS chemical was used.

Inhibitor A and Inhibitor B delayed onset of corrosion, to varying degrees, in the lollipop specimens, but did not prevent corrosion from initiating. No corrosion initiated in Inhibitor A and Inhibitor B slab specimens after approximately one year of testing.

The lollipops were better corrosion specimens than the slabs. The slabs were very awkward to handle, required a large storage area and were more susceptible to localized polarization effects due to specimen geometry. Whereas, the lollipop specimens were



handled and stored quite easily and efficiently, and the circular geometry greatly reduced localized effects during polarization. The 2-inch diameter lollipop specimens gave results within a relatively short time period. Whereas, the 3-inch diameter lollipops and slab specimens required a longer testing period to obtain results.

## **7.6 OVERALL PERFORMANCE SUMMARY: DAS AND DSS CHEMICALS**

When the corrosion, freeze-thaw, absorption, and strength results for the DAS and DSS concretes are analyzed, certain distinctive characteristics of these chemicals in concrete become apparent:

1. Increasing the concentration of DAS or DSS increased the impermeability of the concrete (see Appendix B) and also lowered the compression strength of the concretes (see Appendix C).
2. The percent concentration of DAS and DSS didn't seem to have much effect on corrosion performance or freeze-thaw performance ( at 300 cycles) (see Appendix A).
3. Using the de-foaming agent increased the compression strength of the DAS and DSS concretes significantly, but generally did not have a notable effect on the permeability characteristics of the concretes or their freeze-thaw performance. No reduced air mixes were evaluated in the corrosion program.

If the better chemical of the two, either DAS or DSS, had to be selected, the DSS chemical would be chosen, based on its excellent corrosion, freeze-thaw and absorption

performance. Even though the compression strengths of the DSS mixes were commonly the lowest, they had strengths of about 4000 psi or higher (especially in the lower concentrations of DSS), which does satisfy the requirements of ConnDot's Class "F" concrete for bridges. Furthermore, there was no ammonium odor produced with the DSS concrete, unlike the DAS concrete which did produce a strong ammonium odor.

## CHAPTER 8.0

### CONCLUSIONS AND RECOMMENDATIONS

#### 8.1 CONCLUSIONS

Based on the results to date of the corrosion program being performed at the University of Connecticut, the following conclusions have been made:

1. DAS and DSS act as dual protection inhibitors by reducing permeability and inhibiting corrosion. Adding DAS or DSS to concrete prevented corrosion from initiating in lollipop specimens (2-inch and 3-inch diameter) and slab specimens, and prevented or dramatically reduced corrosion in "cracked" lollipops (see Sections 7.3 and 7.4).
2. The solution resistance of the concrete was increased significantly by adding DAS or DSS (see Section 7.2.4).
3. The DSS chemical had better overall performance than the DAS chemical. Furthermore, no odor problems were encountered when DSS was added to cement.
4. A strong ammonium odor was produced when DAS was added to cement.
5. Inhibitor A and Inhibitor B delayed corrosion onset, to varying degrees, in the lollipop specimens, but did not prevent corrosion from initiating.
6. No corrosion initiated in Inhibitor A and Inhibitor B slab specimens after approximately one year of testing.
7. The lollipop specimens were more efficient specimens than the slab specimens.

8. The 2-inch diameter lollipop specimens made of concrete (not mortar) can be used to evaluate the corrosion performance of new and existing corrosion inhibitors or permeability-reducing-admixtures for use in concrete.
9. The 2-inch diameter lollipop specimens produced reliable corrosion results in a much shorter time period than the 3-inch diameter lollipops or slab specimens.
10. Linear polarization proved to be a dependable method for measuring instantaneous corrosion rates of all the specimens types (see Chapter 7.0).
11. Linear polarization results corresponded quite well to the visual examination of the specimens (see Section 7.4).
12. Positive Feedback was generally an accurate and reliable method for measuring and accounting for the IR drop (see Chapter 6.0).

## **8.2 RECOMMENDATIONS FOR FUTURE RESEARCH**

1. Continue monitoring existing lollipop corrosion specimens, both standard and "cracked", and slab corrosion specimens.
2. Evaluate the corrosion performance of DAS and DSS at concentrations lower than 1/2% using 2-inch diameter lollipop specimens and 3-inch diameter standard and "cracked" lollipop specimens. Also perform absorption testing and compression strength testing on these concentrations.
3. Evaluate the corrosion performance of DAS and DSS concrete with de-foaming agent added.
4. Repeat the freeze-thaw testing with the same (and lower) concentrations of

DAS and DSS, but allow the prisms to dry for about a week, after curing, before testing.

5. Perform electrochemical tests using the DAS and DSS chemicals with only reinforcing steel to obtain the corrosion inhibiting performance of these chemicals on bare steel.
6. Measure the chloride concentration at the level of the reinforcing bar in the concrete specimens.

## REFERENCES

- [1] Walker, H. C., "Parking Structure Durability", *Concrete International*, Vol. 20, No.7, July, 1998, pp. 53-54.
- [2] McDonald, D. B., "Design Options for Corrosion Protection", *Concrete 95 Toward Better Concrete Structures*, Brisbane, Australia, 4-7 September 1995, pp.1-9.
- [3] Clear, K. C., Hartt, W. H., McIntyre, J., Lee, S. K., "Performance of Epoxy-Coated Reinforcing Steel in Highway Bridges", National Cooperation Highway Research Program Report No. 370, Transportation Research Board, 1995.
- [4] Berke, N. S. "Corrosion Inhibitors in Concrete", *Concrete International*, Vol. 13, No. 7, July 1991, pp. 24-27.
- [5] Craig, R. J., Wood, L. E., "Effectiveness of Corrosion Inhibitors and Their Influence on the Physical Properties of Portland Cement Mortars", *Highway Research Record*, No. 328, 1970, pp. 77-88.
- [6] Trepanier, S. M., "Effectiveness of Corrosion Inhibitors in Reinforced Concrete", *Masters Thesis - Queen's University*, Kingston, Ontario, Canada, April, 1994.
- [7] Fontana, M. G., *Corrosion Engineering*, 3<sup>rd</sup> Ed., McGraw Hill, Inc., New York, NY, 1986.
- [8] Scannell, W. T., Sohaghpurwala, A. A., Islam, M., "Assessment of Physical Conditions of Concrete Bridge Components", *FHWA - SHRP Showcase*, US Department of Transportation Federal Highway Administration, July, 1996.
- [9] Lorentz, T., French, C., Leon, R. T., "Corrosion of Coated and Uncoated Reinforcing Steel in Concrete", *Structural Engineering Report No. 92-03*, University of Minnesota Center of Transportation Studies, May, 1992.
- [10] Uhlig, H. H., Revie, R. W., *Corrosion and Corrosion Control - An Introduction to Corrosion Science and Engineering*, 3<sup>rd</sup> Ed., Wiley & Sons, New York, 1985.
- [11] Kruger, J., "The Nature of the Passive Film on Iron and Ferrous alloys", *Corrosion Science*, Vol. 29, No. 2/3, pp. 149-162, 1989
- [12] Toney, M. F., Davenport, A. J., Oblonsky, L. J., Ryan, M. P., Viturs, C. M., "Atomic Structure of the Passive Oxide Film Formed on Iron", *Physical Review Letters*, Vol. 79, No. 21, pp. 4282-4285, 1997.

- [13] Locke, C. E., "Corrosion of Steel in Portland Cement Concrete: Fundamental Studies", *ASTM Special Technical Publication- Symposium on Corrosion Effects of Stray Currents and The Techniques For Evaluating Corrosion of Rebars in Concrete*, STP 906, Nov. 28, 1984, Willamsburg, VA, pp. 5-13.
- [14] Zhang, H., Wheat, H. G., Sennour, M. L., Carrasquillo, R. L., "Corrosion of Steel Bars in Concrete Containing Different Chemical and Mineral Admixtures", *Material Performance*, December 1992, pp. 37-43.
- [15] Borgard, B., Warren, C., Somayaji, S., Heidersbach, R., "Mechanisms of Corrosion of Steel in Concrete", *ASTM Special Technical Publication Symposium on Corrosion Rates of Steel in Concrete*, STP 1065, August 1990, Baltimore, MD, pp. 174-187.
- [16] Berke, N. S., Stark, P., "Calcium Nitrate As An Inhibitor: Evaluation And Testing For Corrosion Resistance", *Concrete International*, September 1985, pp. 42-47.
- [17] Cho, H., Lee, H., Hansen, C., "Laboratory Experiment to Measure Corrosion of Rebar Embedded in Concrete with Corrosion Inhibiting Admixtures", *Transportation Research Board 76 Annual Meeting*, Washington, DC, Jan. 12-16, 1997, Paper No. 97-1304.
- [18] Pfeifer, D. W., Landgren, J. R., Zoob, A., "Protective Systems for New Prestressed and Substructure Concrete", *Report No. FHWA-RD-86-193*, Federal Highway Administration, April 1987.
- [19] Clear, K. C., "Time-To-Corrosion of Reinforcing Steel in Concrete Slabs", *Report No. FHWA-RD-76-70*, Federal Highway Administration, April 1976.
- [20] ASTM C 876 - 91, "Standard Test Method for Half-Cell Potentials of Uncoated Reinforcing Steel in Concrete", *Annual Book of ASTM Standards*, 1991, pp. 434-439.
- [21] Pfeifer, D. W., Landgren, J. R., Krauss, P. D., "Investigation For CRSI on CRSI-Sponsored Corrosion Studies At Kenneth C. Clear Inc., WJE No. 911461", *CRSI Performance Research: Epoxy Coated Reinforcing Steel*, CRSI Final Report - June, 1992.
- [22] ASTM G-109- 92, "Standard Test Method for Determining the Effects of Chemical Admixtures on the Corrosion of Embedded Steel Reinforcement in Concrete Exposed to Chloride Environments", *Annual Book of ASTM Standards*, 1992, pp. 452-455.

- [23] Nami, C. K., Farrington, S. A., Bobrowski, G. S., "OrganicBased Corrosion Inhibiting Admixture for Reinforced Concrete", *Concrete International*, Vol. 14, April 1992, pp. 45-51.
- [24] Stern, M., "A Method For Determining Corrosion Rates From Linear Polarization Data", *Corrosion*, Vol. 14, September 1958, pp. 440t-444t.
- [25] Hack, H. P., Moran, P. J., Scully, J. R., "Influence of Electrolyte Resistance on Electrochemical Measurements and Procedures to Minimize or Compensate for Resistance Errors", *ASTM Special Technical Publication Symposium - The Measurements and Correction of Electrolyte Resistance in Electrochemical Tests*, STP 1056, May, 1988, Baltimore, MD, pp. 5-26.
- [26] EG&G Princeton Applied Research, *Model 273A Potentiostat/Galvanostat User's Guide*, 1993.
- [27] Ehrhart, W. C., "IR Drop in Electrochemical Corrosion Studies - Part 2: A Multiple Method IR Compensation System", *ASTM Special Technical Publication Symposium - The Measurements and Correction of Electrolyte Resistance in Electrochemical Tests*, STP 1056, May, 1988, Baltimore, MD, pp. 78-94.
- [28] McDonald, D. B., Pfeifer, D. W., Krauss, P. D., Sherman, M. R., "Test Methods For New Breeds of Reinforcing Bars", *Corrosion and Corrosion Protection of Steel in Concrete, Proceedings of International Conference held at the University of Sheffield*, 24 - 28 July, 1994, pp. 1155-1171.
- [29] Taylor, S. R., Mason, S. E., Cella, P. A., Clemena, G. G., "An Investigation of New Inhibitors to Mitigate Rebar Corrosion in Concrete", *Report No. FHWA/VA-96-R24*, Virginia Transportation Research Council, April 1996.
- [30] Berke, N. S., Stark, P., "Calcium Nitrate As An Inhibitor: Evaluation And Testing For Corrosion Resistance", *Concrete International*, September 1985, pp. 42-47.
- [31] Berke, N. S., Shen, D. F., Sundberg, K. M., "Comparison of the Polarization Resistance Technique to the Macrocell Corrosion Technique", *ASTM Special Technical Publication Symposium on Corrosion Rates of Steel in Concrete*, June 28, 1988 n 1065 August 1990, Baltimore, MD, pp. 38-51.
- [32] Nmai, C. K., Bury, M. A., Farzam, H., "Corrosion Evaluation of a Sodium Thiocyanate-Based Admixture", *Concrete International*, Vol. 16, April 1994, pp. 22-25.



- [33] Gu, P., Elliot, S., Hristova, R., Beaudion, J. J., Brousseau, R., Baldock, B., "A Study of Corrosion Inhibitor Performance in Chloride Contaminated Concrete by Electrochemical Impedance Spectroscopy", *ACI Material Journal*, Sept.-Oct. 1997.
- [34] McDonald, D. B., Pfeifer, D. W., Krauss, P. D., "The Corrosion Performance of Reinforcing Steel in Concretes Containing Calcium Nitrate, Rheocrete 222 and Rheocrete 222+ During 48-weeks of In-Concrete Testing for Master Builders, Inc", *WJE Report No. 951286*, Wiss, Janney, Elstner Associated, Inc, July 1997.
- [35] Tourney, P., Berke, N. S., "A Call for Standardized Tests for Corrosion Inhibiting Admixtures", *Concrete International*, April 1993, pp. 57-62.
- [36] Gannon, E. J., Cady, P. D., "Condition Evaluation of Concrete Bridges Relative to Reinforcement Corrosion - Vol. 1: State-of-the-Art of Existing Methods", *SHRP - S-323*, Strategic Highway Research Council, Washington, DC, 1993.
- [37] Cady, P. D., Flis, J., Sehgal, A., Li, D., Kho, Y. T., Sabol, S., Pickering, H., Osseo-Asare, K., "Condition Evaluation of Concrete Bridges Relative to Reinforcement Corrosion - Vol. 2: Method for Measuring the Corrosion Rate of Reinforcing Steel", *SHRP -S-324*, Strategic Highway Research Council, Washington, DC, 1992.
- [38] Gannon, E. J., Cady, P. D., "Condition Evaluation of Concrete Bridges Relative to Reinforcement Corrosion - Vol. 8: Procedure Manual", *SHRP -S-330*, Strategic Highway Research Council, Washington, DC, 1992.
- [39] State of Connecticut, Department of Transportation, *Standard Specification for Roads, Bridges and Incidental Construction, Form 814*, 1988.
- [40] Portland Cement Association, *Design and Control of Concrete Mixtures*, 13<sup>th</sup> Ed., Kosmatka, S. H., Panarese, W. C., Editors, 1988.
- [41] State of Connecticut, Department of Transportation, *Bridge Design Manual*, 2<sup>nd</sup> Ed., 1985 with Revision 3 Dated 10/89.
- [42] Shigen, L., Gressert, D. G., Frantz, G. C., Stephens, J. E., "Durability and Bond of High Performance Concrete and Repaired Portland Cement Concrete", *Report No. JHR 97-257*, Joint Highway Research Council of the University of Connecticut and the Connecticut Department of Transportation, June, 1997.
- [43] ASTM C 260 - 94 "Standard Test Method for Air-Entraining Admixtures for Concrete", *Annual Book of ASTM Standards*, 1994, pp. 156-158.

- [44] ASTM C 143 - 90a "Standard Test Method for Slump of Hydraulic Cement Concrete", *Annual Book of ASTM Standards*, 1990, pp. 88-90.
- [45] ASTM C 231 - 91b "Standard Test Method for Air Content of Freshly Mixed Concrete by the Pressure Method", *Annual Book of ASTM Standards*, 1991, pp. 134-141.
- [46] Berke, N. S., Shen, D. F., Sundberg, K. M., "Comparison of the Current Interruption and Electrochemical Impedance Techniques in the Determination of Corrosion Rates of Steel in Concrete", *ASTM Special Technical Publication Symposium - The Measurements and Correction of Electrolyte Resistance in Electrochemical Tests*, STP 1056, May, 1988, Baltimore, MD, pp. 191-201.
- [47] Ahmad, S. H., Zia, P., "High Performance Concretes for Highway Applications", *International Workshop on High Performance Concrete- ACI SP-159*, Bangkok, Thailand, November 1994, pp. 335-349.
- [48] Allyn, M., "Corrosion of Steel Reinforcement Embedded in Concrete: The Evaluation of Two Prototype Concrete Corrosion Inhibitors," Master of Science thesis, The University of Connecticut, Storrs, CT, 1998.

## APPENDIX A

### FREEZE - THAW TESTING

#### A1.0 SPECIMEN PREPARATION AND TEST PROTOCOL

The freeze-thaw durability of each concrete mix was evaluated by ASTM C666-92 "Resistance of Concrete to Rapid Freezing and Thawing", Procedure A. The freeze-thaw test machine held seventeen 4 x 3 x 16-inch prisms in addition to one control prism with temperature probes to control the cabinet operations and record the temperature. Freeze-thaw cycling was set to vary from 0°F to 40°F ( $\pm 3^\circ\text{F}$ ). Prisms were placed into the chamber with the 4-inch side vertical. Dummy concrete specimens were placed in unused containers to ensure consistent performance.

Freeze-thaw specimens were cast and tested prior to casting of the corrosion specimens. The mix design and mixing procedure for the freeze-thaw specimens were essentially the same as in Chapter 5.0. A de-foaming agent was added to some of the DAS and DSS mixes to see how a reduced air content would affect the performance of the mixes. The de-foaming agent was added after step nine of the general mixing procedure. The batches were then mixed for 1.5 minutes before proceeding to step ten.

Mix proportions for freeze-thaw specimens are shown in Table A-1. Batches were 1.0 cu. ft. and used cold tap water (approximately 66°F) for mixing water. Two batches of control concrete were also made without an air entraining agent. One batch was a 1.0 cu. ft. mix using machine mixing (Control-N). The other batch was a 0.64 cu. ft. batch using hand mixing (Control-N-H).

**Table A-1 Freeze-Thaw Mix Proportions.**

Mix Type and No. <sup>1,2,3</sup>	W/C Ratio	Air Entrain Admixture	Inhibitor Concentration <sup>4</sup>	De-foam Agent <sup>5</sup>	Air Content	Slump (in)
Control	0.44	Yes	None	No	7.0	4.5
Control-N	0.41	No	None	No	4.5	3.5
Control-N-H	0.41	No	None	No	2.5	2.25
Inhibitor A	0.40	Yes	4.0 gal/c.y.	No	8.5	2.75
Inhibitor B	0.44	Yes	1.0 gal/c.y.	No	7.5	2.5
2.0% DSS	0.45	No	2%	No	7.5	3.5
2.0% DSS-R	0.43	No	2%	Yes	4.25	2.0
1.0% DSS	0.40	No	1%	No	8.0	3.75
1.0% DSS-R	0.39	No	1%	Yes	4.75	2.0
1/2% DSS	0.38	No	1/2%	No	7.0	3.75
1/2% DSS-R	0.38	No	1/2%	Yes	4.75	2.0
1/4% DSS	0.38	No	1/4%	No	8.0	3.0
1/4% DSS-R	0.38	No	1/4%	Yes	4.5	2.5
2.0% DAS	0.41	No	2%	No	6.5	4.25
1.0% DAS	0.40	No	1%	No	8.0	3.75
1.0% DAS-R	0.40	No	1%	Yes	5.5	3.0
1/2% DAS	0.40	No	1/2%	No	8.5	4.25
1/2% DAS-R	0.40	No	1/2%	Yes	5.0	2.5

<sup>1</sup> All mixes contained Type I/II cement @ 27.85 lb., coarse agg. (oven-dried) @ 48.59 lb., and fine agg. (oven-dried) @ 54.26 lb. - Based on 1.0 cu. ft. mix.

<sup>2</sup> All mixes were 1.0 cf. in size except for Control-N-H which was 0.64 cf.

<sup>3</sup> N- non-air entrained; R- air reduction with de-foaming agent; H- hand mixed.

<sup>4</sup> Concentrations used for Inhibitors A and B were as suggested by the supplier. Concentrations for the DAS and DSS were based on weight of cement.

<sup>5</sup> The quantity of de-foaming agent used in the reduced air mixes was 25.0 ml.

The prism specimens were cast in standard plastic forms with the 4-inch side horizontal. Three forms were clamped on the vibration table at one time. The specimens were cast in two layers and each layer was vibrated for fifteen seconds. Prism tops were finished with a hand trowel. Three specimens were made for each mix.

Freeze-thaw prisms were wet cured for fourteen days in saturated lime water tanks in the moist cure room. On the fifteenth day, specimens were placed in the freeze-thaw

machine for testing. Nine or twelve 3 inch x 6 inch cylinders were also cast for each batch to measure the strength versus age characteristics. The strength cylinders were continuously wet cured in the lime water tanks until required for testing. The cylinders were tested, as stated in Appendix C, at ages of 7, 14, 21, 28 and some at 35 days. Cylinders were tested in a "wet" condition.

The freeze-thaw testing procedure was as follows:

1. On the afternoon of the fourteenth day of wet curing, place specimens in tap water in galvanized containers and place in a large industrial refrigerator at  $38^{\circ}\text{F} (\pm 3^{\circ}\text{F})$  until the following morning.
2. Next morning, weigh and measure the fundamental transverse frequency (FTF) of each specimen.
3. Place specimens in freeze-thaw machine and fill containers with  $38^{\circ}\text{F}$  water.
4. Start freeze-thaw machine.
5. Check water level in containers every two days.
6. Once a week (approximately after 35-40 cycles) remove specimens and rinse with cold water. Rinse out containers.
7. Place specimens in a cold water ( $38^{\circ}\text{F}$ ) bath for 20 minutes.
8. Return containers to freeze-thaw machine in their original position.
9. Weigh and measure the FTF for each specimen.
10. Flip specimens end for end (such that the top front edge becomes the bottom back edge) and then place in freeze-thaw machine at a position five containers

to the right of the removed position.

11. Add water to containers as needed.
12. Repeat steps 4 through 11 for at least 300 cycles or until the FTF reduces to 60% of the original value.

The FTF data was obtained with a resonant frequency analyzer. The 4-inch side of the prism was in the horizontal position during the test. Three specimens for each mix were generally utilized for the freeze-thaw testing program. In a few cases only two specimens were tested due to space limitations. Averaged results are reported in the Section A2.0 below. Relative dynamic modulus of elasticity values,  $P_C$ , were calculated from:

$$P_C = (n_1^2/n^2) \times 100\%, \text{ where}$$

$n$  = The fundamental transverse frequency at *zero* freeze-thaw cycles.

$n_1$  = The fundamental transverse frequency at *c* freeze-thaw cycles.

The relative weight loss,  $\Delta w$ , was calculated from:

$$\Delta w = [1 - (w_1 / w)] \times 100\%, \text{ where}$$

$w$  = The specimen weight a *zero* freeze-thaw cycles

$w_1$  = The specimen weight at *c* freeze-thaw cycles

## A2.0 DISCUSSION OF RESULTS

### A2.1 General

The 28 day strengths of all the freeze-thaw mixes are shown in Figure A-1. Refer to Appendix C for a detailed discussion of the freeze-thaw strength results. The freeze-thaw performance of the mixes is shown in Table A-2 and Figures A-2, A-3, A-4 and A-5. The figures rank the mixes from best to worst performance, left to right, based on relative dynamic modulus of elasticity,  $P_C$ , weight loss, and appearance, respectively. The number in parentheses that appears after each mix name on the horizontal axis of the graphs indicates the number of freeze-thaw cycles completed at the time of the final measurement. The appearance rating was based on a visual evaluation of the 4-inch-wide, non-finished side of the prisms, based on the following criteria:

<u>Rating Number</u>	<u>Description</u>
0	No Scaling
1	< 10% Course Aggregate Visible
2	< 50% Course Aggregate Visible
3	100% Course Aggregate Visible

Ratings in-between these values were interpolated.

In one instance, the freeze-thaw machine malfunctioned after completing 297 cycles. The specimens were in a thawed condition for approximately two days before the problem was discovered. The specimens were then placed in 40°F cold water baths for 30

minutes and the fundamental frequencies were then measured. The specimens, submerged in water, were placed inside the industrial refrigerator, maintained at 38°F, for three days until the freeze-thaw machine was repaired. The freeze-thaw testing then resumed. The mixes effected by this malfunction were the DSS concentrations of 1.0%, 1/2%, and 1/4%, with and without de-foaming agent.

### A2.2 Control Specimens

The air entrained control mix performed very well (Fig. A-6). After 312 freeze-thaw cycles, the dynamic modulus of elasticity,  $P_C$ , was still about 100% with a weight loss of 0.8%. After 519 cycles, the  $P_C$  value remained unchanged and the weight loss increased to 1.8%. The appearance rating was 0.5 and 1.0 after 312 and 519 freeze-thaw cycles, respectively.

The low air control mix, Control-N (air content of 4.5%), also performed very well (Fig. A-6). The  $P_C$  value at the end of 310 freeze-thaw cycles was approximately 95% with a weight loss of 0.9%. This was an unexpected result since these specimens did not have an air entraining admixture added. The reason for this good behavior is not known. These specimens must have had an adequate air void system that created a protective environment even though the air void system was most likely a product of entrapped air. The scaling of the concrete surface was minimal (appearance rating of 0.5).

The control specimens mixed by hand, Control-N-H (air content of 2.50%), failed after 36 freeze-thaw cycles with a  $P_C$  value of 38%. This result was expected due to the extremely low air content.



Table A-2 Relative Dynamic Modulus of Elasticity, Weight Loss, and Appearance Ratings Values.

Specimen	Values At 300 Cycles		Final Values				28 Day Strength (psi)
	Pc (%)	Weight Loss (%)	F/T Cycles	Pc (%)	Weight Loss (%)	Appearance Rating	
Control	99	0.78	312	99	0.81	0.5	6100
Control	99	0.78	519	99	1.81	1.0	6100
Control-N	95	0.90	346	95	0.89	0.5	7072
Control-N-H	Failed	Failed	36	38	0.00	----	6726
Inhibitor A	99	0.21	346	99	0.28	0.0	8161
Inhibitor B	97	0.91	346	96	1.12	1.0	5482
2.0 % DSS	91	0.74	378	89	1.16	1.0	3897
2.0 % DSS - R	80	1.00	378	61	1.34	1.5	4809
1.0 % DSS	92	1.01	381	93	1.80	2.0	4064
1.0 % DSS - R	90	1.62	334	89	1.89	2.5	5708
1/2 % DSS	95	1.11	381	95	1.80	2.0	4580
1/2 % DSS - R	93	1.65	334	91	1.89	2.0	6271
1/4 % DSS	94	1.61	327	94	1.85	2.0	4738
1/4 % DSS - R	82	1.98	327	79	2.16	2.0	6599
2.0% DAS	95	1.21	315	95	1.32	1.5	4318
1.0% DAS	91	1.35	387	89	2.04	3.0	4337
1.0% DAS - R	92	1.99	376	92	2.47	3.0	5447
1/2 % DAS	93	1.66	387	91	2.47	3.0	4419
1/2 % DAS - R	94	1.57	376	93	2.06	3.0	5704

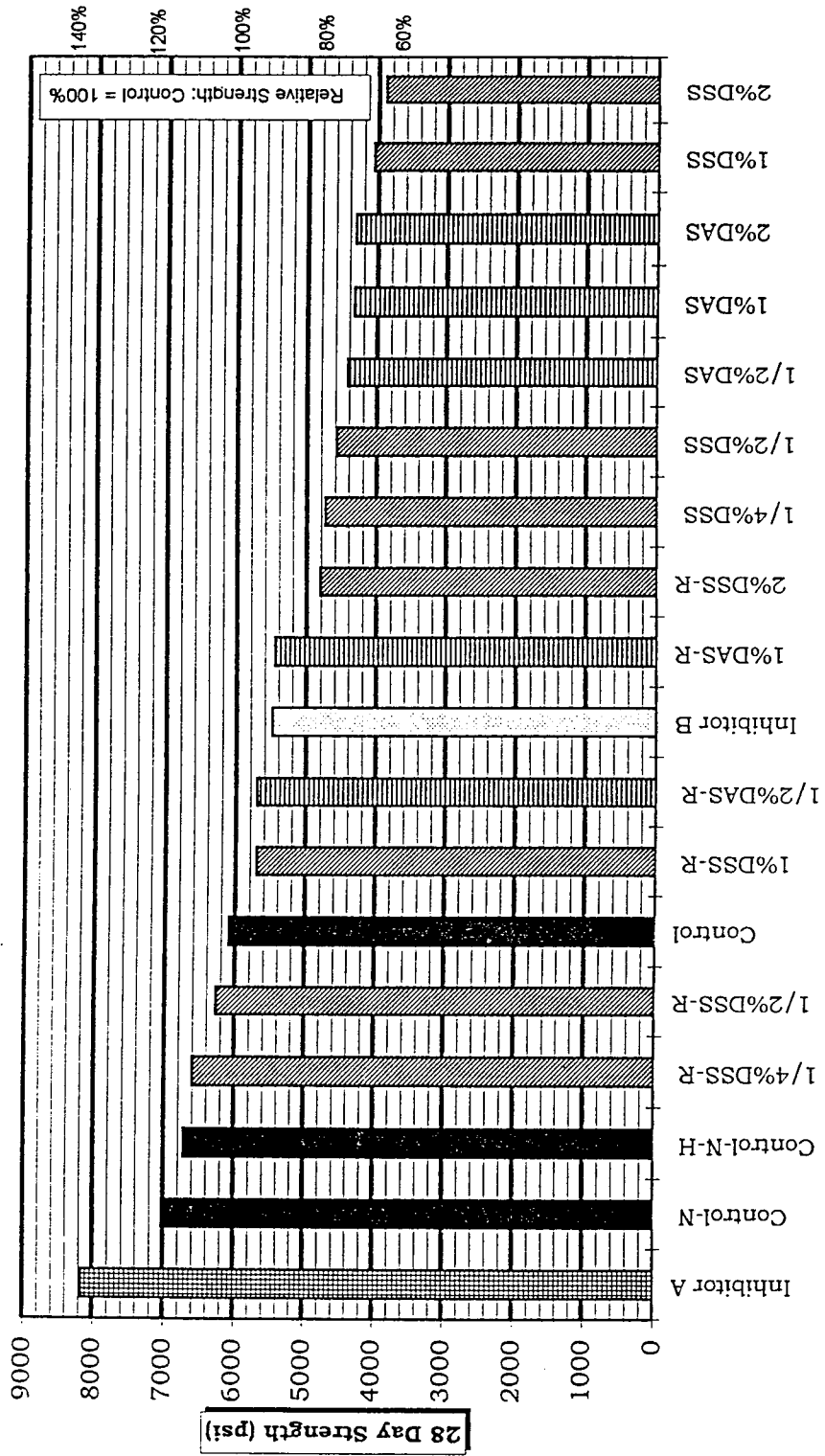


Figure A-1 28 Day Strengths for Freeze-Thaw Mixes.

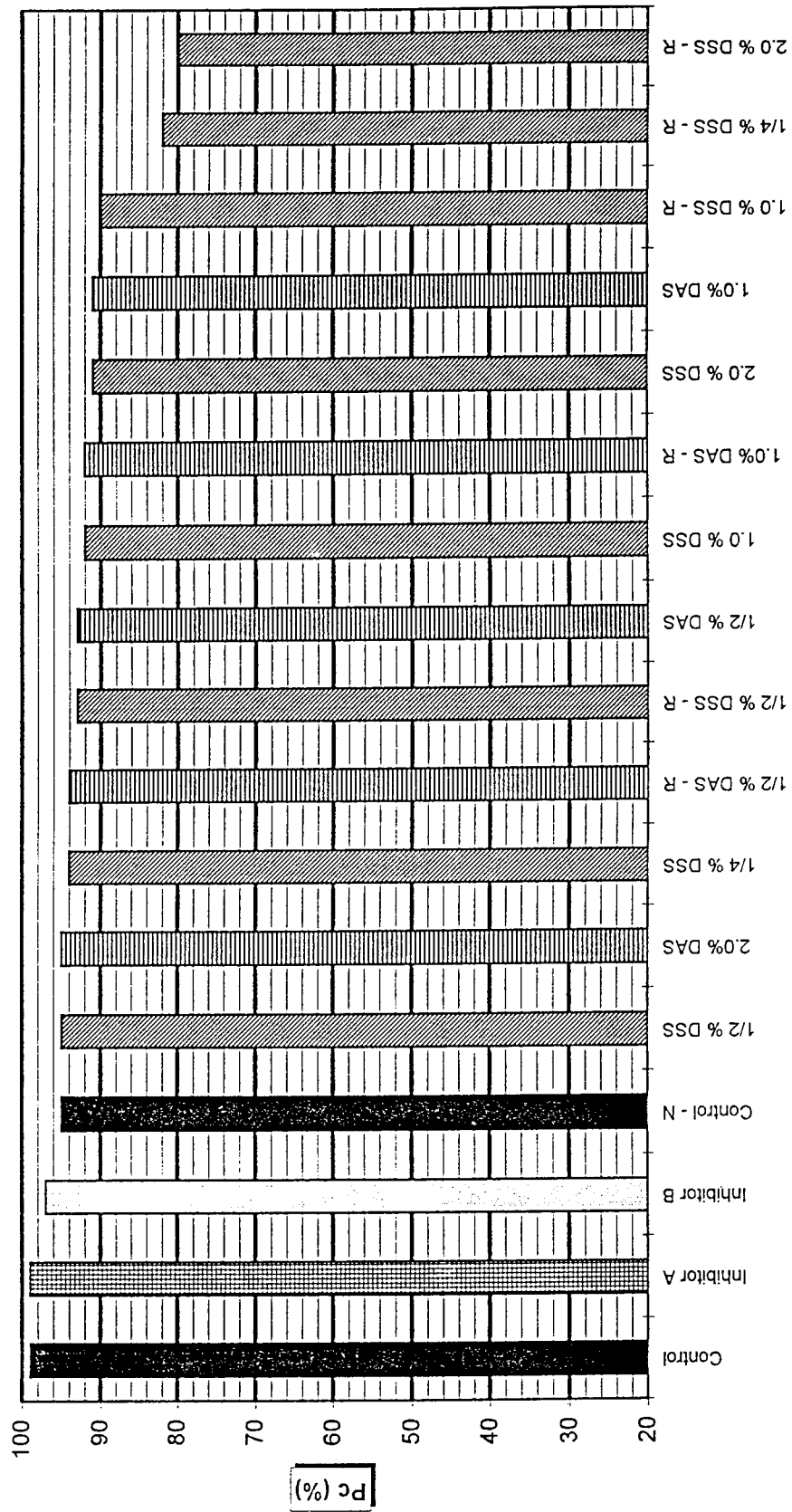


Figure A-2 Relative Dynamic Modulus of Elasticity, all Specimens at 300 Cycles.

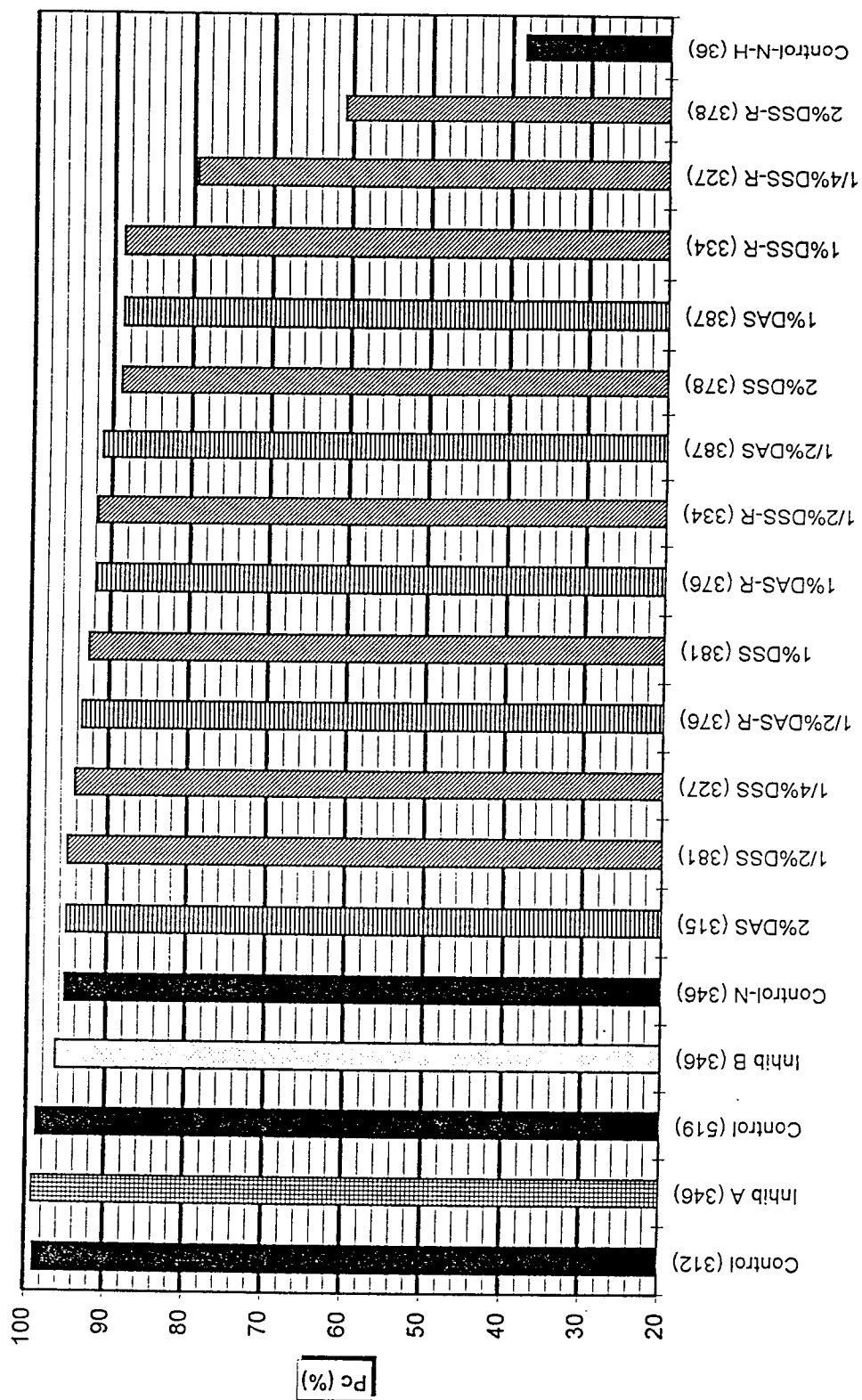


Figure A-3 Relative Dynamic Modulus of Elasticity, all Specimens.

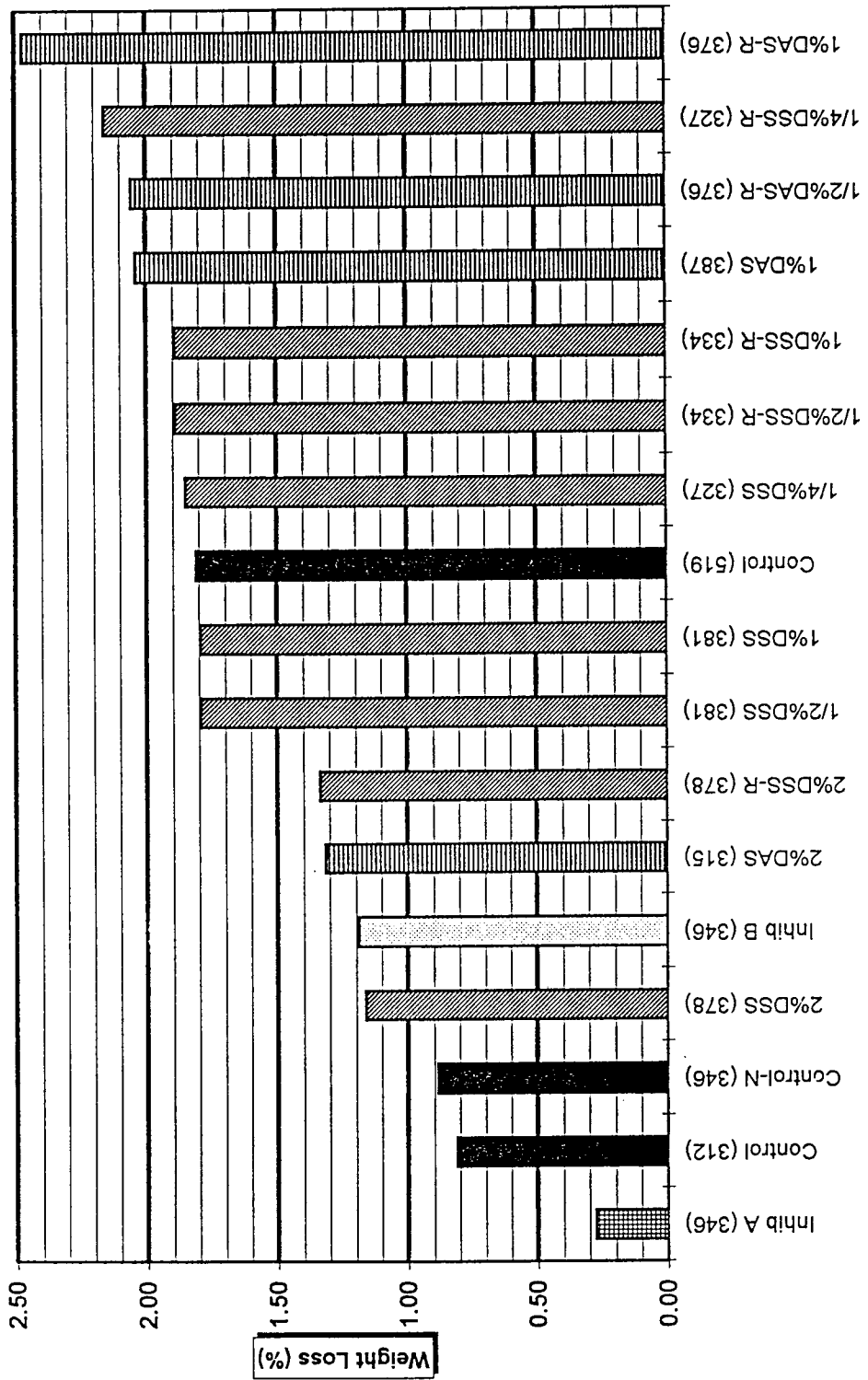


Figure A-4 Weight Loss, all Specimens.

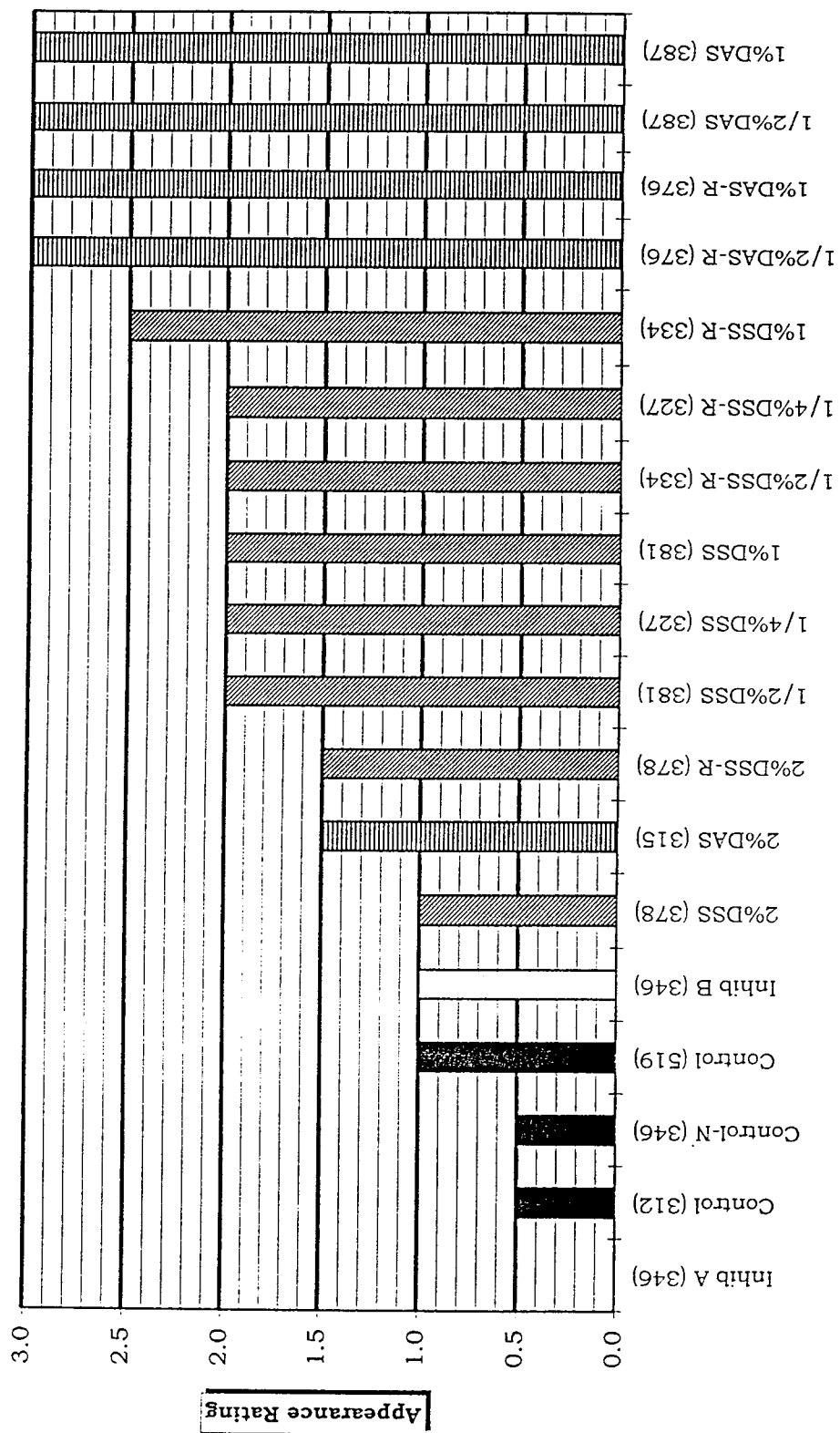


Figure A-5 Appearance Ratings, all Specimens.

### A2.3 Inhibitor A & Inhibitor B Specimens

Figure A-7 shows the freeze-thaw results for Inhibitors A & B. The freeze-thaw performance of Inhibitor A was the best out of all the mixes and had a lower weight loss and less scaling than even the air entrained control concrete. The  $P_C$  value for the Inhibitor A specimens after 346 cycles was 99%. The non-finished side of the prism did not show any signs of surface deterioration. The weight loss was also minimal at 0.28%.

Inhibitor B also performed well. After 346 cycles, the  $P_C$ , weight loss and appearance were 96%, 1.1% and 1.0, respectively.

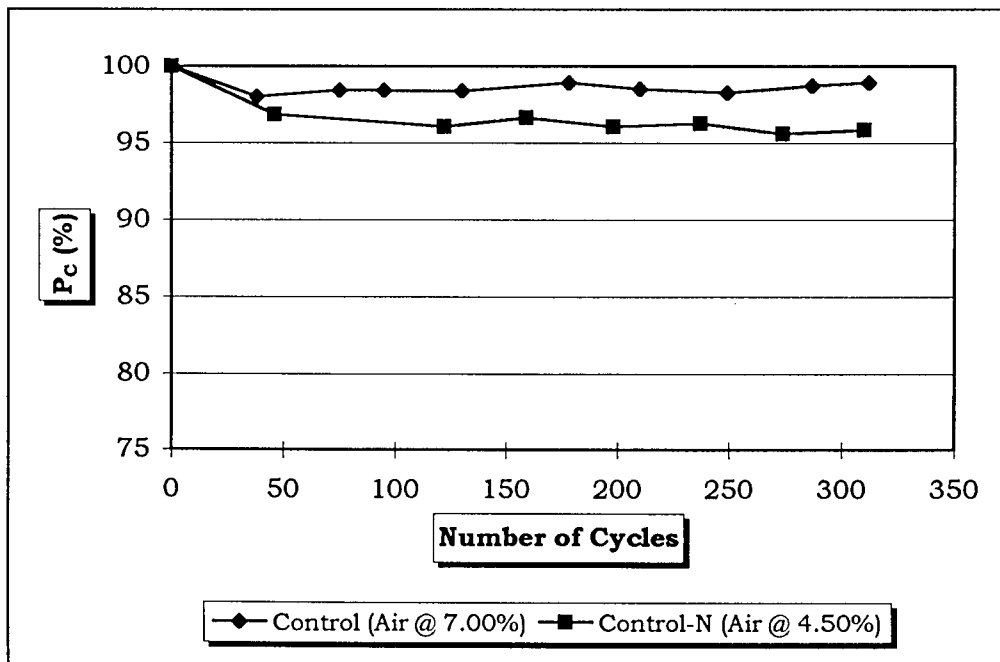


Figure A-6 Relative Dynamic Modulus of Elasticity, Control Mixes.

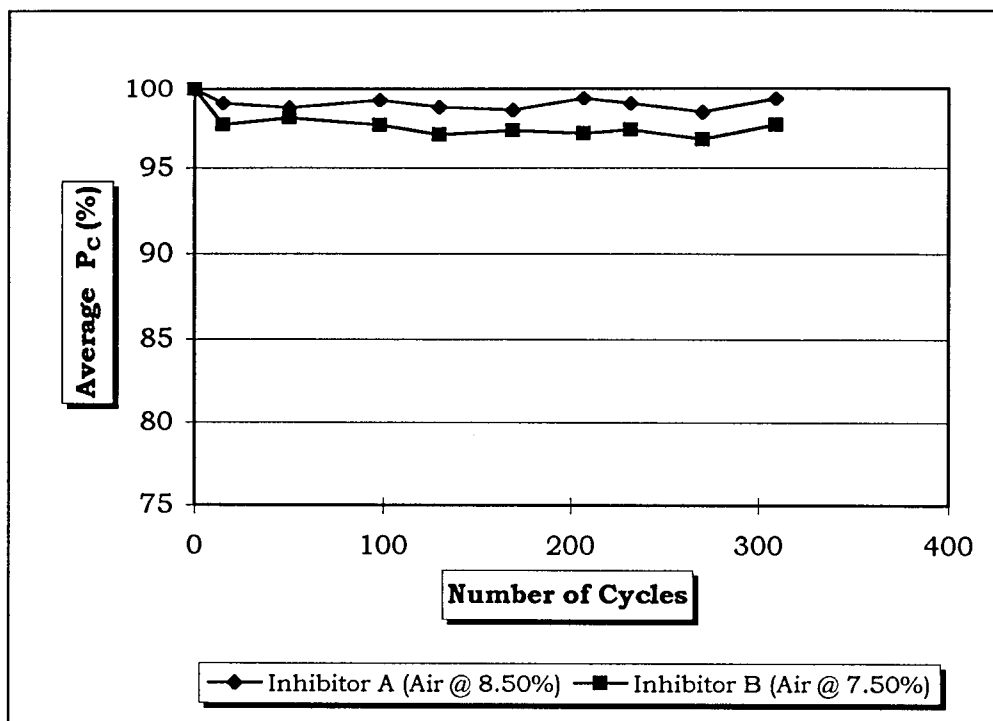


Figure A-7 Relative Dynamic Modulus of Elasticity, Inhibitors A & B Mixes.

#### A2.4 DAS Specimens

The DAS mixes had good freeze-thaw protection with  $P_c$  values of 90% or better after 300 cycles (Figs. A-8 and A-9). The 1% and 1/2% DAS-R mixes had similar results to the companion mixes without the de-foaming agent. The concentration of DAS had little effect on the  $P_c$  value for the mixes either with or without the de-foaming agent. The DAS mixes, both with and without de-foaming agent, generally had the worst surface deterioration (3.0 rating) and highest weight loss (in excess of 2.0%) of all the mixes.

Of the three DAS mixes without the de-foaming agent, the 2% concentration performed the best with values of 1.5, 1.32%, and 95% for appearance, weight loss and  $P_c$ , respectively after 315 freeze-thaw cycles. The 1/2% DAS mix had a slightly higher  $P_c$  value than the 1% DAS mix, and it had only a small increase in weight loss.



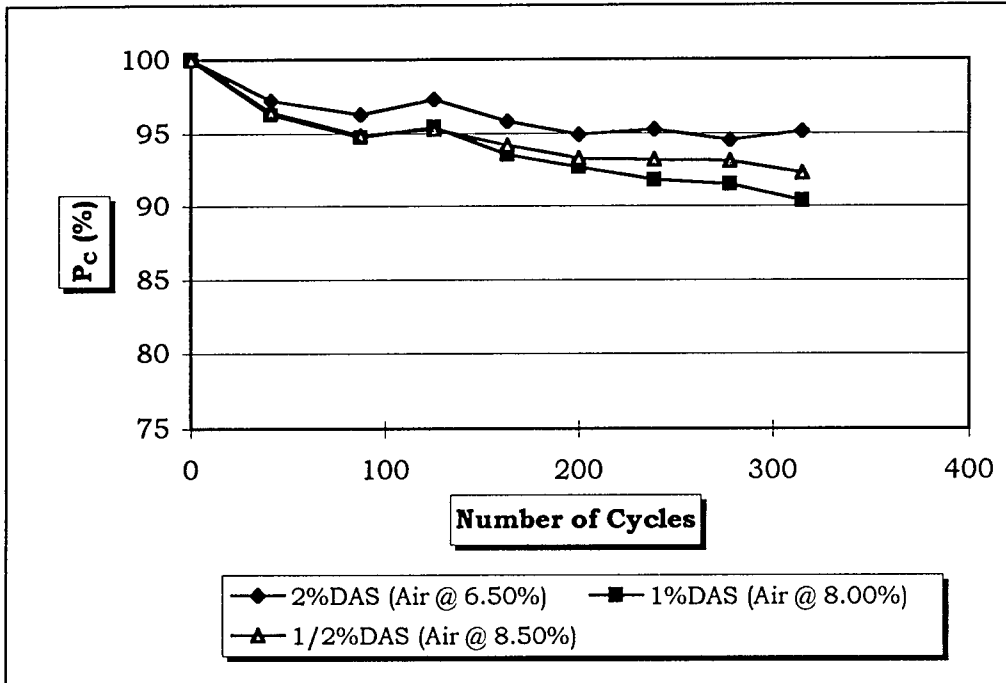


Figure A-8 Relative Dynamic Modulus of Elasticity, DAS Mixes.

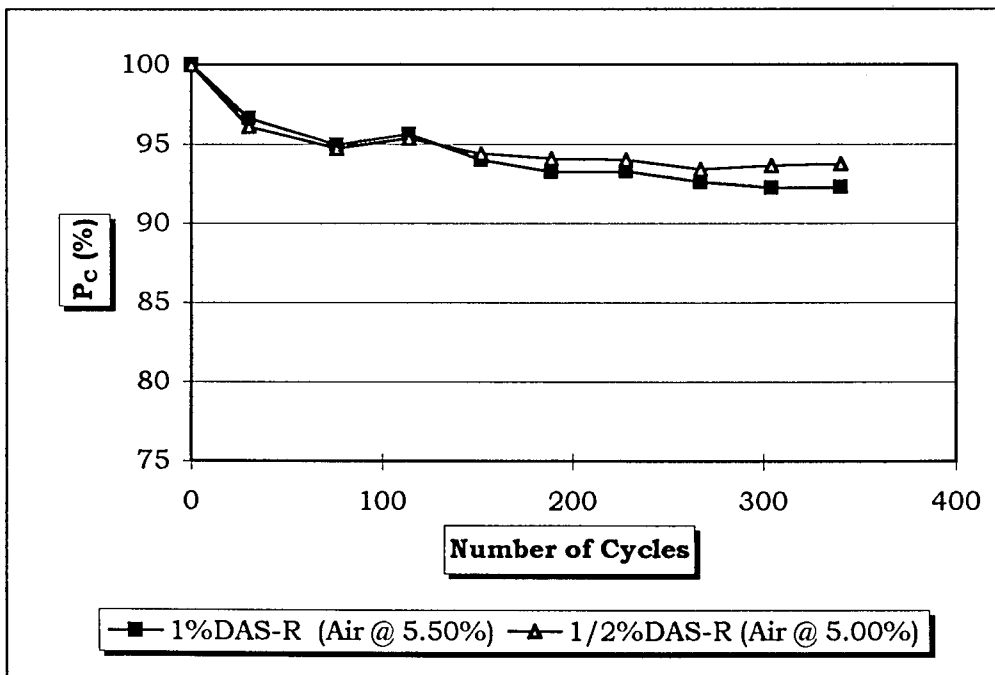


Figure A-9 Relative Dynamic Modulus of Elasticity, DAS-R Mixes.

## A2.5 DSS Specimens

The DSS mixes without de-foaming agent had good freeze-thaw protection. Some DSS-R mixes did not perform as well, overall, as the DSS mixes without de-foaming agent. After 300 cycles, the 1/4%, 1/2%, 1%, and 2% DSS mixes and the 1/2% and 1% DSS-R mixes had  $P_C$  values above 90% (Figs. A-10 and A-11). However, all the reduced air mixes did have  $P_C$  values greater than or equal to 80% after 300 freeze-thaw cycles (Fig. A-11), which is considered adequate freeze-thaw protection for high performance concrete [47]. The relative dynamic modulus for the 2%DSS-R mix decreased to 61% after an additional 78 cycles (378 total), which still satisfied ASTM C666-92 criteria, which is based on 300 cycles. After 378 cycles, the 2%DSS mix dropped slightly to 89%.

Of the four mixes without de-foaming agent, the 1/2% and 1/4% concentrations had the highest  $P_C$  values (approximately 95%). The 2% mixes, both with and without de-foaming agent, had the lowest appearance ratings and weight losses. The appearance ratings and weight loss values for the other DSS mixes without de-foaming agent were very similar to each other.

The 2%DSS-R mix had the lowest appearance rating (1.5) of all the DSS with de-foaming agent mixes, while 1%DSS-R had the highest (2.5). The other two reduced air mixes had ratings of 2.0. The 2%DSS-R mix also had the lowest weight loss (1.34%) and 1/4%DSS-R had the largest (2.16%). The 1%DSS-R and 1/2%DSS-R mixes had weight loss values closer to the 1/4%DSS-R mix (approximately 1.8%).

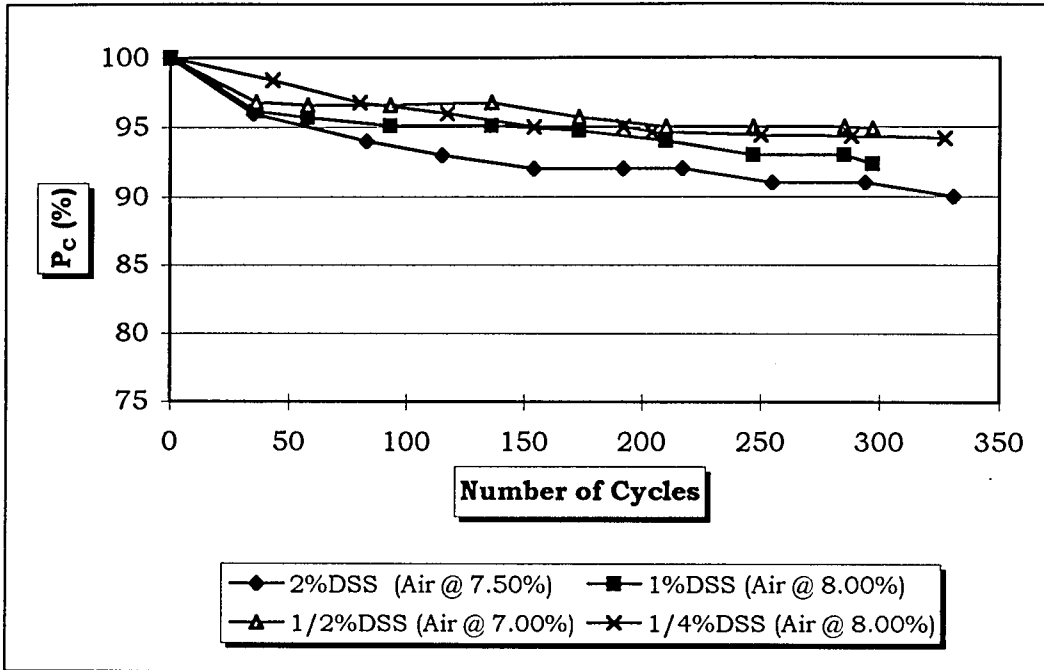


Figure A-10 Relative Dynamic Modulus of Elasticity, DSS Mixes.

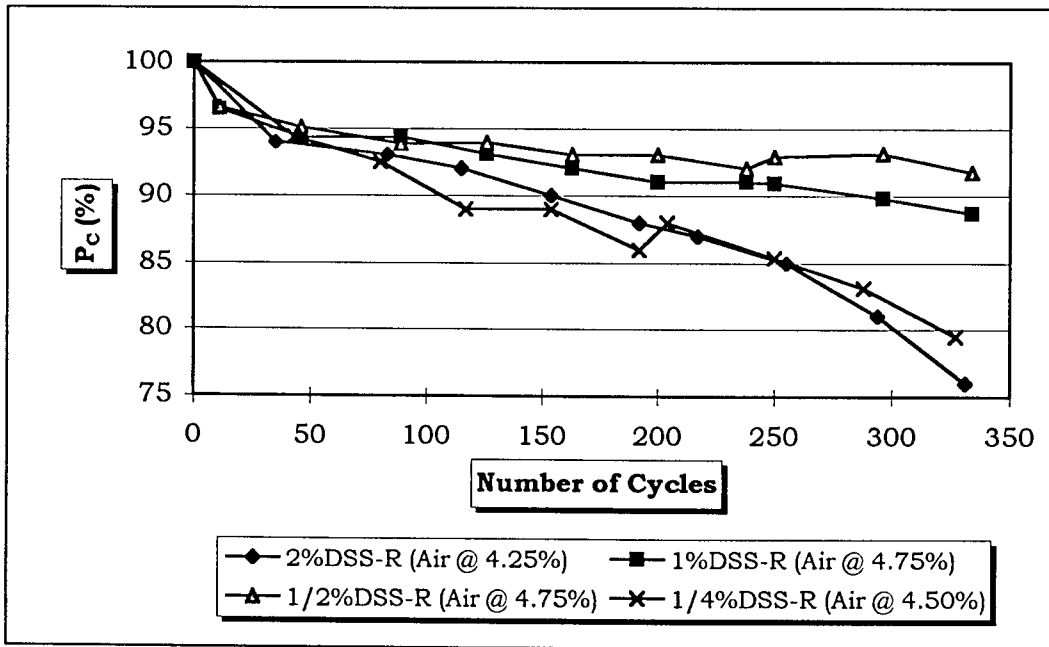


Figure A-11 Relative Dynamic Modulus of Elasticity, DSS-R Mixes.

## A2.6 Summary of Results

The majority of the DAS and DSS mixes, with and without de-foaming agent, had  $P_C$  values of 90% or better after 300 cycles. Only two mixes, 2%DAS-R and 1/4%DSS-R, had  $P_C$  values lower than 90%, but were at least 80% or better. These results indicated good protection when exposed to a harsh freezing and thawing environment.

The air bubble systems in hardened samples of the 2%DAS and 2%DSS were measured according to ASTM C457-90, "Standard Test Method for Microscopical Determination of Parameters of the Air-Void System in Hardened Concrete". The results (Table A-3), based on air volume and bubble spacing, indicated these mixes were "air-entrained" and had air bubble systems similar to the air bubble system of the control concrete that contained an air-entraining admixture.

**Table A-3 Air Bubble Characteristics of the Control, 2%DAS and 2%DSS Mixes.**

Mix Name	Total Air Content (%)	Entrained Air Content (%)	Specific Surface (in <sup>2</sup> / in <sup>2</sup> )	Spacing Factor (inch)
Control	7.0	4.9	799	0.006
2%DAS	6.0	4.7	1068	0.005
2%DSS	7.6	6.3	1065	0.004

The best freeze-thaw performing mix, with and without de-foaming agent, was selected from the DAS and DSS results and compared with the results of the control, Inhibitor-A, and Inhibitor-B mixes (Fig. A-12). A summary of the appearance rating, weight loss,  $P_C$ , and 28 day strength values for these mixes are shown in Table A-4.

Of all the DAS mixes, the 2%DAS and 1/2%DAS-R mixes had the best freeze-thaw performances (based on  $P_C$  value, weight loss and appearance rating). The  $P_C$  values for both mixes were similar, but the 1/2DAS-R had increased surface scaling and overall weight loss. The 1/2%DAS-R mix had the highest 28 day strength (5704 psi) and the 2%DAS mix had the lowest strength (4318 psi) of all the DAS mixes.

The 1/2% concentrations, both with and without de-foaming agent, were chosen for having the best freeze-thaw performance of all the DSS mixes. The 1/2%DSS and 1/2%DSS-R mixes had very similar  $P_C$ , weight loss and appearance rating values. Also, both the 1/2% DSS and 1/2%DSS-R mixes had the second highest 28 day strength (4580 psi and 6271 psi, respectively), when compared to the other DSS mixes with and without de-foaming agent.

**Table A-4 Summary of Relative Dynamic Modulus of Elasticity, Weight Loss, and Appearance Ratings Values for the Best Performing Mixes.**

Specimen	$P_C$ (%) (300 Cycles)	Wt. Loss (%) (300 Cycles)	Appearance Rating	28 Day Strength (psi)
Control	99	0.78	0.5	6100
Inhibitor A	99	0.21	0.0	8161
Inhibitor B	97	0.91	1.0	5482
2.0% DSS	91	0.74	1.0	3897
0.5% DSS	95	1.11	2.0	4580
0.5% DSS - R	93	1.65	2.0	6271
2.0% DAS	95	1.21	1.5	4318
0.5% DAS - R	94	1.57	3.0	5704

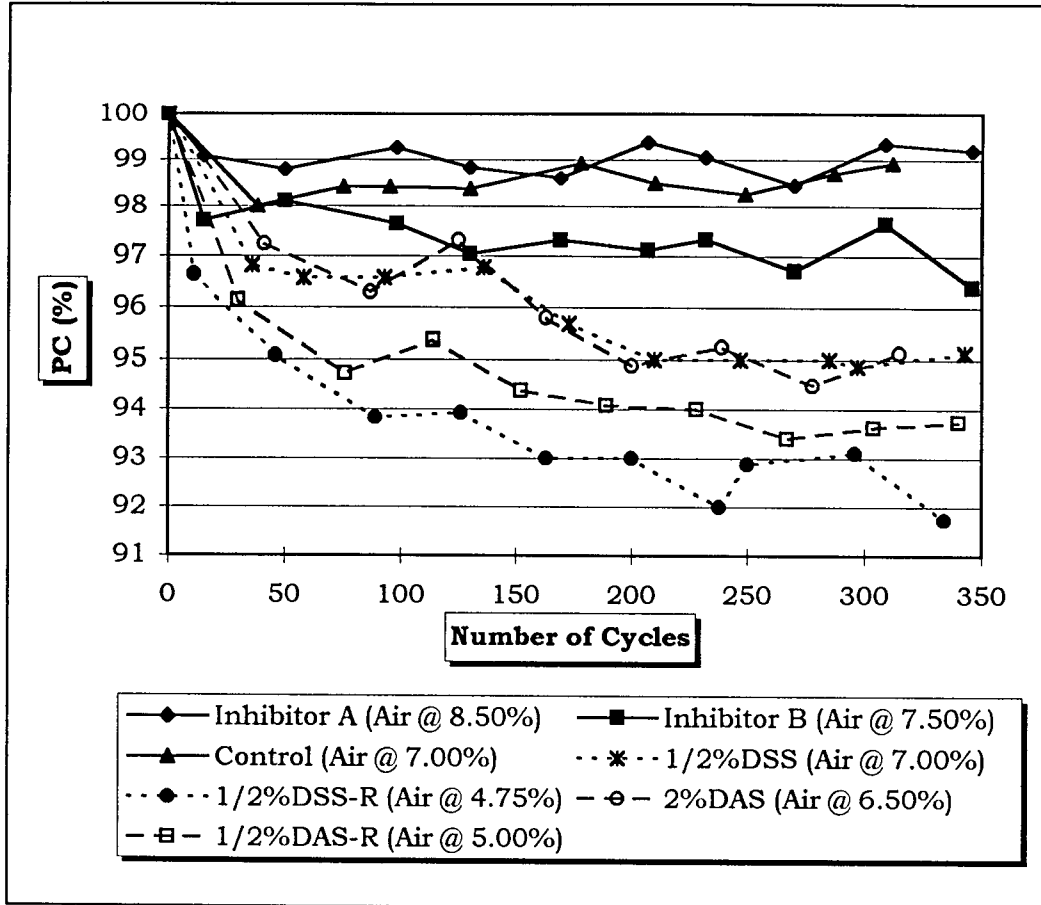


Figure A-12 Relative Dynamic Modulus of Elasticity, Comparison of Best Performing Mixes.

### A3.0 CONCLUSIONS

Test results indicated that the compression strength did not have a significant effect on the freeze-thaw performance of the DAS and DSS mixes without de-foaming agent added. In both cases, the 2% concentrations of DSS and DAS had the lowest strength, but also had the lowest weight loss and surface scaling along with a more than adequate  $P_C$  value.

Except for the 1/4%DSS-R and 2%DSS-R mixes, the percent concentration of DAS and DSS didn't seem to have much effect on freeze-thaw performance at 300 cycles (Fig. A-13). The  $P_C$  value for these two mixes was in the low 80% range but was generally above 90% for all the other DAS and DSS mixes with and without de-foaming agent.

The DSS mixes generally had the lowest weight loss at 300 cycles (Fig. A-14) and the lowest appearance rating (Fig. A-15) for each concentration. The DSS mixes were judged to have the best overall freeze-thaw performance as compared to the DAS mixes, based on all three categories of  $P_C$ , weight loss and appearance. If strength performance was also considered, then the 1/2% and 1% DSS-R and DAS-R mixes would be judged more suitable.

The DAS and DSS mixes had extremely low absorption rates, as described in Appendix B. Based on this fact, it is believed that if the DAS and DSS prisms are allowed to dry for a short period of time (possibly three days to one week) before the freeze-thaw testing commenced, their resistance to freeze-thaw damage might increase very significantly. A partial drying period of the concrete before the start of the freeze-thaw cycling would probably simulate real highway environments more accurately. Also, since Inhibitor B is believed to reduce the ingress of water and chlorides, its freeze-thaw performance might also increase with such a drying period.

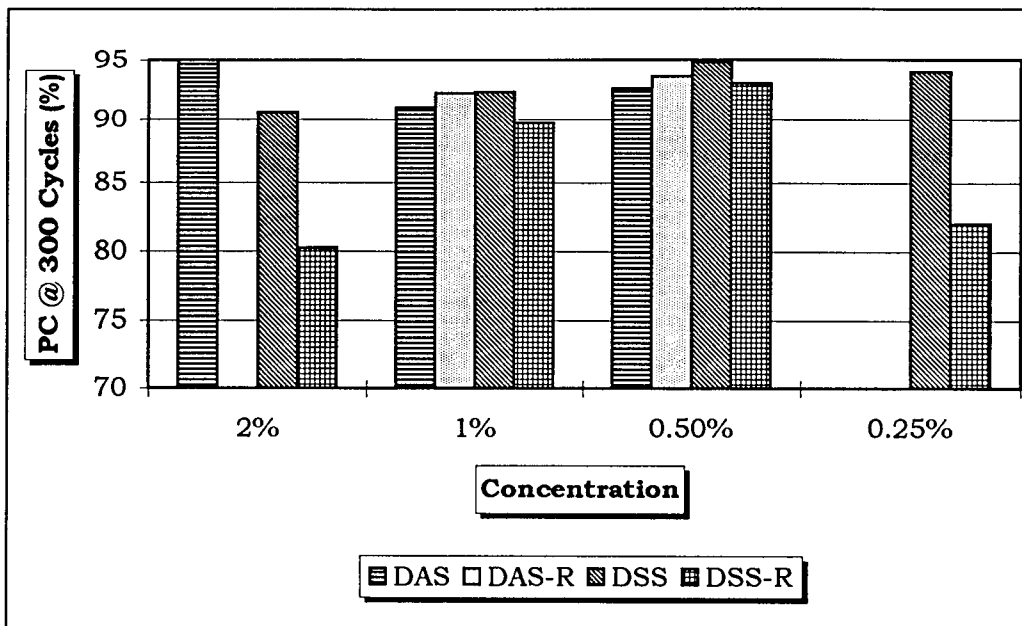


Figure A-13 Relative Dynamic Modulus of Elasticity at 300 Cycles, DSS, DSS-R, DAS and DAS-R Mixes.

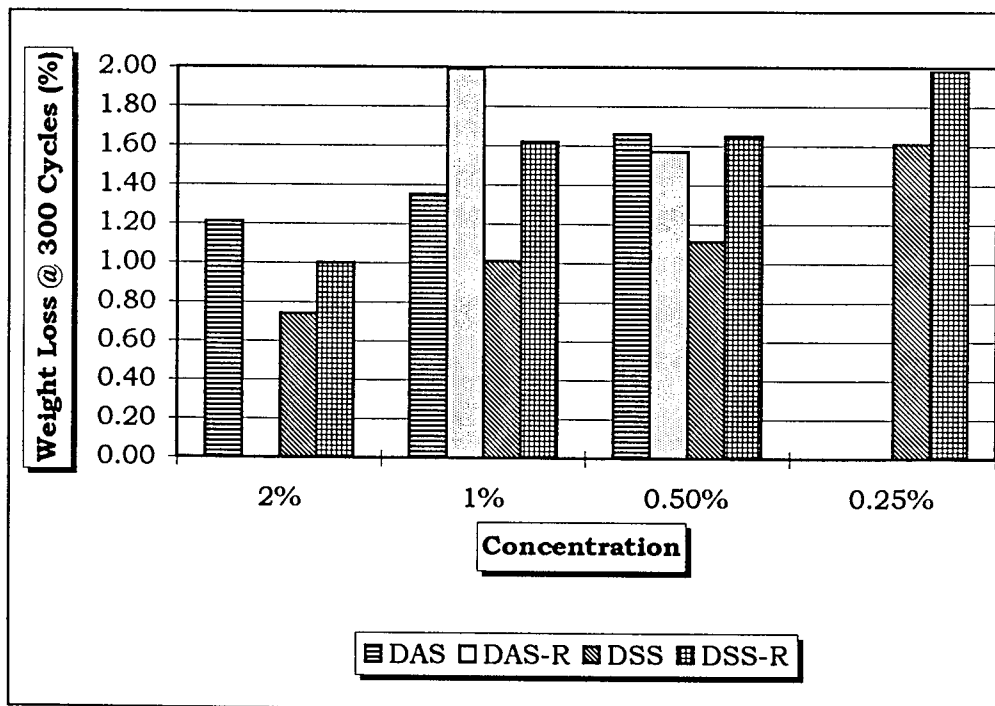


Figure A-14 Weight Loss at 300 Cycles, DSS, DSS-R, DAS and DAS-R Mixes.



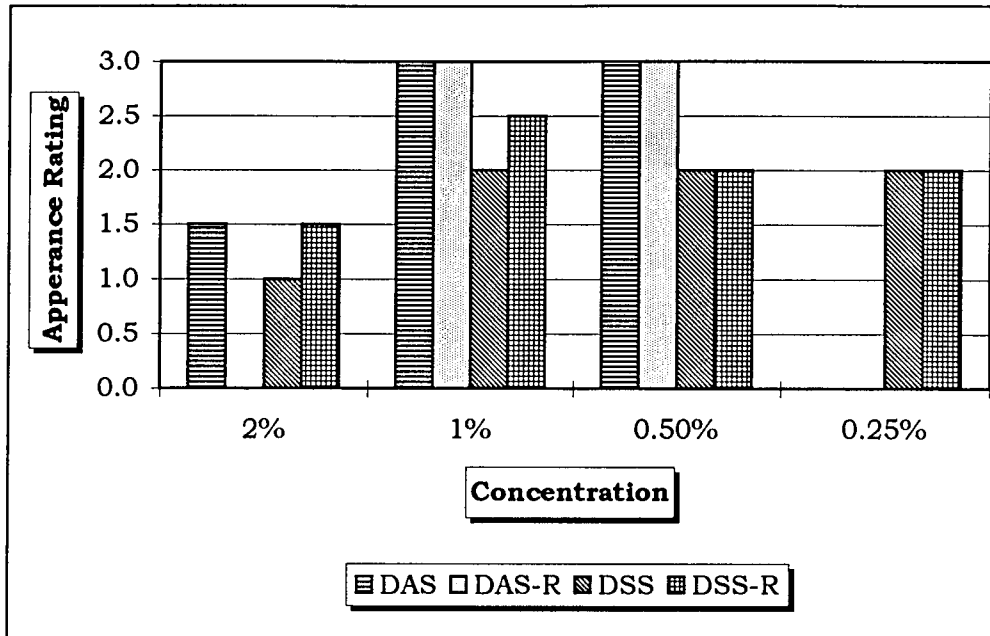


Figure A-15 Appearance Rating, DSS, DSS-R, DAS and DAS-R Mixes.

## APPENDIX B

### ABSORPTION TESTING

#### **B1.0 SPECIMEN PREPARATION AND TEST PROTOCOL**

The absorption characteristics of each concrete mix was evaluated by ASTM C642-90 "Standard Test Method for Specific Gravity, Absorption, and Voids in Hardened Concrete", which was generally adhered to, except the specimens were not boiled.

To see the effects of drying temperature on the total absorption, sixteen specimens were dried at 100°C and seven specimens were dried at 40°C. It was felt that drying at 40°C, instead of at 100°C, would simulate more accurately the temperature environment on actual bridge decks. The specimens of each test mix were made from the same batch, except for Inhibitor A specimens, which used specimens from two similar batches. The absorption specimens were 3 inch by 6 inch cylinders cast from the first set of corrosion mixes, of which all the lollipop specimens were not used for corrosion testing due to surface irregularities, as stated in Chapter 5.0. The surface irregularities were only minor on the 3 inch by 6 inch cylinders and therefore, selected for absorption testing.

Some DAS and DSS mixes had a de-foaming agent added, as done in the freeze-thaw program. These mixes were not used in the corrosion testing program due to time and space limitations, but were selected for absorption testing.

The mix proportions of the specimens without the de-foaming agent added were as stated in Section 5.2. The mix proportions for specimens with de-foaming agent added were essentially the same as stated in Appendix A. Mix proportions for absorption

specimens are shown in Table B-1.

The mixing procedure was essentially the same as stated in Appendix A and Chapter 5.0 for mixes with and without the de-foaming agent added, respectively.

**Table B-1 Absorption Mix Proportions.**

Mix Type and No. <sup>1,2,3</sup>	W/C Ratio	Air Entrain Admixture	Inhibitor Concentration <sup>4</sup>	De-foam Agent <sup>5</sup>	Air Content	Slump (in)
Control	0.38	Yes	None	No	7.5%	3.00
Inhibitor A	0.40	Yes	4.0 gal/c.y.	No	7.0 %	4.50
Inhibitor A-3	0.38	Yes	4.0 gal/c.y.	No	8.0%	4.00
Inhibitor B	0.45	Yes	1.0 gal/c.y.	No	8.5 %	2.75
2.0% DSS	0.40	No	2%	No	8.0%	4.50
2.0% DSS-R	0.40	No	2%	Yes	4.75%	3.75
1.0% DSS	0.40	No	1%	No	8.0%	3.00
1.0% DSS-R	0.40	No	1%	Yes	5.5%	2.75
1/2% DSS	0.39	No	1/2%	No	7.0%	2.50
1/4% DSS	0.38	No	1/4%	No	7.5%	2.25
2.0% DAS	0.41	No	2%	No	6.0 %	4.00
2.0% DAS-R	0.41	No	2%	Yes	4.5%	2.75
1.0% DAS	0.39	No	1%	No	7.0 %	3.00
1.0% DAS-R	0.40	No	1%	Yes	6.0%	2.00
1/2% DAS	0.39	No	1/2%	No	7.0 %	3.00
1/2% DAS-R	0.39	No	1/2%	Yes	5.0 %	2.00
1/4% DAS	0.39	No	1/4%	No	7.0 %	2.50

<sup>1</sup> All mixes contained Type I/II cement @ 27.85 lb., coarse agg. (oven-dried) @ 48.59 lb., and fine agg. (oven-dried) @ 54.26 lb. - Based on 1.0 cu. ft. mix.

<sup>2</sup> All mixes were 1.25 cu. ft. in size except for Control which was made from two 1.0 cu. ft. batches.

<sup>3</sup> R- air reduction with de-foaming agent.

<sup>4</sup> Concentrations used for Inhibitors A and B were as suggested by the supplier. Concentrations for the DAS and DSS were based on weight of cement.

<sup>5</sup> The quantity of de-foaming agent used in the reduced air mixes was 25.0 ml.

The specimens were cast as stated in Chapter 5.0 and were wet cured for fourteen days on shelves in the moist cure room. After fourteen days of wet curing, the specimens were removed and placed in the dry store room until required for testing. The specimens were approximately 28 days old when the absorption testing commenced.

The absorption testing procedure was as follows:

1. Remove cylinders from store room and place in oven at 100°C, or at 40°C, as appropriate.
2. Every three to four days, remove specimens from oven, allow to cool for approximately two hours and weigh. Return specimens to oven.
3. Continue drying, on an individual basis, until the weight loss between successive weighings is equal to or less than 0.1% of the lesser weight.
4. Submerge the cylinders in a water bath at room temperature.
5. Every four to five days, remove specimens from water bath, towel dry excess surface moisture and weigh. Return specimens to water bath.
6. Continue the immersion, on an individual basis, until the weight gain between successive weighings is equal to or less than 0.1% of the heavier weight.

Generally, it took approximately three to four weeks to dry the specimens and six to eight weeks to saturate them. The final absorption values were based on the average of two specimens, except only one specimen was used with the 40°C tests. The absorption

was calculated as:

$$\text{Absorption} = [(B - A) / A] \times 100\%, \text{ where}$$

A = Final weight, in air, of oven dried sample.

B = Final weight, in air, of surface-dry sample after immersion.

## B2.0 DISCUSSION OF RESULTS

The absorption results are shown in Table B-2 and Figures B-1 & B-2, which rank the mixes from lowest to highest absorption. Figures B-3 and B-4 show absorption verses time results for some of the mixes. Figures B-5, B-6 and B-7 compare the DAS and DSS results.

**Table B-2 Final Absorption: all Specimens.**

Specimen	Average Absorption (%)	
	Dried @ 100°C	Dried @ 40°C
Control	8.49	5.10
Inhibitor A	7.43	----
Inhibitor A-3	----	5.06
Inhibitor B	7.39	3.88
2%DAS	2.69	1.28
2%DAS-R	3.09	----
1%DAS	2.89	1.45
1%DAS-R	3.34	----
1/2%DAS	3.39	----
1/2%DAS-R	4.64	----
1/4%DAS	6.04	----
2%DSS	2.95	1.51
2%DSS-R	3.29	----
1%DSS	3.22	1.82
1%DSS-R	3.57	----
1/2%DSS	3.85	----
1/4%DSS	5.09	----

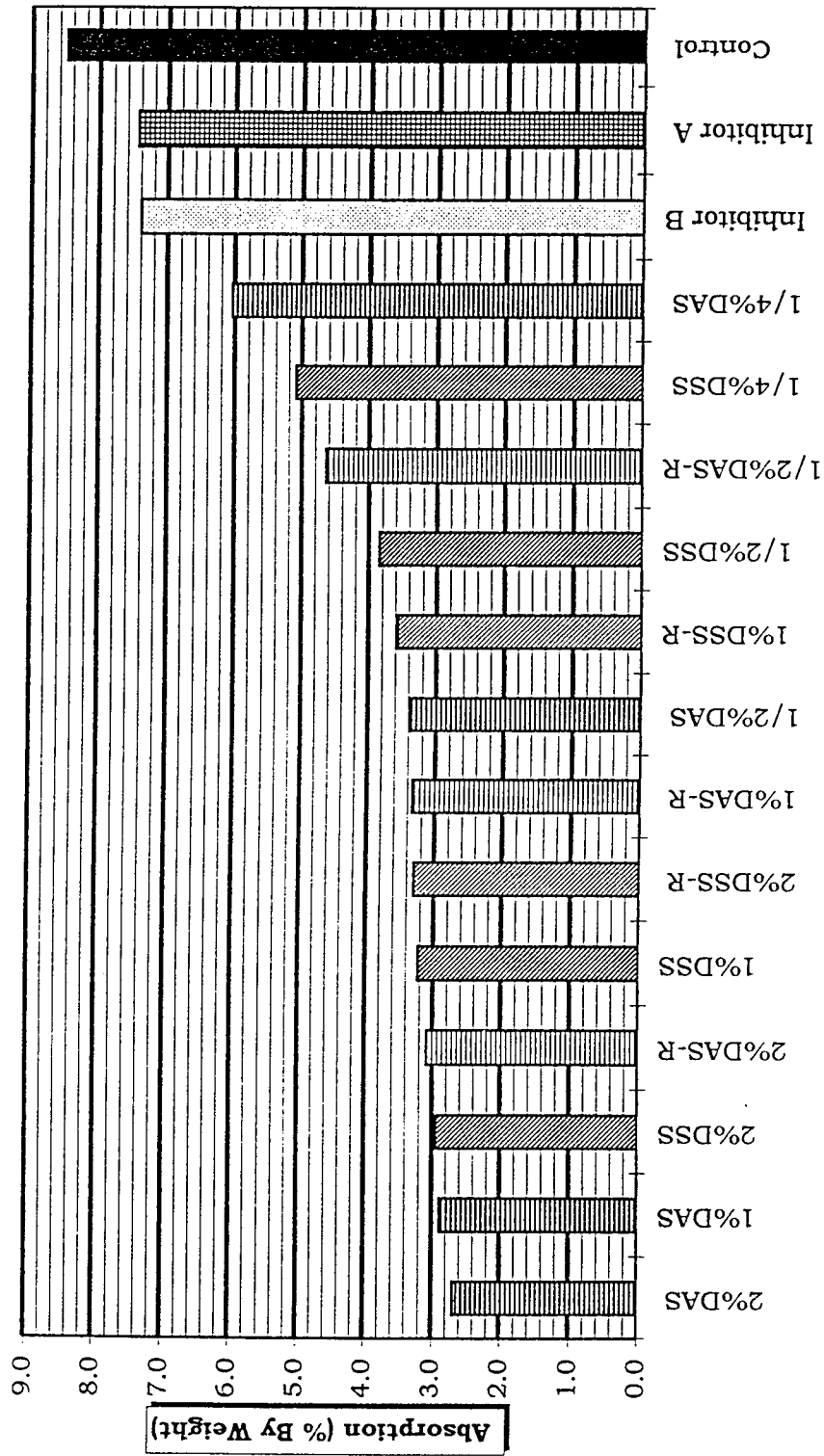


Figure B-1 Final Absorption: all Specimens, Dried at 100°C.

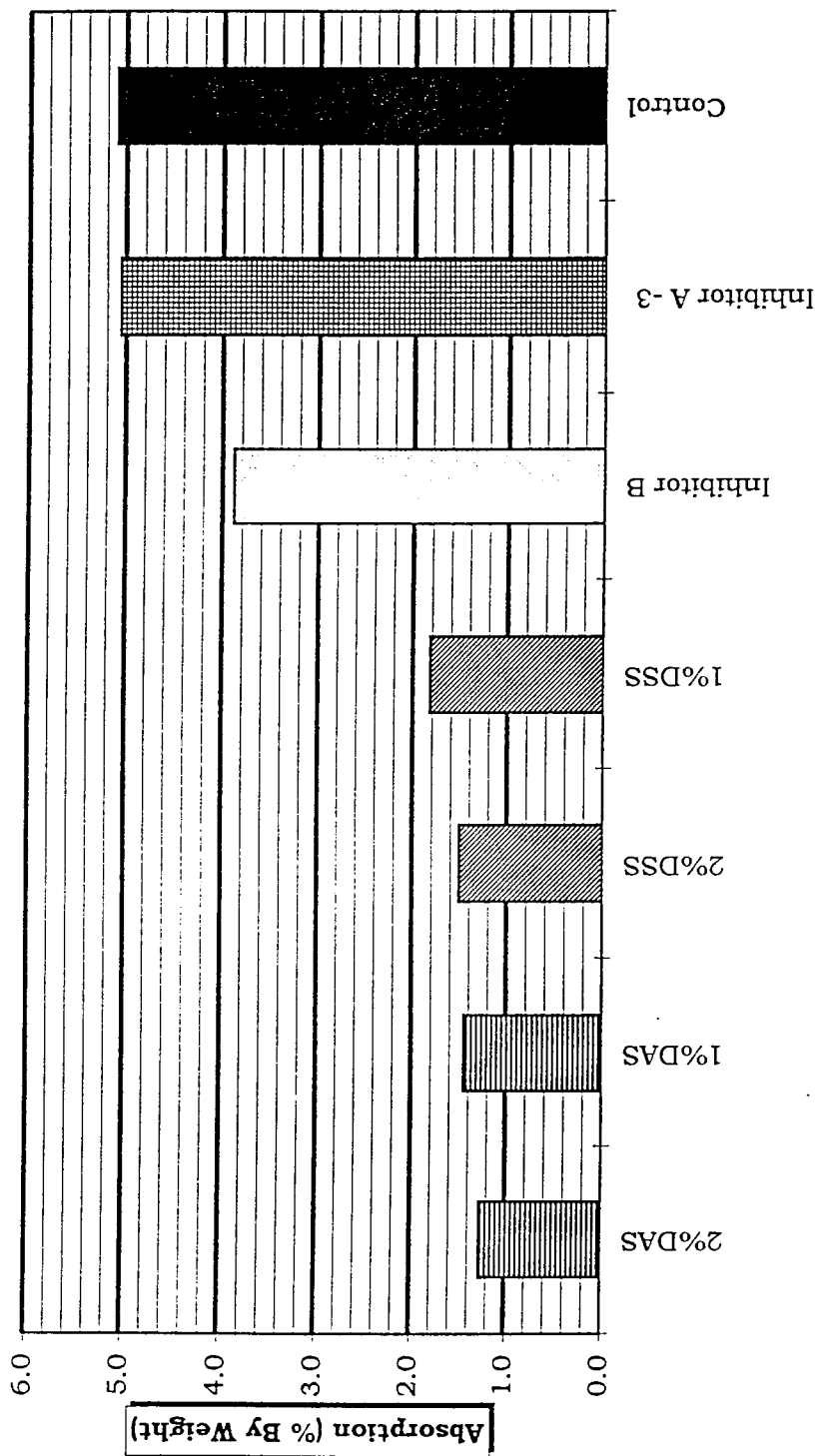


Figure B-2 Final Absorption: all Specimens, Dried at 40°C.

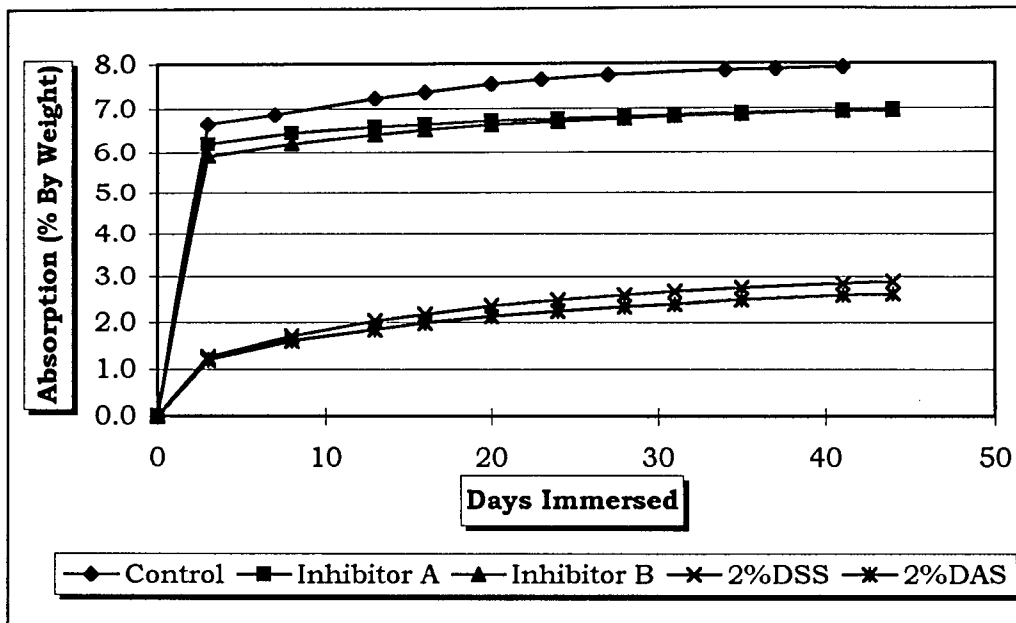


Figure B-3 Absorption Verses Time: Control, Inhibitors A & B, DAS and DSS Specimens, Dried at 100°C.

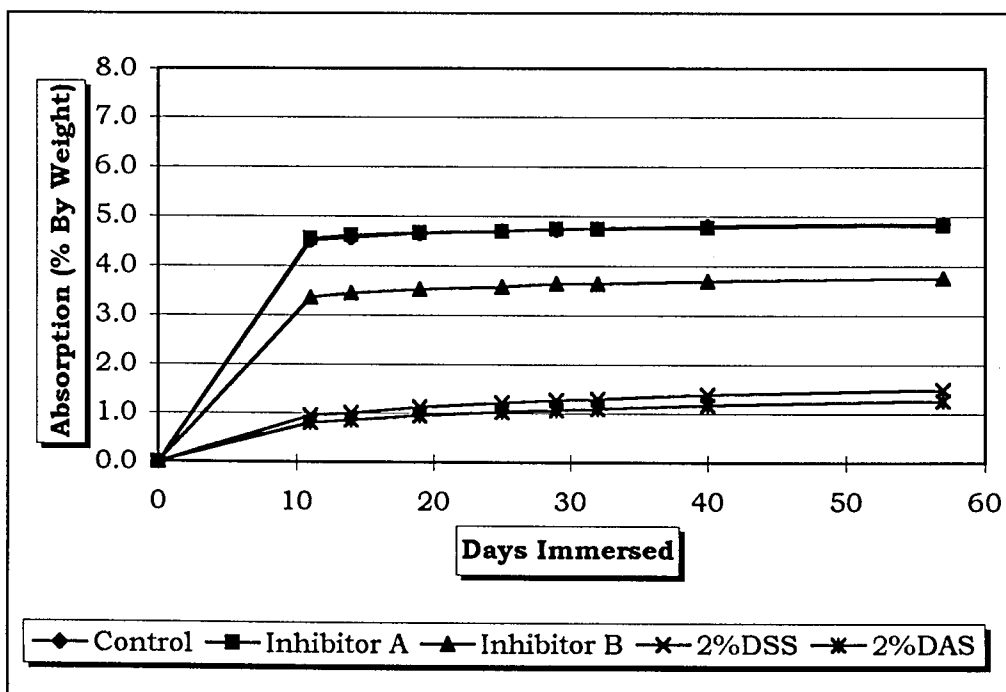


Figure B-4 Absorption Verses Time: Control, Inhibitors A & B, DAS and DSS Specimens, Dried at 40°C.



The control mix had the highest absorption with values of 8.5% and 5.1% for drying at 100°C and 40°C, respectively.

Inhibitors A and B had about the same absorption value, 7.4%, when the specimens were dried at 100°C. This was an unexpected result. The manufacture of Inhibitor B indicated that this product should reduce moisture absorption.

The DAS chemical made the concrete quite impervious, compared to the control, Inhibitor A, and Inhibitor B mixes, regardless of the drying temperature. The results showed that as the DAS concentration increased, the impermeability of the concrete also increased. The same trend occurred with the DAS-R mixes, with air reduction. The final absorption values for the DAS mixes, dried at 100°C, for concentrations of 2%, 1%, 1/2% were 2.7%, 2.9%, and 3.4%, respectively. There was a significant increase in the absorption, approximately by a factor of two (from 3% to 6%), when the concentration of DAS decreased from 1/2% to 1/4%. The 2%DAS and 1%DAS mixes had slightly lower absorption than their reduced air companion mixes, with de-foaming agent. The 1/2%DAS mix had about 1% lower absorption than the 1/2%DAS-R mix. A 1/4%DAS-R mix was not evaluated.

The DSS results and trends were similar to the DAS and DAS-R mixes. DSS concentrations of 2%, 1%, 1/2%, and 1/4% produced absorption values of 2.9%, 3.2%, 3.9% and 5.1%, respectively, when dried at 100°C. There was not as large an increase, as compared to the DAS mixes, in absorption values when the DSS concentration was decreased from 1/2% to 1/4%.

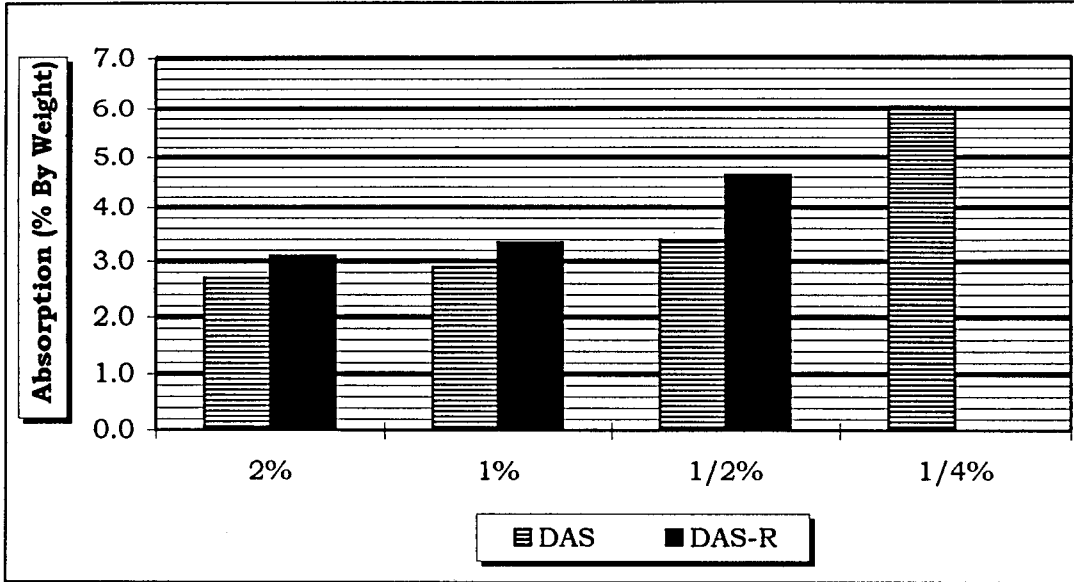


Figure B-5 Final Absorption: DAS and DAS-R Specimens, Dried at 100°C.

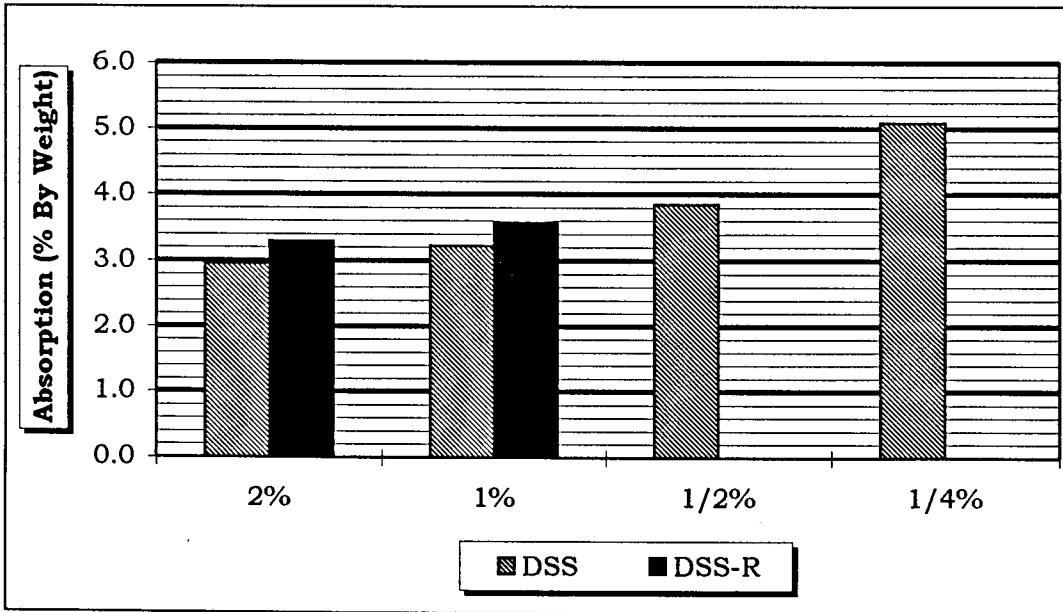


Figure B-6 Final Absorption: DSS and DSS-R Specimens, Dried at 100°C.

Reducing the drying temperature from 100°C to 40°C, reduced the final absorption values by approximately 50% for all specimens and the absorption rates also decreased. Inhibitor B had a slight, but not dramatic, improvement in relative overall absorption performance. At 100°C drying, Inhibitor B had the same final absorption as Inhibitor A (7.4%), but when dried at 40°C, the absorption for Inhibitor B was approximately 1% less than for Inhibitor A (3.9% vs. 5.1%). The DAS and DSS mixes outperformed both Inhibitors A & B and the control mixes with absorption values less than 1.8% when dried at 40°C.

### **B3.0 CONCLUSIONS**

The best mixes, based on absorption performance, were the 2%, 1% and 1/2% concentrations of DAS and DSS, both with and without the de-foaming agent added. Generally, the absorption values for these mixes were at least fifty percent lower than the values for the control, Inhibitor A and Inhibitor B mixes.

Overall, the DAS mixes had slightly lower absorption than the DSS mixes (Fig. B-7), except for the 1/4%DSS mix which was a little more impermeable than the 1/4%DAS mix. The reduction of air content in the DAS and DSS mixes did not have a significant effect on the absorption performance of these mixes.

The 1/4% concentration of the DAS and DSS mixes had moderately higher absorption rates than the other DAS and DSS mixes, which indicated that there was a limiting concentration based on absorption. Based on the results, the concentration of

DAS and DSS should be 1/2% or greater to obtain superior impermeability characteristics in concrete.

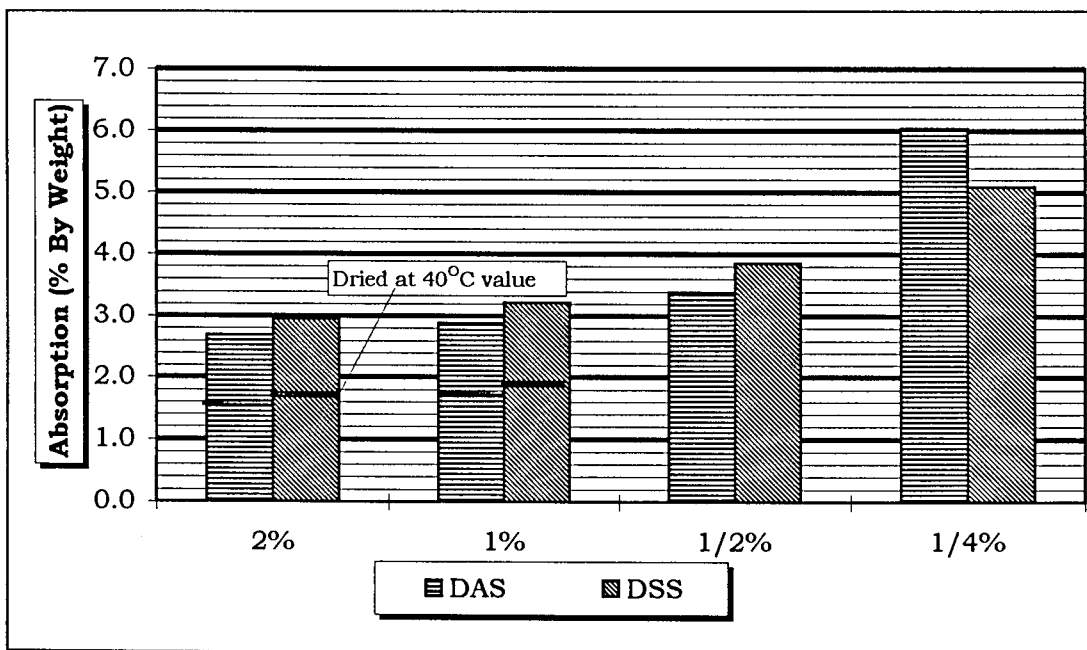


Figure B-7 Final Absorption: DAS and DSS Specimens, Dried at 100°C.

## APPENDIX C

### COMPRESSION STRENGTH

#### C1.0 SPECIMEN PREPARATION AND TEST PROTOCOL

The compressive strength of each corrosion and freeze-thaw mix was evaluated by ASTM C39-94 "Standard Test Method for Compressive Strength of Cylindrical Concrete Specimens".

With each corrosion batch, six 3-inch x 6-inch cylinders were cast and wet cured for 14 days and then stored in air until tested (See Chapter 5.0 for mix details). With each freeze-thaw mix, nine or twelve 3-inch x 6-inch cylinders were cast and wet cured continuously until tested (See Appendix A for mix details). As noted before, the water/cement ratio was not held constant for all the mixes. Rather, sufficient water was added to produce an acceptable consistency.

Additional cylinders were cast from mixes (Table C-1) that were not used for corrosion testing due to time constraints or because of casting problems encountered with some of the corrosion specimens. These problems had no effect on the quality of the strength cylinders. Some of these additional mixes for the DAS and DSS batches had a defoaming agent added after step nine of the general mixing procedure (Chapter 5.0). The batches were then mixed for 1.5 minutes before proceeding with step ten.

Cylinders were tested using elastomeric end caps and were loaded at a rate of 15 kips per minute. The freeze-thaw mix cylinders were tested wet and the other cylinders

were tested dry. Generally, the results of three cylinders were averaged together for each test age, for each mix.

**Table C-1 Additional Mix Proportions.**

Mix Type and No. <sup>1,2</sup>	W/C Ratio	Air Entrain Admixture	Inhibitor Concentration <sup>3</sup>	De-foam Agent <sup>4</sup>	Air Content	Slump (in)
Inhibitor A-2	0.38	Yes	4.0 gal/c.y.	No	7.00	3.50
Inhibitor B-2	0.40	Yes	1.0 gal/c.y.	No	8.50	4.25
2.0% DAS-R-1	0.41	No	2%	Yes	4.50	2.75
1.0% DAS-R-1	0.40	No	1%	Yes	6.00	2.00
1/2% DAS-R-1	0.39	No	1/2%	Yes	5.00	2.00
1/2% DAS-R-2	0.40	No	1/2%	Yes	5.00	2.50
1/4% DAS-1	0.39	No	1/4%	No	7.00	2.50
2.0% DSS-R-1	0.40	No	2%	Yes	4.75	3.75
1.0% DSS-R-1	0.40	No	1%	Yes	5.50	2.75
1/2% DSS-1	0.39	No	1/2%	No	7.00	2.50
1/2% DSS-2	0.41	No	1/2%	No	9.00	4.00
1/4% DSS-1	0.38	No	1/4%	No	7.50	2.25

<sup>1</sup> All mixes contained Type I/II cement @ 27.85 lb., coarse agg. (oven-dried) @ 48.59 lb., and fine agg. (oven-dried) @ 54.26 lb. - Based on 1.0 cu. ft. mix.

<sup>2</sup> R- air reduction with de-foaming agent.

<sup>3</sup> Concentrations used for Inhibitors A and B were as suggested by the supplier. Concentrations for the DAS and DSS were based on weight of cement.

<sup>4</sup> The quantity of de-foaming agent used in the reduced air mixes was 25.0 ml.

## C2.0 DISCUSSION OF RESULTS

The strength results for the corrosion monitored mixes and additional mixes, both identified hereafter as corrosion mixes, and freeze-thaw mixes are shown in Table C-2 and Figures C-1, C-2, C-3 and C-4. The batch numbers shown in Table C-2 correspond to the corrosion mixes only. The relative strengths of the corrosion mixes and freeze-thaw mixes are shown as a percentage of the corrosion Control-2 mix and the freeze-thaw Control mix, respectively.

Table C-2 28 Day Strengths for Corrosion and Freeze-Thaw Mixes.

Mixes <sup>1,2,3</sup>	Corrosion Mixes			Freeze-Thaw Mixes		
	w/c	Compression	Strength	w/c	Compression	Strength
		28 Day (psi)	Relative (%) <sup>4</sup>		28 Day (psi)	Relative (%) <sup>5</sup>
Control-2*	0.38	5941	100	0.44	6100	100
Inhibitor-A-1*	0.40	7381	124	0.40	8161	134
Inhibitor-A-2	0.38	7590	128	----	----	----
Inhibitor-A-3*	0.38	6884	116	----	----	----
Inhibitor-B-1*	0.45	4932	83	0.44	5482	90
Inhibitor-B-2	0.40	5032	85	----	----	----
Inhibitor-B-3*	0.39	4839	81	----	----	----
2% DAS-1*	0.41	5217	88	0.41	4318	71
2% DAS-2*	0.41	4489	76	----	----	----
2% DAS-R-1	0.41	5065	85	----	----	----
1% DAS-1*	0.39	5038	85	0.40	4337	71
1% DAS-2*	0.40	4758	80	----	----	----
1% DAS-R-1	0.40	5490	92	0.40	5447	89
1/2% DAS-1*	0.39	5367	90	0.40	4419	72
1/2% DAS-2*	0.40	4996	84	----	----	----
1/2% DAS-R-1	0.39	5863	99	0.40	5704	94
1/2% DAS-R-2	0.40	5909	99	----	----	----
1/4% DAS-1	0.39	5352	90	----	----	----
2% DSS-1*	0.40	3744	63	0.45	3897	64
2% DSS-2*	0.41	3741	63	----	----	----
2% DSS-R-1	0.40	4277	72	0.43	4809	79
1% DSS-1*	0.40	4232	71	0.40	4064	67
1% DSS-2*	0.40	3873	65	----	----	----
1% DSS-R-1	0.40	5072	85	0.39	5708	94
1/2% DSS-1	0.39	4981	84	0.38	4580	75
1/2% DSS-2	0.41	4099	69	----	----	----
1/2% DSS-R-1	----	----	----	0.38	6271	103
1/4% DSS-1	0.38	5157	0.87	0.38	4738	78
1/4% DSS-R-1	----	----	----	0.38	6599	108

<sup>1</sup> Number after specimen name indicates batch number for corrosion mixes only.

<sup>2</sup> R- air reduction with de-foaming agent (25 ml for 1.0 cu. ft. mix).

<sup>3</sup> \* - Corrosion Monitored Mixes.

<sup>4</sup> Relative strength: corrosion Control-2 mix equals 100%.

<sup>5</sup> Relative strength: freeze-thaw Control mix equals 100%.

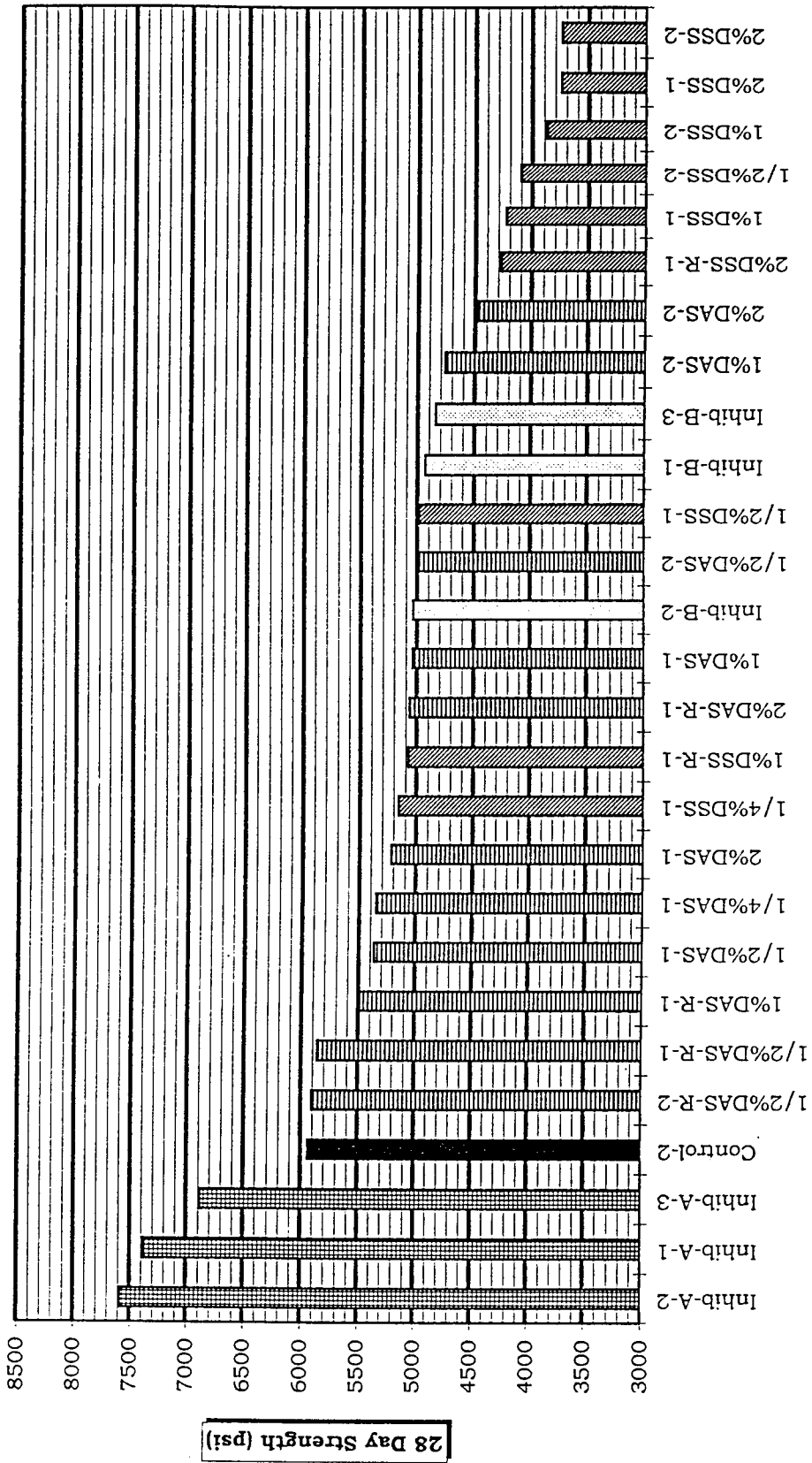


Figure C-1 28 Day Compression Strengths for Corrosion Mixes.



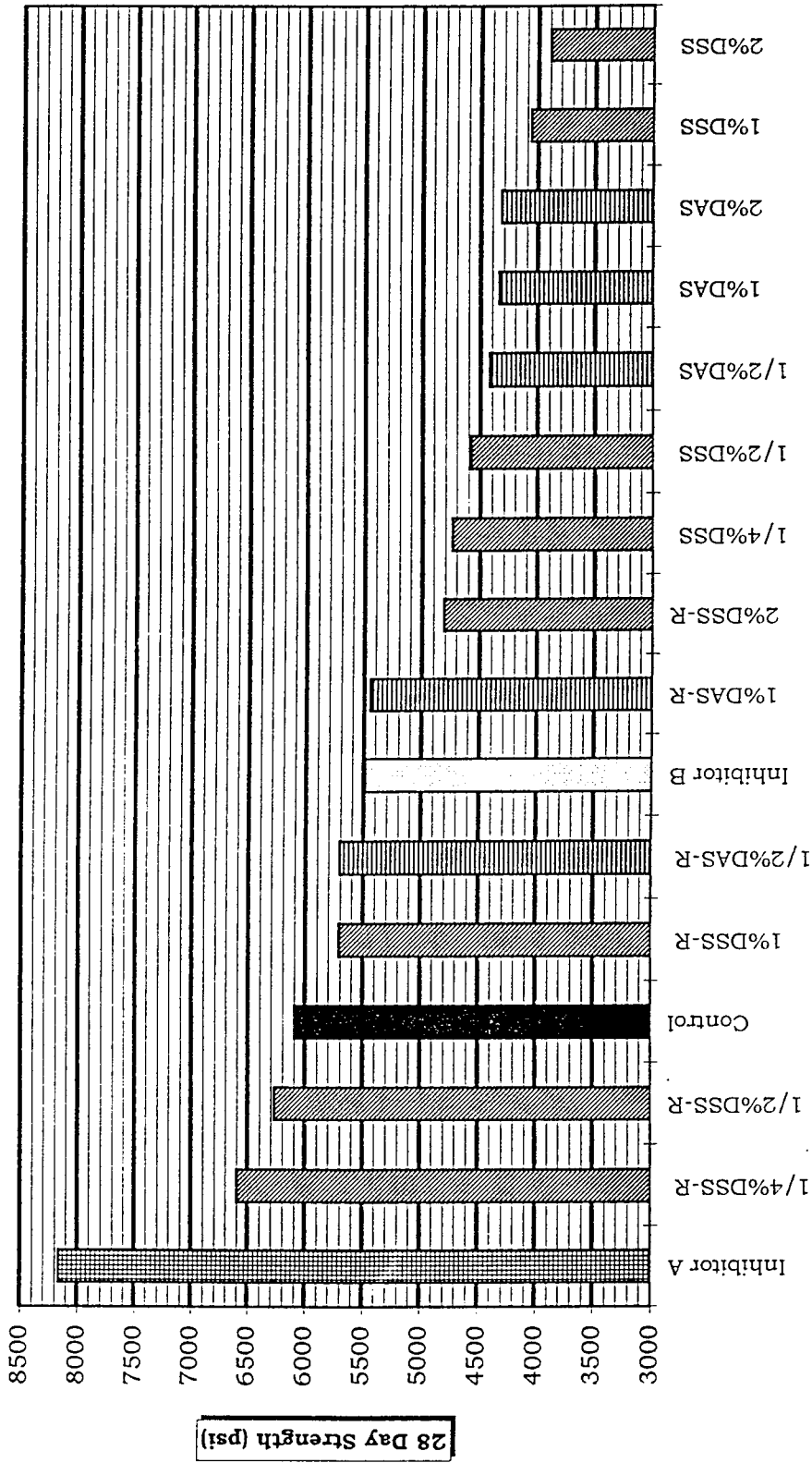


Figure C-2 28 Day Compression Strengths for Freeze-Thaw Mixes

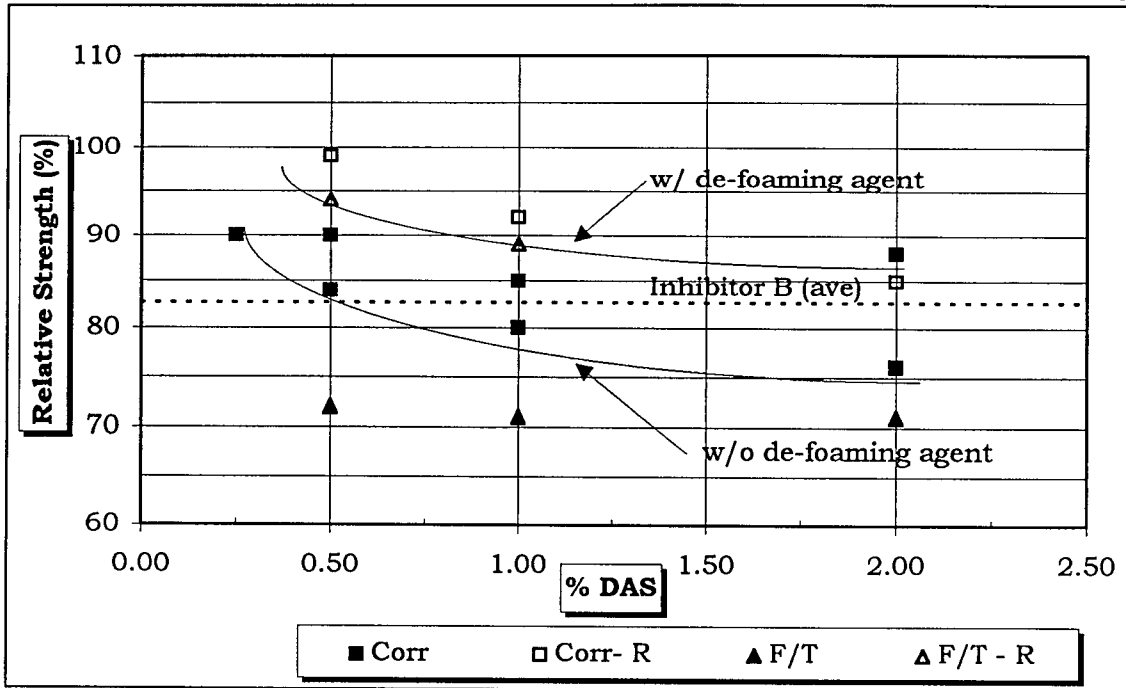


Figure C-3 Relative 28 Day Compression Strengths: all DAS Mixes (Control Mixes = 100%).

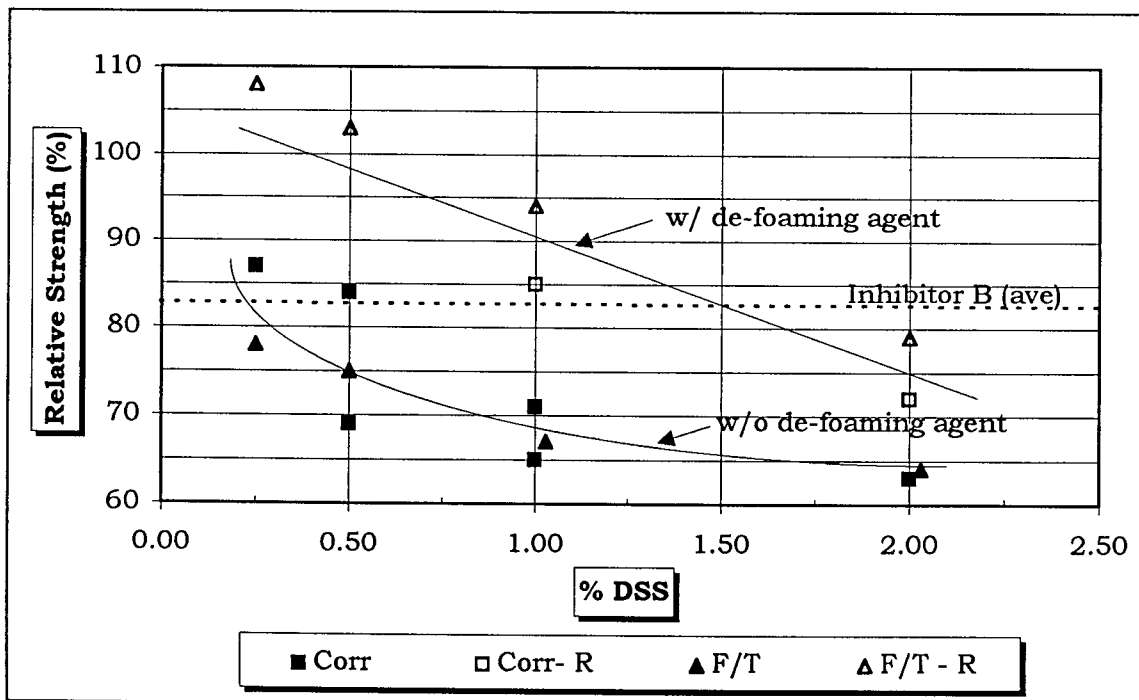


Figure C-4 Relative 28 Day Compression Strengths: all DSS Mixes (Control Mixes = 100%).

The control mixes for the corrosion and freeze-thaw specimens had approximately the same 28 day strengths (The corrosion monitored Control-1 mix had a 56 day strength of about 7000 psi, but a 28 day strength was not obtained and therefore this mix was not listed in Table C-2).

Inhibitor A had the highest strength, approximately 120% or higher of the control mixes. Inhibitor B was about 84% the strength of the control mixes.

The corrosion and freeze-thaw mixes used different curing conditions. However, the DAS data (Fig. C-3) and the DSS data (Fig. C-4), showed very similar trends when grouping all the data together. Visual "best fit" (i.e., "eyeballed") trend lines are shown.

All of the corrosion DAS mixes, with and without de-foaming agent, had 28 day relative strengths of 90% and 80% of the control, respectively, except for the 2% concentrations, which were within 85% and 75%, respectively. The freeze-thaw DAS mixes with de-foaming agent had relative strengths of a least 93% or better and mixes without de-foaming agent had relative strengths of about 70%. The strengths of the DAS mixes, both with and without de-foaming agent, generally increased with decreasing DAS concentrations, except for the freeze-thaw mixes without de-foaming agent for which the strengths remained relatively unchanged.

Typically, the DSS mixes without de-foaming agent had the lowest strengths of all the mixes. The DSS corrosion mixes, with and without de-foaming agent, had relative strengths from 72% to 85% and 63% to 87%, compared to the control, respectively. The DSS freeze-thaw mixes had relative strengths from 79% to 108% for mixes with de-foaming agent and from 64% to 78% for mixes without de-foaming agent. The DSS

strength results also indicated that mix strength increased as concentration of DSS decreased (Figure C-4).

### C3.0 CONCLUSIONS

Comparing the 28 day strengths of the corrosion (using a combination of wet and air curing) and the freeze-thaw mixes (using continuous wet curing), the strength performance of companion mixes were very similar. In both, Inhibitor A mixes generally had the highest strengths (at 120% of Control) and the 2%DSS mix without de-foaming agent had the lowest (at 60% of Control). Inhibitor B averaged about 84% of the Control.

Increasing the concentration for both DAS and DSS produced lower compression strengths without much difference between the two chemicals. Compared to the mixes without de-foaming agent, adding de-foaming agent increased the strengths of the DAS and DSS mixes by 4% to 25% for the corrosion mixes and by 23% to 40% for the freeze-thaw mixes. Generally the strength increase due to the de-foaming agent was higher for the DSS mixes. Also, the strength increase due to the de-foaming agent was higher for the lower DAS and DSS concentrations. For 1% or lower DAS and DSS concentrations with de-foaming agent, the reduced air mixes had relative strengths of about 90% or better of the control mixes, which were comparable to the strengths of the Inhibitor B mixes.

Except for a few mixes (the 2%DSS corrosion and freeze-thaw mixes and the 1%DSS corrosion mix, all without de-foaming agent), all the DAS and DSS mixes had 28 day compression strengths greater than 4000 psi, which satisfied the requirements of ConnDot's Class "F" concrete for bridges. Even the lowest strength DSS mixes were within 6.5% of the required strength of 4000 psi.

## APPENDIX D

### SOLUTION RESISTANCE AND CORROSION RATE DATA

$R_s$  verses time and  $1/R_p$  verses time (corrected for IR error) plots for each individual specimen of each group and type (i.e., not averaged) are presented here. Note that any obviously "bad" data points (such as in Fig. D-8) were not included in the data reduction process and/or in results presented in Chapter 7.0. Also, some of the control specimens were cut open during the monitoring program, therefore the data for those specimens (such as Fig. D-1) ends abruptly.

Solution Resistance verses time results are presented as follows:

2-Inch Diameter Lollipops	Figures D-1 to D-8
3-Inch Diameter Lollipops	Figures D-9 to D-16
Slab Specimens	Figures D-17 to D-26

Corrosion rates ( $1/R_p$ ) verses time results are presented as follows:

2-Inch Diameter Lollipops	Figures D-27 to D-34
3-Inch Diameter Lollipops	Figures D-35 to D-42
Slab Specimens	Figures D-43 to D-52

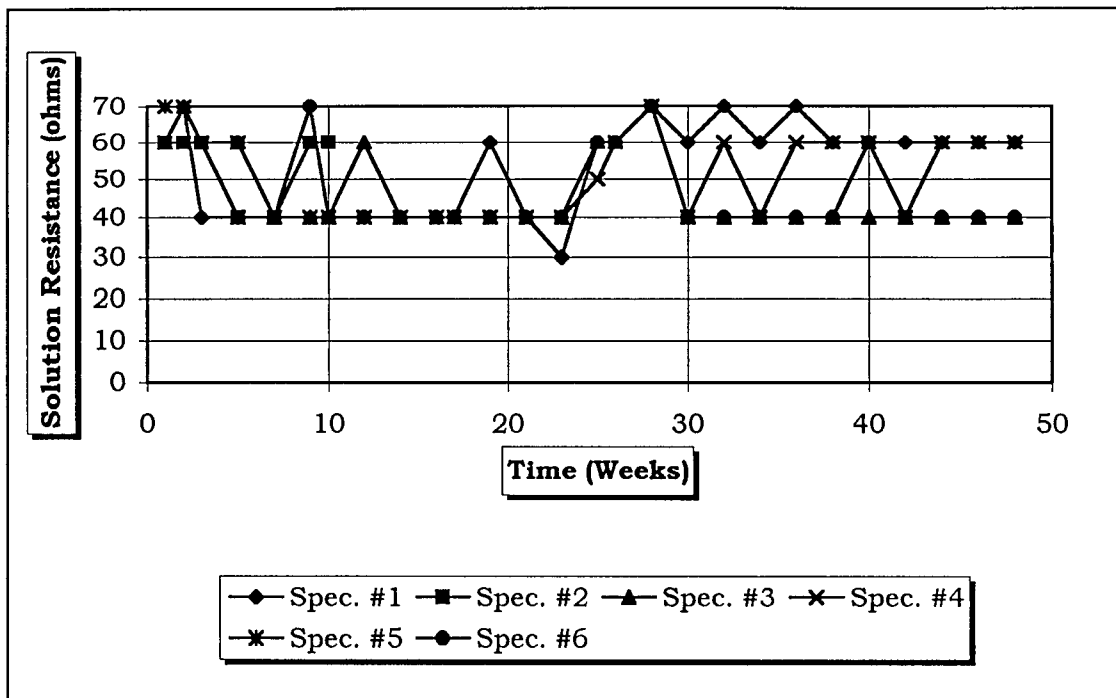


Figure D-1 Solution Resistance, 2-Inch Diameter Lollipops: Control.

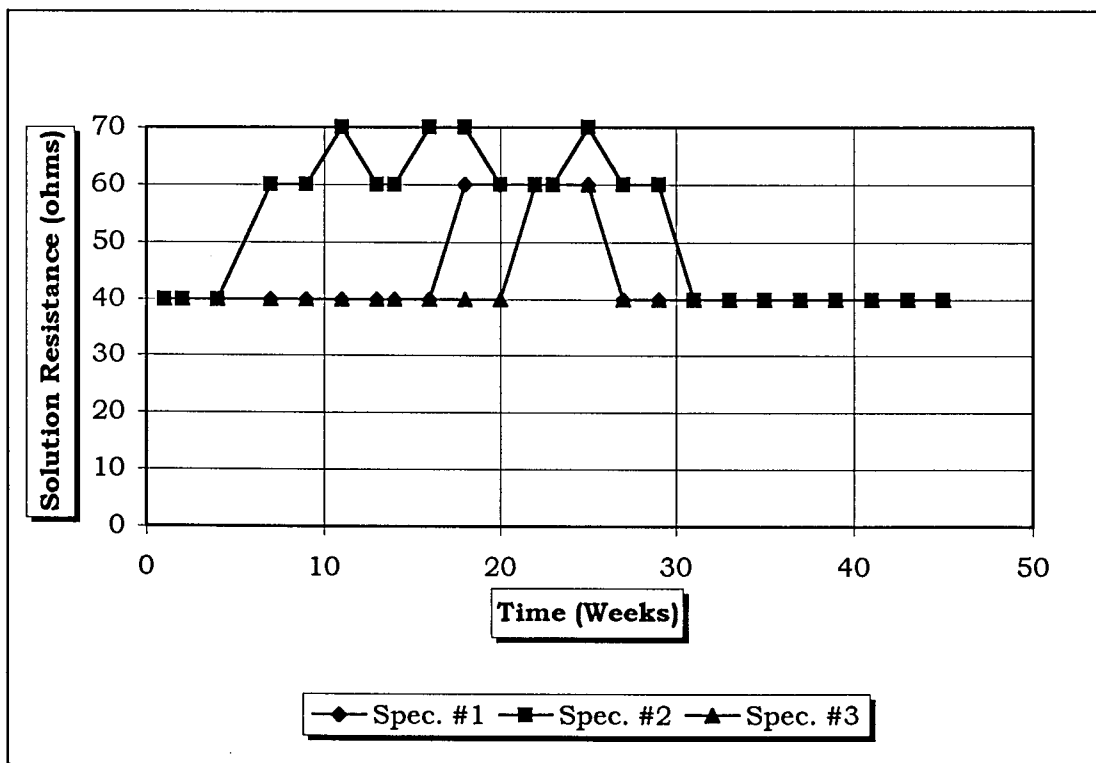


Figure D-2 Solution Resistance, 2-Inch Diameter Lollipops: Inhibitor A.

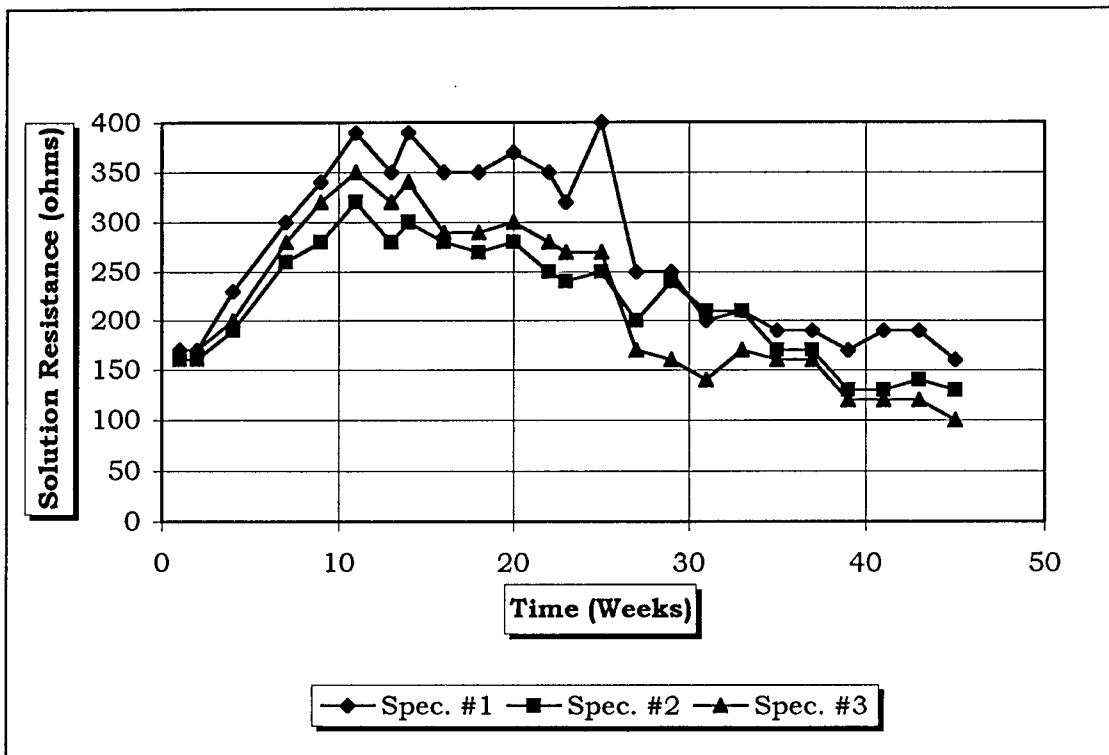


Figure D-3 Solution Resistance, 2-Inch Diameter Lollipops: Inhibitor B.

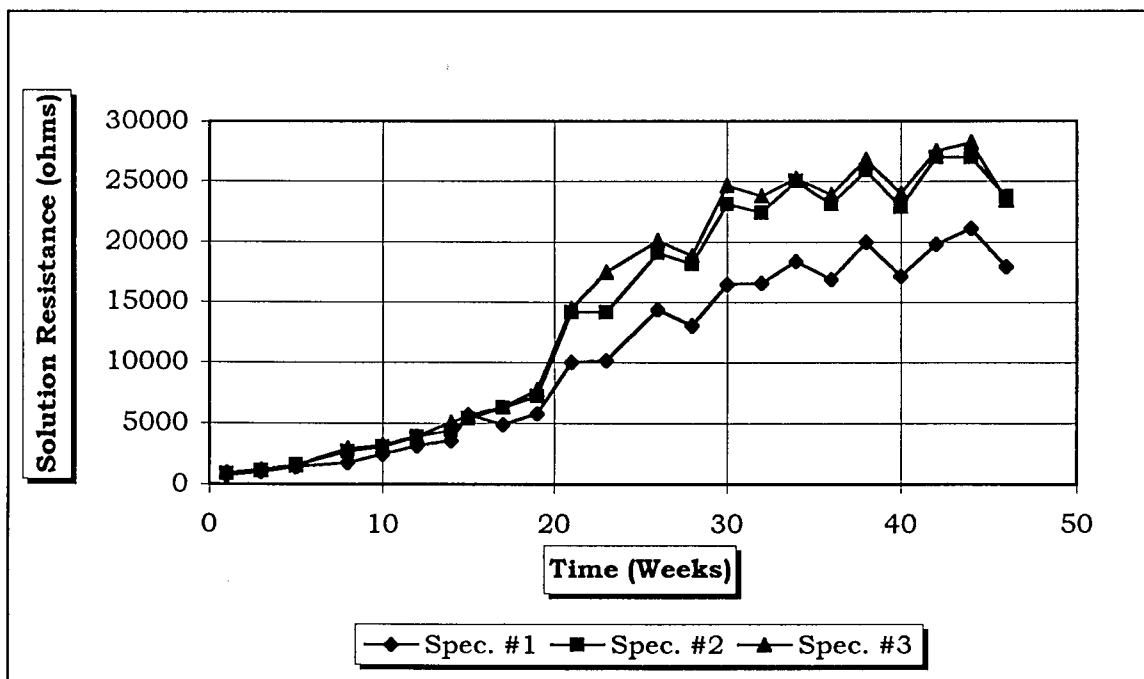


Figure D-4 Solution Resistance, 2-Inch Diameter Lollipops: 2%DAS.

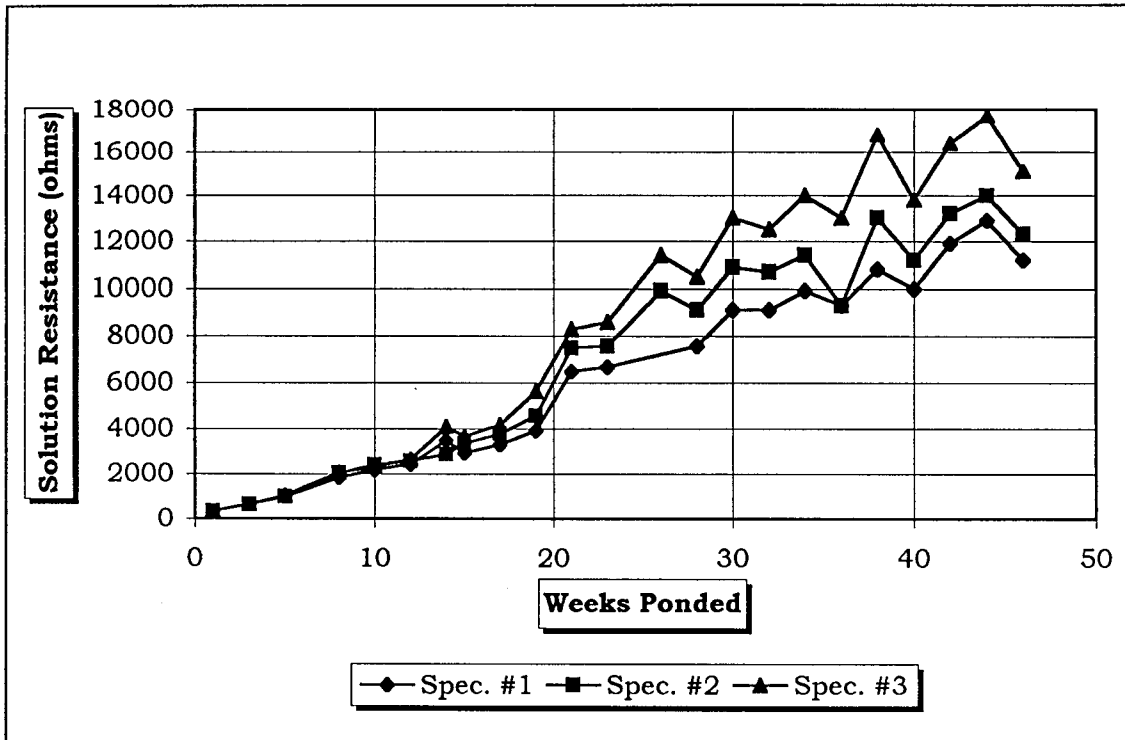


Figure D-5 Solution Resistance, 2-Inch Diameter Lollipops: 1%DAS.

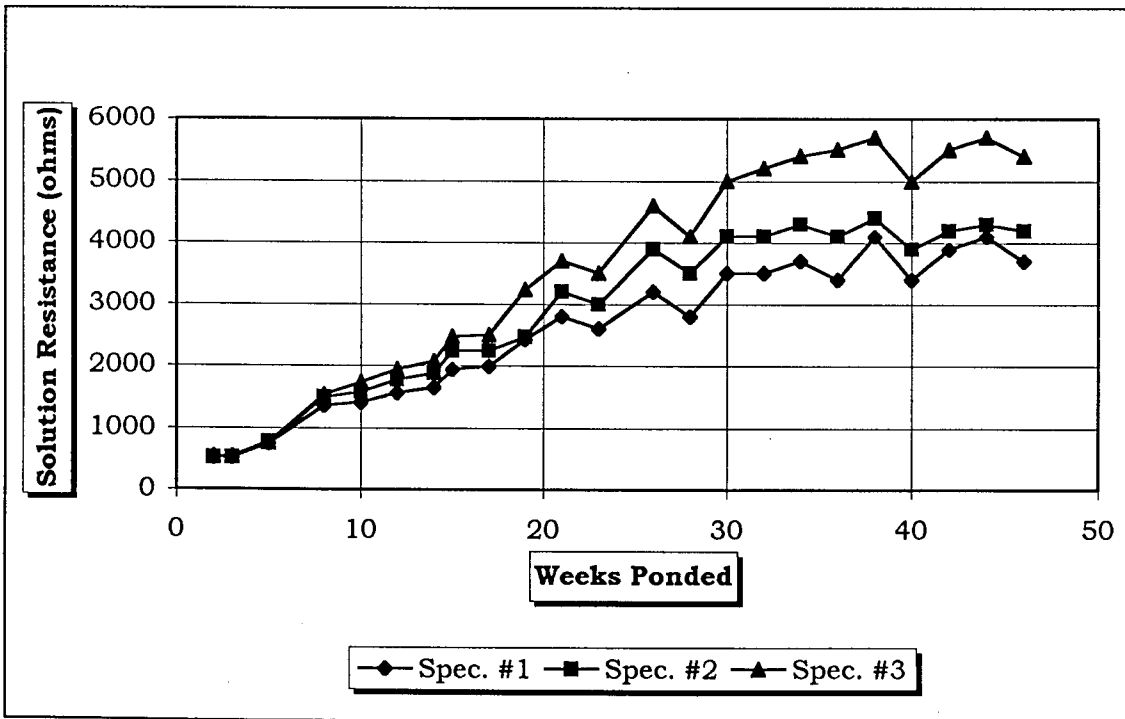


Figure D-6 Solution Resistance, 2-Inch Diameter Lollipops: 1/2%DAS.



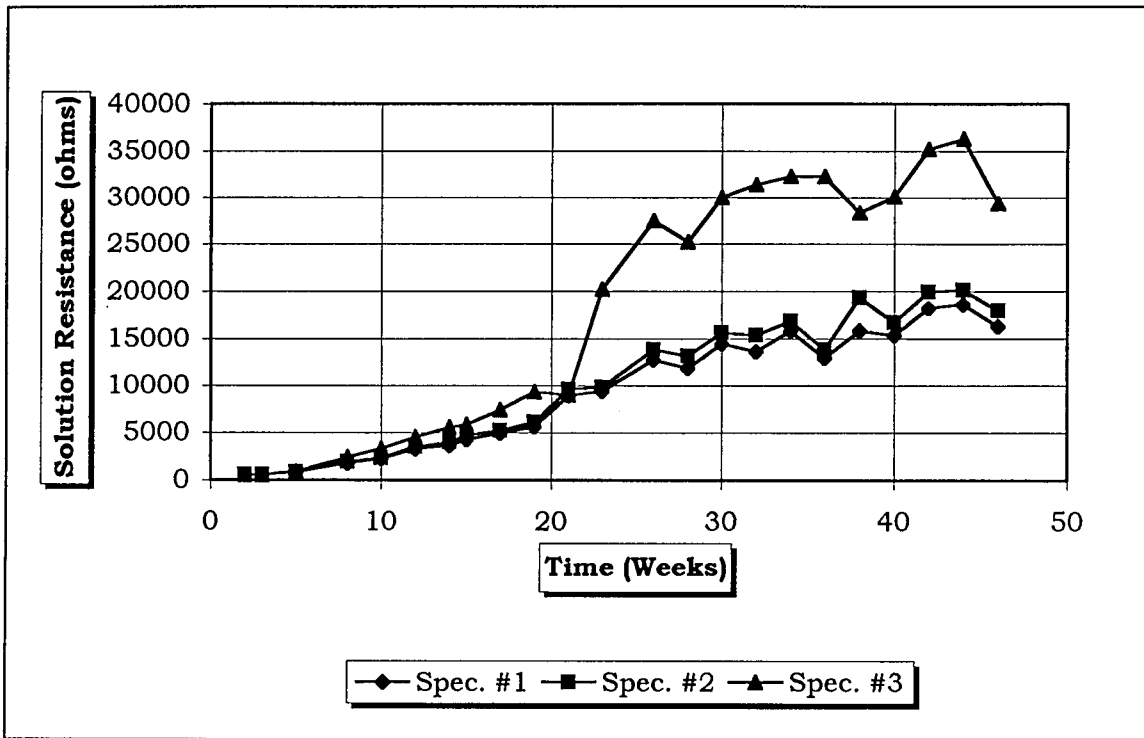


Figure D-7 Solution Resistance, 2-Inch Diameter Lollipops: 2%DSS

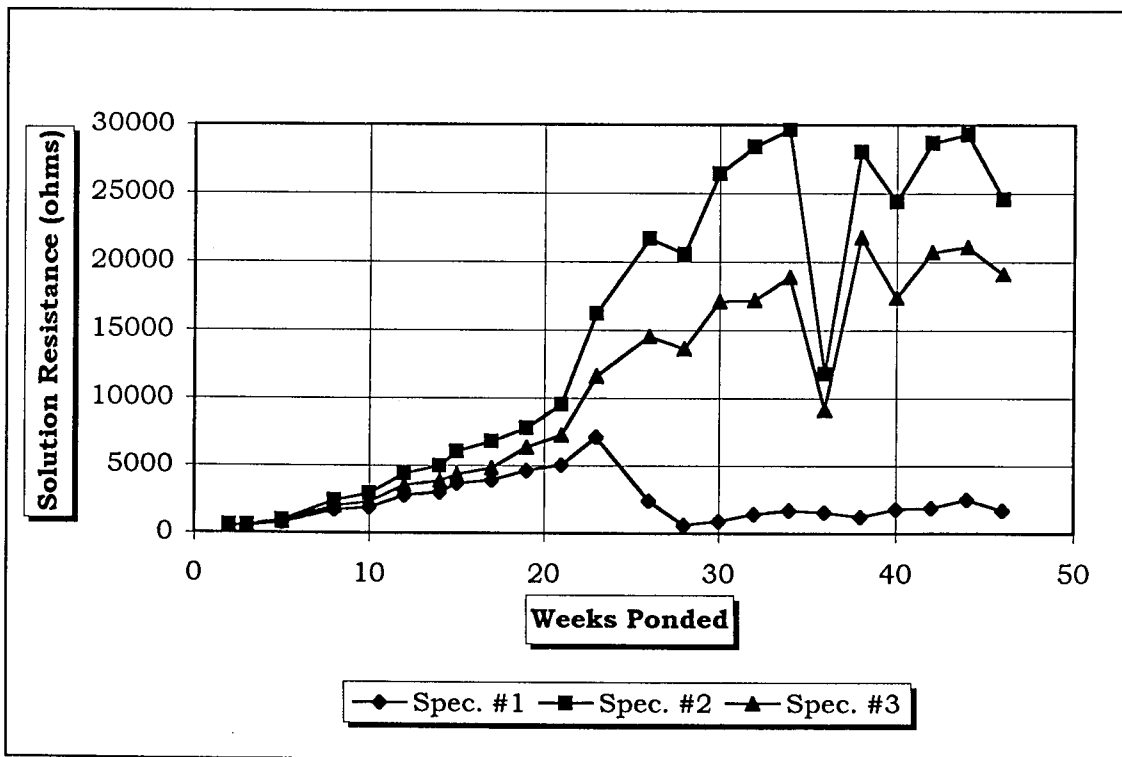


Figure D-8 Solution Resistance, 2-Inch Diameter Lollipops: 1%DSS

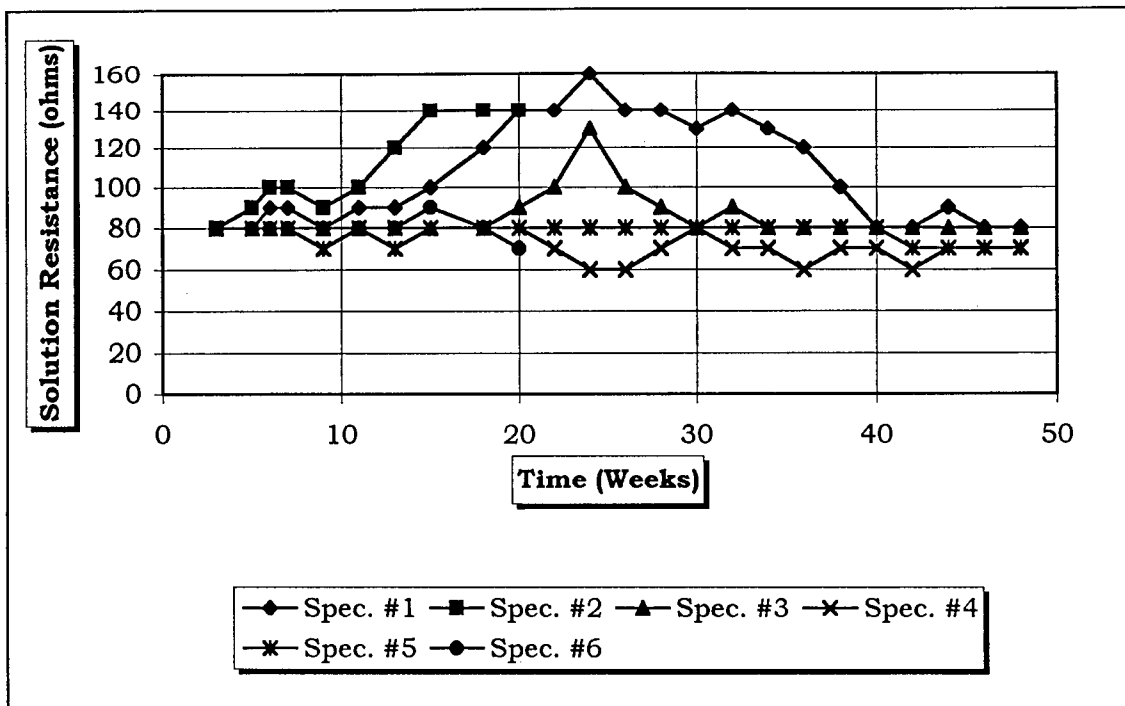


Figure D-9 Solution Resistance, 3-Inch Diameter Lollipops, Control.

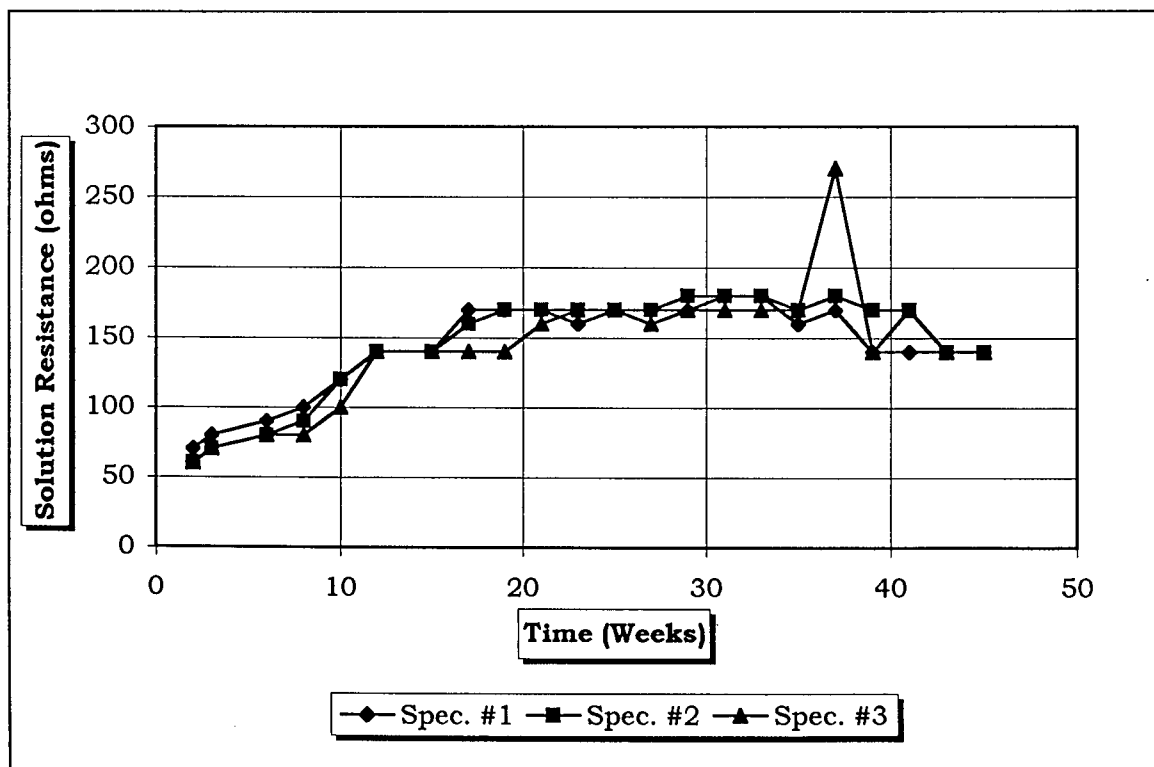


Figure D-10 Solution Resistance, 3-Inch Diameter Lollipops, Inhibitor A.

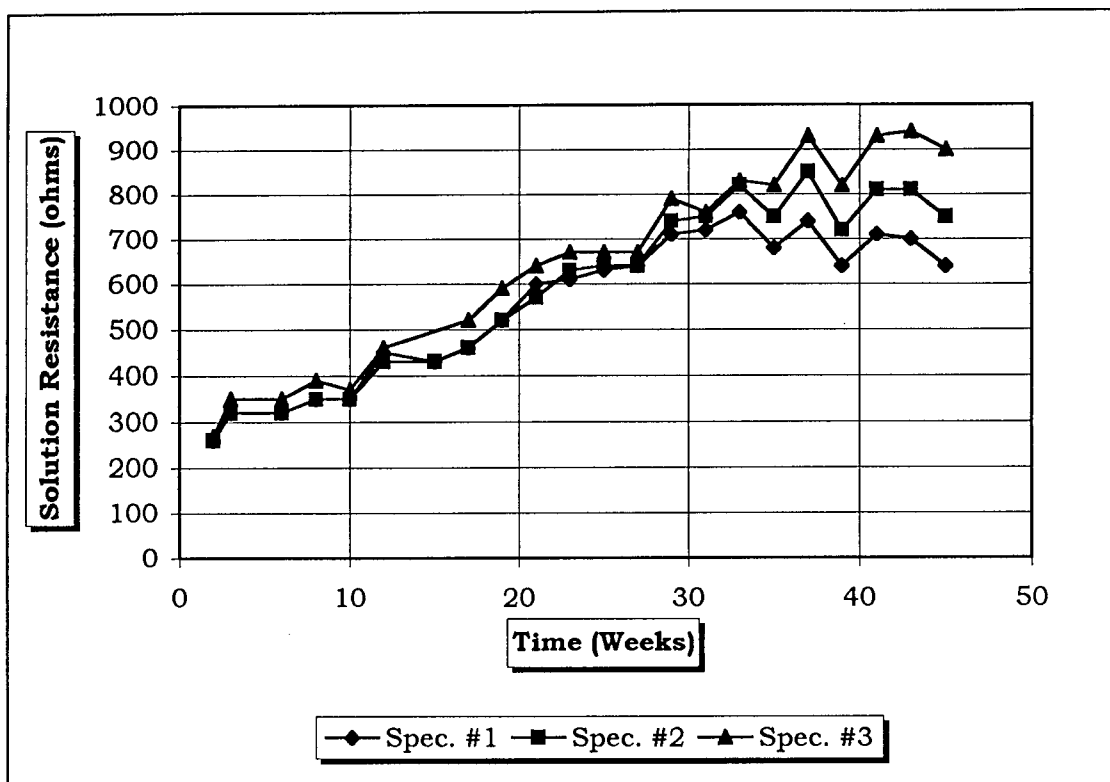


Figure D-11 Solution Resistance, 3-Inch Diameter Lollipops, Inhibitor B.

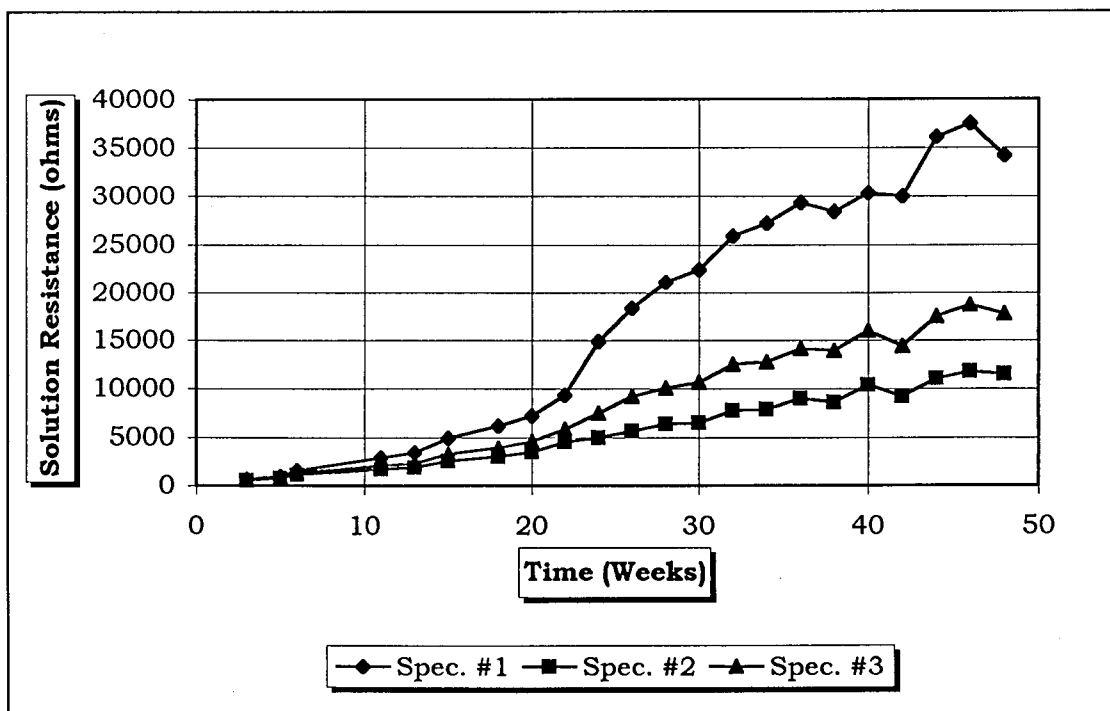


Figure D-12 Solution Resistance, 3-Inch Diameter Lollipops, 2% DAS.

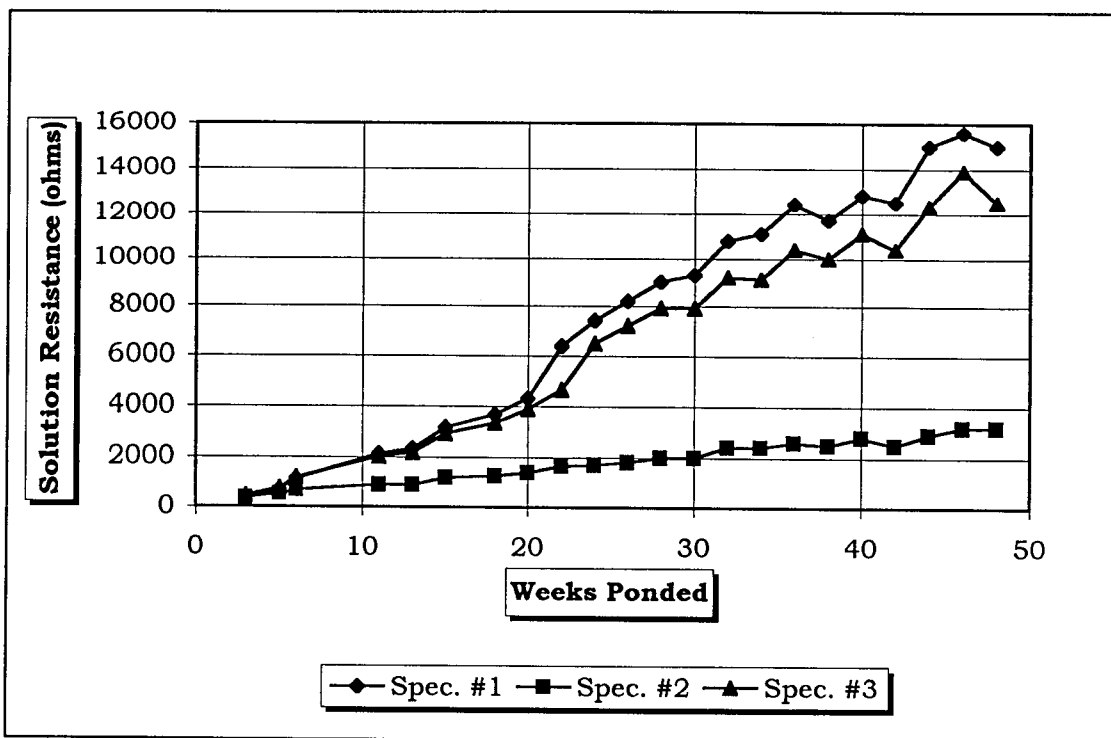


Figure D-13 Solution Resistance, 3-Inch Diameter Lollipops, 1% DAS.

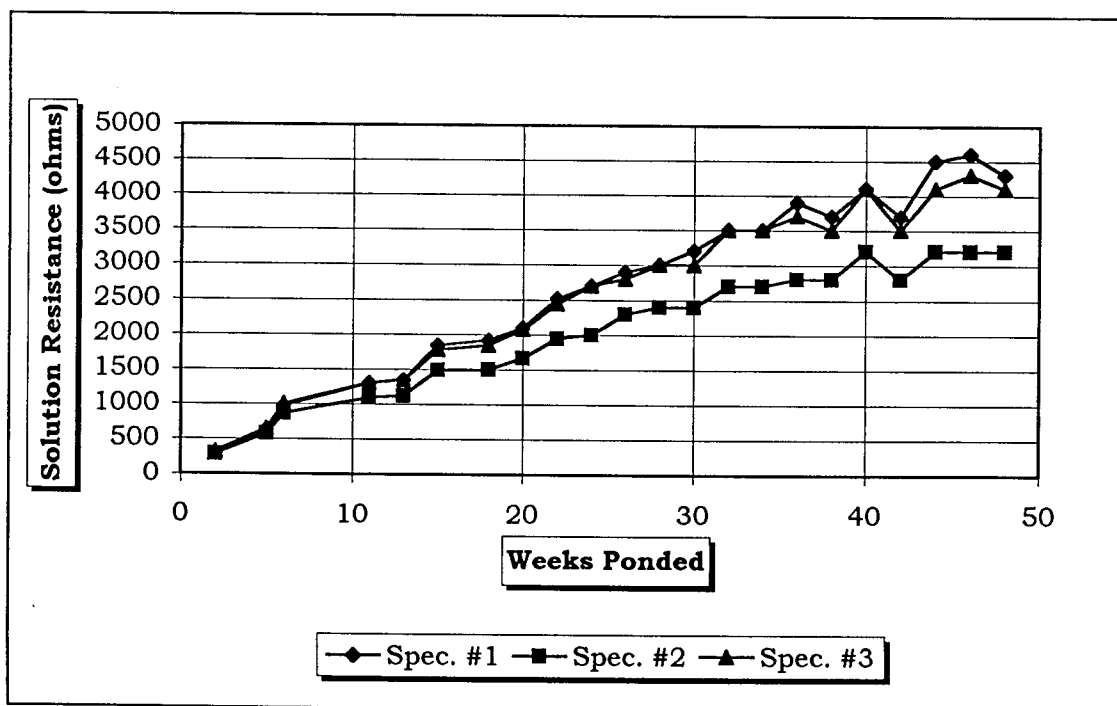


Figure D-14 Solution Resistance, 3-Inch Diameter Lollipops, 1/2% DAS.

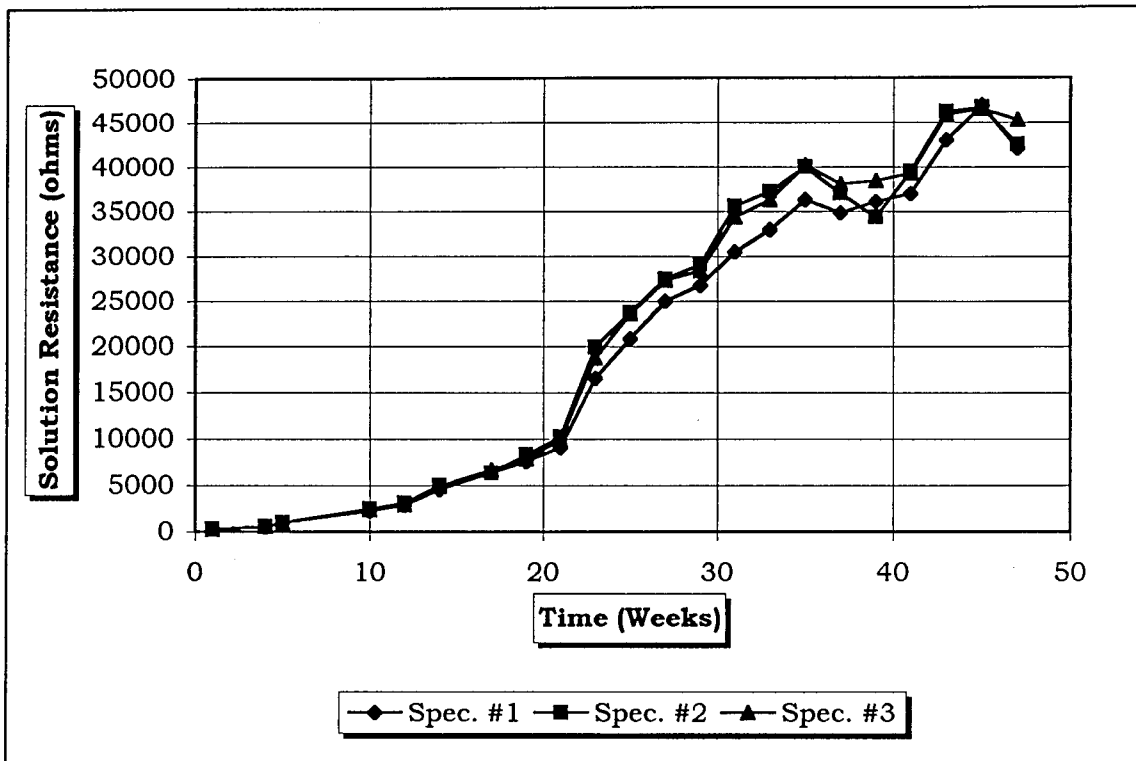


Figure D-15 Solution Resistance, 3-Inch Diameter Lollipops, 2% DSS.

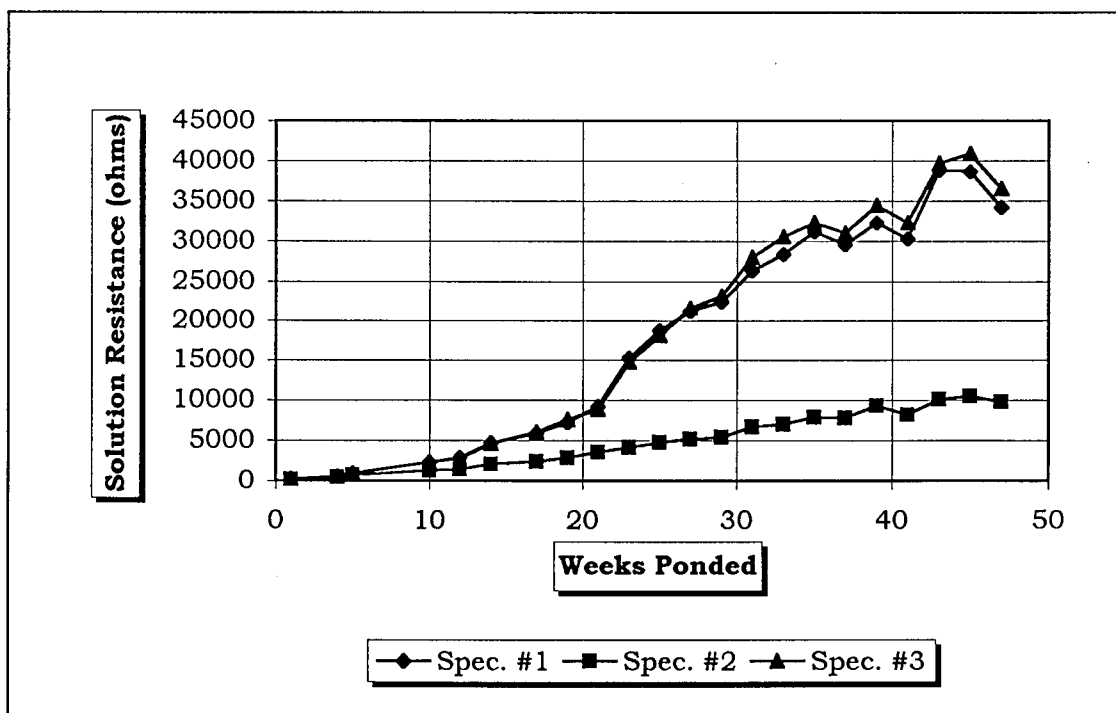


Figure D-16 Solution Resistance, 3-Inch Diameter Lollipops, 1% DSS.

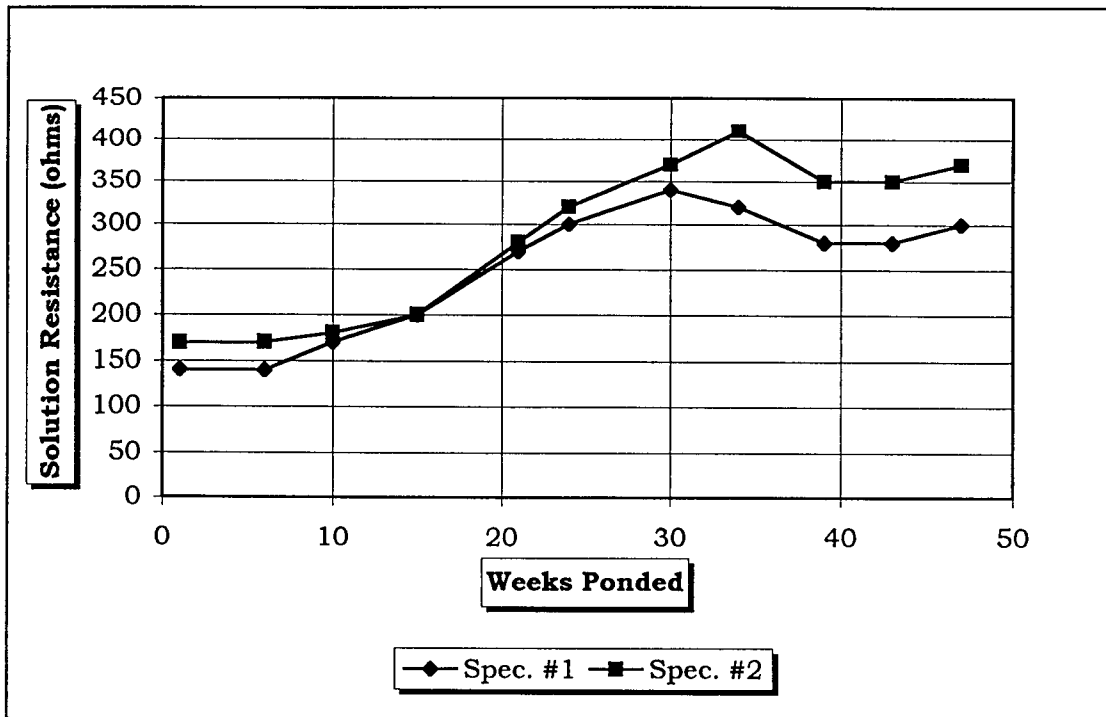


Figure D-17 Solution Resistance, Slabs, Control-1 Mixes Conn.

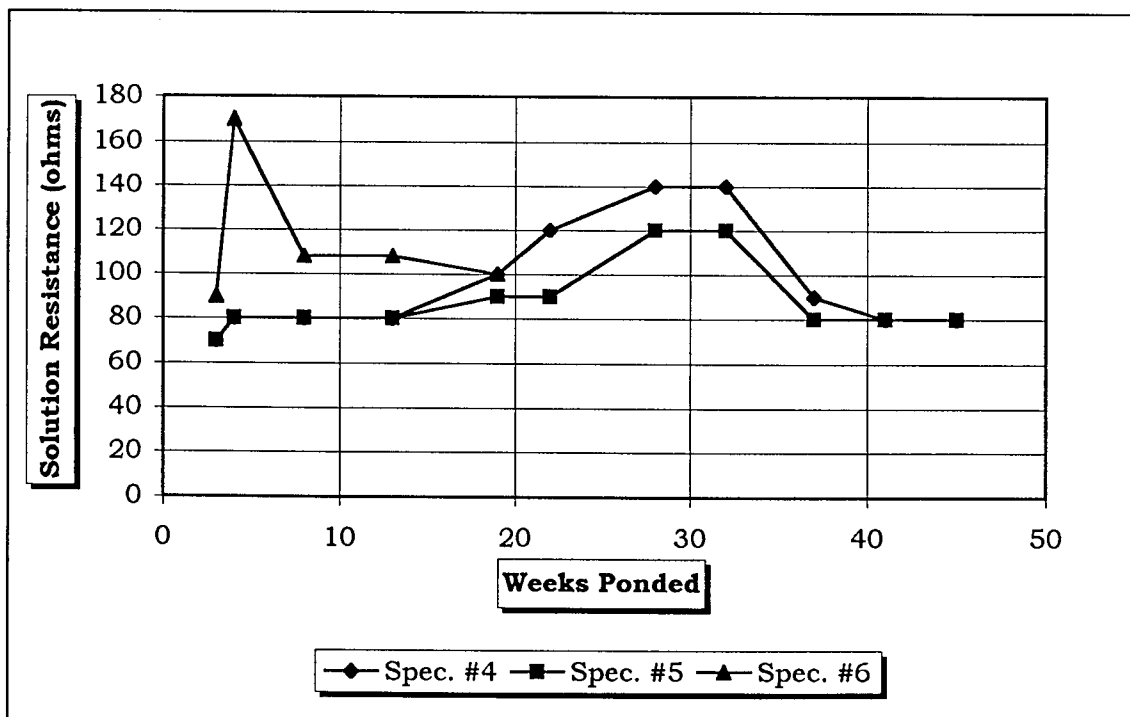


Figure D-18 Solution Resistance, Slabs, Control-2 Unconn.

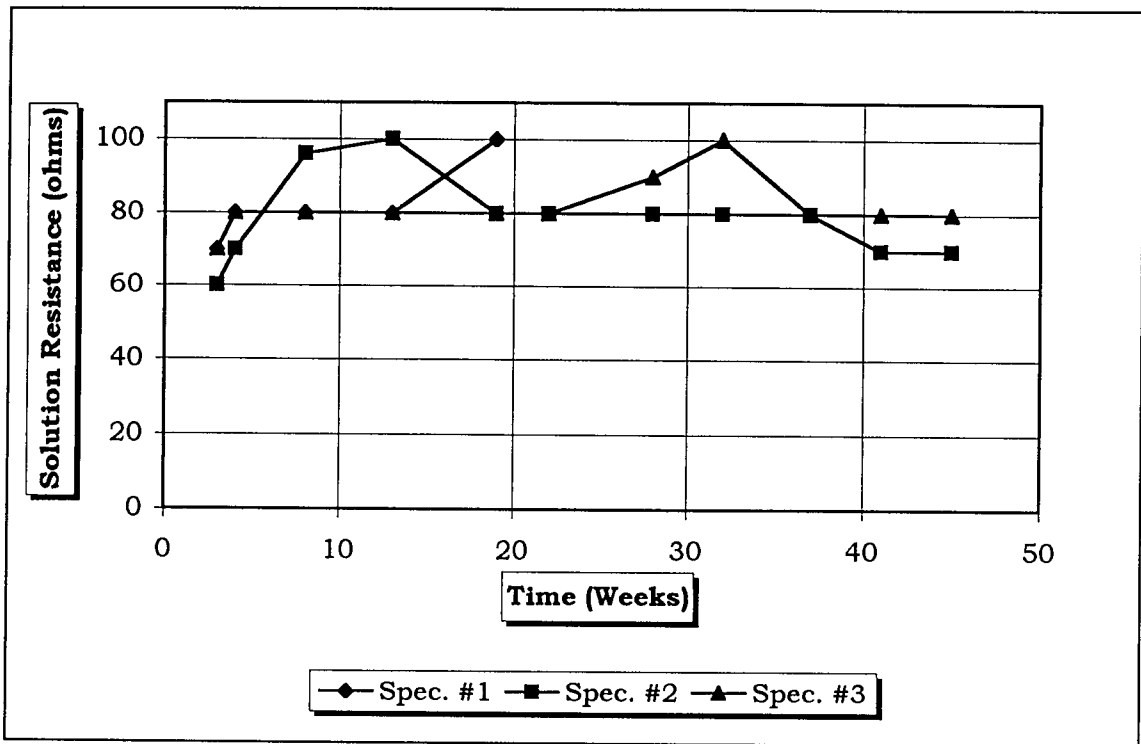


Figure D-19 Solution Resistance, Slabs, Control-2 Mixes Conn.

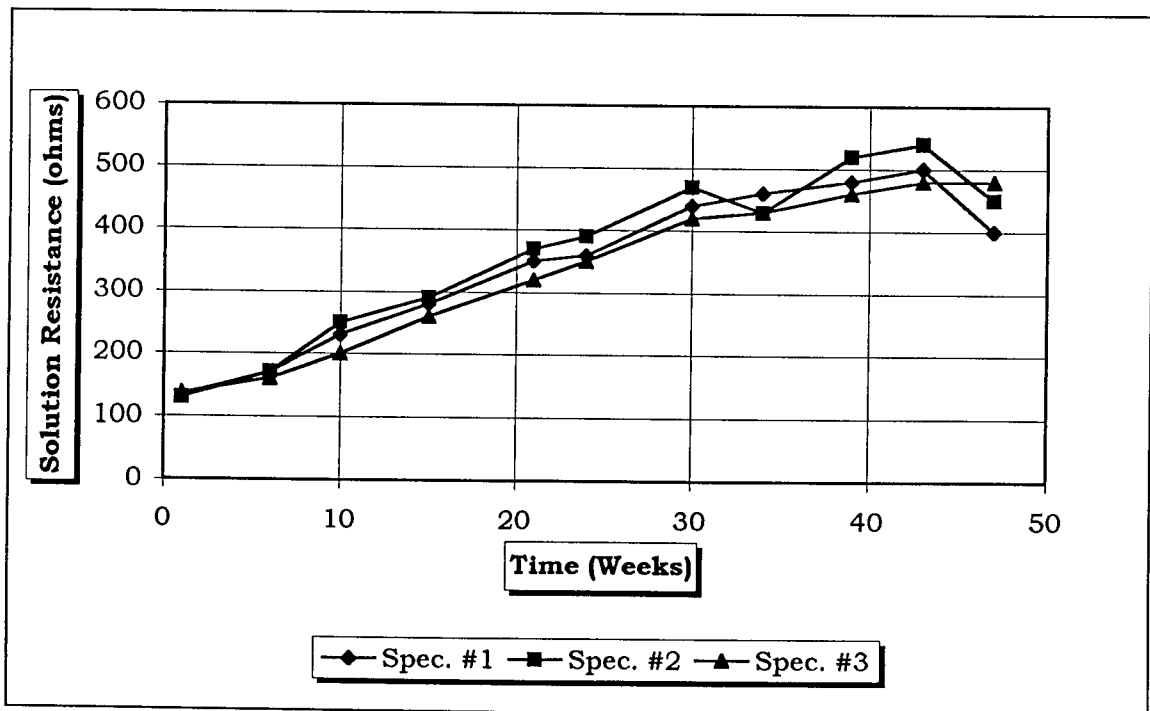


Figure D-20 Solution Resistance, Slabs, Inhibitor A.

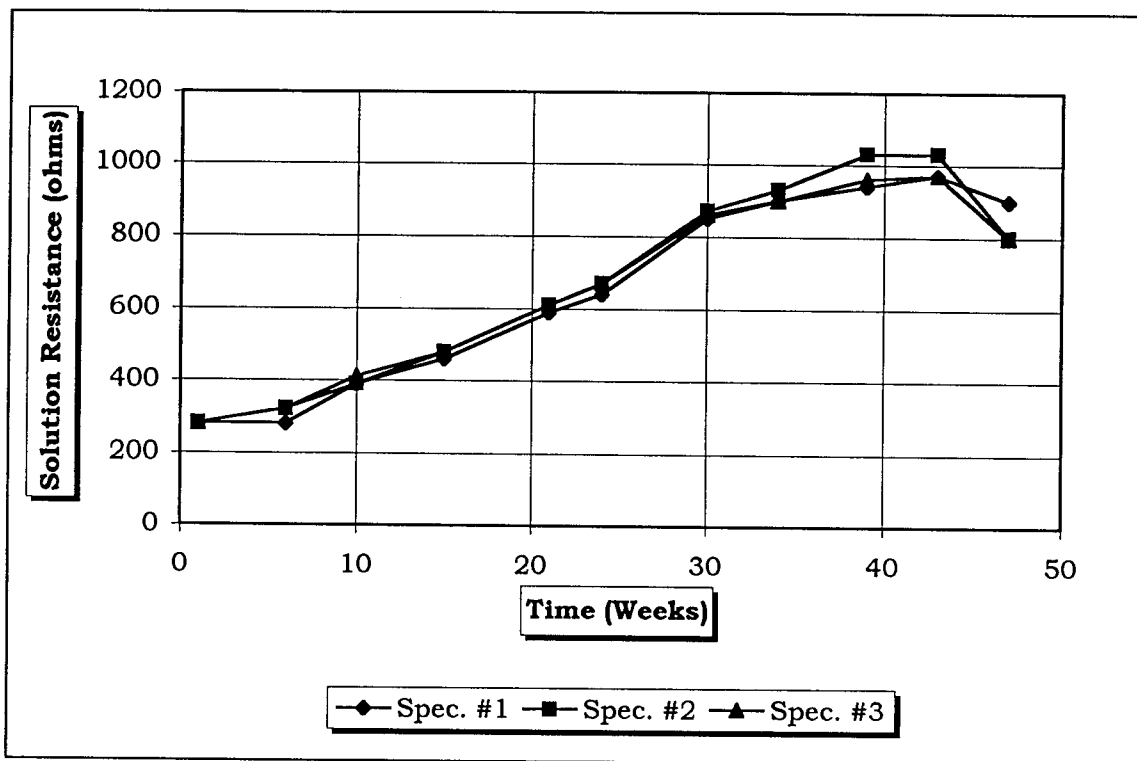


Figure D-21 Solution Resistance, Slabs, Inhibitor B.

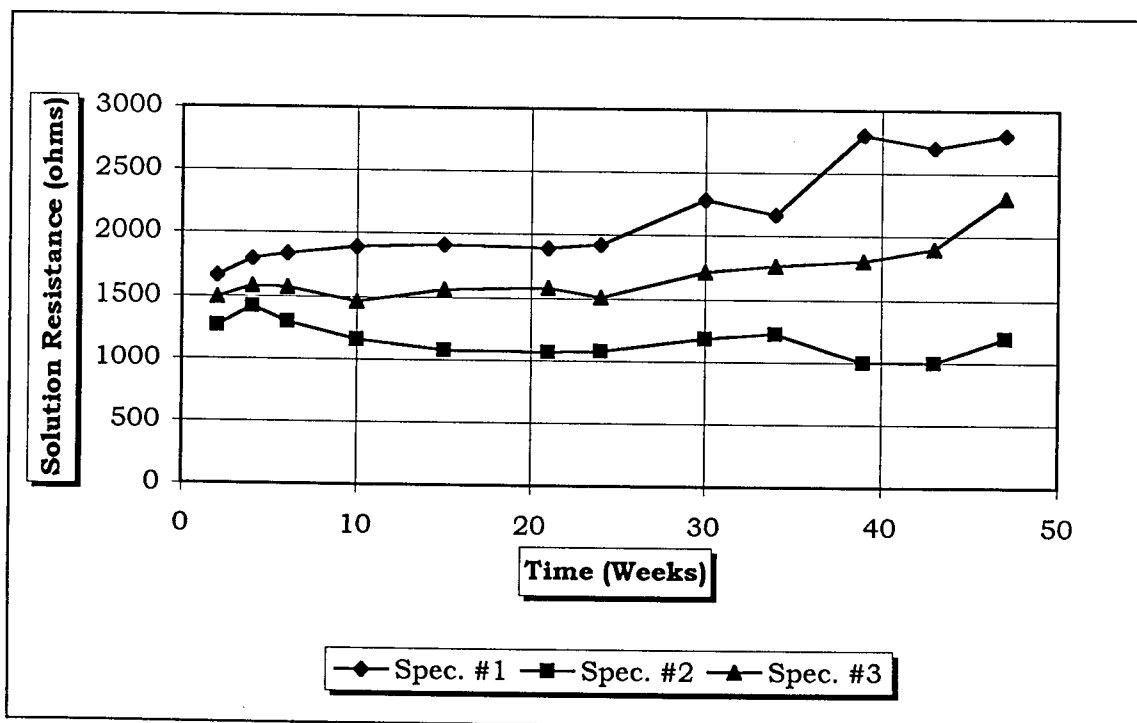


Figure D-22 Solution Resistance, Slabs, 2% DAS.



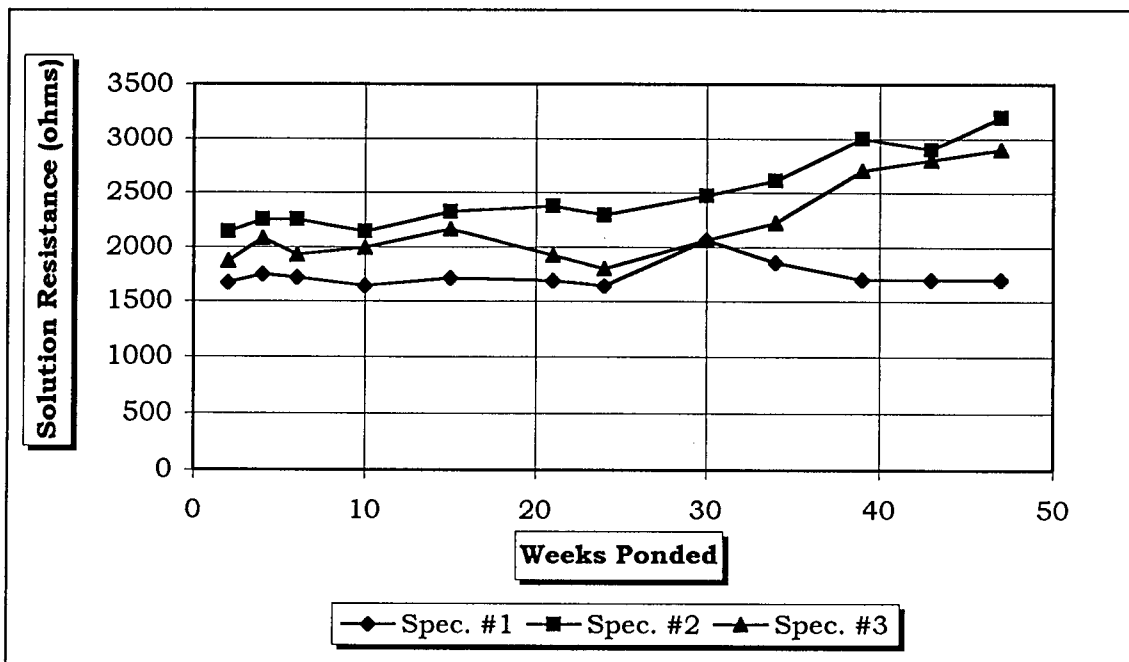


Figure D-23 Solution Resistance, Slabs, 1% DAS.

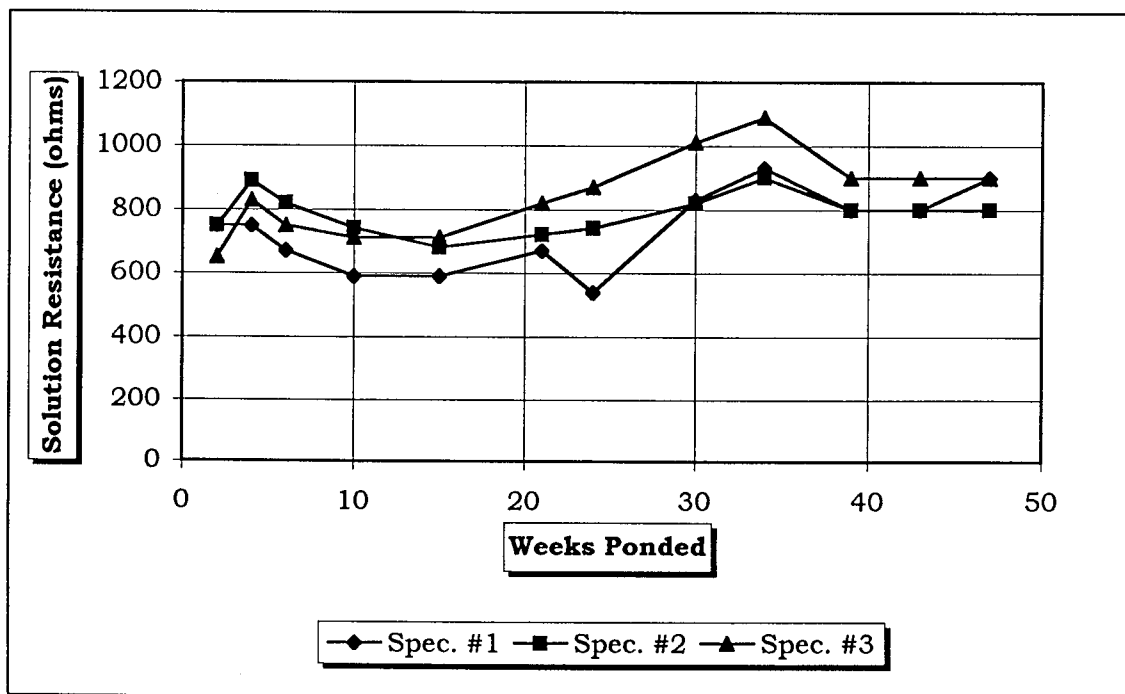


Figure D-24 Solution Resistance, Slabs, 1/2% DAS.

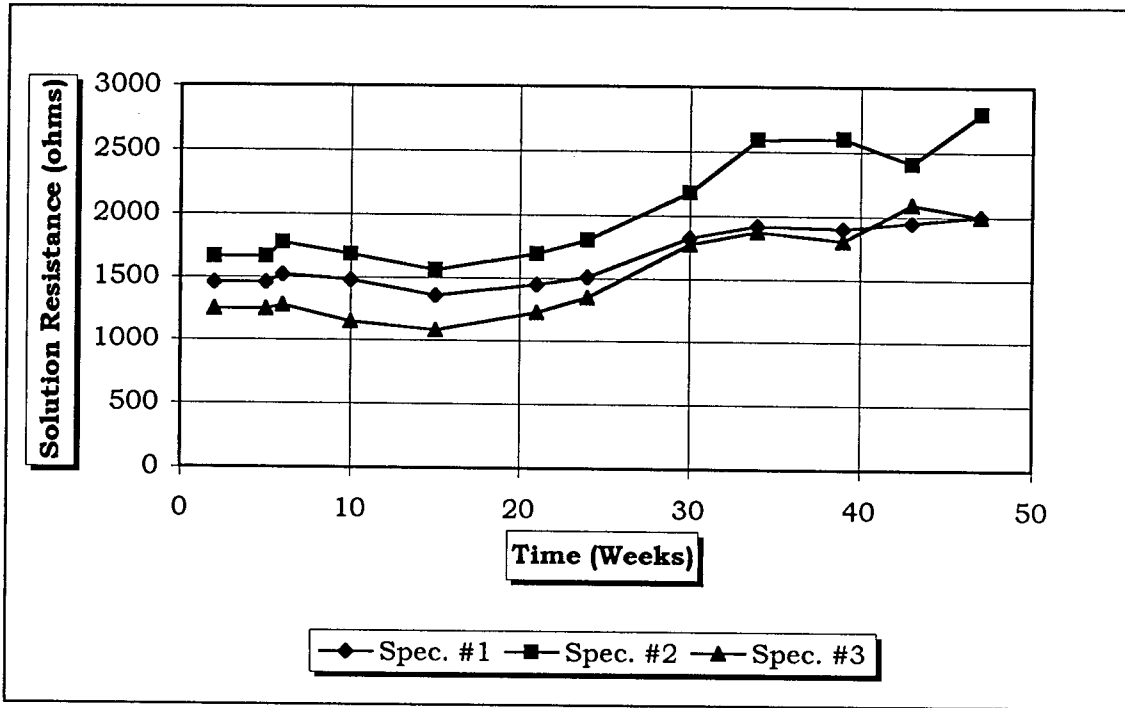


Figure D-25 Solution Resistance, Slabs, 2% DSS.

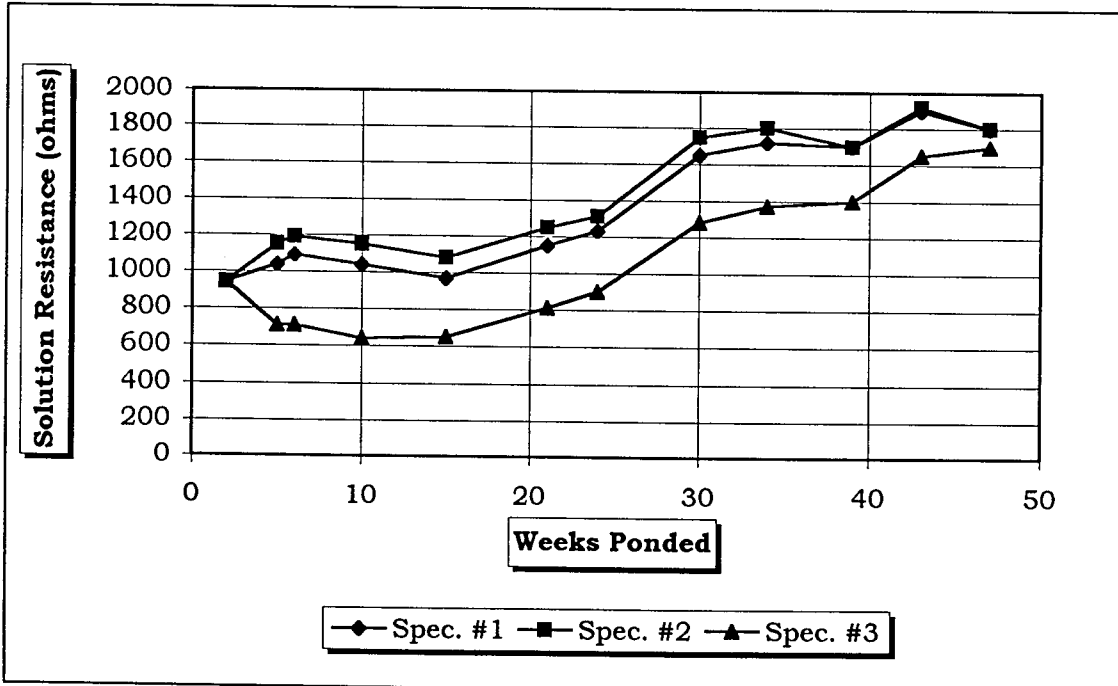


Figure D-26 Solution Resistance, Slabs, 1% DSS.

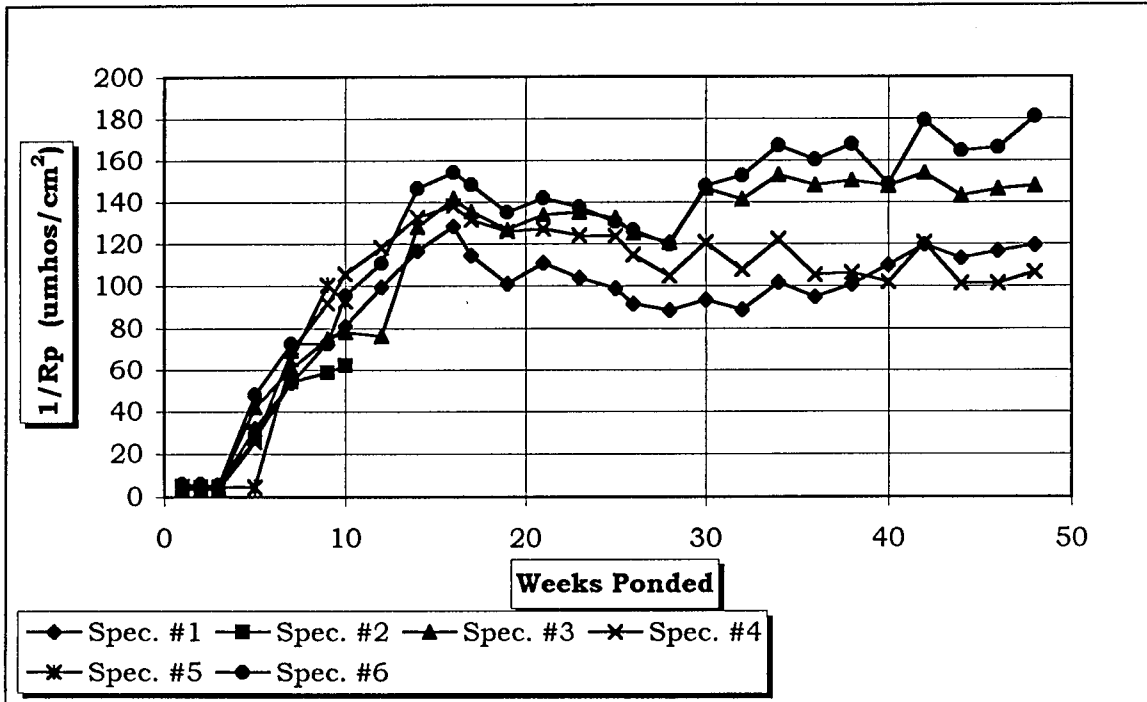


Figure D-27 Corrosion Rate, 2-Inch Diameter Lollipops: Control.

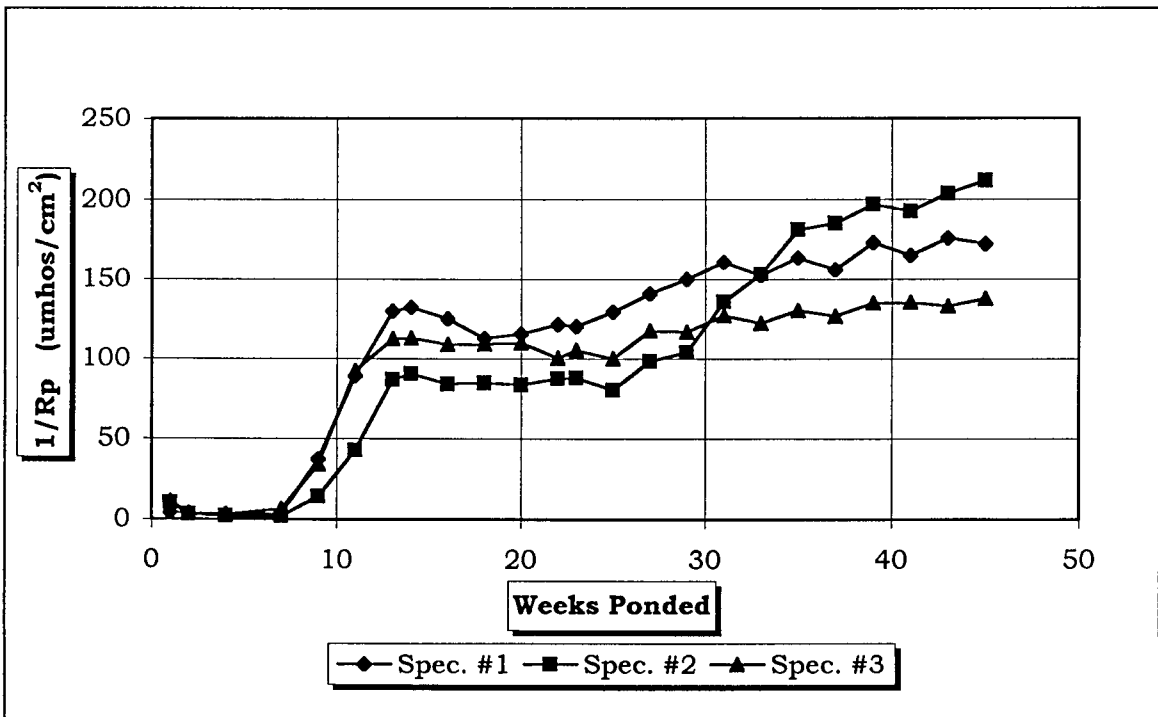


Figure D-28 Corrosion Rate, 2-Inch Diameter Lollipops: Inhibitor A.

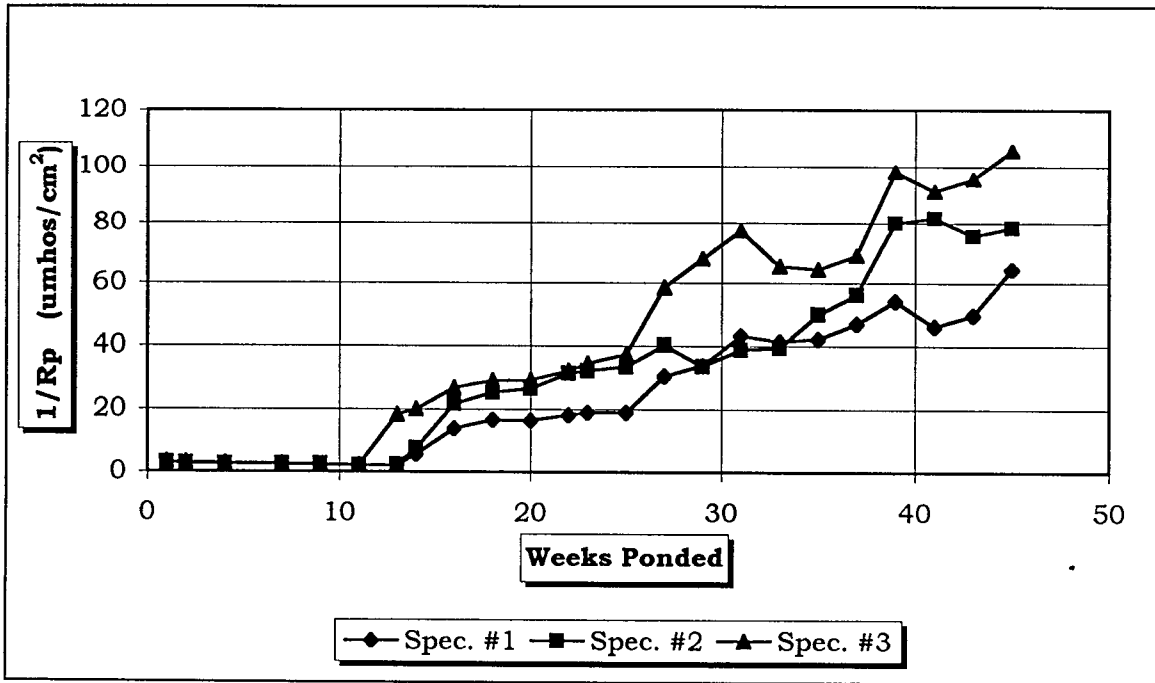


Figure D-29 Corrosion Rate, 2-Inch Diameter Lollipops: Inhibitor B.

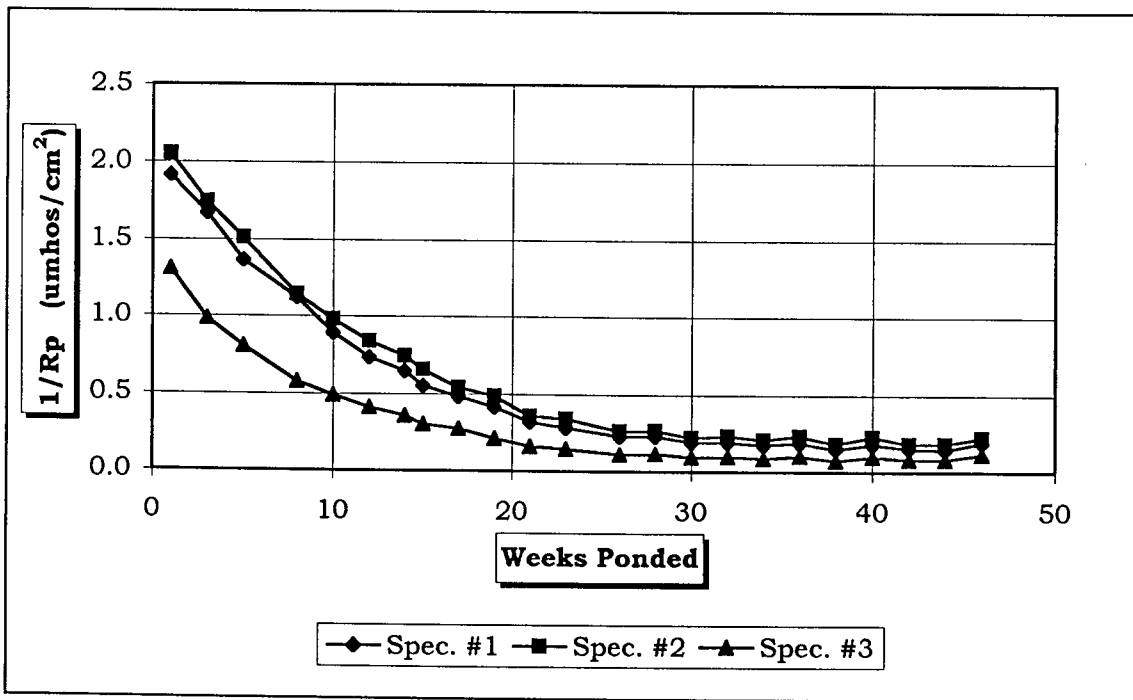


Figure D-30 Corrosion Rate, 2-Inch Diameter Lollipops: 2%DAS.

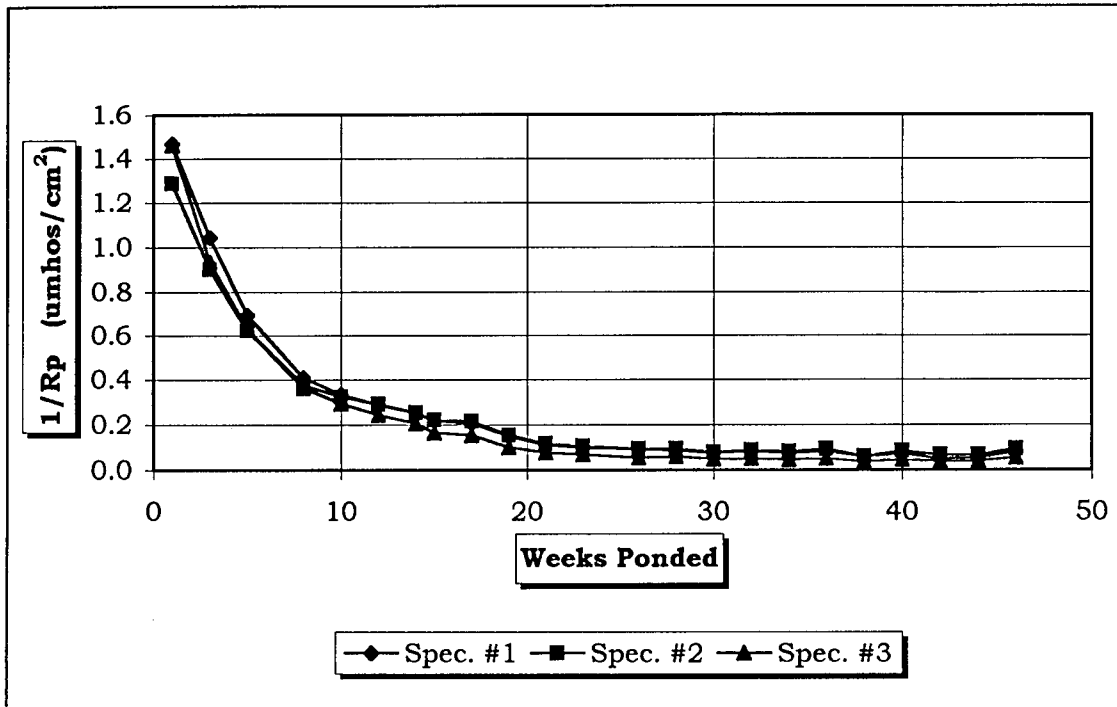


Figure D-31 Corrosion Rate, 2-Inch Diameter Lollipops: 1%DAS.

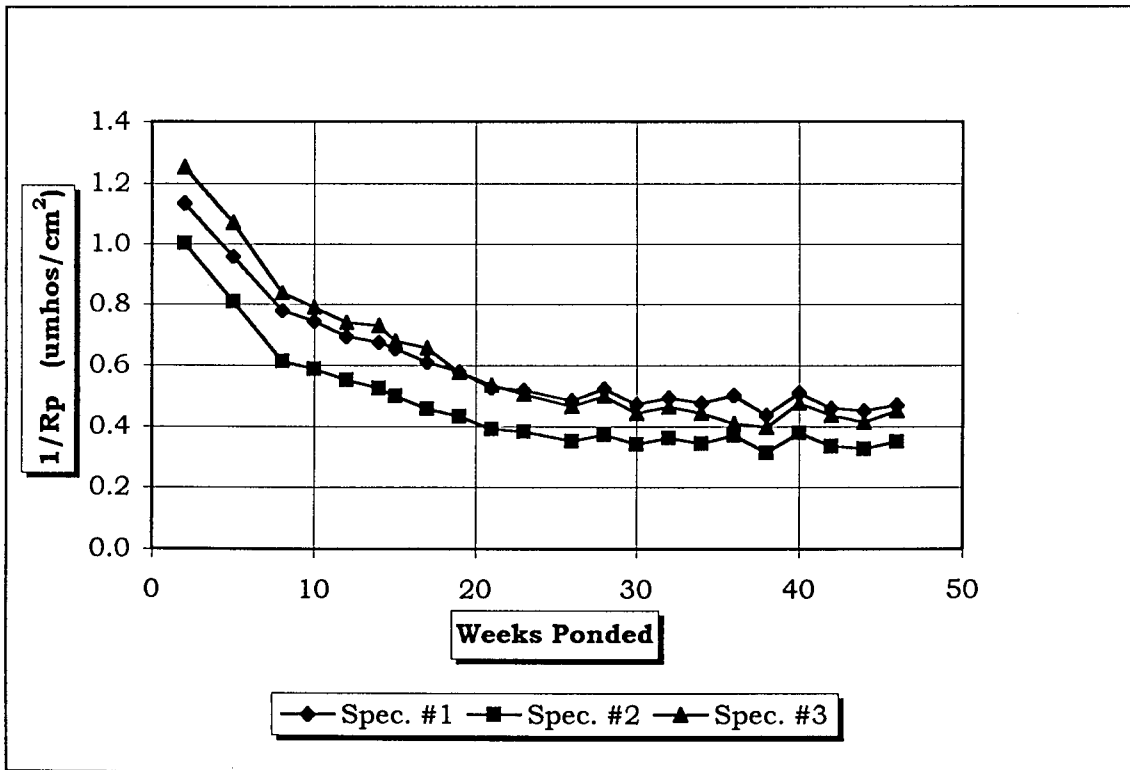


Figure D-32 Corrosion Rate, 2-Inch Diameter Lollipops: 1/2%DAS.

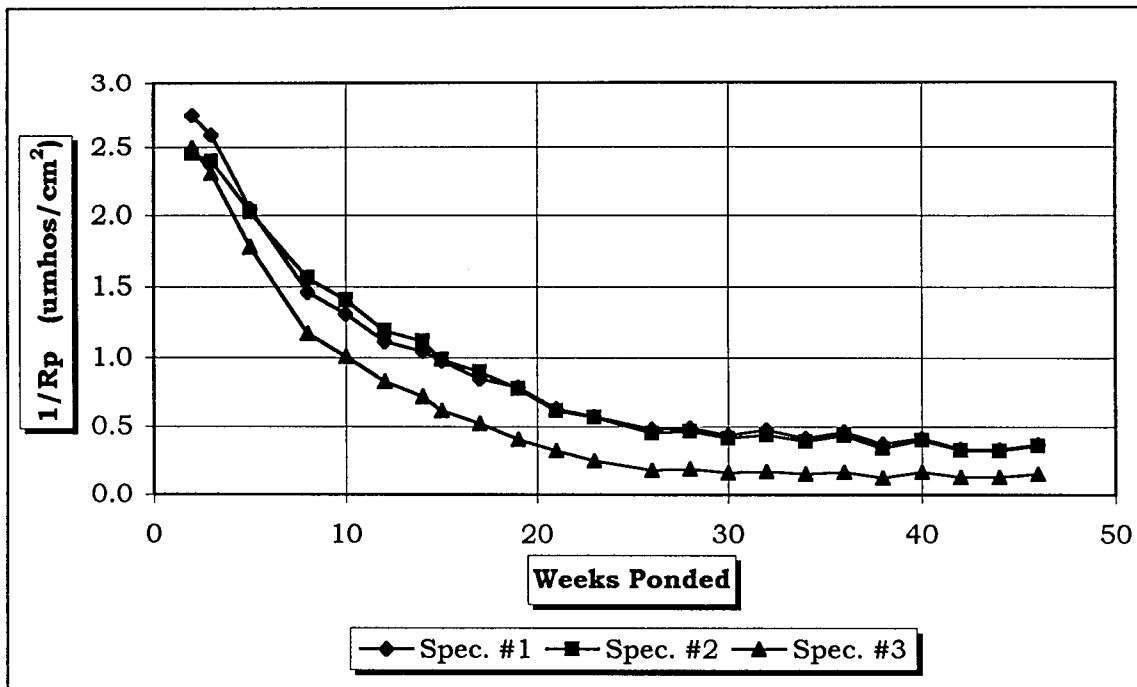


Figure D-33 Corrosion Rate, 2-Inch Diameter Lollipops: 2%DSS.

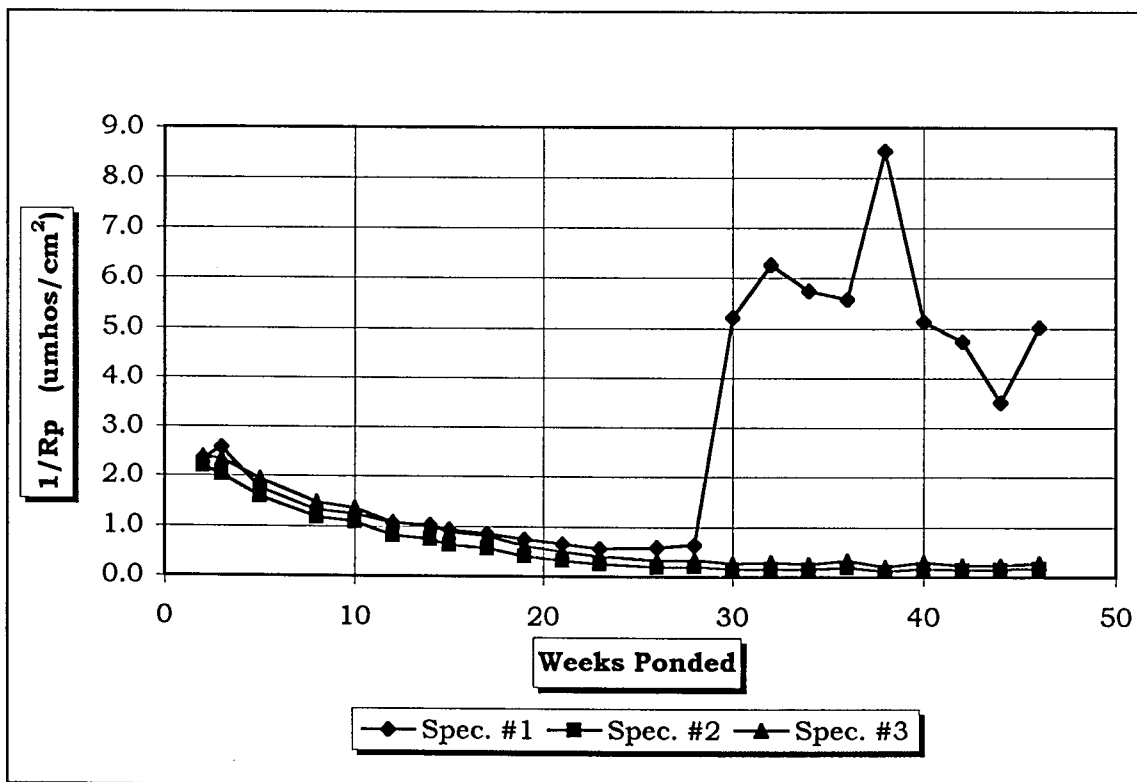


Figure D-34 Corrosion Rate, 2-Inch Diameter Lollipops: 1%DSS.

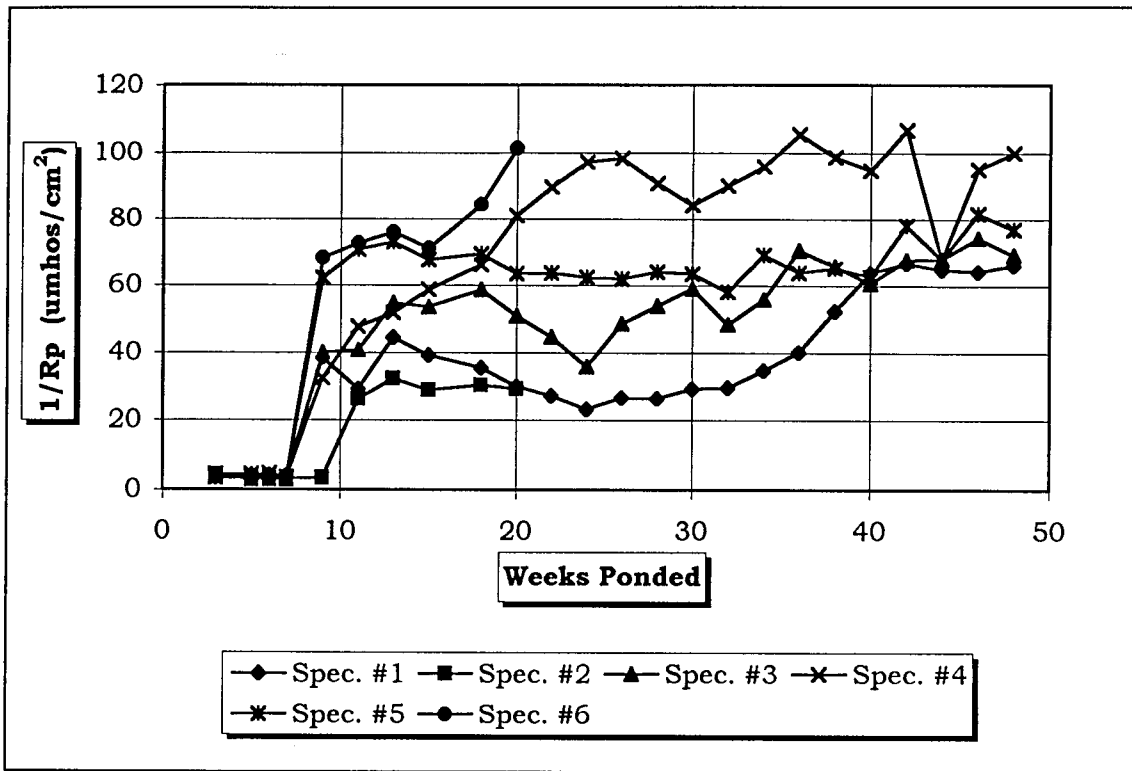


Figure D-35 Corrosion Rate, 3-Inch Diameter Lollipops, Control.

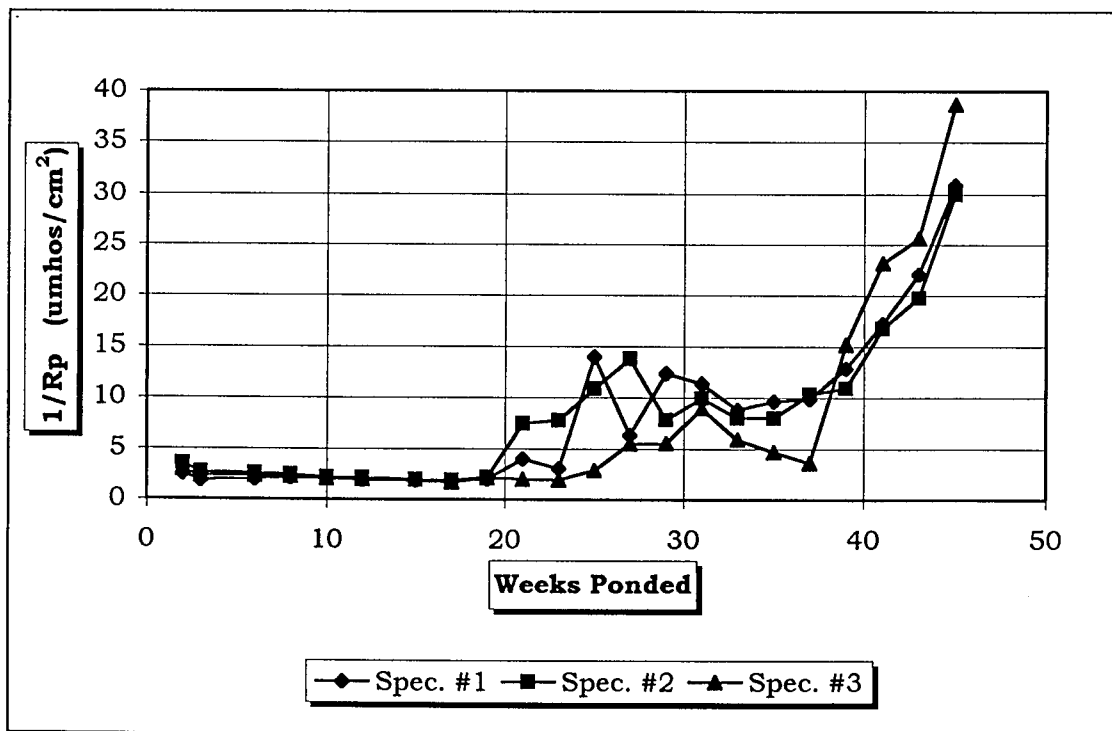


Figure D-36 Corrosion Rate, 3-Inch Diameter Lollipops, Inhibitor A.

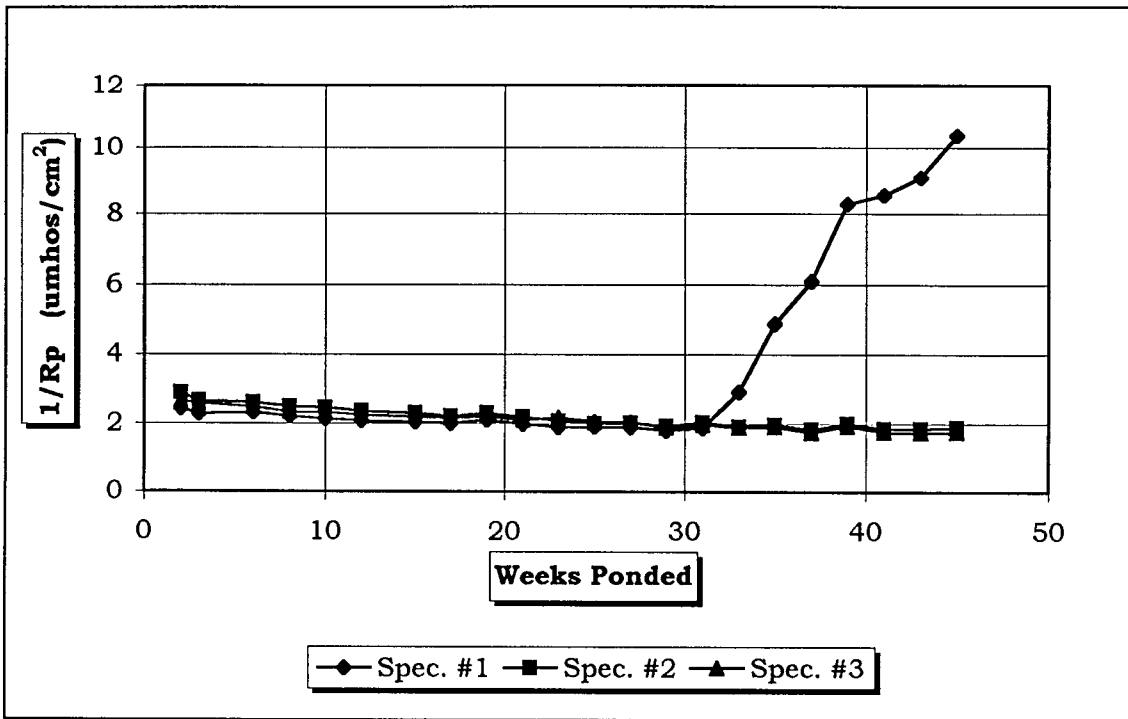


Figure D-37 Corrosion Rate, 3-Inch Diameter Lollipops, Inhibitor B.

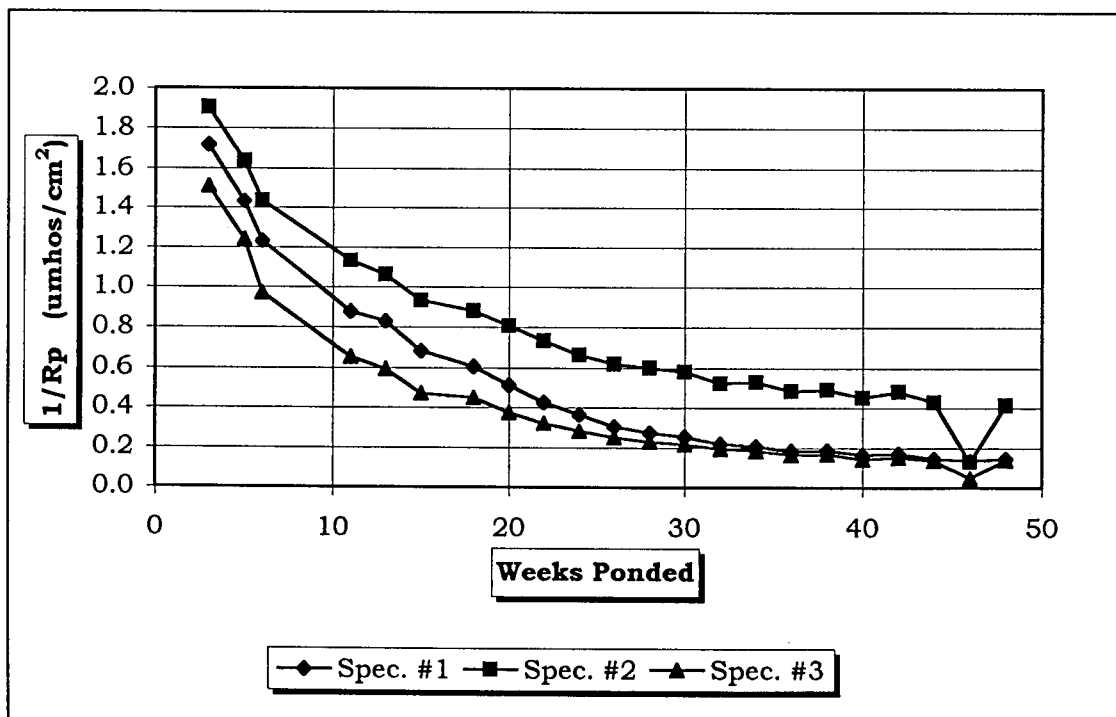


Figure D-38 Corrosion Rate, 3-Inch Diameter Lollipops, 2% DAS.



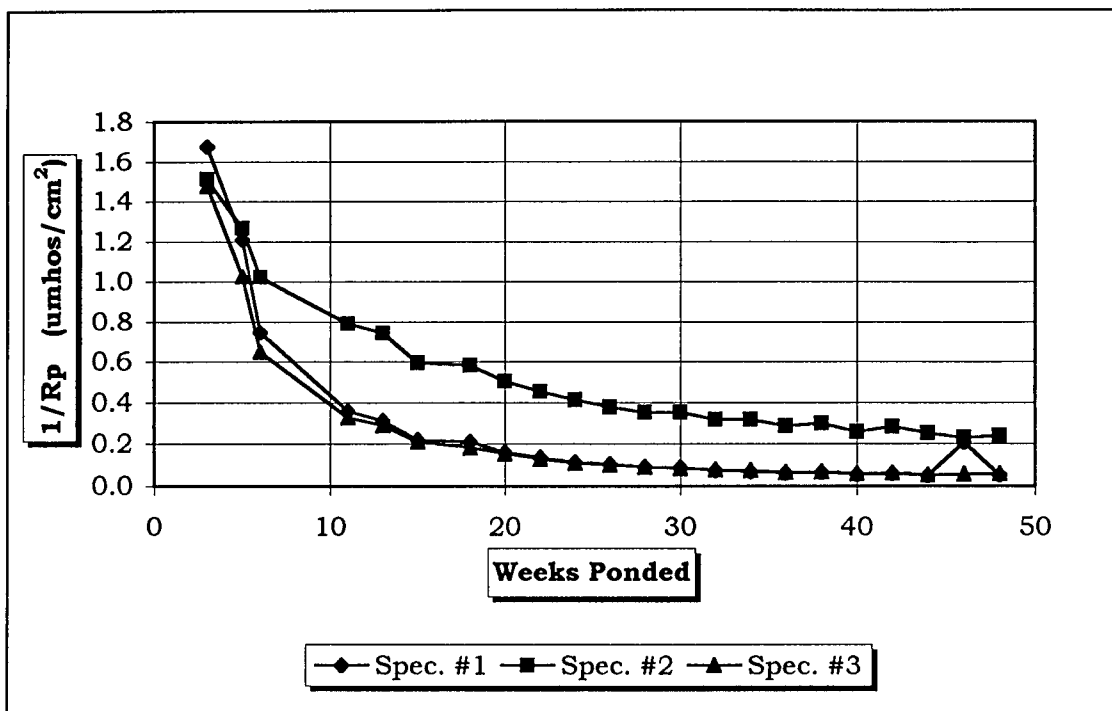


Figure D-39 Corrosion Rate, 3-Inch Diameter Lollipops, 1% DAS.

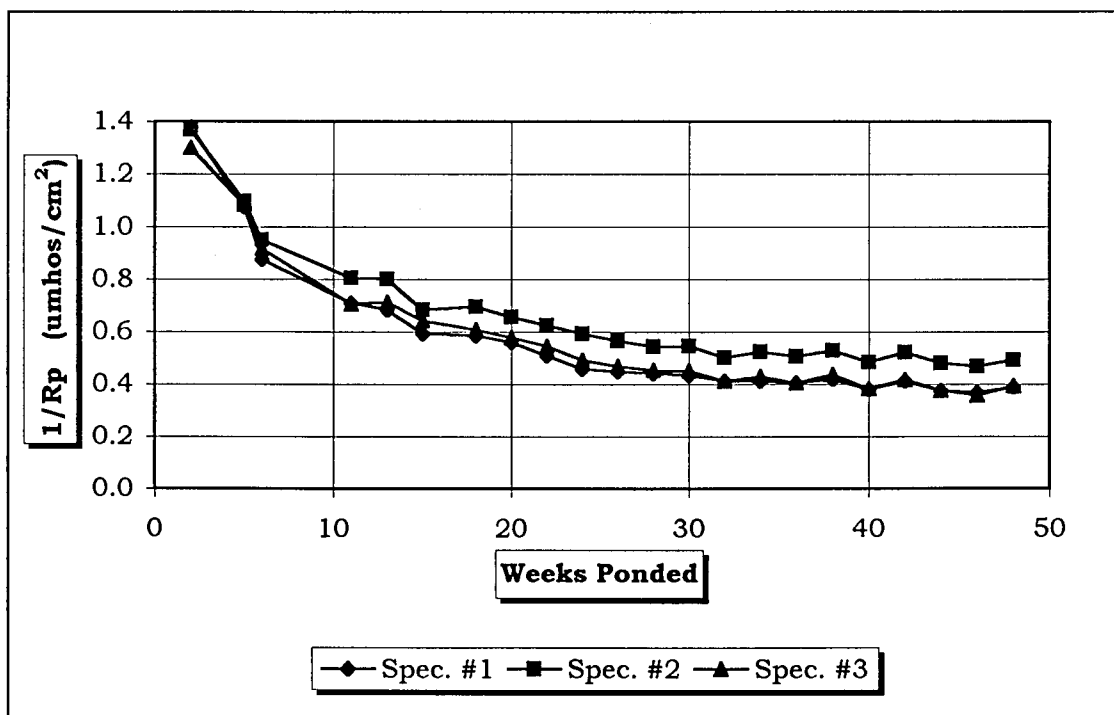


Figure D-40 Corrosion Rate, 3-Inch Diameter Lollipops, 1/2% DAS.

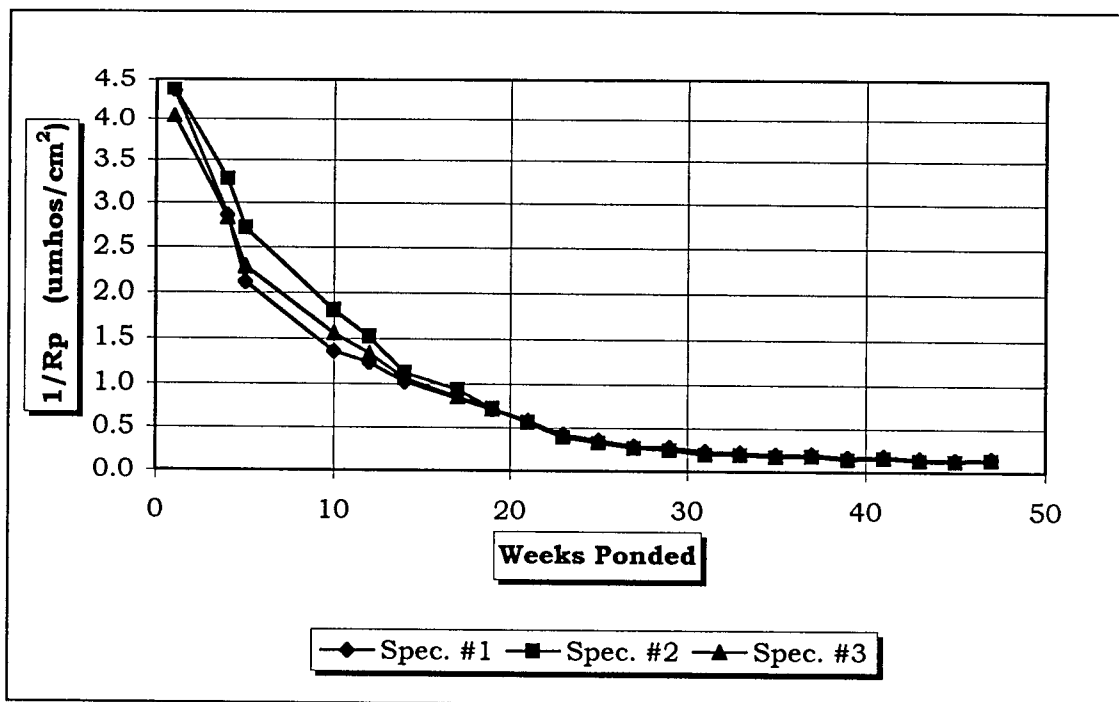


Figure D-41 Corrosion Rate, 3-Inch Diameter Lollipops, 2% DSS.

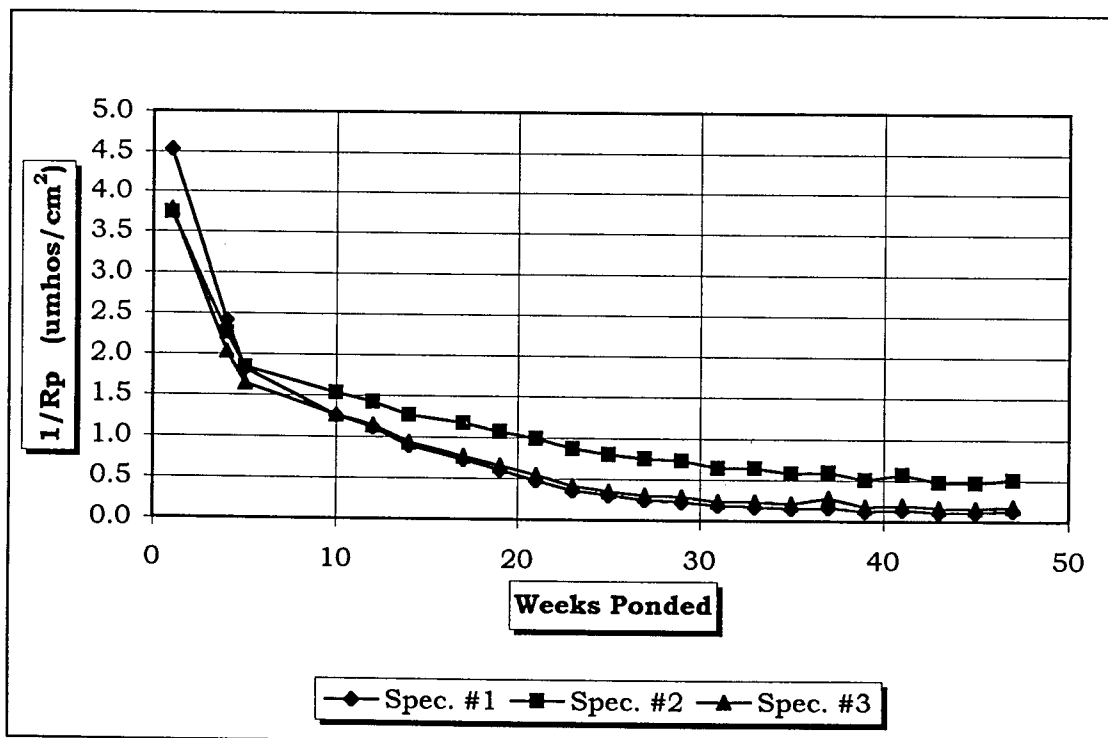


Figure D-42 Corrosion Rate, 3-Inch Diameter Lollipops, 1% DSS.

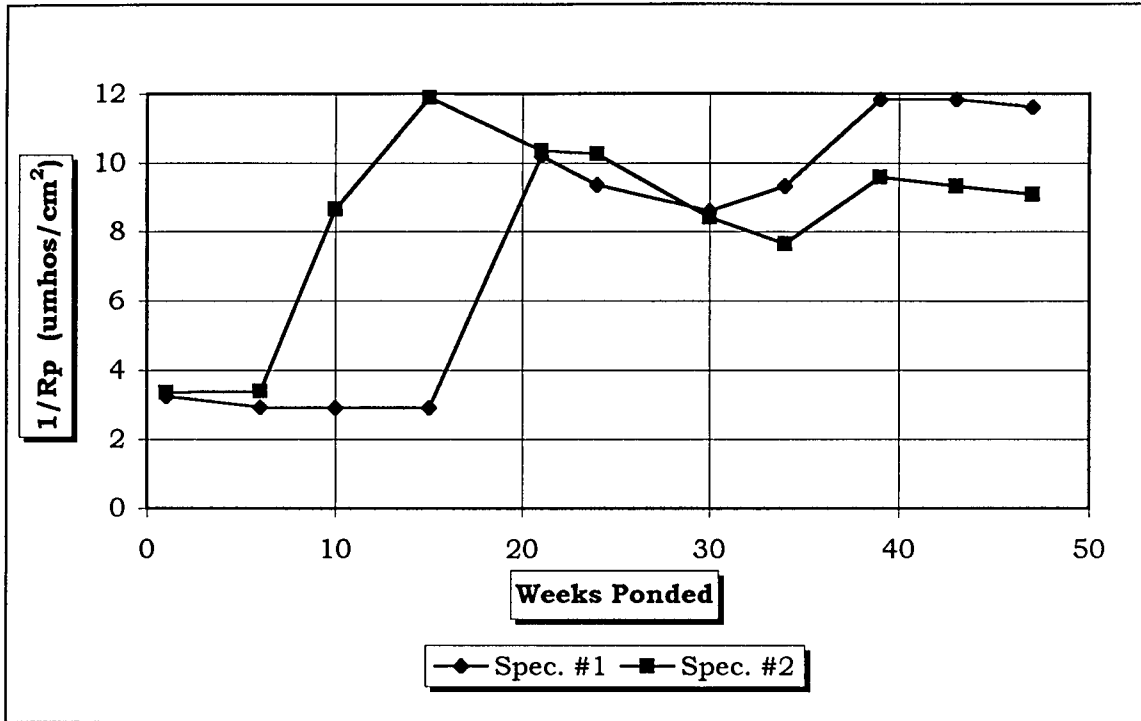


Figure D-43 Corrosion Rate, Slabs, Control-1 Mixes Conn.

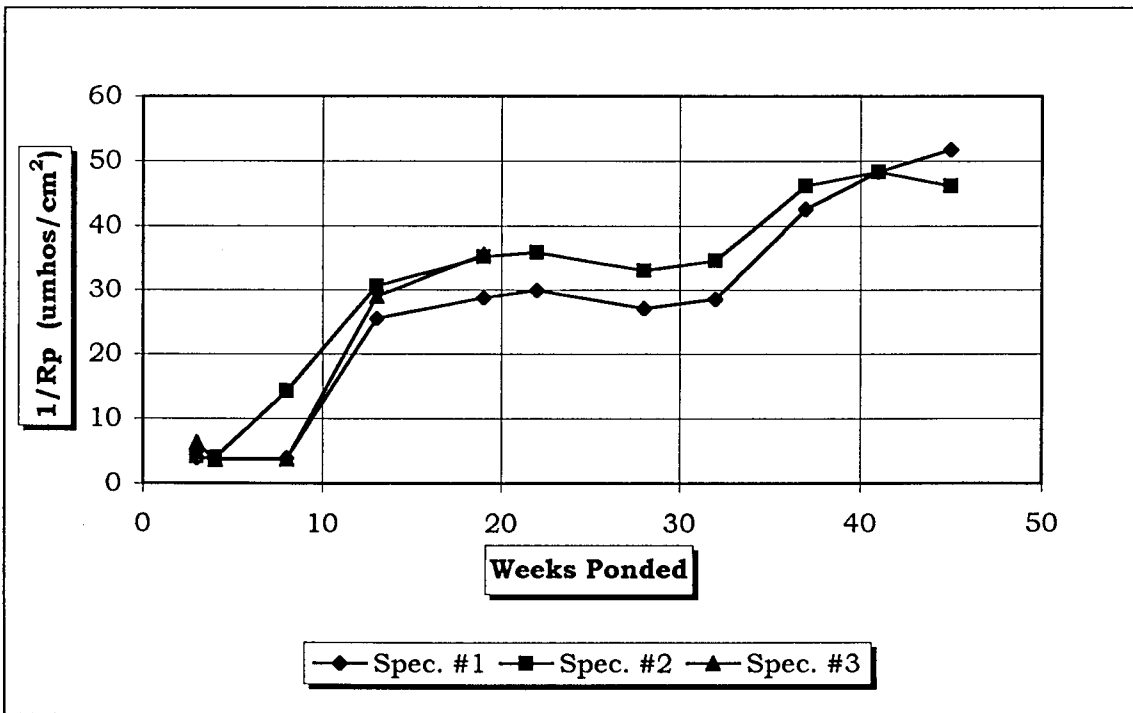


Figure D-44 Corrosion Rate, Slabs, Control-2 Unconn.

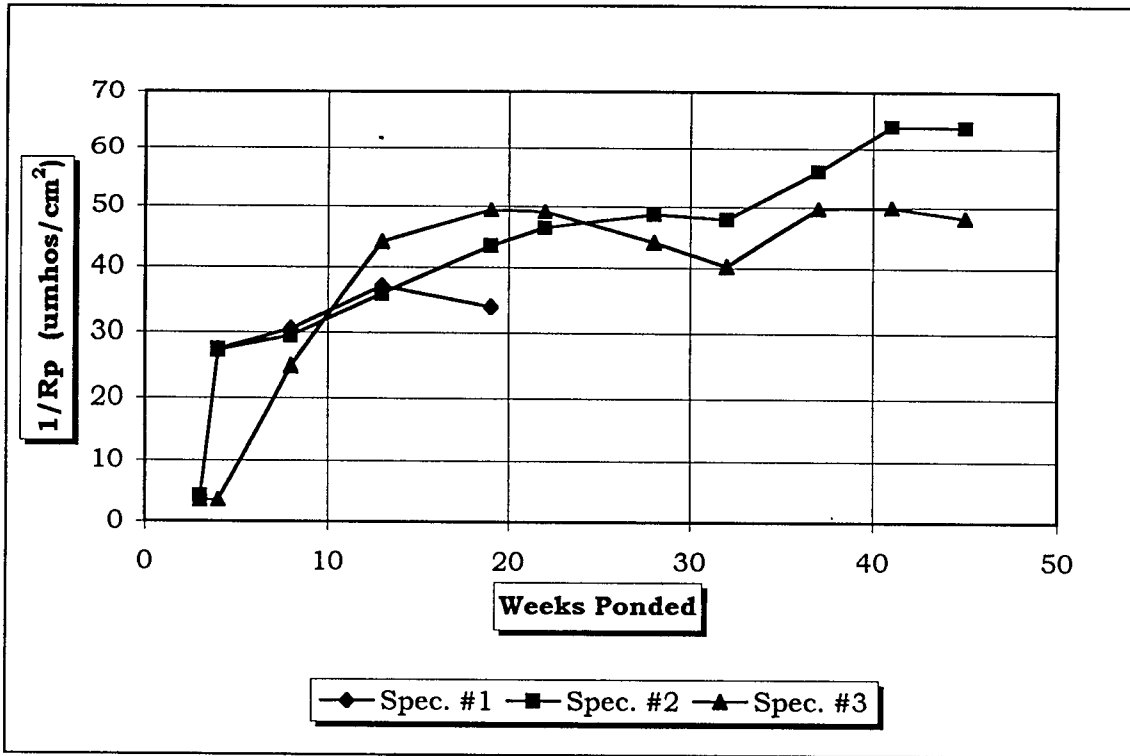


Figure D-45 Corrosion Rate, Slabs, Control-2 Mixes Conn.

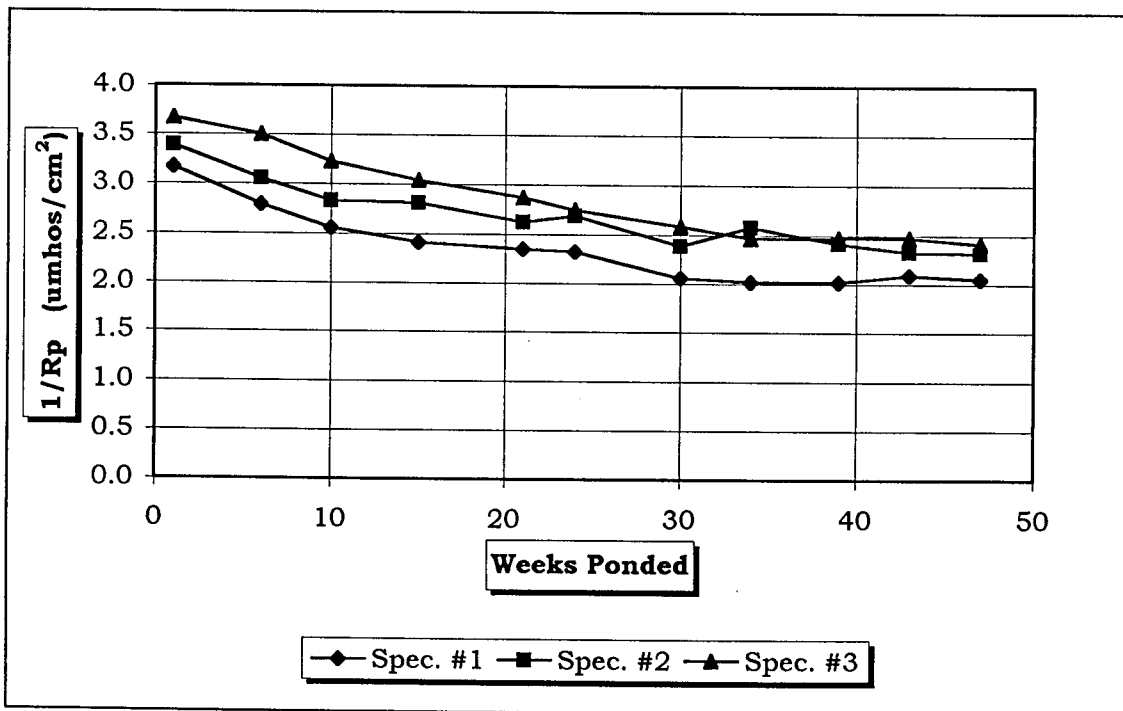


Figure D-46 Corrosion Rate, Slabs, Inhibitor A.

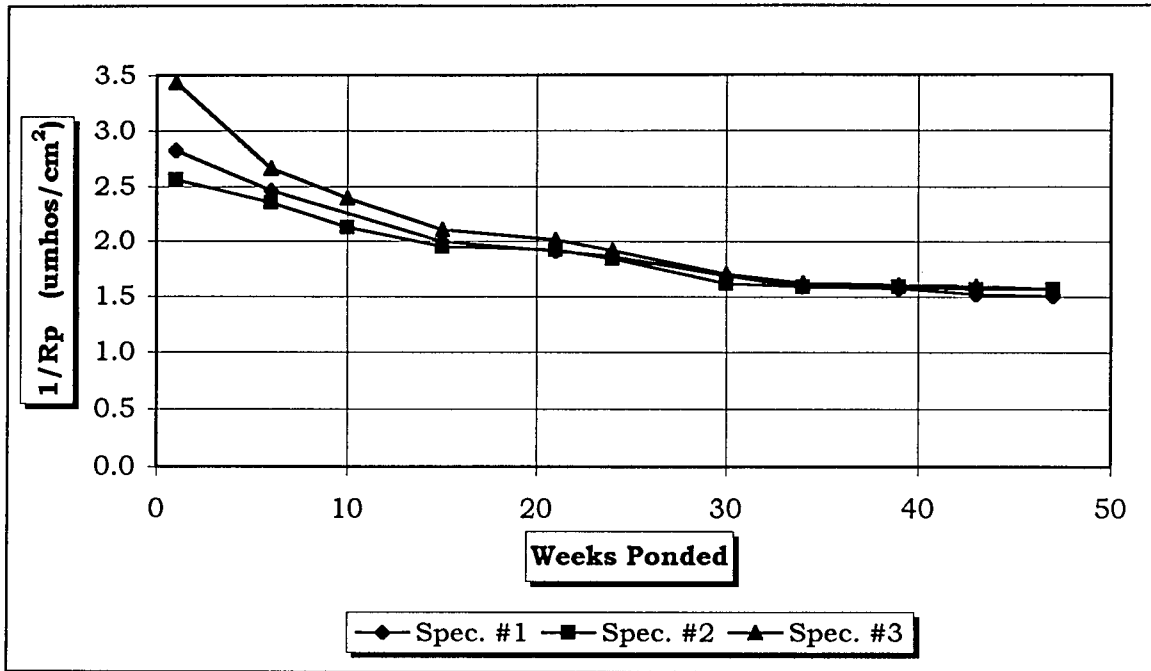


Figure D-47 Corrosion Rate, Slabs, Inhibitor B.

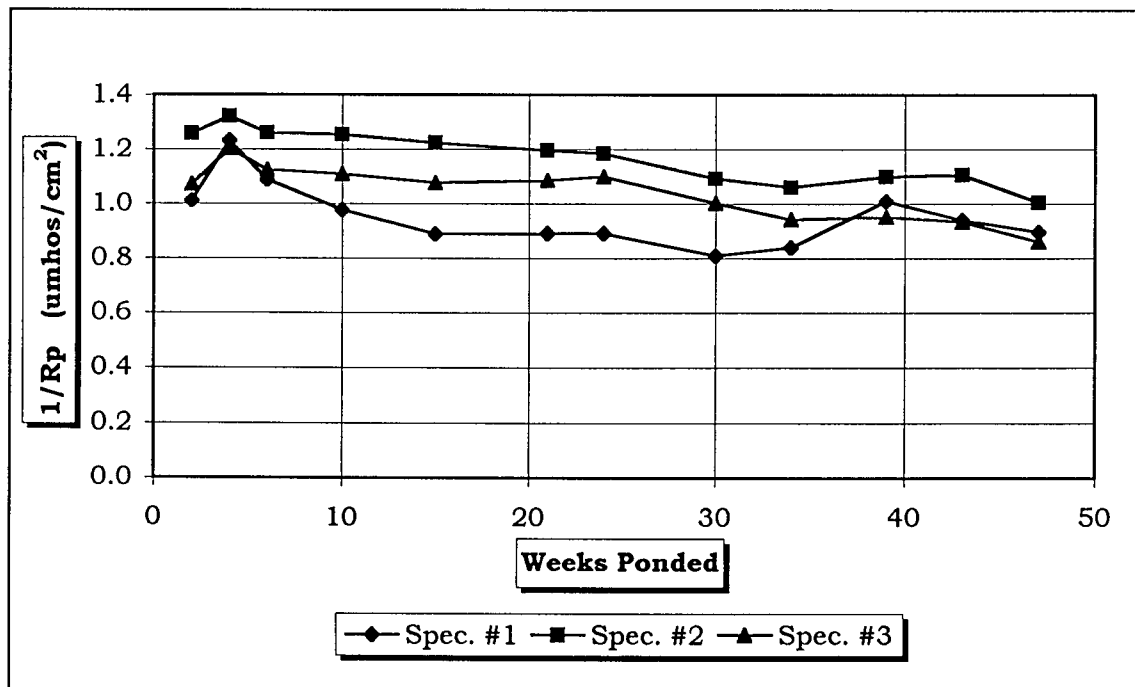


Figure D-48 Corrosion Rate, Slabs, 2% DAS.

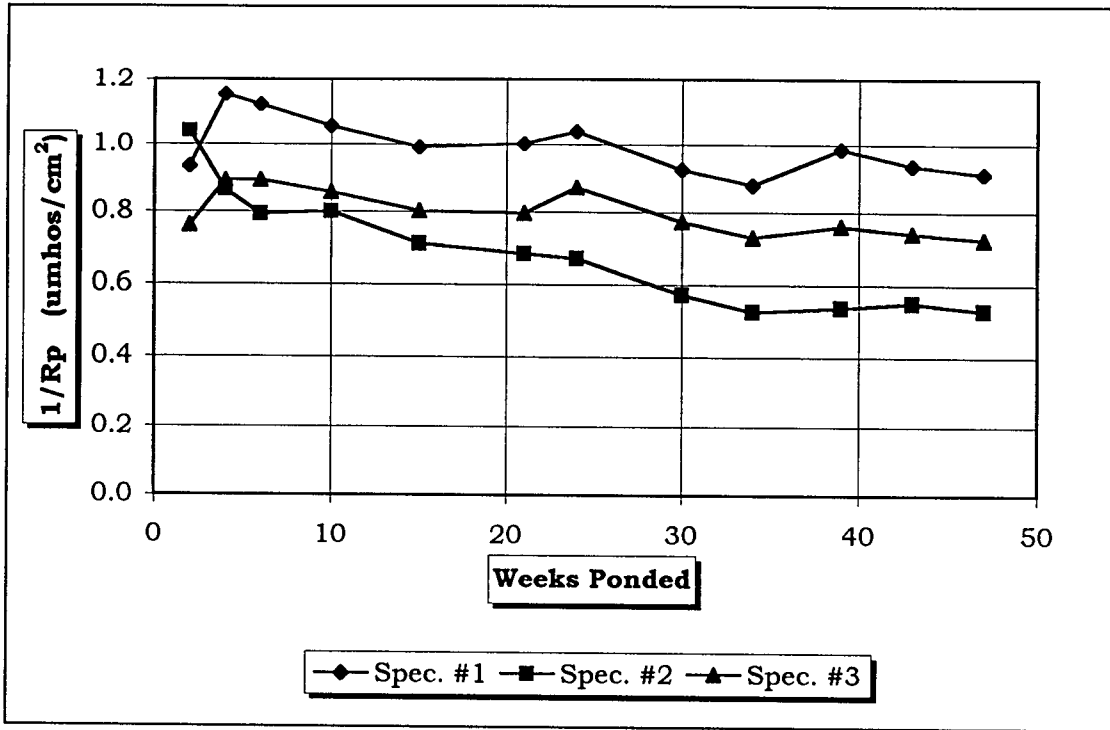


Figure D-49 Corrosion Rate, Slabs, 1% DAS.

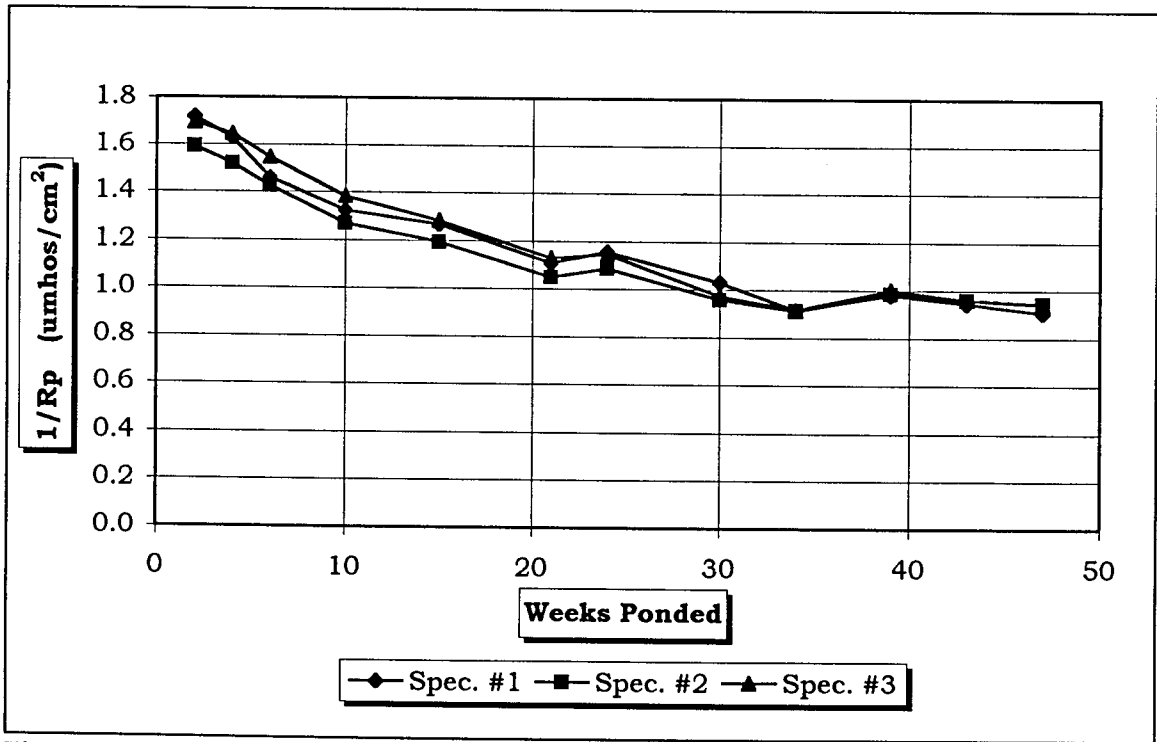


Figure D-50 Corrosion Rate, Slabs, 1/2% DAS.

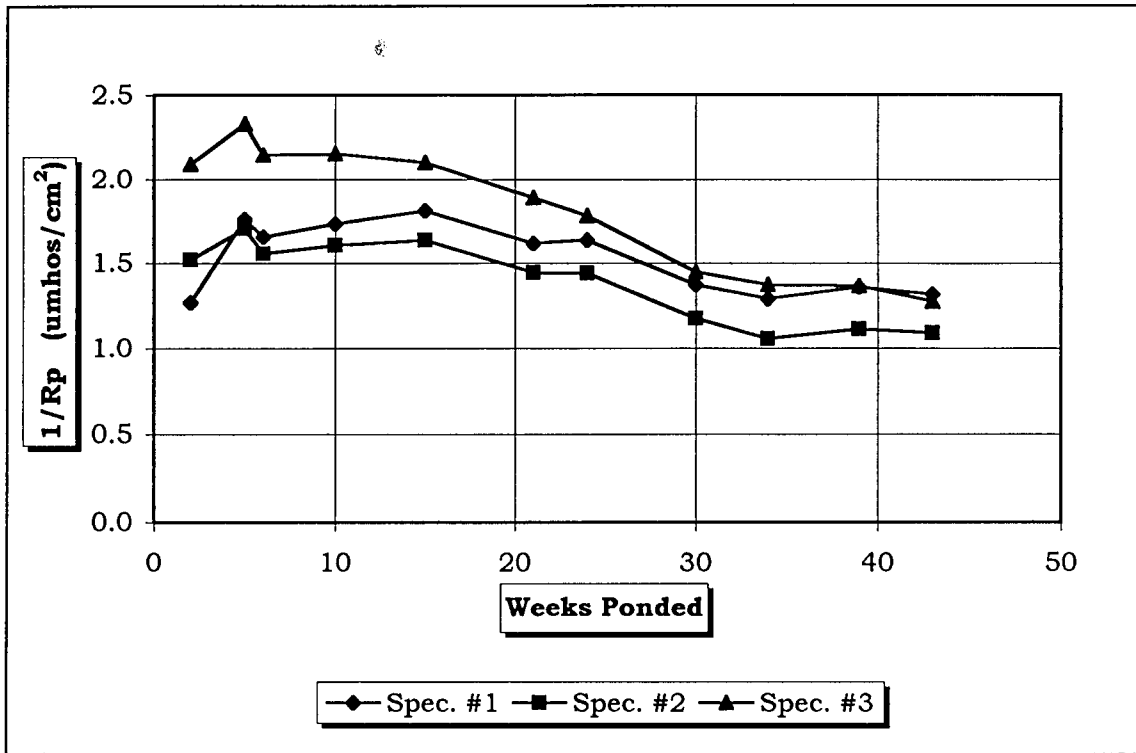


Figure D-51 Corrosion Rate, Slabs, 2% DSS.

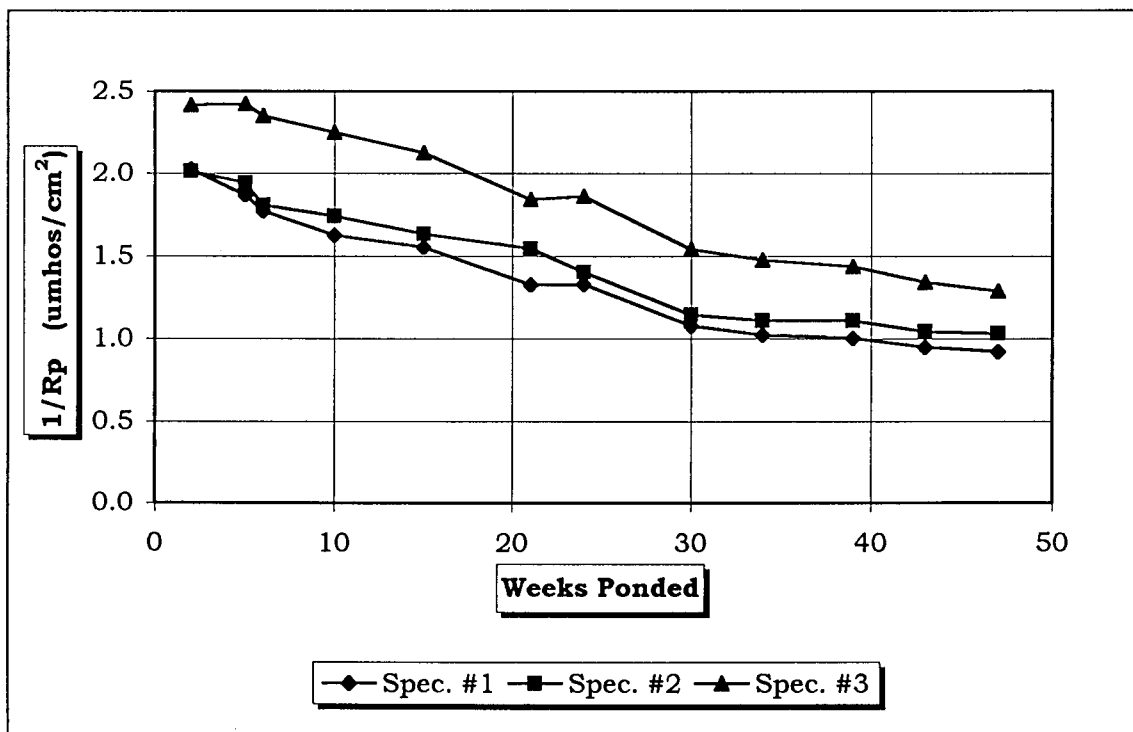


Figure D-52 Corrosion Rate, Slabs, 1% DSS.

